N° d'ordre NNT : 2024ISAL0088

THESE de DOCTORAT DE L'INSA LYON, membre de l'Université de Lyon

Ecole Doctorale N° 206
(Ecole Doctorale de chimie de Lyon)

Spécialité/ discipline de doctorat : Génie des procédés

Soutenue publiquement le 13/11/2024, par :

(Caroline Kimie Miyazaki)

Optimization of hybrid aerated vertical/horizontal flow treatment wetland

Devant le jury composé de :

GALVAO	Ana	Professor (PhD)	University of Lisbon	Rapporteure
ROUSSEAU	Diederik	Professor (PhD)	Ghent University	Rapporteur
GAUTIER	Mathieu	Professor (HDR)	INSA-Lyon	Président
MASI	Fabio	Directeur technique/R&D (PhD)	IRIDRA	Examinateur
MOLLE	Pascal	Directeur de recherche (HDR)	INRAE	Directeur de thèse
NIVALA	Jaime	Directrice de recherche (HDR)	INRAE	Co-directrice de thèse
MORVANNOU	Ania	Chargée de recherche (PhD)	Ecobird	Invitée

Thèse accessible à l'adresse : https://theses.insa-lyon.fr/publication/2024ISAL0088/these.pdf © [C.K. Miyazaki], [2024], INSA Lyon, tous droits réservés

INSA INSTITUT NATIONAL DES SCIENCES APPLIQUÉES LYON

Département de la Formation par la Recherche et des Études Doctorales (**FEDORA**)

Bâtiment Charlotte Perriand 3e étage
17, av. des Arts
69621 Villeurbanne Cédex
fedora@insa-lyon.fr

Référence : TH1162_MIYAZAKI Caroline

L'INSA Lyon a mis en place une procédure de contrôle systématique via un outil de détection de similitudes (logiciel Compilatio). Après le dépôt du manuscrit de thèse, celui-ci est analysé par l'outil. Pour tout taux de similarité supérieur à 10%, le manuscrit est vérifié par l'équipe de FEDORA. Il s'agit notamment d'exclure les auto-citations, à condition qu'elles soient correctement référencées avec citation expresse dans le manuscrit.

Par ce document, il est attesté que ce manuscrit, dans la forme communiquée par la personne doctorante à l'INSA Lyon, satisfait aux exigences de l'Etablissement concernant le taux maximal de similitude admissible.

INSA LYON
Campus LyonTech La Doua
20, avenue Albert Einstein - 69621 Villeurbanne cedex - France
Tél. +33 (0)4 72 43 83 83 - Fax +33 (0)4 72 43 85 00
www.insa-lyon.fr

membre de UNIVERSITÉ DE LYON

Thèse accessible à l'adresse : https://theses.insa-lyon.fr/publication/2024ISAL0088/these.pdf © [C.K. Miyazaki], [2024], INSA Lyon, tous droits réservés

Département FEDORA – INSA Lyon - Écoles Doctorales

SIGLE	ECOLE DOCTORALE	
ED 206 CHIMIE	**CHIMIE DE LYON** https://www.edchimie-lyon.fr Sec. : Renée EL MELHEM Bât. Blaise PASCAL, 3e étage secretariat@edchimie-lyon.fr	**M. Stéphane DANIELE** C2P2-CPE LYON-UMR 5265 Bâtiment F308, BP 2077 43 Boulevard du 11 novembre 1918 69616 Villeurbanne directeur@edchimie-lyon.fr
ED 341 E2M2	**ÉVOLUTION, ÉCOSYSTÈME, MICROBIOLOGIE, MODÉLISATION** http://e2m2.universite-lyon.fr Sec. : Bénédicte LANZA Bât. Atrium, UCB Lyon 1 Tél : 04.72.44.83.62 secretariat.e2m2@univ-lyon1.fr	**Mme Sandrine CHARLES** Université Claude Bernard Lyon 1 UFR Biosciences Bâtiment Mendel 43, boulevard du 11 Novembre 1918 69622 Villeurbanne CEDEX e2m2.codir@listes.univ-lyon1.fr
ED 205 EDISS	**INTERDISCIPLINAIRE SCIENCES-SANTÉ** http://ediss.universite-lyon.fr Sec. : Bénédicte LANZA Bât. Atrium, UCB Lyon 1 Tél : 04.72.44.83.62 secretariat.ediss@univ-lyon1.fr	**Mme Sylvie RICARD-BLUM** Laboratoire ICBMS - UMR 5246 CNRS - Université Lyon 1 Bâtiment Raulin - 2ème étage Nord 43 Boulevard du 11 novembre 1918 69622 Villeurbanne Cedex Tél : +33(0)4 72 44 82 32 sylvie.ricard-blum@univ-lyon1.fr
ED 34 EDML	**MATÉRIAUX DE LYON** http://ed34.universite-lyon.fr Sec. : Yann DE ORDENANA Tél : 04.72.18.62.44 yann.de-ordenana@ec-lyon.fr	**M. Stéphane BENAYOUN** Ecole Centrale de Lyon Laboratoire LTDS 36 avenue Guy de Collongue 69134 Ecully CEDEX Tél : 04.72.18.64.37 stephane.benayoun@ec-lyon.fr
ED 160 EEA	**ÉLECTRONIQUE, ÉLECTROTECHNIQUE, AUTOMATIQUE** https://edeea.universite-lyon.fr Sec. : Philomène TRECOURT Bâtiment Direction INSA Lyon Tél : 04.72.43.71.70 secretariat.edeea@insa-lyon.fr	**M. Philippe DELACHARTRE** INSA LYON Laboratoire CREATIS Bâtiment Blaise Pascal, 7 avenue Jean Capelle 69621 Villeurbanne CEDEX Tél : 04.72.43.88.63 philippe.delachartre@insa-lyon.fr
ED 512 INFOMATHS	**INFORMATIQUE ET MATHÉMATIQUES** http://edinfomaths.universite-lyon.fr Sec. : Renée EL MELHEM Bât. Blaise PASCAL, 3e étage Tél : 04.72.43.80.46 infomaths@univ-lyon1.fr	**M. Hamamache KHEDDOUCI** Université Claude Bernard Lyon 1 Bât. Nautibus 43, Boulevard du 11 novembre 1918 69 622 Villeurbanne Cedex France Tél : 04.72.44.83.69 direction.infomaths@listes.univ-lyon1.fr
ED 162 MEGA	**MÉCANIQUE, ÉNERGÉTIQUE, GÉNIE CIVIL, ACOUSTIQUE** http://edmega.universite-lyon.fr Sec. : Philomène TRECOURT Tél : 04.72.43.71.70 Bâtiment Direction INSA Lyon mega@insa-lyon.fr	**M. Etienne PARIZET** INSA Lyon Laboratoire LVA Bâtiment St. Exupéry 25 bis av. Jean Capelle 69621 Villeurbanne CEDEX etienne.parizet@insa-lyon.fr
ED 483 ScSo	**ScSo**[1] https://edsciencessociales.universite-lyon.fr Sec. : Mélina FAVETON Tél : 04.78.69.77.79 melina.faveton@univ-lyon2.fr	**M. Bruno MILLY** (INSA : J.Y. TOUSSAINT) Univ. Lyon 2 Campus Berges du Rhône 18, quai Claude Bernard 69365 LYON CEDEX 07 Bureau BEL 319 bruno.milly@univ-lyon2.fr

[1] ScSo : Histoire, Géographie, Aménagement, Urbanisme, Archéologie, Science politique, Sociologie, Anthropologie

Thèse accessible à l'adresse : https://theses.insa-lyon.fr/publication/2024ISAL0088/these.pdf © [C.K. Miyazaki], [2024], INSA Lyon, tous droits réservés

Acknowledgements

I undertook the challenge of pursuing a PhD with the intention of enhancing my professional capabilities, expanding my scientific knowledge, and, if only to a modest extent, contributing the advancement of research. At the conclusion of the three-year period, it is evident that the experience exceeded my expectations and I am profoundly grateful for the opportunity. The demanding journey, which involved overcoming numerous challenges, has resulted in personal and professional growth. I was privileged to learn from leading researchers in a large research infrastructure, which allowed me to contribute, even on a small scale, to the advancement of wastewater treatment system research. I must acknowledge the invaluable support of several individuals who played a pivotal role in my success:

To my advisors Pascal Molle, Jaime Nivala, Ania Morvannou and Laura Delgado-Gonzales for their guidance and support throughout the duration of this process. Their advice and mentorship have been invaluable, and I am deeply appreciative of their willingness to dedicate their time to teaching me. I am honored to have had the opportunity to learn from such esteemed specialists in my field.

To the jury who have accepted to participate in my PhD defense. Your valuable comments and remarks will undoubtedly enhance the quality of this research. I would also like to thank Mathieu Sperandio and Jérôme Harmand for their contributions during my PhD Steering Committee. Your feedback throughout the years have been helpful in shaping the structure of my research.

To Office Français de la Biodiversité, Rhône–Méditerranée–Corse and Adour-Garrone water agencies as well as EUR H2O'Lyon for its financial support of the TONIC research project. The quality of this research project would not have been possible without their support.

To the whole REVERSAAL unit for the collaboration during these years, we had rich discussions and shared special convivial moments together. Most of all, I had an immense support to be able to conduct my experiments (thanks to Olivier, Jérémie, Gael, Arnold, Rémi Clément). Special thanks for Jean Marc Choubert for guiding the research unit and always supporting my research; to Olivier Garcia for helping and teaching me all these years the best practice on the field, he knows more than anyone does how hard and tiring it was being there when everything went wrong. I am sure my research would not go further without him.

To Arthur Fendrich, for the endless support and love. I would had giving up without you, thank you for being my rock when I needed. I never felt alone in this path, you gave me not only emotional support, but also wise advices, always wishing the best for me.

To my family, Ester, Celso, Caio, Chris, for inspiring and encouraging me to perform to the best of my abilities. Despite the physical distance between us, your words of encouragement and support have been fundamental in driving me forward. I will forever grateful for the amazing family I have. I could not forget to acknowledge Eunice, Lais, Leila, Andre, Oswaldo, Kiyomi, Paulinho, Erica and Vitor and my special friends from Brazil, France and others that are all over the world, always cheering me up, giving hopeful words and reason to laugh and light down the stressful moments.

Thèse accessible à l'adresse : https://theses.insa-lyon.fr/publication/2024ISAL0088/these.pdf © [C.K. Miyazaki], [2024], INSA Lyon, tous droits réservés

Contents

List of publications and communications **11**

List of figures **16**

List of tables **19**

1 General introduction **21**

2 Literature review **25**
2.1 Blue-green infrastructure and nature based-solutions for wastewater treatment 25
2.2 Treatment wetland 26
2.3 Aerated treatment wetland 29
2.4 Rhizosph'air® 32
2.5 Oxygen transfer in aerated wetlands 34
2.6 Nitrogen dynamics in treatment wetland 37
2.7 Research questions and thesis outline 42

3 Hydraulic characterization of a hybrid aerated vertical and horizontal treatment wetland **45**
3.1 Introduction 47
3.2 Material and methods 48
3.2.1 Pilot system description 48
3.2.2 Impact of aeration strategies: tracer test 50
3.2.3 Full-scale system 53
3.2.4 Limitations 53
3.3 Results and discussion 55
3.3.1 Tracer response curves (pilot scale) 55
3.3.2 Modelling outlet tracer curve 58
3.3.3 Internal tracer measurement 61
3.3.4 Comparison between pilot versus full-scale 64
3.4 Conclusions and perspectives 66
3.5 Learnings 66

4 Aeration strategies and total nitrogen removal in a hybrid aerated treatment wetland **69**
4.1 Introduction 71

Thèse accessible à l'adresse : https://theses.insa-lyon.fr/publication/2024ISAL0088/these.pdf © [C.K. Miyazaki], [2024], INSA Lyon, tous droits réservés

4.2 Material and methods . . . 72
4.2.1 Treatment wetland pilot . . . 72
4.2.2 Pilot operation and experimental conditions . . . 73
4.2.3 Pilot monitoring – chemical parameters . . . 75
4.3 Results and discussion . . . 77
4.3.1 Treatment performances and limitations: Timing aeration strategy . 77
4.3.2 Treatment performance and limitations: Aeration strategy according to batch feeding periods . . . 82
4.4 Conclusion . . . 85
4.5 Learnings . . . 86

5 Optimization of total nitrogen removal in a hybrid aerated vertical and horizontal treatment wetland 89
5.1 Introduction . . . 91
5.2 Material and methods . . . 93
5.2.1 Treatment wetland pilot . . . 93
5.2.2 Optimizing total nitrogen removal . . . 94
5.2.3 Controlling total nitrogen removal with online sensors . . . 98
5.3 Results and discussion . . . 101
5.3.1 Optimizing total nitrogen removal . . . 101
5.3.2 Exploratory control of total nitrogen removal with online sensors . . 108
5.4 Conclusions and perspectives . . . 112
5.5 Learnings . . . 113

6 Conclusion and perspectives 115
6.1 General conclusion . . . 115
6.2 Perspectives . . . 117
6.2.1 Electrical resistivity tomography . . . 118
6.2.2 Biological activity . . . 119
6.2.3 Biokinetics model . . . 120
6.2.4 Aeration control through models . . . 120

References 123

7 Appendix 143
7.1 Hydraulic characterization of a hybrid aerated vertical and horizontal treatment wetland . . . 143
7.2 Aeration strategies and total nitrogen removal in a hybrid aerated treatment wetland . . . 147
7.3 Optimization of total nitrogen removal in a hybrid aerated vertical and horizontal treatment wetland . . . 158
7.4 Methodology for hydraulic characterization based on ERT . . . 163
7.4.1 Introduction . . . 163
7.4.2 Methodology . . . 164
7.4.3 Results . . . 166
7.4.4 Conclusions . . . 167
7.5 Methodology for nitrogen kinetics . . . 168

Thèse accessible à l'adresse : https://theses.insa-lyon.fr/publication/2024ISAL0088/these.pdf © [C.K. Miyazaki], [2024], INSA Lyon, tous droits réservés

Abstract

Passive treatment wetlands (TWs) have limited capacity to treat total nitrogen. Consequently, TW research has concentrated efforts on exploring various designs and configurations to optimize these systems and enhance their performance. One of the most innovative developments is the Rhizosph'air® system, which combines a first-stage French vertical flow (VF) TW with an aerated horizontal flow (HF) TW. This work focused on this system, with the objective of optimizing total nitrogen removal by studying hydraulic behavior and different aeration strategies. All the experiments were conducted on a pilot scale with a surface area of 20 m^2 (approximately 26 PE) in Craponne, France.

The first objective was to assess the influence of aeration strategies on the hydraulic behavior of the pilot. This study made notable contributions in two key areas. Firstly, it evaluated the hydraulic response in the middle and at the outlet of the pilot to different aeration strategies. Secondly, it validated the possibility of upscaling the results to a higher-capacity system. Internal measurements revealed flow heterogeneity, with some paths exhibiting higher flow velocities than others, indicating the presence of preferential pathways. The primary filter is directly affected by the water distribution on the surface and the different flow directions (vertical and horizontal). Therefore, it plays an important role in the overall hydraulic performance. Increasing the aeration time helps to reduce preferential pathways by improving the mixing process. The results indicated that the total duration of aeration on the primary filter should be longer than that on the secondary filter. In order to achieve optimal hydraulic performance, a minimum of six hours of aeration per day on the secondary filter. Finally, the results obtained in the pilot system were applicable and representative of what could occur in hydraulics at larger scales. The HRT was 39.1 hours for the pilot system and 41.4 hours for the full-scale system, while the NTIS values were 5.4 and 4.1, respectively.

The second objective of this PhD thesis was to evaluate the impact of different experimental conditions on total nitrogen removal. The experimental conditions included variations in inlet ammonium concentration, duration of aeration, setting the time of aeration, synchronizing the aeration with the inflow, and different hydraulic loading rates. The results indicated that total nitrogen removal was limited when the aeration was based on time (time slot control). In this strategy, the optimal experimental condition was the one in which both the hydraulic loading rate (from 0.15 m/d to 0.35 m/d) and the ammonium loading rate (from 8 g NH_4-N/m^2/d to 24 g NH_4-N/m^2/d) increased. The outcome saw a significant improvement, with TN removal increasing from 47% to 71%. The denitrification process was limited due the lack of carbon with 17.6 ± 4.9 mg NO_3-N/L at the outlet. By transitioning from a time-based to a inflow-based aeration strategy, the system was able to provide the necessary aerobic and anoxic durations for nitrification

Thèse accessible à l'adresse : https://theses.insa-lyon.fr/publication/2024ISAL0088/these.pdf © [C.K. Miyazaki], [2024], INSA Lyon, tous droits réservés

and denitrification, occurring at optimal times, resulting in a better denitrification with 8.70 ± 4.40 mg NO_3-N/L at the outlet.

The final objective was to test another aeration strategy better suited to optimize TN removal, to assess its limitations, and to explore rules for controlling the aeration system. With the new aeration strategy based on the inflow, the system demonstrated superior performance than result experiments on Chapter 3, with 81% TN removal and 13.7 ± 6.4 mg TN/L at the outlet, when the organic loadings were comparable to those observed in small communities. Such aeration strategy, based on the inflow, has the potential to be an effective solution for optimizing the removal of TN with normal organic loadings at the inlet. Moreover, when the system was submitted to high inlet ammonium concentrations ($>$ 100 mg NH_4-N/L), the performance achieved 83% TN removal rate and an average concentration of 27.2 ± 12.0 mg TN/L at the outlet. In this case, the strategy was unable to achieve very low TN concentrations, i.e., reducing the TN concentration to below 15 mg/L due to limitations in the nitrification process. Additional oxygenation in the system proved necessary to meet the desired specification. The results of the N-k-C* model applied to TKN and TN indicated that it is not accurate enough and may not be suitable for design purposes to meet strict compliance criteria ($<$15mg TN/L). The feasibility of using a bending-points strategy to automate this system was assessed using the DO and Eh sensors' signal and identifying a correlation between inflection points and the end of nitrification or denitrification. This strategy may present some challenges due to the low frequency of occurrences of these bending points, as well as inconsistencies in their occurrence and NH_4-N and NO_3-N concentrations during the bending points. Finally, the feasibility of using linear predictive models to predict the system outlet was investigated. However, the values provided by the online sensors showed non-linear relationships, which made this approach unsuitable.

Thèse accessible à l'adresse : https://theses.insa-lyon.fr/publication/2024ISAL0088/these.pdf © [C.K. Miyazaki], [2024], INSA Lyon, tous droits réservés

Résumé

Les filtres plantés de roseaux (FPR) passifs (sans apport d'énergie) ont une capacité limitée à traiter l'azote global (NGL). C'est la raison pour laquelle la recherche sur les FPR a concentré ses efforts sur l'exploration de diverses conceptions et configurations, visant à optimiser ces systèmes et à en améliorer les performances. L'un des développements les plus innovants est le systèmeRhizosph'air® qui combine un FPR à écoulement vertical (premier étage) avec un FPR à écoulement horizontal aéré. Cette thèse s'est concentrée sur ce système particulier, avec pour objectif d'optimiser l'élimination du NGL par l'étude de son comportement hydraulique et de différentes stratégies d'aération. Toutes les expériences sur le terrain ont été menées à l'échelle d'un pilote de 20 m^2 (environ 26 EH) à Craponne, en France.

Le premier objectif était d'évaluer l'influence de différentes stratégies d'aération sur le comportement hydraulique du pilote. Cette étude a apporté des contributions notables dans deux domaines clés. Tout d'abord, elle a évalué la réponse hydraulique au milieu et à la sortie du pilote en fonction des différentes stratégies d'aération. Deuxièmement, elle a validé la possibilité d'extrapoler les résultats à des capacités plus importantes. Les mesures internes ont révélé une hétérogénéité des écoulements, certains chemins présentant des vitesses d'écoulement plus élevées que d'autres, ce qui indique la présence de voies préférentielles. Le filtre primaire est directement affecté par la distribution de l'eau à la surface et par les différentes directions d'écoulement (verticale et horizontale). Il joue donc un rôle important dans la performance hydraulique globale. L'augmentation de la durée d'aération contribue à réduire les voies préférentielles en améliorant le processus de mélange. Les résultats indiquent que la durée totale de l'aération sur le filtre primaire devrait être plus longue que sur le filtre secondaire. Afin d'atteindre des performances hydrauliques optimales, un minimum de six heures d'aération par jour devrait être attribué dans le filtre primaire. Enfin, les résultats obtenus dans le pilote sont applicables et représentatifs de ce qui pourrait se produire en hydraulique à plus grande échelle. Le temps de séjour hydraulique était de 39,1 heures pour le pilote et de 41,4 heures pour le système à grande échelle, tandis que les valeurs NTIS étaient respectivement de 5,4 et 4,1.

Le deuxième objectif de cette thèse de doctorat était d'évaluer l'impact de la variation des conditions expérimentales sur l'élimination du NGL. Les conditions expérimentales comprenaient des variations dans la concentration en ammonium en entrée, la durée de l'aération, le réglage de la durée de l'aération, la synchronisation de l'aération avec le débit entrant, les différentes charges hydrauliques. Les résultats ont indiqué que l'élimination du NGL pouvait être limité lorsque l'aération était appliquée sur une base temporelle (asservissement sur tranche horaire). Dans cette stratégie, la condition expérimentale optimale était celle dans laquelle le taux de charge hydraulique (de 0,15 m/j à 0,35 m/j)

Thèse accessible à l'adresse : https://theses.insa-lyon.fr/publication/2024ISAL0088/these.pdf © [C.K. Miyazaki], [2024], INSA Lyon, tous droits réservés

et le taux de charge en ammonium (de 8 g NH_4-N/m^2/j à 24 g NH_4-N/m^2/j) étaient les plus élevés; L'élimination de l'azote global passant de 47 % à 71 %. Le processus de dénitrification a été limité par le manque de carbone avec 17,6 ± 4,9 mg NO_3-N/L à la sortie. En passant d'une stratégie d'aération basée sur le temps à une stratégie d'aération basée sur le débit, le système a pu fournir les durées aérobies et anoxiques nécessaires à la nitrification et à la dénitrification, à des moments optimaux, ce qui a entraîné une meilleure dénitrification avec 8,70 ± 4,40 mg NO_3-N/L à la sortie.

L'objectif final était de tester une stratégie d'aération pour optimiser l'élimination du NGL, d'évaluer ses limites et d'explorer les règles de contrôle du système d'aération. Avec les nouveaux paramètres, le système a démontré une performance supérieure que les expériences de résultats du Chapitre 4, avec 81 % d'élimination du NGL et 13.7 ± 6.4 mg NGL/L à la sortie, lorsque les charges organiques appliquées étaient comparables à celles mesurées dans les petites collectivités. Cette stratégie d'aération, basée sur le débit, a le potentiel de devenir une solution efficace pour optimiser l'élimination du NGL. De plus, lorsque le système a été soumis à des concentrations élevées d'ammonium en entrée (> 100 mg NH_4-N/L), les performances ont atteint 83% d'élimination du NGL et une concentration moyenne de 27.2 ± 12.0 mgNGL/L à la sortie. Dans ce cas, la stratégie n'a pas permis d'atteindre des concentrations très basses, à savoir la réduction de la concentration en NGL en dessous de 15 mg/L, en raison des limites du processus de nitrification. Une oxygénation supplémentaire du système était nécessaire pour atteindre la concentration souhaitée en sortie. Les résultats du modèle N-k-C* appliqué à l'azote Kjeldahl et au NGL indiquent qu'il n'est pas suffisament précis et ne peut pas convenir à des fins de dimensionnement pour répondre à des critères de conformité stricts (<15mg NGL/L). La faisabilité de l'utilisation des points d'inflexion pour automatiser ce système a été évaluée en utilisant le signal des capteurs DO et Eh et en identifiant une corrélation entre les points d'inflexion et la fin de la nitrification ou de la dénitrification. Cette stratégie peut présenter quelques difficultés en raison de la faible occurrence de ces points d'inflexion, ainsi que des incohérences entre leurs occurrences et les concentrations de NH_4-N et de NO_3-N mesurées au moment des points d'inflexion. Enfin, la faisabilité de l'utilisation de modèles prédictifs linéaires pour prédire la sortie du système a été étudiée. Cependant, les valeurs fournies par les capteurs en ligne présentaient des relations non linéaires, ce qui rendait cette approche inadaptée.

Thèse accessible à l'adresse : https://theses.insa-lyon.fr/publication/2024ISAL0088/these.pdf © [C.K. Miyazaki], [2024], INSA Lyon, tous droits réservés

List of publications and communications

Publications:

- Miyazaki, C.K., Morvannou, A., Higelin, E., Nivala, J., Molle, P., 2023. Aeration strategies and total nitrogen removal in a hybrid aerated treatment wetland. Blue-Green Systems 5, 321–335. https://doi.org/10.2166/bgs.2023.045
- Miyazaki, C.K., Morvannou, A., Petitjean, A., Nivala, J., Molle, P., 2024. Hydraulic characterization of a hybrid aerated vertical and horizontal treatment wetland. Ecological engineering, 206, 107301. https://doi.org/10.1016/j.ecoleng.2024.107301

International Conferences:

- Miyazaki, C.K., Delgado-Gonzalez, L., Morvannou, A., Molle, P. 2022. Hydraulic characterization in a hybrid vertical/horizontal treatment wetland with forced aeration. IWA 17th International Conference on Wetland Systems for Water Pollution Control. Lyon, France. (Poster presentation)
- Miyazaki, C.K., Nivala, J., Morvannou, A., Clément, R., Molle, P. 2023. Hydraulic characterization in a hybrid vertical/horizontal treatment wetland with forced aeration. WETPOL. Bruges, Belgium. (Oral presentation)
- Miyazaki, C.K., Morvannou, A., Petitjean, A., Nivala, J., Molle, P. 2024. Optimization of total nitrogen removal in a hybrid aerated treatment wetland. IWA 18th International Conference on Wetland Systems for Water Pollution Control. Martinique, France. (Oral presentation)
- Silveira, D.D., Miyazaki, C.K., Sorgato, A.C., Lapolli, F.R., Morvannou, A., Kela, P., Nivala, J., Molle, P. 2024. Microbial insights in a hybrid aerated treatment wetland for total nitrogen removal. IWA 18th Conference on Wetland Systems for Water Pollution Control. Martinique, France. (Oral presentation)
- Kisielius, V., Miyazaki, C.K., Morvannou, A., Nivala, J., Molle, P., Carvalho, P.N. 2024. A hybrid aerated treatment wetland for removal of water contaminants and micropollutants. IWA 18th Conference on Wetland Systems for Water Pollution Control. Martinique, France. (Oral presentation)

Thèse accessible à l'adresse : https://theses.insa-lyon.fr/publication/2024ISAL0088/these.pdf © [C.K. Miyazaki], [2024], INSA Lyon, tous droits réservés

Thèse accessible à l'adresse : https://theses.insa-lyon.fr/publication/2024ISAL0088/these.pdf © [C.K. Miyazaki], [2024], INSA Lyon, tous droits réservés

List of Figures

2.1 Overview schematics of TWs. Top left: horizontal flow; top right: vertical flow; bottom left: French vertical flow, first stage; bottom right: French vertical flow, second stage. Source; Dotro et al. (2017) 27
2.2 Removal effects of ammonia in TW with/without aeration. Source: Zhuang et al., 2019 31
2.3 Scheme of the Rhizosph'air® wastewater TW (schematic courtesy of Ecobird). 34
2.4 Overview of nitrogen transformations in a hybrid TWs. Source: Adapted from Kadlec and Wallace (2009) and Hallin et al. (2018) 38
2.5 Research outlines for each chapter and the interaction between them. . . . 43

3.1 Representation of the hybrid aerated system and the location of each material. In this representation, the filter 1 is primary filter (fed) and filter 2 is secondary filter (rest). The filter 2 would be become primary filter after the alternation. Source: Adapted from **Chapter \ref {chap4}** 49
3.2 Aeration strategy for each experimental condition for the pilot system . . . 50
3.3 Conductivity meter installed inside the filter, at the inlet and outlet in a top view and transversal section A-A. 52
3.4 Normalized frequency over time for each aeration strategy 57
3.5 A (left) – Normalized frequency over time for overall result for each gamma distribution for tracer 0h. B (right) - Normalized frequency over time for each individual, unweighted, gamma that compose the final mixture distribution, which is the 3 gamma (tracer 0h). 61
3.6 Normalized frequency over time for 24h, 9h1, 9h2 and 6h aeration per day. The conductivity meters were placed according to Figure 3.3. CM stands for conductivity meter. 63
3.7 Normalized frequency over time for the pilot and full-scale with 6-hours of aeration per day 65

4.1 Hydraulic operating scheme of the hybrid aerated vertical/horizontal flow TW pilot 74
4.2 Parameters for each experimental condition. 76

Thèse accessible à l'adresse : https://theses.insa-lyon.fr/publication/2024ISAL0088/these.pdf © [C.K. Miyazaki], [2024], INSA Lyon, tous droits réservés

4.3 Position and type of sensor at the inlet, inside and outlet of the pilot, and location of the 24-hour composite sampling. The sensors were strategically placed to have a different vertical and horizontal profile and to have a view of the processes taking place in each filter and in half of the pathway. . . . 77

4.4 Applied and treated loads for NH_4-N (A) and TN (B), for experimental conditions C1 (T-9h-0.15), C2 (T-3h-0.15), C3 (T-3h-0.25), C4 (T-3h-0.35) and C5 (T-3h-0.35-NH_4) 78

4.5 Duration in hours per day of aerobic condition (> 0.2 mg O2/L) and anoxic condition (< 0.2 mg O2/L) for the experimental conditions employing the time-based aeration strategy. A single oxygen sensor is exhibited for a period of one month. The red dash lines represent the filter alternation, PF stands for primary filter and SF for secondary filter 80

4.6 Applied and treated loads for NH_4-N and TN, for experimental conditions C1 (T-9h-0.15), C2 (T-3h-0.15), C3 (T-3h-0.25), C4 (T-3h-0.35), C5 (T-3h-0.35-NH_4), C6 (F-3.3h-1.7h-0.35-NH_4) and C7 (F-2.5h-0h-0.35-NH_4) 83

4.7 Duration in hours per day of aerobic condition (> 0.2 mg O2/L) and anoxic condition (< 0.2 mg O2/L) for the experimental conditions employing aeration strategy based on batch time. A single oxygen sensor is exhibited for a period of one month. PF = Primary filter and SF = secondary filter . 84

4.8 DO concentration during 24 hours for multiple days for the condition C7 (F-2.5h-0h-0.35-NH_4). A single oxygen sensor is exhibited, located at vertical 1 (84cm depth). Dash black lines represent the batches sent to the primary filter 85

5.1 Position and type of sensors at the inlet, inside and outlet of the pilot, and location of the 24-hour composite sampling and for the bending-points validation. In this scheme, primary filter is on the left side and secondary filter is on the right side. 94

5.2 Aeration strategy for the current study. 96

5.3 Aeration strategies applied for the bending-points validation experiments. EC = experimental conditions. 100

Thèse accessible à l'adresse : https://theses.insa-lyon.fr/publication/2024ISAL0088/these.pdf © [C.K. Miyazaki], [2024], INSA Lyon, tous droits réservés

5.4 Principal component analysis showing the relationship between TN removal and other variables. The points represent the TN removal. TN_rem = TN removal, Water_temp = Water temperature, BOD_TKN = BOD_5inlet concentration / TKN inlet concentration, Anoxic_PR = Anoxic duration (< 0.2 mg O_2/L) in a day on the primary filter, Aerobic_PR = Aerobic (> 0.2 mg O_2/L) duration in a day on the primary filter, Anoxic_SC = Anoxic duration (< 0.2 mg O_2/L) in a day on the secondary filter, Aerobic_SC = Aerobic duration (> 0.2 mg O_2/L) in a day on the secondary filter, NH_4_out = NH_4-N concentration at the outlet, NO_3_out = NO_3-N concentration at the outlet, group 1 = normal organic loading, group 2 = high organic loading, group 3 = winter time. 102

5.5 Comparison between experimental and predicted values for NTK and TN concentrations at the outlet. The model accuracy was pointed out as R^2 and RMSE. 106

5.6 Trend curves for each online sensor considering only periods where the organic loading was < 100 NH_4-N/L and < 1200 mg COD/L. Black line represent the mean concentration, the grey region the 95% confidence interval, blue dashed line the batch hour, red region the aeration period. NH_4 middle, NO_x middle, Eh middle, O2 F1, Eh F1 and pH F1 were place in filter 1 and they are playing the primary filter. O2 F2 and Eh F2 were place in filter 2 and they are as secondary filter. 107

5.7 A. DO concentration versus ammonium concentration for the primary filter, the red dashed line represents the "DO elbow". B. Eh measurement versus ammonium concentration for the primary filter, the red dashed line represents the "ORP plateau". C. Eh measurement versus nitrate concentration for the secondary filter, the red dashed line represents the "Nitrate knee". 109

5.8 Pearson correlation matrix (upper-right), density function and histograms (diagonal), and scatter plot (lower-left) for the sensor. Statistical significance of rank correlations: dot means $p < 0.1$, *** means $p < 0.001$, ** means $p < 0.01$,* means $p < 0.05$. In the diagonal, the red curve represents the kernel density estimates, and below the diagonal, the red line represents the association between variables. 111

7.1 Concentration in amino-G acid (mg/L) at the pilot outlet over time for each aeration strategy. 144

7.2 Comparison between different fitting methodologies for each tracer test. . . 144

7.3 Comparison between amino-G acid and salt for the 24h tracer test. 145

7.4 Comparison between amino-G acid and salt for the 9h1 tracer test. 145

Thèse accessible à l'adresse : https://theses.insa-lyon.fr/publication/2024ISAL0088/these.pdf © [C.K. Miyazaki], [2024], INSA Lyon, tous droits réservés

7.5 Comparison between amino-G acid and salt for the 9h2 tracer test. 145
7.6 Comparison between amino-G acid and salt for the 6h tracer test. 146
7.7 Comparison between amino-G acid and salt for the 0h tracer test. 146
7.8 Inlet salt concentrations for each tracer test. 146
7.9 Inlet, outlet concentrations and concentration removal for the seven experimental condition tested, considering COD, fCOD and TSS. 150
7.10 Inlet, outlet concentrations and concentration percent removal for the seven experimental conditions tested, considering NH_4-N, NO_3-N and TN. 151
7.11 Dissolved oxygen concentrations measured at different pilot depths for the seven experimental conditions tested. Depths are indicated from the bottom of the pilot 151
7.12 Bending points strategy for aerobic and anoxic phase. Source: Jaramillo et al. (2018) 158
7.13 Matrix of correlation result (all variables) 158
7.14 Scree plot for PCA analysis using the dataset 159
7.15 Contribution of each variable to PC1. 159
7.16 Contribution of each variable to PC2. 160
7.17 Left side – Applied load versus treated load for NH_4-N and TN. Right side - Inlet and outlet concentrations for COD, NH_4-N and TN. The TN concentration removal on the right y-axis represent the values in percentage. 160
7.18 Curves characteristics for each online sensor considering only periods where the organic loadings were $>$ 100 mg NH_4-N/L and $>$ 1200 mg COD/L. Black line represent the mean concentration, the grey region the 95% confidence interval, blue dashed line the batch hour, red region the aeration period. . 161
7.19 Eh and DO curve patterns for primary and secondary filters. Black dashed lines represent the batch hour and the blue region the aeration period. . . 161
7.20 A. Eh measurement versus nitrate concentration for the primary filter, the red dashed line represents the “Nitrate knee”. B. Eh measurement versus nitrate concentration for the primary filter, the red dashed line represents the “Nitrate knee”. C. DO concentration versus ammonium concentration for the secondary filter, the red dashed line represents the “DO elbow”. . . 162
7.21 Methodology for ERT data treatment 165
7.22 Validation for the ERT data 166
7.23 ERT results from the study case in a y-axis slice. A = minimum ratio (%), B = minimum ratio (%) at the back and minimum time from 56 to 130 time-step, C = minimum ratio (%) at the back and minimum time from 130 to 200 time-step 167
7.24 Sampling location and the sensors used for the kinetic experiment. 168

Thèse accessible à l'adresse : https://theses.insa-lyon.fr/publication/2024ISAL0088/these.pdf © [C.K. Miyazaki], [2024], INSA Lyon, tous droits réservés

List of Tables

1.1 Minimum treatment performance for the parameters COD, BOD_5, and TSS according to legal requirements, and recommended maximum requirements based on EPNAC (2015) 23

2.1 Removal efficiencies and treatment area required for each type of wetland. HF = horizontal flow, VF= vertical flow. Source: Dotro et al. (2017). . . . 28

2.2 Removal efficiencies and treatment area required for each type of hybrid TW (Vymazal, 2013) 29

3.1 Operational parameters for each aeration strategy at the pilot system. PR= primary filter, SC = secondary filter, NB = number of cycles per day, Operation = aeration ON (h per cycle), Stop = aeration OFF (h per cycle), HLR = hydraulic loading rate (m/d 51

3.2 Operational parameters for the pilot and full-scale systems. NB = number of cycles per day, Operation = aeration ON (h per cycle), Stop = aeration OFF (h per cycle), HLR = hydraulic loading rate (m/d 54

3.3 Results for each experimental condition. $_{t}$HRT = theoretical HRT; $T_{initial}$ = the moment when the tracer was initially detected at the outlet; T_{median} = the duration required for 50% of the measured tracer mass reach the outlet; T_{mode} = time for reaching tracer concentration peak; T_{90}/T_{10} = Morrill dispersion index (T_{90} and T_{10} are the dimensionless times taken when the first 10% and 90% of the tracer reaches the outlet) 56

3.4 Results for gamma fitting model for each aeration strategy. t = theoretical; e_v = volumetric efficiency; WD = weighted distribution; σ^2 = variance $\left(\int_0^\infty (time - HRT)^2 f(t)dt\right)$; σ_θ^2 = normalized variance $\left(\frac{\sigma^2}{HRT^2}\right)$. When appropriate, values are reported with the corresponding distribution (e.g., #1 referring to the first gamma distribution). *The weighted HRT was calculated by computing numerically the first moment of the gamma mixture. The weighted NTIS is the individual NTIS multiplied by their corresponding flow fractions. 59

Thèse accessible à l'adresse : https://theses.insa-lyon.fr/publication/2024ISAL0088/these.pdf © [C.K. Miyazaki], [2024], INSA Lyon, tous droits réservés

3.5 Results for the salt tracer tests. $T_{initial}$ = time of the first detection of the tracer at the outlet; T_{median} = Time for exiting of 50% of measured tracer mass in the effluent; T_{mode} = time for reaching tracer concentration peak T_{90} = Time for exiting of 90% of measured tracer mass in the effluent . . . 62
3.6 Results for the pilot and full-scale 64

4.1 Experimental conditions parameters. T= time, F = feeding, PR = primary filter, SF = secondary filter, NB = number of cycles per day, Operation = aeration ON (min per cycle), Stop = aeration OFF (min per cycle), HLR = hydraulic loading rate (m/d) 75
4.2 Inlet, outlet concentrations and concentration removal for each condition, considering temperature inside the filter, COD, TSS, TN, NH_4-N and NO_3-N, where Avg = average, Std dev = standard deviation and n= number of observations 79
4.3 Inlet, outlet concentrations and concentration removal s for each condition, considering temperature inside the filter, COD, TSS, TN, NH_4-N and NO_3-N, where Avg = average, Std dev = standard deviation and n= number of observations 82

5.1 Inlet, outlet concentrations and concentration removal for normal and high organic loads, for COD, TSS, TN, NH_4-N and NO_3-N. Avg = average and Std dev = standard deviation. 103
5.2 First-order reaction using the N-k-C^* model approach, based on input and output average concentration for each month, as well as the main model assumptions. C^* stands for background concentration in mg/L. 105
5.3 Nitrogen form concentrations at D0 and Eh inflexion points ("DO elbow", "ORP plateau", "Nitrate knee"). PR = primary filter, SC = secondary filter, - = no bending-points found. 110

7.1 Weather condition and water height for the different tracer experiments . . 143
7.2 Values used for calibration the amino-G acid 143
7.3 Parametric coefficients: COD 147
7.4 Parametric coefficients: fCOD 147
7.5 Parametric coefficients: TSS 147
7.6 Parametric coefficients: NH_4-N 147
7.7 Parametric coefficients: TN 148
7.8 Inlet, outlet concentrations and concentration removal for each condition, considering temperature inside the COD,fCOD, TSS, TN, NH_4-N, NO_3-N,NO_2-N, PO_4-P,HCO_3-,where Avg = average, Std dev = standard deviation and n= number of observations 149

Thèse accessible à l'adresse : https://theses.insa-lyon.fr/publication/2024ISAL0088/these.pdf © [C.K. Miyazaki], [2024], INSA Lyon, tous droits réservés

7.9 Analysis of the lack of organic carbon for C1: T-9h-0.15 152
7.10 Analysis of the lack of organic carbon for C2: T-3h-0.15 152
7.11 Analysis of the lack of organic carbon for C3: T-3h-0.25 152
7.12 Analysis of the lack of organic carbon for C4: T-3h-0.35 153
7.13 Analysis of the lack of organic carbon for C5: T-3h-0.35-NH_4 153
7.14 Analysis of the lack of organic carbon for C6: F-3.3h-1.7h-0.35-NH_4 153
7.15 Analysis of the lack of organic carbon for C7: F-2.5h-0h-0.35-NH_4 154
7.16 Weather condition - Part 1 155
7.17 Weather condition - Part 2 156
7.18 Weather condition - Part 3 157

Thèse accessible à l'adresse : https://theses.insa-lyon.fr/publication/2024ISAL0088/these.pdf © [C.K. Miyazaki], [2024], INSA Lyon, tous droits réservés

Thèse accessible à l'adresse : https://theses.insa-lyon.fr/publication/2024ISAL0088/these.pdf © [C.K. Miyazaki], [2024], INSA Lyon, tous droits réservés

Chapter 1

General introduction

Water pollution is a global problem and represents a significant and current challenge. The main source of degradation and pressure on freshwater ecosystems is human activities. A recent study has highlighted the issue of chemical contamination in 13,000 European river bodies, which is attributable to urban wastewater treatment plants (European Environment Agency et al., 2018). Discharging wastewater from households, industry, and commerce introduces various environmental pollutants in water bodies. These contaminants compromise the water quality, impact public health, undermine socioeconomic growth, and impact global biodiversity (du Plessis, 2022). Consequently, this deterioration contributes to the scarcity and stress of water resources, further accentuating the magnitude of water pollution.

The presence of nutrients, mainly nitrogen and phosphorus, in wastewater effluent contributes significantly to the deterioration of water quality. The overabundance of these compounds stimulates the growth of algae, a phenomenon referred to as eutrophication. This widespread occurrence is one of the main causes of deterioration in freshwater and coastal marine ecosystems globally (Chislock et al., 2013). Algal blooms exert multiple impacts on ecosystem dynamics, profoundly affecting biodiversity. These blooms create unfavorable conditions for aquatic organisms by impeding sunlight penetration. Some species of algae produce potent toxins that pose a threat to human and fish lives. Once dead, algae decompose, depleting dissolved oxygen concentrations and rendering the environment anoxic or anaerobic. Consequently, the effects of eutrophication go beyond the deterioration of water quality, encompassing the loss of biodiversity and the disruption of natural ecological balances.

To avoid this unfortunate outcome, legislation requires appropriate treatment measures before wastewater is discharged into water bodies. The European water policy has established Directives to protect the environment, stipulating distinct threshold values based on the scale of the wastewater treatment facility and the sensitivity of the discharge

Thèse accessible à l'adresse : https://theses.insa-lyon.fr/publication/2024ISAL0088/these.pdf © [C.K. Miyazaki], [2024], INSA Lyon, tous droits réservés

area (Council Directive of the European Communities, 1991). In the French context, the current decree published on July 31, 2020, aligns with the European Directive. The treatment requirement will depend on the receiving loads (i.e., more or less than 120 kg BOD_5/d or 2,000 person equivalent [PE]), and the decree defines the maximum effluent concentration and the minimum concentration to be removed for COD, BOD_5, and TSS (Table 1.1).

In regard to nitrogen, there is no requirement for nutrient removal for loads less than 600 kg BOD_5/d (10,000 PE). The regulation begins with larger systems, defined as treatment capacities between 600 kg BOD_5/d and 6000 kg BOD_5/d (100,000 PE), and applies only to plants discharging into eutrophication-sensitive areas. It should be noted that some local regulators have set more stringent requirements, particularly for treatment systems with lower capacities. In light of these considerations, indicative values of the maximum performance achievable were proposed for each agglomeration (EPNAC, 2015). For capacities below 2,000 PE, the recommendation sets a maximum requirement of 10 mg NH_4-N/L and 15 mg NTK/L. For capacities between 2,000 and 5,000 PE, the recommendations become more stringent, with a maximum of 8 mg NH_4-N/L, 10 mg NTK/L, 5 mg NO_3-N/L, and 15 mg NTK/L. For systems with a capacity of 5,000 PE and 10,000 PE, the recommendation is to increase nitrogen removal to reach 5 mg NH_4-N/L, 8 mg NTK/L, 5 mg NO_3-N/L, and 15 mg NTK/L.

Nature-based solutions (NbS) provide a promising approach to managing water pollution, particularly through treatment wetlands (TW). These systems are effective in decentralized sanitation, in the context of small communities up to 2,000 PE because they use natural components—such as vegetation, soil, and microorganisms—to remove contaminants, capable of meeting the legal requirements for COD, BOD_5, and TSS (Dotro et al., 2017). However, in areas with high sensitivity to nitrogen discharges, as well as regions with growing populations, environmental deterioration, and climate change pressure, other solutions are required. To address these requirements, system intensification through mechanized aeration has emerged as a promising solution, enabling high-rate treatment processes (Wallace et al., 2020). Aerated wetlands, in particular, have gained recognition for their effectiveness in treating ammonium up to 99% removal (Zhuang et al., 2019). They are suitable for communities with populations up to 10,000 PE (Nivala et al., 2014), making them cost-effective alternative to activated sludge and compact system that fits in context of decentralized system in urban areas.

The latest research indicates that switching from continuous to intermittent aeration can increase TN removal. This strategy allows the system to be more flexible, and studies are investigating the possibility of delivering nitrogen according to demand, either discharging it into rivers or reusing the effluent for non-potable use (Farouk et al., 2020). In the event that the system is situated in close proximity to a water body, it is necessary to

Thèse accessible à l'adresse : https://theses.insa-lyon.fr/publication/2024ISAL0088/these.pdf © [C.K. Miyazaki], [2024], INSA Lyon, tous droits réservés

Table 1.1: Minimum treatment performance for the parameters COD, BOD_5, and TSS according to legal requirements, and recommended maximum requirements based on EPNAC (2015)

Capacity	**Range**	**Minimum legal requirements**	**Recommended maximum requirements (EPNAC, 2015)**
<200 PE		COD: 200 mg/L or 60% BOD_5: 35 mg/L or 60% TSS: 50%	COD: 125 mg/L BOD_5: 25 mg/L TSS: 35 mg/L NH_4-N: 10 mg/L NTK: 15 mg/L
>200 and <2,000 PE		COD: 200 mg/L or 60% BOD_5: 35 mg/L or 60% TSS: 50%	COD: 90 mg/L BOD_5: 15 mg/L TSS: 20 mg/L NH_4-N: 10 mg/L NTK: 15 mg/L
>2,000 and <10,000 PE	>2,000 and <5,000 PE	COD: 125 mg/L or 80% BOD_5: 25 mg/L or 75% TSS: 35 mg/L or 90%	COD: 90 mg/L BOD_5: 15 mg/L TSS: 15 mg/L NH_4-N: 8 mg/L NTK: 10 mg/L NO_3-N: 5 mg/L TN: 15 mg/L
	>5,000 and <10,000 PE	COD: 125 mg/L or 80% BOD_5: 25 mg/L or 75% TSS: 35 mg/L or 90%	COD: 90 mg/L BOD_5: 15 mg/L TSS: 15 mg/L NH_4-N: 5 mg/L NTK: 8 mg/L NO_3-N: 5 mg/L TN: 15 mg/L

implement a TN removal process in order to facilitate the discharge of the effluent. In light of the current water scarcity crisis, cities are exploring alternative methods for water reuse. Wastewater effluents, rich in nutrients, have the potential to be repurposed for agricultural or landscape irrigation, representing a valuable source of water for these applications. In view of the aforementioned considerations and the potential for aeration control, it would be prudent to investigate treatment processes capable of producing water quality tailored to specific applications. To achieve these objectives from a technical standpoint, the system optimization process must place a high priority on gaining a comprehensive understanding of specific system processes, with a particular focus on hydrodynamics and mass transport (Regmi et al., 2018). This approach will ensure that aerated wetlands continue to meet evolving environmental standards and contribute to sustainable water management in small and medium-sized communities.

Thèse accessible à l'adresse : https://theses.insa-lyon.fr/publication/2024ISAL0088/these.pdf © [C.K. Miyazaki], [2024], INSA Lyon, tous droits réservés

This current PhD thesis is set in this broader global context and focuses on an aerated wetland that offers resilience and robustness for implementation in urban areas and operational flexibility to reuse the wastewater and promote water circularity. The following literature review will present the fundamental concepts, the most recent research, and the research gaps in this area. The following sections provide an overview of green infrastructures and nature-based solutions for wastewater treatment. They also present comprehensive information about treatment wetlands, aerated treatment wetlands, and a cutting-edge technology called Rhizosph'air®, which is the system studied in this PhD thesis. Subsequently, two specific topics are particularly targeted as part of the parameters of interest for this system: oxygen transfer in aerated treatment wetlands and nitrogen dynamics in treatment wetlands.

Thèse accessible à l'adresse : https://theses.insa-lyon.fr/publication/2024ISAL0088/these.pdf © [C.K. Miyazaki], [2024], INSA Lyon, tous droits réservés

Chapter 2

Literature review

2.1 Blue-green infrastructure and nature based-solutions for wastewater treatment

The combination of rapid urbanization, climate change, and increasing water scarcity is placing significant strain on city infrastructure. Urban areas must adapt in order to maintain pleasant living conditions. In light of these circumstances, urban water resources face significant constraints, prompting cities to integrate sustainable urban water management practices into their planning frameworks. One strategy to address these challenges is adopting nature-based solutions (NbS), which bridge the gap between biodiversity conservation and conventional engineering systems. By leveraging the inherent capabilities of natural ecosystems, NbS propose to integrate solutions to tackle societal challenges, e.g., water pollution, flood risk, drought, etc. This approach aims to create more resilient cities by transforming them into more efficient and sustainable resource-circular systems (Bozovic et al., 2017; Liquete et al., 2016; Oral et al., 2020).

The International Union created the term NbS for the Conservation of Nature (IUCN) in 2016 (IUCN, 2016) and encompasses a range of many existing technologies. The optimal integration of NbS into urban landscapes involves decentralizing systems and implementing smart wastewater collection methods to connect treated water with areas where water reuse is in demand, thereby promoting water circularity (Stefanakis, 2024). This approach enables water loops to be closed and reconnected, generating multiple co-benefits and employing a fit-for-purpose approach (Atanasova et al., 2021; Masi et al., 2018; Tsatsou et al., 2023). It also emphasizes control at source, where greener areas promote greater permeability in urban areas. In the context of wastewater management, the traditional treatment system approach is to be straightforward, replicable, and predictable (Eggermont et al., 2015), providing an "end-of-the-pipe" solution as opposed to a "process

Thèse accessible à l'adresse : https://theses.insa-lyon.fr/publication/2024ISAL0088/these.pdf © [C.K. Miyazaki], [2024], INSA Lyon, tous droits réservés

integrated" approach (Stefanakis, 2019). The NbS approach has gained popularity due to its greener technologies, which provide co-benefits and ecosystem services.

NbS represent an effective approach to water pollution control, particularly through the use of blue-green infrastructure (BGI) such as treatment wetlands (TW). These systems are well-suited for decentralized sanitation, as they integrate natural elements like plants, soil, and bacteria to remove pollutants from wastewater, including nitrogen compounds, thereby supporting sustainable water management.

2.2 Treatment wetland

TW are engineered systems that mimic natural wetlands to control water pollution. They are a well-established technology for wastewater treatment in small communities (with populations of less than 2,000 population equivalent, PE.) due to their robustness in the face of input variations, low operation and maintenance requirements, and the high water quality they provide (Morvannou et al., 2015). Among the variants, the main group consists of subsurface flow TW, either horizontal flow (HF) or vertical flow (VF), as illustrates Figure 2.1. The HF TW is a fully saturated reactor, in which the water flows horizontally below the surface through the pores of the media. Due to its configuration, there is limited oxygen mass transfer between the atmosphere and the water, resulting in a low concentration of dissolved oxygen in the water. This creates an anoxic/anaerobic environment. The system requires a primary treatment to remove the organic matter and to prevent clogging caused by high organic loads. It is then employed as a secondary or tertiary treatment to polish pollutants (Dotro et al., 2017; Vymazal, 2008).

Conversely, the classical VF TW is designed for use in unsaturated conditions, rather than in water-saturated environments. The wastewater is applied to the surface in intermittent batches, with a relatively high flow rate, in order to achieve uniform coverage across the surface area. Subsequently, the effluent percolates vertically through the sand media towards the bottom. The unsaturated zone allows the air to enter the pores , thereby increasing oxygenation and aerobic activity, which in turn facilitates the degradation of organic matter and oxidation of ammonium. As with the HF TW, the VF TW cannot treat organic matter directly from raw wastewater, so a preliminary treatment is required to reduce the organic loading.

The French VF TW was developed with the objective of transforming the classic VF TW system into a primary treatment, directly applying raw wastewater and integrating sludge management. The system comprises two stages, operating in series and with cells in parallel (Molle et al., 2005). The primary stage represents the main innovation, with a gravel media, and receives the entire organic load directly on the surface without needing a prior sedimentation tank. Some organic matter is retained on the surface, forming the

Thèse accessible à l'adresse : https://theses.insa-lyon.fr/publication/2024ISAL0088/these.pdf © [C.K. Miyazaki], [2024], INSA Lyon, tous droits réservés

organic deposit layer. One cell is fed in batches for 3.5 days, after which the cell enters a rest period, and another parallel cell is fed. These alternating phases allow for controlling the biomass growth attached to the media and the mineralization of the deposited layer on the surface, thus avoiding clogging problems (Molle et al., 2005). The effluent is then applied to the second stage, a classic VF TW, where it further treats dissolved water pollution, specifically to remove ammonium.

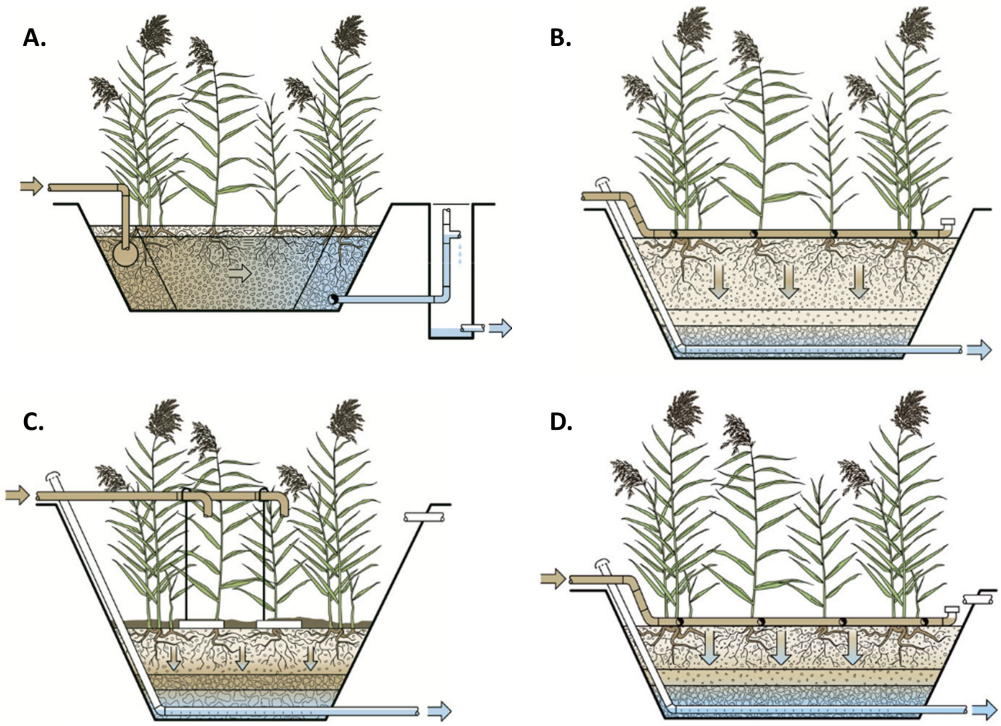

Figure 2.1: Overview schematics of TWs. Top left: horizontal flow; top right: vertical flow; bottom left: French vertical flow, first stage; bottom right: French vertical flow, second stage. Source; Dotro et al. (2017)

One significant advantage of these TWs is that they do not necessitate any external energy input when local context allows gravity feeding. The majority of the system can operate through gravitational force alone, and they do not require the use of air blowers or other high-intensity equipment to inject air. This results in reduced maintenance and operational costs. However, TW systems demand a large footprint (Dotro et al., 2017). According to Molle et al. (2005), the classic French two-stage VF TW requires 2 $m^2.PE^{-1}$ in temperate climate, while the HF TW requires 5 $m^2.PE^{-1}$. Wastewater treatment typically requires the use of a specific type of wetland, operating in a series configuration, with the total footprint determined by the selected design. As a result, numerous studies have determined that the high land requirements of passive TW systems present a significant

Thèse accessible à l'adresse : https://theses.insa-lyon.fr/publication/2024ISAL0088/these.pdf © [C.K. Miyazaki], [2024], INSA Lyon, tous droits réservés

limitation in contexts where land availability is restricted, particularly in urban areas (Ghosh and Gopal, 2010; Ilyas and Masih, 2017; Kivaisi, 2001; Zapater-Pereyra et al., 2015). Additionally, they require a significant surface area compared with traditional wastewater treatment systems (UASB reactor: 0.03 – 0.1 $m^2.PE^{-1}$; activated sludge: 0.12 – 0.3 $m^2.PE^{-1}$) (Dotro et al., 2017).

Table 2.1 provides an overview of the main characteristics, removal efficiencies and land requirements for each type of wetland in temperate climate. All the systems are highly efficient at removing solids (total suspended solids – TSS) and organic pollutants. The VF TW and the French VF have excellent oxygen transfer, which enables them to achieve high ammonium removal (up to 90%) (Molle et al., 2005). However, in terms of total nitrogen (TN) performance, these types of TWs achieve about 20-50% TN removal (Cross et al., 2021). Insufficient oxygenation in HF TWs leads to incomplete nitrification and affects ammonium removal capacity (Vymazal, 2008). In this case, the nitrification process represents the main constraint on removing TN. VF TW allows for nitrification to occur, but the denitrification process can only take place in anoxic conditions with the presence of organic carbon. However, such conditions are not present in VF TW (Val del Río et al., 2017).

Table 2.1: Removal efficiencies and treatment area required for each type of wetland. HF = horizontal flow, VF= vertical flow. Source: Dotro et al. (2017).

Parameters	**HF**	**VF**	**French VF**
Treatment step	Secondary	Secondary	Combined primary and secondary
TSS	> 80%	> 90%	> 90%
Organic matter	> 80%	> 90%	> 90%
Ammonia nitrogen	20 – 30%	> 90%	> 90%
TN	30-50%	< 20%	30 – 50%
Total phosphorus	10-20%	10-20%	10-20%
Coliforms	2 log10	2 – 4 log10	1 – 3 log10
Treatment area required ($m^2.PE^{-1}$)	3 - 10	1.2 – 5	2 – 2.5

The strict compliance criteria have forced the TW designers to develop other configurations to enhance TN removal. Hybrid TWs are primarily designed for this purpose and consist of a combination of VF, HF or FWS arrangements. These configurations

Thèse accessible à l'adresse : https://theses.insa-lyon.fr/publication/2024ISAL0088/these.pdf © [C.K. Miyazaki], [2024], INSA Lyon, tous droits réservés

allow different redox conditions that favor TN removal. The VF-HF TW and HF-VF TW have an average NH_4-N removal of 69% and 73%, respectively. In terms of TN removal, a study of 60 hybrid systems showed a better performance of the hybrid free water surface (FWS) (Vymazal, 2013). On the contrary, another study showed that the VF–FWS–HF configuration had the highest TN removal (53%), and the HF had the highest potential nitrification rate as a second stage filter (Xiong et al., 2022).The first stage French VF-HF TW promoted a TN removal of 83% during summer period (Molle et al., 2008). Table 2.2 summarizes the removal efficiencies for each type of hybrid TW. The VF plays a significant role in nitrification and is an effective first stage, while the HF can be used as a second stage due to its denitrification capacity (Tunçsiper, 2009; Xiong et al., 2022). The table also demonstrated considerable variability and imprecision in ammonia and TN removal. This highlights an opportunity for further research and development in achieving better nitrogen efficiency with this two-stage TW.

Table 2.2: Removal efficiencies and treatment area required for each type of hybrid TW (Vymazal, 2013)

Parameters	**VF-HF**	**HF-VF**	**VF-VF-HF**	**Hybrid FWS**
BOD_5	63-96%	85-95%	66-99%	48-95%
COD	51-90%	77-95%	70-97%	63-98%
TSS	32-98%	81-98%	55-98%	56-94%
NH_4-N	19-91%	64-85%	36-99%	35-99%
TN	42-70%	33-80%	39-89%	37-99%

2.3 Aerated treatment wetland

Alternative designs have been developed to improve treatment performance by introducing units that can act on energy, chemical, or operational aspects (Fonder and Headley, 2010). In particular, the oxygen-intensified system can be particularly used to improve oxygen availability and increase the removal of compounds such as ammonium and nitrate nitrogen, in which case it is the known as an aerated TW. In such a system, the air blower compresses and injects gaseous oxygen into the saturated zone, converting it from a gaseous to a dissolved state. Aerated TW systems were created 20 years ago, but their implementation has increased over the last decade. Around 500 aerated TW systems are in operation worldwide (Nivala et al., 2020).

The aeration process optimizes the system by adding a unit of energy, reducing the required footprint to around 1 $m^2.PE^{-1}$. This represents a significant enhancement over

Thèse accessible à l'adresse : https://theses.insa-lyon.fr/publication/2024ISAL0088/these.pdf © [C.K. Miyazaki], [2024], INSA Lyon, tous droits réservés

passive TW, for which the land requirement exceeds 2 $m^2.PE^{-1}$. As a result, passive TW is rarely applied for large communities or in urban areas due to space limitations and a few studies focus on its implementation in this environment (Oral et al., 2020). Thus, aeration opens a horizon for integration in a new context with higher population density (Stefanakis, 2019). Although this is an important advantage, the installed air blowers require more energy, operation and maintenance than passive and natural treatment systems. The aeration process operates at low pressure (low water level in the filter), which, according to the designers, results in low energy consumption (between 0.16 and 0.49 kWh/m^3 of treated water), compared to intensive processes where, for an equivalent level of treatment, the aeration-related energy consumption is higher (generally above 0.6 kWh/m^3 of treated water) (Austin and Nivala, 2009; Kadlec and Wallace, 2009; Labella et al., 2015; Rochard, 2017a). This energy requirement refers to a continuous aeration mode, i.e., aeration for 24 hours a day, whereas more often, this strategy is switched to intermittent aeration (0.064 kWh/m^3 energy consumption in an aerated HF TW (Khan et al., 2022) to save even more energy consumption. Thus, the energy cost justifies the reduction in surface area required (including the cost of land and excavation) (Labella et al., 2015).

Moreover, aeration in intermittent mode could allow the system to be more flexible, which studies have been investigating the possibility of delivery the nitrogen in accordance with defined objectives, such as discharging into the water body or reusing the effluent in agriculture (Farouk et al., 2020). Removing TN is extremely important to avoid eutrophication and meet the effluent compliance criteria. In the context of water scarcity, the circular economy movement has been supporting the recovery of nitrogen in wastewater facilities to reuse purpose. Furthermore, this approach reduces energy demand in the wastewater treatment plants and helps reduce the need for industrial fertilizers in agriculture. The strategy is to retain nitrogen compounds in the wastewater, either in the NH_4^+ form or oxidized NO_3^- form, according to crop requirement, soil type, and specific environmental conditions (Alva et al., 2006; Farouk et al., 2020; Ribaudo et al., 2011). In other words, the aerated wetlands could be operated in a flexible way to be reused in different context (Neto et al., 2021).

The incorporation of air optimizes the treatment efficiency, particularly in terms of carbon and ammonium removal, exceeding 90% (Cross et al., 2021; Masih, 2017; Zhuang et al., 2019), as illustrates Figure 2.2. The TN removal is typically influenced by aeration strategy (Zhuang et al., 2019), dissolved oxygen (DO) concentration and COD/TN ratio (Zhang et al., 2024). Denitrification remains limited in continuous aeration mode, reaching 15-60% of TN removal (Cross et al., 2021; Nivala et al., 2019b). This is due to a number of factors, including excessive aeration, nitrate accumulation and the lack of soluble and biodegradable organic matter (Khan et al., 2022; Uggetti et al., 2016). Intermittent aeration in time-based aeration mode can potentially remove up to 80% of the TN for

Thèse accessible à l'adresse : https://theses.insa-lyon.fr/publication/2024ISAL0088/these.pdf © [C.K. Miyazaki], [2024], INSA Lyon, tous droits réservés

aerated VF TW or HF TW (Liu et al., 2019; Masih, 2017). This approach favors the nitrification and denitrification processes (Wallace et al., 2020). In the case of carbon source addition, this efficiency could reach 90% for a COD/N ratio of 10 for an intermittent (4 hours per day) VF TW (Fan et al., 2013), and even to 96% with a layer of wheat straw as a carbon source (Jia et al., 2018). The C/N ratio for aerated TW can be increased from 40% TN removal with a C/N ratio of 3 to 90% TN removal with a C/N ratio of 9 (Zhuang et al., 2019).

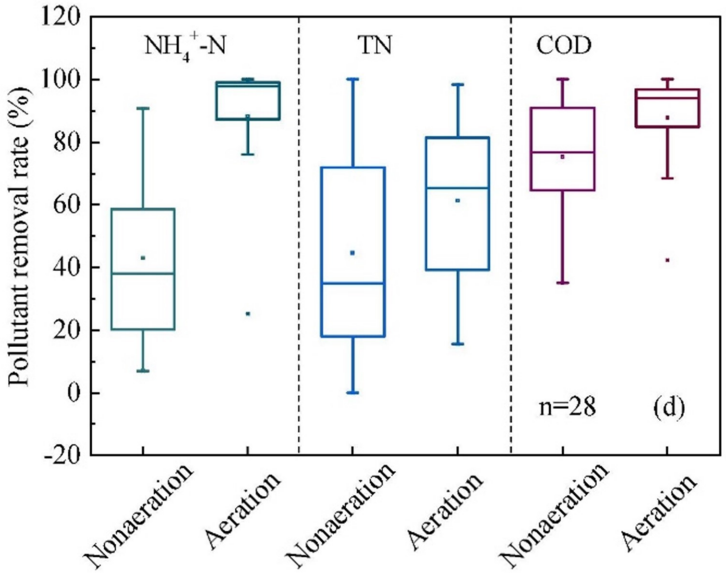

Figure 2.2: Removal effects of ammonia in TW with/without aeration. Source: Zhuang et al., 2019

Other studies explored the use of dissolved oxygen concentration as a set point to maintain an optimal environmental condition (Khan et al., 2022; Uggetti et al., 2016), with a maximum TN removal of 80%. The studies conducted to date have demonstrated a significant interest in optimizing the system, and there is an urgent need to address research gaps for aerated TW:

- The TN removal can/should be further optimized (Jia et al., 2018).
- The response of aerated TW to organic overload is unknown (Nivala et al., 2020).
- The rate of oxygen transfer within a porous media was studied in clear water, but no study investigated the effect of biomass development on oxygen transfer efficiency (Séranne et al., 2021).
- Automation using online sensors (e.g., DO, NH_4-N, pH, redox potential) could be used to control the aeration to optimize the performance and save energy consumption (Nivala et al., 2020). Data-driven and soft-sensors model approaches could go further on establishing rules for controlling the system (Dong and Kuang, 2024).

Thèse accessible à l'adresse : https://theses.insa-lyon.fr/publication/2024ISAL0088/these.pdf © [C.K. Miyazaki], [2024], INSA Lyon, tous droits réservés

- The aeration strategy can directly affect the water quality at the outlet, but the aeration effect on hydraulics in hybrid systems remains unknown (Boog et al., 2020; Boog et al., 2014; Butterworth et al., 2016a). The studies consider the system as a 'black box' without exploring the actual flow inside the system.
- Efforts should be made to do mechanistic modeling of aerated TW, combining the kinetics and hydraulics (Nivala et al., 2020).

2.4 Rhizosph'air®

The combination of VF and HF TW in a hybrid system has the potential to achieve TN removal, which is why research trends are focusing on different multi-stage configurations (Vymazal, 2013). A single-single stage configuration, the Rhizosph'air®, features an innovative process and high-tech capabilities to optimize treatment. This patented technology (Troesch et al., 2020) is designed to enhance the efficiency and effectiveness of wastewater treatment. This compact system allows for a significant reduction in the required footprint, from 2 $m^2.PE^{-1}$ (classical two-stage French VF wetland) to 0.8 – 1.2 $m^2.PE^{-1}$ depending on the conditions (Molle et al., 2005; Petitjean et al., 2021; Troesch et al., 2020). Therefore, reducing surface area alters the feasibility of implementing TW in urban areas. The system operates as a primary and secondary treatment, with a French VF TW above an aerated HF TW.

The system consists of a two parallel unsaturated filters filled with finer gravel (2-6mm) as shown in Figure 2.3. The raw wastewater is distributed evenly across the surface of the unsaturated filter in operation, where it is fed into the system and percolates vertically through the pores. The filter is dosed in batches, with the volume of a single batch set at a minimum of 2 cm and a maximum of 5 cm (minimum water flow of 0.5 $m^3/h/m^2$) to ensure homogenous distribution (Dotro et al., 2017). The suspended solids are retained by filtration in the gravel layer, where they are accumulate and are mineralized over time. The dissolved matter is treated by bacteria present in the porosity of the gravel layer. The two filter in parallel are alternated every 3.5 days, allowing one filter to be active and the other to be at rest. This strategy is crucial to stabilize the sludge layer on the surface of the filter during the rest period, reducing the risk of system clogging, avoiding plant stress (e.g., lack of water) (Dotro et al., 2017).

The transition layer has the function of intermediate two different gravel sizes. Then, the last layer is completely saturated filled with coarse gravel. Contrary to the unsaturated layer, where the flow is vertical, in this saturated layer the flow is mainly horizontal. Typically, HF TW is an oxygen-deprived environment. However, in this hybrid system, oxygen demand is met by an aeration network, with driplines sending fine air bubbles throughout the entire layer. This design could provide the flexibility needed for the

Thèse accessible à l'adresse : https://theses.insa-lyon.fr/publication/2024ISAL0088/these.pdf © [C.K. Miyazaki], [2024], INSA Lyon, tous droits réservés

system to operate according to treatment requirements. However, further studies should be conducted to explore this idea in more depth. This saturated part removes dissolved and colloidal contaminants, including ammonium and even nitrate. The aeration strategy can be either continuous, to nitrify all the ammonium pollution present, or intermittent, enabling both nitrification and denitrification processes.

The first unsaturated layer functions as a French VF TW, with reeds (i.e., P. australis) planted in this fine support. Regarding the nitrogen cycle, plants may play a role in TW in the following ways: by assimilation of nutrients, by producing organic matter, by releasing oxygen from the root zone, and by releasing organic carbon (Val del Río et al., 2017). Nevertheless, nutrient uptake plays a relatively minor role in TW compared to the applied loads (Langergraber and Simunek, 2005). The main role of the plants is the mechanical process, where the wind swings the stems, creating tubular spaces around them and facilitating water percolation and passive air penetration into these zones. This physical phenomenon prevents clogging and increases the mineralization of the accumulated sludge (Lombard Latune et al., 2017; Molle et al., 2006). The mineralization process is also accelerated by the oxygen supplied by the air blowers, where air bubbles rise from the bottom to the surface, providing additional oxygenation to accelerate the degradation of organic matter.

This hybrid system has been installed at various sites in France (18 plants), and is designed to treat raw wastewater from small and medium-sized agglomerations (the largest one is 4,500 PE). One of the plants was installed in Tarcenay, France, with a capacity to serve 1,400 PE (Prost-Boucle et al., 2021; Prost-Boucle and Molle, 2021). This TW was used to treat domestic wastewater, and it was monitored for a period of two years. The treatment performance for COD, BOD_5, and TSS remained consistently high and stable, regardless of the aeration strategy employed. However, when an aeration strategy of 12 hours per day was applied, divided into four cycles, ammonium was completely oxidized and nitrate exited the system as it was not used in the denitrification process due to insufficient carbon availability. Reducing the daily aeration duration proved an effective solution to enhance the denitrification process and improve TN removal. By implementing a four-cycle aeration strategy for a total of three hours per day, the system achieved a 97% removal rate of COD and an 82% removal rate of TN, with a remaining concentration of 19 mg TN/L at the outlet. The results suggest that optimization by aeration could be competitive with activated sludge treatment performance (Prost-Boucle and Molle, 2021). However, it should be noted that the study was conducted as part of a report and evaluation of a system, and not in the context of scientific purpose and a limited aeration strategy was tested under conditions of high variability in inflow and outflow.

The general limitations of Rhizosph'air® and areas requiring further research are as follows:

Thèse accessible à l'adresse : https://theses.insa-lyon.fr/publication/2024ISAL0088/these.pdf © [C.K. Miyazaki], [2024], INSA Lyon, tous droits réservés

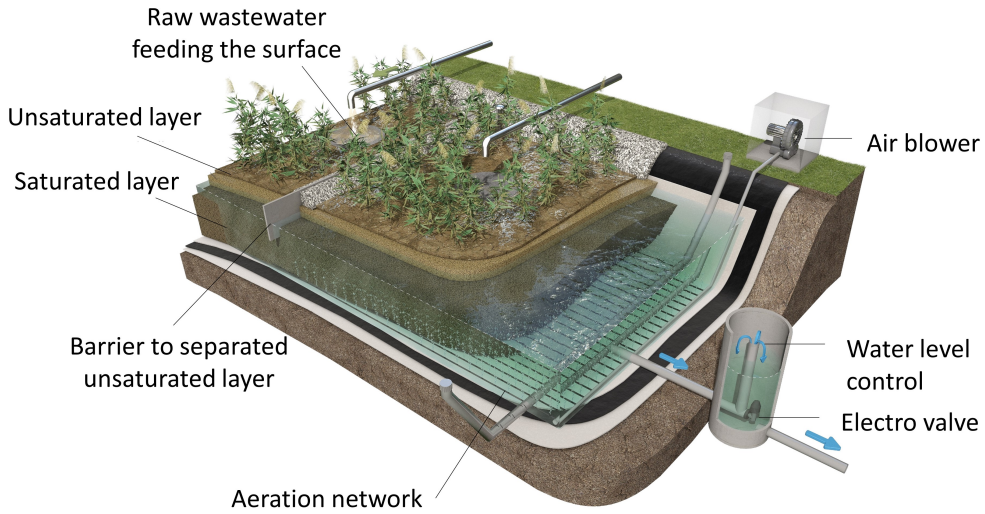

Figure 2.3: Scheme of the Rhizosph'air® wastewater TW (schematic courtesy of Ecobird).

- The lack of organic carbon (insufficient C/N ratio) hinders an optimal denitrification process (Higelin, 2021; Prost-Boucle and Molle, 2021).
- The use of oxygen sensors inserted inside the filter does not provide an overall view of the general conditions regarding spatial heterogeneity of oxygen supply and consumption (Prost-Boucle and Molle, 2021).
- Intermittent aeration is controlled by an air blower with a time set point (frequency on/off), and these operating conditions may limit the nitrogen removal rates (Durot and Molle, 2017).
- The aeration cycle is not adapted to different organic loads (variation in inlet wastewater characteristics).

The system shows great potential for further development. Future steps should further investigate oxygen transfer, the impact of aeration strategies on system performance, the development of hydraulic models, and the optimization of TN removal.

2.5 Oxygen transfer in aerated wetlands

In the context of biological treatment processes, mass transfer across the gas-liquid interface represents a critical operation within an aerated system. The two-film theory posits that mass transfer occurs between the gas and liquid phases across two interfaces: the gas phase and the liquid phase. The transfer process involves two simultaneous processes: absorption, where the substance transitions from the gaseous state to the liquid state; and desorption, which is the opposite effect, where the substance passes from the liquid to the

Thèse accessible à l'adresse : https://theses.insa-lyon.fr/publication/2024ISAL0088/these.pdf © [C.K. Miyazaki], [2024], INSA Lyon, tous droits réservés

gaseous state. Both processes encounter resistance to molecular movement, which impacts the efficiency of mass transfer (Metcalf et al., 2004). The practical application of this theory is the transfer of oxygen from air into liquid, which can be achieved by introducting oxygen bubbles. The most common equipment used in conventional wastewater treatment is the submerged-bubble aeration system, which generates air bubbles using orifices, injectors, and nozzles (Metcalf et al., 2004). In aerated TW, the air diffusers are mainly alternative pipes or tubing with driplines installed at the bottom of the system to ensure uniform air distribution (Wallace et al., 2020).

A number of factors affect oxygen transfer to meet oxygen demand in the system, including the airflow rate delivered by the air blower, bubble size, immersion depth of the air distribution system and temperature (Harris et al., 1996). Furthermore, the addition of a media component introduces further complexity when aeration takes place in wetlands. Considering only the effect of the media, oxygen transfer efficiency would be enhanced by increasing the contact time between the air bubble and the water. This is achieved when the former is trapped in the pore spaces and the tortuous path lengthens the distance the air bubble has to travel before reaching the surface (Harris et al., 1996). However, when air bubbles reach the bulk liquid, they coalesce with other bubbles, increasing their size and reducing their surface area. This makes oxygen transfer less efficient (Nivala et al., 2020). This duality poses a challenge in clearly determining the overall effect of granular media on Standard Oxygen Transfer Efficiencies (SOTE). Efficiency is estimated to be intermediate between fine-bubble and coarse-bubble diffusers (Wallace et al., 2020). Further research is needed to clarify these opposing effects and provide a comprehensive understanding of the mechanisms involved (Nivala et al., 2020).

SOTE can vary depending on the media type and the size of the gravel. According to Wallace et al. (2007), fine-bubble diffusers achieved an efficiency of 6.6% in one-meter deep bench-scale tanks without media and 4.7% in tanks with gravel media. Araya et al. (2016) highlighted a notable difference in oxygen transfer efficiency between gravel and zeolite. Butterworth (2014) investigated the impact of orifice size and air flow rate on SOTE performance with and without media. She observed that systems without media exhibited lower SOTEs. The smallest orifice with a lower airflow rate demonstrated the most optimal performance in a system with media.

Vera-Puerto et al. (2022) highlighted the impact of gravel size, noting that larger gravel sizes led to higher SOTEs, ranging from 0.7 to 1.6% for coarse gravel and 0.4 to 1.1% for fine gravel. However, the authors defined coarse gravel with a porosity of 50% and fine gravel with a porosity of 44%, which is inconsistent with the generally accepted relationship between grain size and porosity. Furthermore, the percentages are similar, and a statistical analysis should be conducted to determine their significance. Therefore, the paper does not provide sufficient clarity on the relationship between gravel size and SOTE.

Thèse accessible à l'adresse : https://theses.insa-lyon.fr/publication/2024ISAL0088/these.pdf © [C.K. Miyazaki], [2024], INSA Lyon, tous droits réservés

Conversely, increasing the airflow rate (up to 10.7 $m^3.N.h^{-1}.m^2$) will result in a reduction in residence time and, consequently, a decrease in SOTE values. In contrast to the findings of Vera-Puerto et al. (2022), Séranne et al. (2021) observed that SOTEs reached higher values (11 to 18%/m) in fine gravel than in coarse gravel (5 to 10%/m), regardless of the airflow rate. However, increasing the airflow rate, it reaches a plateau (0.46 $m^3.N.h^{-1}.m^2$) and a subsequent decrease in SOTE. As Vera-Puerto et al. (2022) tested higher airflow rates, this could reflect the decrease in results after the "plateau". Additionally, the authors assess air distribution images using electrical resistivity tomography, which yields an air cone distribution within the initial 10-20 centimeters, along with oxygen heterogeneity across the column height. The coarse gravel produces an even more heterogeneous air distribution, which can only be mitigated by increasing the diffuser density or the air flow. Furthermore, the study demonstrated that the volume of air occupied in the water is higher in fine gravel (10 - 12.5%) and lower in coarse gravel (0 - 5%) for one diffuser. All of the studies were conducted on a mesocosm or column scale, with experiments conducted in clean water. As a result, there are still research questions regarding the possibility of upscaling these results and the effect of SOTE in wastewater, including gravel-attached biofilm.

Once released from the diffuser, the bubbles follow an upward trajectory to reach the surface. This trajectory can follow different directions. The distribution of bubbles across the surface of the system can be uniform, sparse, or sporadic (Nivala et al., 2020). The bubble pattern is dependent on the air distribution system and is indicative of broader operational issues, such as broken connectors or clogged driplines. Fouling of air distribution lines may be caused by the precipitation of organic or inorganic compounds into the orifices during the non-aeration period when intermittent aeration occurs. A case of iron precipitation in the air distribution pipes has been reported in the literature, and the cleaning procedure included the addition of chloridric acid (HCl) (Van Oirschot et al., 2015; Wallace et al., 2020). Given the increasing use of this intermittent aeration strategy to reduce energy costs and enhance TN removal, further research should concentrate on how aerated TWs respond to this phenomenon (Vera-Puerto et al., 2022).

The current method for estimating oxygen consumption rates is through the use of gaseous tracers, respirometry, or interference from water quality data (Nivala et al., 2013). The most commonly used method is the latter, which estimates oxygen usage based on pollutant degradation, stoichiometric relationships, and water quality data (Durot and Molle, 2017; Nivala et al., 2013). Together with this data, the oxygen required can be calculated using airflow rate, aeration time per day, density of air and mass fraction of oxygen in air (Rous et al., 2019). In passive TW, there is an imbalance between the oxygen requirements of the system and the actual supply of oxygen, which requires additional oxygenation within the system. To address this deficit, aerated TWs are used to enhance

Thèse accessible à l'adresse : https://theses.insa-lyon.fr/publication/2024ISAL0088/these.pdf © [C.K. Miyazaki], [2024], INSA Lyon, tous droits réservés

oxygen transfer and meet demand up to tenfold (Prost-Boucle and Molle, 2021). A review study found that aerated TWs had an aeration efficiency (AE) (ratio between oxygen consumed and oxygen delivered) of about 2.45 and 5.03%. The intermittent aeration strategy generally had higher values of AE (Rous et al., 2019).

It is evident that there is an imbalance between oxygen consumption and supply. This highlights the necessity for the implementation of additional oxygen, which will require further knowledge to understand how to operate the aerated treatment works (TW) effectively. However, there is currently limited information available on oxygen transfer in aerated TWs (Rous et al., 2019; Vera-Puerto et al., 2022). In that sense, further study of oxygen transfer is essential to enable the development of effective design procedures, the development of a robust aeration control strategies, and the improvement of energy efficiency through a deeper understanding of the actual oxygen transfer dynamics (Vera-Puerto et al., 2022).

2.6 Nitrogen dynamics in treatment wetland

The dynamics of nitrogen in advanced and conventional wastewater treatment plants are subject to different interactions than those in TW, where the soil and plants contribute to a more complex environment. Several processes take place simultaneously in the water, sediment and biomass, and nitrogen can be transformed physically or chemically. The main nitrogen transformations and degradation processes are: ammonification, nitrification, denitrification, plant uptake and ammonia adsorption (Kadlec and Wallace, 2009; Vymazal, 2007). Even though there are several nitrogen transformations, microbial processes are the dominant removal pathways (Allen et al., 2023). The major nitrogen compounds found in wastewater are organic and inorganic (NH_4-N, NO_2-N, and NO_3-N) nitrogen.

There are three main mechanisms for removing nitrogen from wastewater: physical, chemical or biological. The latter is the most common employed, offering high pollutant degradation efficiency, preventing secondary pollution and being cost-effective (Zhou et al., 2023). The classical pathway to remove nitrogen from wastewater is through the nitrification and denitrification processes, which uses the natural bacteria metabolism. The process requires two steps: aerobic autotrophic nitrification and anoxic heterotrophic denitrification. These steps are necessary to transform ammonium into nitrogen gas. It is important to note that both phases require specific environmental conditions (pH, temperature, DO concentration, C/N ratio, heavy metals, recalcitrant compounds, hydraulic retention time) and source requirements, foremost dissolved oxygen concentration and carbon source (Mishra et al., 2022). The main chemical and microbiological transformations taking place inside the hybrid TW studied are outlined in Figure 2.4.

Thèse accessible à l'adresse : https://theses.insa-lyon.fr/publication/2024ISAL0088/these.pdf © [C.K. Miyazaki], [2024], INSA Lyon, tous droits réservés

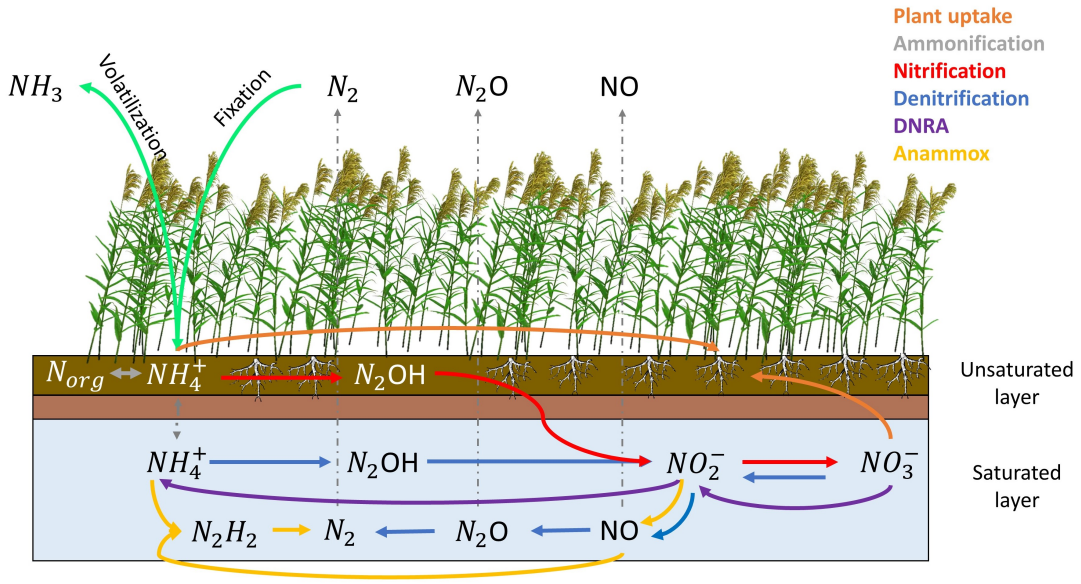

Figure 2.4: Overview of nitrogen transformations in a hybrid TWs. Source: Adapted from Kadlec and Wallace (2009) and Hallin et al. (2018)

- Ammonia volatilization

This physicochemical process is the loss of NH_3 in aqueous form to the atmosphere by volatilization. This inorganic form of nitrogen can be either ammonia (NH_3 – unionized) or ammonium (NH_4^+ - ionized). The ionic form is dependent on the soil pH value. Values below 7.5 favor ionization, which significantly reduces the likelihood of volatilization. Conversely, alkaline pH values (above 9.3) drastically increase the likelihood of this phenomenon, forming unionized forms (Reddy et al., 2022; Vymazal, 2007). Furthermore, water temperature impacts the solubility of ammonia. As temperature rises, ammonia solubility declines while volatilization rates increase (Reddy et al., 2022. In the case of the Rhizosph'air® system, there is no free water surface and no algal activity. Consequently, pH values remain stable (Vymazal, 2005). This process is, therefore, assumed to be insignificant for the hybrid system under study.

- Ammonification or mineralization of organic nitrogen

The process involves the conversion of organic nitrogen (e.g., amino acids) into ammonium. Mineralization of organic nitrogen can occur in both aerobic and anaerobic environments. However, the kinetic reaction is faster in the aerobic phase (Parde et al., 2021; Saeed and Sun, 2012). Accordingly, in the event of the prevalence of organic nitrogen in the influent, the majority of the reactions will occur in the upper layer (Saeed and Sun, 2012). In the Rhizosph'air® system, this process will occur specifically in the deposit and unsaturated layer. Heterotrophic microorganisms are the main agents involved in this process, and their reaction kinetics are faster than nitrification. Typically, 60 - 70 % of the

Thèse accessible à l'adresse : https://theses.insa-lyon.fr/publication/2024ISAL0088/these.pdf © [C.K. Miyazaki], [2024], INSA Lyon, tous droits réservés

total Kjeldahl nitrogen (TKN) in domestic wastewater is present in the form of ammonia (Kadlec and Wallace, 2009) and 74% in small communities in France (Mercoiret, 2009). The reactions depend on several factors, including temperature, pH, C/N ratio, available nutrients, and soil conditions (Vymazal, 2007). Ideally, the pH should be between 6.5 and 8.5 (Saeed and Sun, 2012; Vymazal, 2007). The optimum temperature should be between 40 and 60°C (Vymazal, 2007).Thus, the remaining 30-40% of the organic nitrogen in the influent can be mineralized in the upper layer of the studied system, given the rapid reaction and ready transformation in the aerobic environment.

- Nitrification

This process involves the oxidation of ammonia with oxygen as the electron acceptor to oxidized nitrogen using CO_2 as the carbon source. First, NH_4 is oxidized to NO_2 by ammonium-oxidizing bacteria (AOB), which are autotrophic bacteria (Kadlec and Wallace, 2009). They use CO_2 or carbonates as a carbon source (Vymazal, 2007). These bacteria require oxygen and are active in a strictly aerobic environment (Vymazal, 2007). In the second step, NO_3 is formed by nitrite oxidizing bacteria (NOB – autotrophic bacteria), which operate in a facultative environment, either aerobic or anaerobic (Vymazal, 2007). In the absence of inhibition, the conversion of nitrite to nitrate is typically faster than ammonia to nitrite, resulting in minimal nitrite accumulation. Studies in aerated TWs have shown that the relative abundance of AOB and NOB can increase threefold compared to an unaerated system (Fan et al., 2016; Zhang et al., 2024). The nitrification process in TWs consumes approximately oxygen (4.2-4.5 g O_2) (Saeed and Sun, 2012) and they require more alkalinity (7.1 - 8.64 g) (Kadlec and Wallace, 2009; Saeed and Sun, 2012). The production of nitrate results in a consumption of alkalinity and a decrease in pH values in the water.

The nitrification process is influenced by a number of environmental factors, including temperature, pH, alkalinity, inorganic carbon source, microbial population, and concentrations of ammonium and dissolved oxygen (Vymazal, 2007). The optimal temperature for nitrification in soils is between 30 and 40°C (Reddy et al., 2022; Saeed and Sun, 2012). Nevertheless, nitrification was still observed at temperatures between 0 and 5°C in TW (Faulwetter et al., 2009). It is important to note that no nitrification occurs when the DO concentration is below 0.5 mg/L. (Pascual et al., 2018). Regarding aerated TWs, the optimal balance between ammonium removal and energy consumption efficiency was found to be 2-3 mg O_2/L (Khan et al., 2022). The simple oxidation equation in TWs can be described (Saeed and Sun, 2012) by Eq. 1.1 and Eq. 1.2.

Nitritation:

$$NH_3 + 1.5O_2 \rightarrow H^+ + H_2O + NO_2^- \qquad \text{(Eq. 1.1)}$$

Thèse accessible à l'adresse : https://theses.insa-lyon.fr/publication/2024ISAL0088/these.pdf © [C.K. Miyazaki], [2024], INSA Lyon, tous droits réservés

Nitrification:

$$2NO_2^- + O_2 \rightarrow 2NO_3^- \quad \text{(Eq. 1.2)}$$

The complete nitrification equation, including the cell biomass synthesis is described by Eq. 1.3 (Saeed and Sun, 2012).

$$NH_4^- + 1.83O_2 + 0.98HCO_3^- \rightarrow 0.021C_5H_7NO_2 + 1.04H_2O + 0.98NO_3^- + 1.88H_2CO_3 \quad \text{(Eq. 1.3)}$$

- Denitrification

Facultative heterotrophs are capable of converting nitrate into dinitrogen (gas form) using organic matter as a carbon source in TWs. In conventional wastewater treatment the addition of an external carbon source (e.g., methanol or ethanol) could be necessary during this process. However, in TWs, dead and decomposed biomass can supply a portion of organic carbon. This quantity may prove insufficient in the event of a high nitrate load. It is recommended that a ratio of C:N of 5:1 be used to ensure that carbon is not a limiting factor (Li et al., 2019; Zhu et al., 2014) or at least 2:1 to achieve optimal denitrification rates (Morvannou et al., 2017). The denitrification process can occur at low dissolved concentration, between 0.2 and 0.5 mg/L (Pascual et al., 2018), under an oxidation/reduction potential (Eh) between +350 and +100 mV (Kadlec and Wallace, 2009). Furthermore, microbial denitrification may be constrained by temperatures below 15°C (Liu et al., 2024).

The denitrification process produces 3.0 g of alkalinity as $CaCO_3$ per gram of NO_3-N reduced (Kadlec and Wallace, 2009), resulting in an increase in the pH value of the water. The reduction equation in TWs can be described by Eq. 1.4.

$$2NO_3^- \rightarrow 2O_2 \rightarrow 2NO \rightarrow N_2O \rightarrow N_2 \quad \text{(Eq. 1.4)}$$

- Nitrate-ammonification

Dissimilatory nitrate-nitrogen reduction to ammonium (DNRA), or nitrate-ammonification, has the potential to compete with denitrifying bacteria for nitrate reduction. In this process, NO_3 to NH_4-N under anaerobic conditions (Saeed and Sun, 2012). This process occurs when fermentative bacteria are present under anaerobic conditions. These bacteria are not dependent on nitrate for growth and development. Dissimilatory NO_3-N reduction was observed in HF TW, but its contribution was insignificant compared to the denitrification process (Liu et al., 2018). Furthermore, according to Tang et al. (2020) the aforementioned reaction only becomes significant when

Thèse accessible à l'adresse : https://theses.insa-lyon.fr/publication/2024ISAL0088/these.pdf © [C.K. Miyazaki], [2024], INSA Lyon, tous droits réservés

the carbon-to-nitrate ratio exceeds 12. Therefore, the confirmation of this process in the studied system should be confirmed with metagenomic analysis.

- Anammox

Further pathways have been identified as potential means of achieving TN removal. These include simultaneous nitrification–denitrification, partial nitrification–denitrification, anammox, and CANON (Hameed et al., 2022; Negi et al., 2022; Saeed and Sun, 2012; Tang et al., 2020; Wallace and Austin, 2008).Among them, the anammox process is particularly well known for its 60% reduction in energy requirements, sludge reduction by 90%, and minimal footprint requirement (Negi et al., 2022). Furthermore, TWs involve a slow-growing bacteria that attaches to the media by forming a biofilm, with a mean cell residence time of greater than 200 days (Wallace and Austin, 2008). This particular condition is conducive to other nitrogen pathways, especially anammox. These autotrophic bacteria convert ammonium directly into dinitrogen gas, using nitrite as an electron acceptor. The anammox process has specific requirements and is susceptible to several environmental conditions, including pH values (6.5 - 8.3), temperature (20 - 30°C), dissolved oxygen concentration (ideally less than 0.04 mg/L) and a C/N ratio less than 2 (Cho et al., 2020), type of TW, vegetation type, organic loading rate, hydraulic retention time and substrate material (Negi et al., 2022). Therefore, DNA analysis should be used to confirm the presence and role of this process in nitrogen transformation in the system under study.

- Plant uptake (assimilation)

Nitrogen uptake by plants is defined as the use of inorganic nitrogen compounds as a nitrogen source for cell synthesis and tissue construction (Vymazal, 2007). The assimilation of ammonia or nitrate is dependent on the preference of the plant species. However, research indicates that ammonia is the most important nitrogen source for plants when both ammonia and nitrate are available (Rampuria et al., 2021). It should be noted that there is significant variation in the uptake of nitrogen by plants between different species. The process is influenced by a number of factors, including rhizosphere development, root penetration, above-ground biomass, seasonal changes, and other environmental factors that influence the process (Vymazal, 2007). The uptake of nitrogen by plants acts to counteract the ammonification process (Reddy et al., 2022). In systems implemented in temperate and cold regions, this process is negligible due to the timing of harvesting, which occurs during the winter rather than during the peak of nutrient availability in late summer (Vymazal, 2005). In addition, the net removal of ammonia from plant uptake is approximately 10 $gN/m^2 \cdot yr$, which represents 0.07% of the NH_4-N applied load into the Rhizosph'air® pilot system (Chapter 4).

Thèse accessible à l'adresse : https://theses.insa-lyon.fr/publication/2024ISAL0088/these.pdf © [C.K. Miyazaki], [2024], INSA Lyon, tous droits réservés

- Nitrogen adsorption

The ionized ammonia (dissolved cation) present in pore water can be adsorbed by cation exchange onto negatively charged inorganic sediments, soils, or detritus (Reddy et al., 2022). This phenomenon is reversible. When ammonium concentrations in the liquid are high, the rate of adsorption increases. Conversely, desorption releases ammonia back to the liquid when the concentration decreases (Vymazal, 2007). It should be noted that this process does not result in nitrogen removal. Rather, it is a transformation during which the compound is retained on the solid part.

The principal factor that can influence ammonium exchange in a first stage French VF TW is the organic matter (OM). Ammonium is adsorbed by OM accumulated in the first layer and soil minerals (Molle, 2014). Morvannou et al. (2014) developed a model to simulate the nitrogen dynamic in a first-stage VF TW with gravel. Their findings demonstrated that approximately one-third of the applied ammonium was adsorbed during the feeding period. Subsequently, the ammonium can be nitrified between batches and during rest periods (Molle et al., 2006). In the case of the saturated layer, the porous medium employed is gravel, which has a low adsorption capacity (Tan et al., 2021). The organic matter that accumulates on the surface of the primary filter top of the Rhizosph'air® can have a significant impact on nitrogen dynamics.

2.7 Research questions and thesis outline

The main objective of this doctoral research was to optimize nitrogen removal performance in a hybrid aerated vertical and horizontal TW. All the experiments were done in a research platform called REFLET, in France. In order to support this optimization, studies were made to understand the effect of airflow in the hydraulic of the system, to evaluate the impact of aeration strategies on TN removal and to establish an optimized aeration strategy and to explore aeration control rules for TN removal. Figure 2.5 illustrates the research outlines for each chapter and the interaction between them. To achieve this goals, the thesis was separated in three main chapters:

- Chapter 2: The hybrid system under study has a complex function, and the main questions regarding its hydraulic were: *Changing the aeration strategy, what are the effects on the hydraulics? Going beyond the 'black-box' analysis, how the system behaves internally? Are the results on a pilot scale applied to a larger scale?*. Therefore, this chapter goal was to evaluate the impact of aeration strategies on the hydrodynamic behavior of the studied system, assessing the outlet and in the middle of the pilot system. The results were then compared to assess their applicability at full scale. This chapter was based on the findings of a six-month experiment

Thèse accessible à l'adresse : https://theses.insa-lyon.fr/publication/2024ISAL0088/these.pdf © [C.K. Miyazaki], [2024], INSA Lyon, tous droits réservés

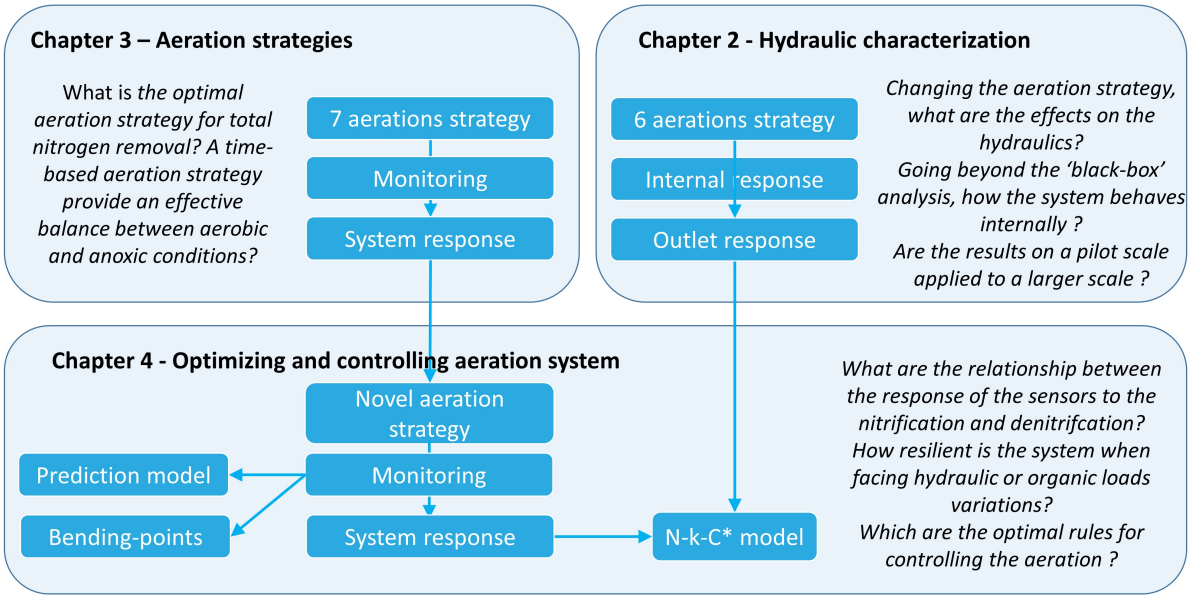

Figure 2.5: Research outlines for each chapter and the interaction between them.

conducted during the second year of the PhD thesis.

- Chapter 3: Previous studies have investigated the impact of intermittent aeration on TN removal. Nevertheless there were still remaining questions that require further investigation: *What is the optimal aeration strategy for TN removal? A time-based aeration strategy provide an effective balance between aerobic and anoxic conditions?*. This chapter objective was to investigate the impact of TN removal under various hydraulic loading, ammonium inlet concentration, and aeration strategies either based on time or on batch-hours (flows). Sampling campaigns were conducted from 2019 to 2021 as part of the Syntea pilot study. The treatment and results analysis were included in the first-year PhD thesis to incorporate the knowledge gained from a previous study on the pilot.
- Chapter 4: This chapter continues the investigations found in Chapter 3, where the questions arised as conclusions were: *What is the optimal aeration stretagy that could enhance the TN removal? How resilient is the system when facing hydraulic or organic loads variations? Which are the optimal rules for controlling the aeration ? What are the relationship between the response of the sensors to the nitrification and denitrifcation process?*. The objetive of this chapter was to evaluate a novel aeration strategy for the removal of TN and to explore rules for controlling the aeration in this hybrid system. The field experiment were conducted during the second/third year of the PhD thesis.
- Chapter 5 provides the main conclusion of this PhD thesis and outlines the per-

Thèse accessible à l'adresse : https://theses.insa-lyon.fr/publication/2024ISAL0088/these.pdf © [C.K. Miyazaki], [2024], INSA Lyon, tous droits réservés

spectives for future research. This section highlights some of the work conducted in parallel with the aforementioned chapters. However, due to time constraints, it was not possible to reach a conclusion regarding certain aspects. Further development should continue working on topics such as the electrical tomography resistivity, which was carried out in parallel with the tracer test, and the bio-kinetic model, which couples the engineer process model with nitrification and denitrification coefficient rates.

Thèse accessible à l'adresse : https://theses.insa-lyon.fr/publication/2024ISAL0088/these.pdf © [C.K. Miyazaki], [2024], INSA Lyon, tous droits réservés

Chapter 3

Hydraulic characterization of a hybrid aerated vertical and horizontal treatment wetland

Abstract

Characterizing the performance of any treatment wetland (TW) system requires a fundamental understanding of the hydraulic behavior of the system. In aerated treatment, the air supply increases complexity, and the internal behavior of TWs can vary according to the adopted aeration strategy. Understanding these changes can provide insights into an optimized operation for aerated TWs. In this sense, the present work characterizes the hydraulics of a hybrid aerated vertical and horizontal TW through parallel tracer testing under different aeration strategies (varying aeration duration and aeration between the different compartments). The tracer test was conducted using amino-G acid and salt on a pilot scale system and measured at the outlet and inside the system. These results are subsequently compared to a full-scale system of a similar design to assess the validity of the results on a larger scale. The results allowed a characterization of actual retention time, the estimated number of tanks-in-series (NTIS), the volume of dead zones, and the identification of the hydraulic behavior under different aeration conditions. The results indicated that decreasing aeration duration led to more heterogeneity within the filter, the aeration on the primary filter plays an important role in mixing, and the pilot scale results can be upscaled for a larger scale. It also highlighted the impact of aeration in the different compartments of this hybrid aerated wetland system, which can contribute to an accurate characterization of specific pollutant removal kinetics.

Keywords: Amino-G acid, Aeration, Constructed wetland, Tracer study, Wastewater

Thèse accessible à l'adresse : https://theses.insa-lyon.fr/publication/2024ISAL0088/these.pdf © [C.K. Miyazaki], [2024], INSA Lyon, tous droits réservés

This chapter was published as: Miyazaki, C.K., Morvannou, A., Petitjean, A., Nivala, J., Molle, P., 2024. Hydraulic characterization of a hybrid aerated vertical and horizontal treatment wetland. Ecological engineering. Ecological Engineering, 206, 107301.https://doi.org/10.1016/j.ecoleng.2024.107301

Thèse accessible à l'adresse : https://theses.insa-lyon.fr/publication/2024ISAL0088/these.pdf © [C.K. Miyazaki], [2024], INSA Lyon, tous droits réservés

3.1 Introduction

Decentralized solutions such as treatment wetlands (TWs) have emerged as viable options for meeting local discharge regulations while reducing operational and maintenance costs (Morvannou et al., 2015; Nivala et al., 2020; Vymazal and Kröpfelová, 2008). However, increased land constraints and stringent requirements demanded more resilient solutions, like aerated TWs, which have been significantly developed over the past decade. In aerated TWs, the ascent movement of air bubbles leads to the oxygen transfer from a gaseous to a dissolved state. This leads to higher oxygen transfer rates compared to regular TWs, enhanced pollutant removal, and improved final effluent quality (Nivala et al., 2020).

One of the aerated TW designs is the Rhizosph'air® system, described by the patented technology of Troesch et al. (2020) and consists of a hybrid aerated TW fed with raw wastewater. It integrates two cells of an unsaturated vertical flow (VF) over a saturated horizontal flow (HF) in a single stage. This compact system reduces the required footprint from 2 m^2 per population equivalent (PE) (classical two-stage French VF wetland) to 0.8 – 1.2 $m^2.PE^{-1}$ depending on the conditions (Molle et al., 2005; Petitjean et al., 2021; Troesch et al., 2020). The system has a shallow unsaturated layer on the top (Figure 2.3), followed by a saturated zone where the flow is a mix of vertical and horizontal flow, and a third saturated zone where the flow is horizontal. Each saturated zone can be aerated in a differentiated mode. With these settings, the oxygen transfer can be increased by a factor of three compared to passive saturated TW, leading to more efficient TW design and implementation (Petitjean et al., 2022; Troesch et al., 2020).

The pollutant removal efficacy of TWs is highly influenced by characteristics such as the hydraulic retention time (HRT), the volume of dead zones, and the existence of short-circuiting (Headley and Kadlec, 2007). In the case of aerated TWs, the air supply can change the hydraulic behavior. Tracer experiments in the literature reported that aerated VF TWs improve aeration mixing properties, functioning with similar conditions as continuously stirred tank reactor (CSTR) (Boog et al., 2014), whereas 4.5 tanks-in-series (NTIS) are required to represent hydraulic behavior in aerated HF TWs (Nivala et al., 2020). The aeration strategy has been reported to affect the tracer response and, thus, the hydraulic functioning of the system. For example, Boog et al. (2014) reported a similar theoretical HRT but a higher tracer mass recovered with intermittent aeration (2 cycles per day of 8 hours on, 4 hours off) than with continuous aeration in an aerated VF TW. Boog et al., 2020 also observed a slight difference in the tracer mass recovery between continuous aeration over the entire area of a HF TW (64%) and continuous aeration over only 70% of the area for a HF TW (47%). The results showed a lower peak and NTIS value (3.2 for bromide tracer) for the test condition compared to fully aerated over the entire area, indicating a faster and more variable flow. In addition, Butterworth et al.

Thèse accessible à l'adresse : https://theses.insa-lyon.fr/publication/2024ISAL0088/these.pdf © [C.K. Miyazaki], [2024], INSA Lyon, tous droits réservés

(2016b) investigated the mixing pattern on aerated and non-aerated HF TW, and the aerated TW showed a better mixing effect than the non-aerated TW.

The existence of different zones and flow directions in the Rhizosph'air® system, as shown in Figure 2.3, significantly complicates the water flow, raising questions about its hydraulic behavior. The first and only hydraulic study in this TW design was carried out on a full-scale plant of 1,400 PE (Tarcenay, France), receiving 340 m^3/d of raw wastewater, with 4 cycles per day of 1.5 hours on, 4.5 hours off (a total 6h per day of aeration). The TW had a hydraulic retention time of 3.5 days with a tracer mass recovery rate of 99% (Prost-Boucle and Molle, 2021). The results demonstrated the absence of short-circuiting or preferential pathways, with similar characteristics to a combination of CSTR and a plug-flow reactor (PFR) (Prost-Boucle and Molle, 2021). Overall, the study represents the current hydraulic state of the filter but did not explore how the different aeration strategies might impact the water flow and the hydraulic behavior. Additionally, most published studies on aerated TWs tested only a few aeration conditions for strict conventional HF and VF TWs (Boog et al., 2020; Butterworth et al., 2016b) and did not analyze spatial heterogeneity inside the filter (Delgado-Gonzalez et al., 2023). In this sense, evaluating the impact of the aeration strategy on the behavior of the Rhizosph'air® system could provide valuable information for its design and operation for a specific outlet quality target.

Therefore, the present work investigates how different aeration strategies affect the hybrid system. To do so, tracer experiments with different durations and compartment aeration were tested. Tracers (amino-G acid and NaCl) were injected into the system, and results were measured at the system's outlet and internally. The tracer response curves and several hydraulic parameters were calculated and compared for each experiment.

3.2 Material and methods

3.2.1 Pilot system description

The study was conducted at the REFLET research platform (INRAE, 2019) located in Craponne (France) on a pilot (Figure 3.1) with a surface area of 20 m^2 (two cells, each 2.5 m x 4 m). The industrial pilot was commissioned in January of 2019, with a one-month period of start-up, receiving a low hydraulic load during the first months. The TW receives raw wastewater from a combined sewer and is fed with 10 batches of 400 L (4 m^3 per day). The hybrid aerated TW has an upper layer, divided in two filters (10 m^2 each – left is filter 1 and right is filter 2,as shown in Figure 3.1), functioning as a first-stage French VF TW.

The two filters are alternately fed (herein referred to as primary filter and secondary filter) every 3.5 days, ensuring the mineralization of the solid accumulation at the surface. The filter actively receiving wastewater is termed the "primary filter" (in the case of Figure

Thèse accessible à l'adresse : https://theses.insa-lyon.fr/publication/2024ISAL0088/these.pdf © [C.K. Miyazaki], [2024], INSA Lyon, tous droits réservés

3.1, filter 1 is the primary filter), while the rest filter is labeled the "secondary filter" (Figure 3.1 represents filter 2 as secondary filter). The drainage system is configured to direct the outflow to the outlet of the secondary filter. The solids are retained on the top of the filter as it is the design intention for French VF wetlands (Molle, 2014).

The raw wastewater is applied to flood the entire surface of the primary filter (applied volume of 4 cm). The wastewater infiltrates through a layer of unsaturated gravel (2 – 6 mm nominal size, 20 cm deep), then to a transition layer of gravel (10 – 20 mm nominal size, 15 cm deep). Finally, the water reaches an aerated saturated gravel zone (20-40 mm nominal grain size, 100 cm deep), which is connected between the two filters. The aeration system comprises 120 driplines installed at the bottom of the 20 m^2 surface area (diffuser density: 60 diffuser/m^2) and are connected to air blowers. An air flowmeter, temperature sensor and pressure sensor were installed after the air blowers. The air blowers are fixed speed drive type and when they are running, the pressure fluctuates around 160-180 mbar with an airflow rate of 5-6 m^3/h.

The methodology of this study consisted of: i) conducting tracer tests at a pilot scale with a batch injection of amino-G acid and salt under various aeration strategies (further detailed in the next Section); ii) conducting tracer test at a full-scale system with a batch injection of amino-G acid with 6 hour aeration per day. Figure 3.1 represents the pilot system configuration and the location of the materials used for the experiment.

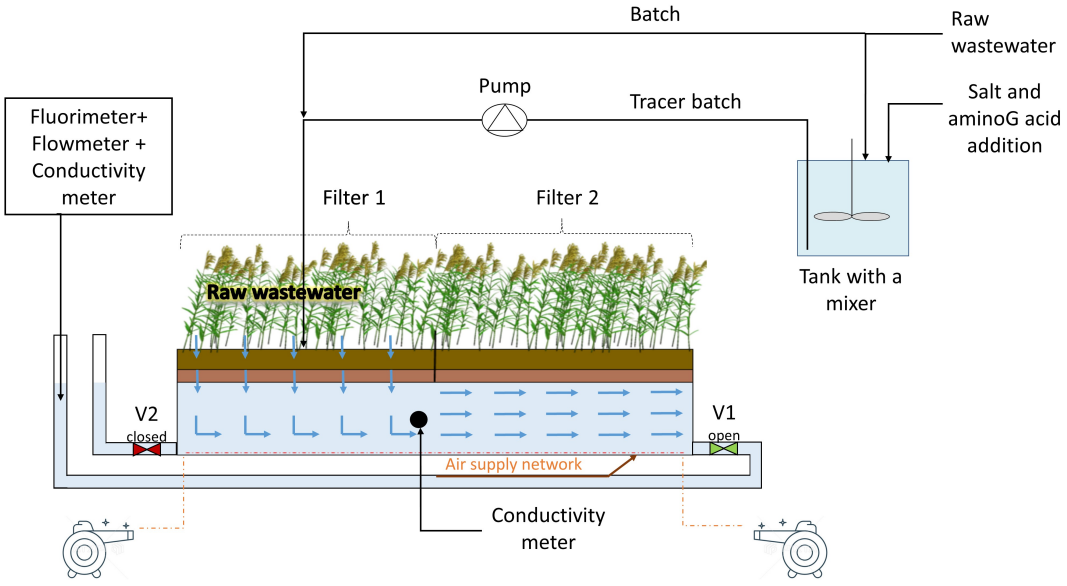

Figure 3.1: Representation of the hybrid aerated system and the location of each material. In this representation, the filter 1 is primary filter (fed) and filter 2 is secondary filter (rest). The filter 2 would be become primary filter after the alternation. Source: Adapted from **Chapter \ref {chap4}**

Thèse accessible à l'adresse : https://theses.insa-lyon.fr/publication/2024ISAL0088/these.pdf © [C.K. Miyazaki], [2024], INSA Lyon, tous droits réservés

3.2.2 Impact of aeration strategies: tracer test

- Aeration strategies

In order to evaluate the influence of aeration on the hydraulics, experiments with six different aeration strategies were conducted (Figure 3.2). The first four experimental conditions maintained the same aeration duration for both filters, starting from 24 hours per day and decreasing to 9h/d, 6h/d, and no aeration at all. In the last two experimental conditions, aeration was differentiated between primary and secondary filters, with 9h1 aerating for 9h per day in the primary filter (filter fed) and no aeration in the secondary filter. The last condition, 9h2, was the opposite of 9h1.

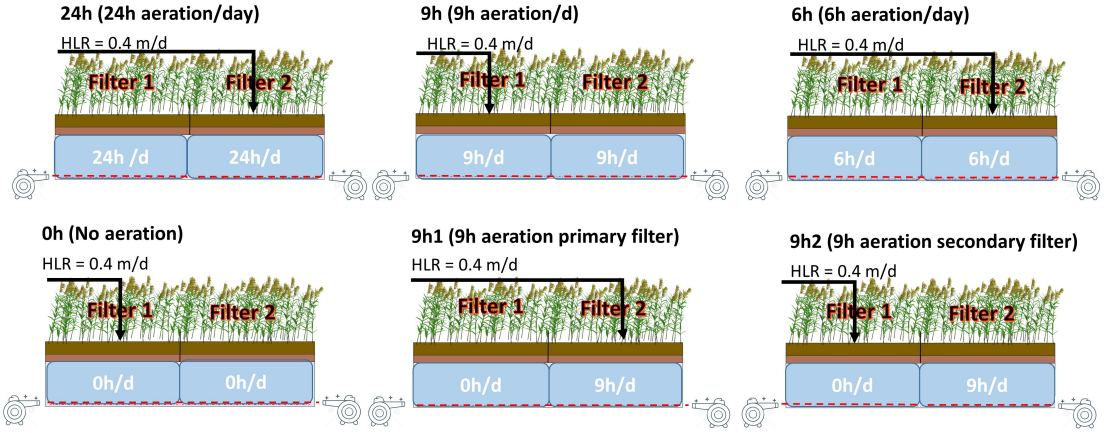

Figure 3.2: Aeration strategy for each experimental condition for the pilot system

In all conditions involving 9h and 6h aeration per day, the aeration was divided into 8 cycles equally distributed over the day, as shown in Table 3.1. The hydraulic loading rate on the primary filter remained fixed throughout the experiment at 0.4 m/d , with a total 10 batches per day and no filter alternation done over the course of each tracer test. There were no strong rainfall events during all tracer tests (refer to Table 7.1 in the Appendix for specific weather conditions for each experimental test).

- Tracer tests

The tracer test involves the introduction of a non-reactive and soluble tracer at the system's inlet to subsequently analyze its response at the outlet (Kadlec and Wallace, 2009). Previous experiments have established that amino-G acid exhibits minimal sorption to wetland soils and sediments typically associated with wetland environments (Valhondo et al., 2016). Consequently, owing to its favorable attributes as a tracer, amino-G acid was employed to assess the response at the outlet. Another tracer, the salt, was employed to assess the system's internal hydraulic behavior. This selection was driven by the need to use a tracer that could change the resistivity of the water for another parallel experiment

Thèse accessible à l'adresse : https://theses.insa-lyon.fr/publication/2024ISAL0088/these.pdf © [C.K. Miyazaki], [2024], INSA Lyon, tous droits réservés

Table 3.1: Operational parameters for each aeration strategy at the pilot system. PR= primary filter, SC = secondary filter, NB = number of cycles per day, Operation = aeration ON (h per cycle), Stop = aeration OFF (h per cycle), HLR = hydraulic loading rate (m/d

Experimental condition		24h	9h	6h	0h	9h1	9h2
Aeration on the PR	NB	1	8	8	0	8	0
	Operation	24h	1.1h	0.75h	0h	1.1h	0h
	Stop	0h	1.9h	2.25h	24h	1.9h	24h
Aeration on the SC	NB	1	8	8	0	0	8
	Operation	24h	1.1h	0.75h	0h	0h	1.1h
	Stop	0h	1.9h	2.25h	24h	24h	1.9h
HLR		0.4	0.4	0.4	0.4	0.4	0.4
Filter fed		2	1	2	1	2	1

(Electrical Resistivity Tomography) that is not present in the current paper. However, as the salt is highly variable, it was important to place a conductivity meter at the outlet to compare the results from another tracer to guarantee the replicability and the possibility of validating the outlet results.

The amino-G acid (12 g) and salt (approximately ten times the background concentration, amounting to 3 kg of salt) were mixed in the batch volume and injected directly at the feeding point of the filter (impulse technique) (Headley and Kadlec, 2007; Kadlec and Wallace, 2009), involving a single batch (400 L) followed by subsequent batches without tracers. Continuous measurements of inlet and outlet flow rates were made using flowmeters (Hendress & Hauser) at one-minute time step. The hydraulic response was measured with one-minute step at the pilot outlet using a fluorimeter (GGUN-FL) (Figure 3.3). The calibration curve (to transform mV to g/m^3) was made at the end of each tracer test (values for calibration is shown in Table 7.2 in the Appendix).

The conductivity of the water was modified by the addition of salt and conductivity meters (CM) were used to detect its concentration. They were strategically positioned both vertically and horizontally within the filter, with a total of six conductivity meters, including four inside (CM2 to CM5), one at the inlet (CM1), and one at the outlet (CM6), as illustrated in Figure 3.3. When the system was conceived, two large piezometers were installed, where we placed the conductivity meters 4 and 5. When the current tracer experiment took place, the pilot was already active and had been running for four years, so installing an additional large piezometers to accommodate the new sensors was unfeasible. To preserve the integrity of the system and prevent any damage, two small piezometers were instead inserted in the middle and on the other side of the filter. Extraction of the

Thèse accessible à l'adresse : https://theses.insa-lyon.fr/publication/2024ISAL0088/these.pdf © [C.K. Miyazaki], [2024], INSA Lyon, tous droits réservés

water was facilitated by a peristaltic pump, directing the water to a small container to enable conductivity to be measured by online sensors (CM2 and CM3). Subsequently, the water was reintroduced into the system via small piezometers located nearby downstream.

The internal measurements were used to observe the heterogeneity at the interface between primary and secondary filters. A comparison of the results obtained at the outlet for the saline tracer and amino-G acid is shown in Figures 7.3 – 7.7 (Appendix) to check the replicability of the amino-G results.

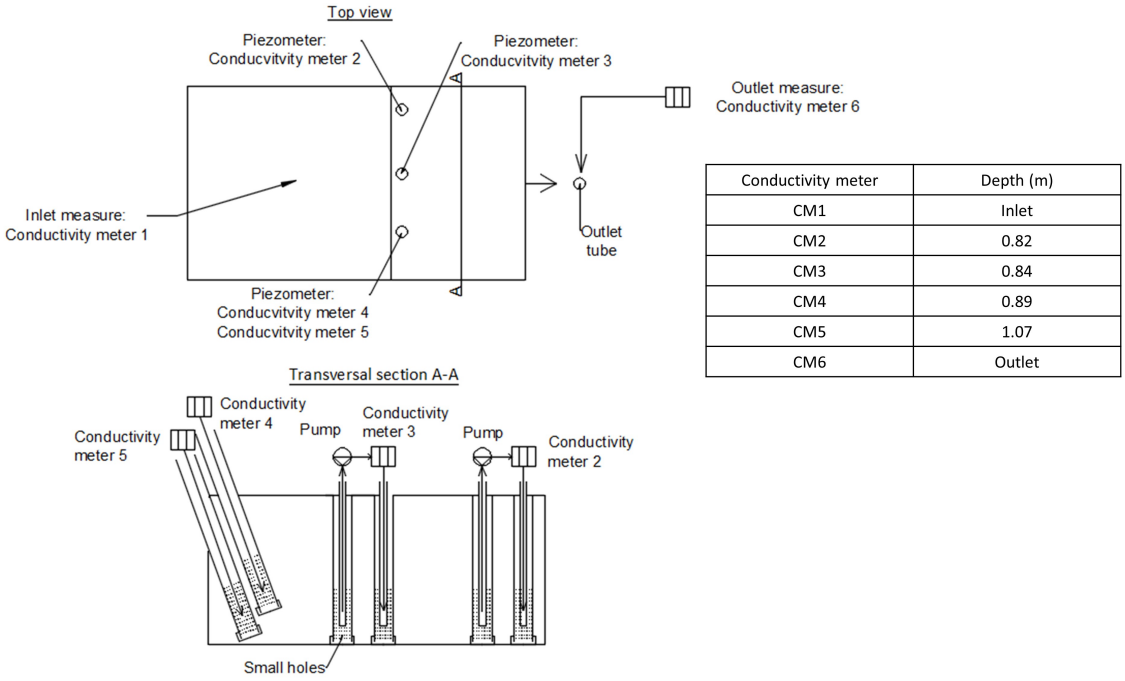

Conductivity meter	Depth (m)
CM1	Inlet
CM2	0.82
CM3	0.84
CM4	0.89
CM5	1.07
CM6	Outlet

Figure 3.3: Conductivity meter installed inside the filter, at the inlet and outlet in a top view and transversal section A-A.

The tracer data were analyzed to find the HRT, volumetric efficiency and the possible existence of preferential pathways (Kadlec and Wallace, 2009). Two methods were compared to obtain the best fit to the detention time distribution, the tank-in-series (TIS) and the parallel-path model (Kadlec and Wallace, 2009) (refer to Figure 7.2 in Appendix to compare each method). In the TIS model, a single Gamma distribution is calibrated with the method of the moments, and in the parallel-path model, a mixture of multiple gamma distributions is adopted. The latter was used to represent, for example, the short-circuit on a free wetland surface in Florida (Kadlec and Wallace, 2009; Wang and Jawitz, 2006).

The detention time distribution curve is obtained by normalizing the outlet concentration (Headley and Kadlec, 2007), as shown in Eq. 3.1.

Thèse accessible à l'adresse : https://theses.insa-lyon.fr/publication/2024ISAL0088/these.pdf © [C.K. Miyazaki], [2024], INSA Lyon, tous droits réservés

$$\text{Frequency} = \frac{C(t)}{\int_0^\infty C(t)\,dt} \qquad \text{(Eq. 3.1)}$$

Where C(t) is the tracer concentration at time t.

In this study, the parallel-path model characterized the curve shape better from the experimental data, thus it was the one chosen. The parameterization used for each Gamma distribution is a generalization of the Levenspiel curve for real-valued parameters. It depends on N, the Number of Tanks In Series parameter (NTIS), and τ, the hydraulic retention time. The finite mixture model of Gamma distributions are described by Eq. 3.2 and Eq. 3.3:

$$\text{f(t)} = \sum_{i=1}^{K} \alpha_i f_i(t) \qquad \text{(Eq. 3.2)}$$

$$\text{f}_i(t) = \frac{1}{\Gamma(N) \cdot \tau^N \cdot N^{-N}} t^{N-1} \cdot \exp\left(-\frac{tN}{\tau}\right) \qquad \text{(Eq. 3.3)}$$

With $f(t)$ being the mixture of $K = \{1, 2, 3, 4\}$ Gamma probability distribution function (pdf), denoted by $f_i(t)$, $\Gamma(N)$ being the gamma function, α_i being the mixture fraction of the i-th Gamma pdf, respecting Eq. 3.4, and t being the time.

$$\sum_{i=1}^{K} \alpha_i = 1 \qquad \text{(Eq. 3.4)}$$

N and τ were estimated by minimizing the sum of square error (SSE) between the experimental data and the pdf calculated (Kadlec and Wallace, 2009; Levenspiel, 2012; Wallace and Knight, 2006).

3.2.3 Full-scale system

In order to validate the replicability of the results for a larger scale, the same strategy used in the tracer test with 6 hours of aeration per day at a pilot scale (0.75h on, 2.25h off) was used at a full-scale hybrid aerated TW with similar configuration (Petitjean et al., 2023). The main parameters from the pilot and the full-scale are described in Table 3.2.

3.2.4 Limitations

Several unexpected issues during data collection influenced the quality of the information obtained. In the tracer 9h, the air blower failed during the first 10h of the tracer test, leading to an unstable behavior at the beginning of the concentration curve.

Thèse accessible à l'adresse : https://theses.insa-lyon.fr/publication/2024ISAL0088/these.pdf © [C.K. Miyazaki], [2024], INSA Lyon, tous droits réservés

Table 3.2: Operational parameters for the pilot and full-scale systems. NB = number of cycles per day, Operation = aeration ON (h per cycle), Stop = aeration OFF (h per cycle), HLR = hydraulic loading rate (m/d

Parameters	**6h/d – Pilot scale**	**6h/d – Full-scale**
Area size (m^2)	20	103
Batches per day	10	16
Applied volume (cm)	0.4	2.3
Feeding point	1 point/10 m^2	1 point/50 m^2
HLR	0.4	0.37
Period of the tracer test	March	June
Amino-G acid addition (g)	12	5.9
Aeration strategy	6h aeration/day	6h aeration/day each network (16 cycles)
NB	8	8
Operation	0.75h	0.75h
Stop	2.25h	2.25h
Unsaturated layer	0.35m depth	0.35m depth
Saturated layer	1m depth	1m depth

Thèse accessible à l'adresse : https://theses.insa-lyon.fr/publication/2024ISAL0088/these.pdf © [C.K. Miyazaki], [2024], INSA Lyon, tous droits réservés

Consequently, this tracer test was invalid, and the results are not presented hereafter. Analogous field-related issues involving pump malfunctions also affected the tracer test 9h, leading to inconclusive results for CM2 and CM3 (Figure 3.3 illustrates their location). Furthermore, an increased background concentration during the tracer test 0h with salt affected the interpretation of its results (refer to Figure 7.8 in Appendix to see the inlet - CM1). Nevertheless, it remains valid for the amino-G acid analysis.

Moreover, numerous tracer tests were conducted in the pilot-scale system, being the last one the tracer 0h. Even if filters were alternated between each tracer test, the long period of feeding without alternation for each tracer test (10 days) might have increased the solid accumulation rate on the surface and thus affected water distribution and infiltration at the surface of the primary filter. This might have impacted the hydrodynamics, especially on the tracer 0h, although quantifying is not possible.

3.3 Results and discussion

3.3.1 Tracer response curves (pilot scale)

The results for each experimental condition using amino-G acid are shown in Table 3.3. The theoretical HRT was calculated based on the saturated water depth, porosity, and surface area. The surface area is 20 m^2, according to the filter geometry. The porosity was assumed to be 40%, equivalent to a uniform gravel layer (Uggetti et al., 2016), and slightly higher than the range 25 - 34.5% of TWs filled with dune and river sand reported by Welz et al. (2018). The saturation level of the pilot varied between 0.84 m and 1 m due to batch volume and the difference in water height between outlet of filter 1 and 2 during the construction (5-8 cm difference). Table 7.1 (Appendix) presents the water depth details for each tracer test. The estimated theoretical residence time in this saturated zone is calculated to be around 1.9 days (43 - 44 h). Consequently, the hydraulic percolation time in the unsaturated zone (35 cm), considering the water content of 0.1, is around 2 - 3 hours. It is consistent with previous studies on this filter (Molle, 2003; Ruiz-Ocampo et al., 2022) and similar to those found for a VF TW in Brazil (Decezaro et al., 2019). Therefore, the total theoretical HRT was around 45h for all the tracer time (see Table 3.3).

The mass recovery rates in tracer tests 24h and 9h1 were 87% and 98%, respectively. These rates exceeded the 80% threshold considered conservative and suitable for deriving accurate hydraulic indices (Headley and Kadlec, 2007). The tracer tests 9h2 and 6h had lower mass recovery rates, 72%. The values found in the present work were similar to the 77% obtained in an aerated HF TW with continuous aeration between 8 am and 8 pm (Butterworth et al., 2016b), and are closer to the upper bound of the range 43 - 91% reported by HF TW and free water surface wetland (Gikas et al., 2017; Seeger et al., 2013;

Thèse accessible à l'adresse : https://theses.insa-lyon.fr/publication/2024ISAL0088/these.pdf © [C.K. Miyazaki], [2024], INSA Lyon, tous droits réservés

Table 3.3: Results for each experimental condition. $_{t}$HRT = theoretical HRT; $T_{initial}$ = the moment when the tracer was initially detected at the outlet; T_{median} = the duration required for 50% of the measured tracer mass reach the outlet; T_{mode} = time for reaching tracer concentration peak; T_{90}/T_{10} = Morrill dispersion index (T_{90} and T_{10} are the dimensionless times taken when the first 10% and 90% of the tracer reaches the outlet)

Parameter	**24h**	**9h1**	**9h2**	**6h**	**0h**
Filter fed	2	2	1	2	1
$_{t}$HRT (h)	45.4	45.2	45.1	45.0	45.0
$T_{initial}$ (h)	6.4	2.5	2.5	0.2	0.1
T_{median} (h)	35.7	38.2	28.6	36.1	28.2
T_{mode} (h)	31.5	28.1	22.3	30.7	14.2
T_{90}/T_{10}	3.0	3.6	4.5	3.7	6.4
Mass recovery rate (%)	87	98	72	72	65

Shih et al., 2016; Wang et al., 2023). The amount of tracer loss could be due to the tracer's degradation on the surface of the filter as a result of its photosensitivity or its adsorption on the organic matter (Kadlec, 2007; Kadlec and Wallace, 2009).

The lowest tracer mass recovery was for tracer test 0h, 65%. It could be due tracer degradation or sorption onto a solid surface (Kadlec and Wallace, 2009; Levenspiel, 2012). The total duration of the tracer test 0h was 164 h, 3.6 times the $_{t}$HRT. According to Levenspiel (2012)), when this duration is more than three times the $_{t}$HRT, some of the fluid is stagnant (dead zones) and flow velocity is low in these areas. When this happens, there is a risk of density effects and, consequently, density stratification, where the tracer sinks to the bottom (Headley and Kadlec, 2007). The findings suggest an increasing relationship between oxygen supply to the filter and the recovery rate (i.e., 0h $<$ 6h $<$ 24h). This correlation arises from the mixing promoted by aeration, which prevents the formation of stagnant zones where the tracer could be trapped.

The time of the first detection of tracer at the outlet ($T_{initial}$) was found to increase from the 0h to the 24h experiment. The first amino-G acid concentration was detected after 0.1h in the former and 6.4h in the latter. Such a delay may indicate that the absence of aeration favors preferential pathways while aeration vertically mixes the tracer, leading to a longer time to reach the outlet. The time necessary for reaching a peak concentration at the outlet (T_{mode}) indicated an influence of aeration of the primary filter. While the experiments 0h and 9h2 (i.e., without aeration on the primary filter) presented T_{mode} of 14.2h and 22.3h, respectively, the experiments 6h, 9h1 (i.e., aerated only on the

Thèse accessible à l'adresse : https://theses.insa-lyon.fr/publication/2024ISAL0088/these.pdf © [C.K. Miyazaki], [2024], INSA Lyon, tous droits réservés

primary filter) and 24h presented values of 30.7h, 28.1h and 31.5h, respectively. These results indicate that the aeration may positively affect the distribution of the tracer in its saturated layer, increasing the homogeneity inside the system and minimizing the creation of preferential pathways.

The normalized outlet tracer response curve are shown in Figure 3.4 and Figure 7.1 (Appendix) presents the concentration curves. For the tracer test 0h shows distinct minor peaks throughout the experiment, representing the batch effect. On the contrary, in the other tracer tests, the curve appears smoother, devoid of minor small peaks. This effect can be attributed to the amortization caused by aeration. Hence, these effects operate in divergent manners: the increase of tracer concentration at the outlet upon batch arrival and the retention of the tracer during aeration periods.

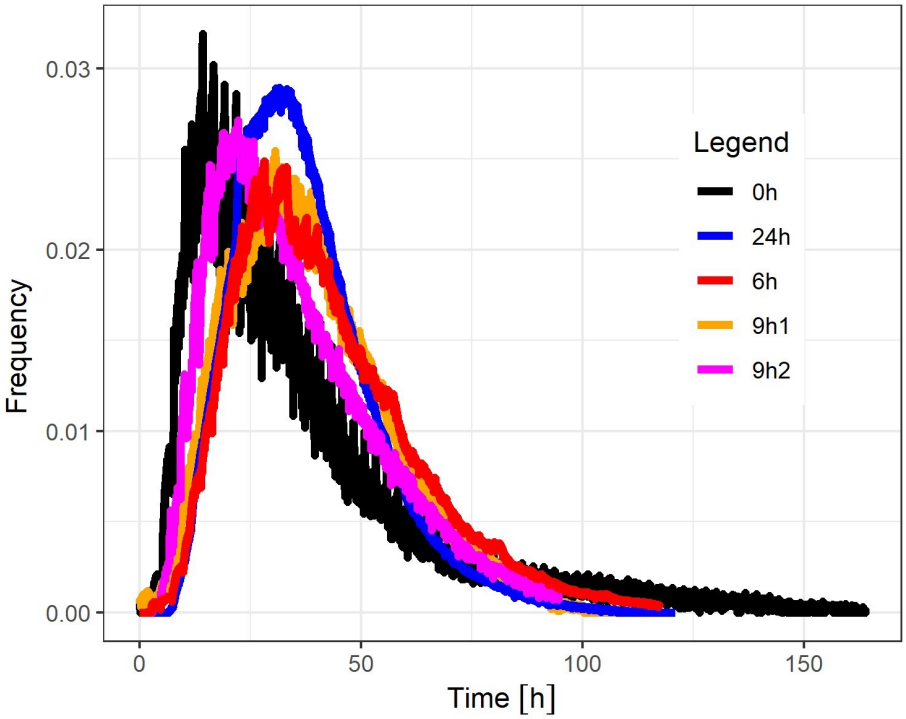

Figure 3.4: Normalized frequency over time for each aeration strategy

Moreover, the tracer test 0h has sharp peak, indicating short-circuiting, and a remarkably longer tail than the other tests, representing the impact of stagnant regions and dead zones inside the system (Levenspiel, 2012). In those zones, the volume is not being used, leading to a lower effective volume and possibly compromising the efficiency of the treatment (Cota et al., 2011). Concerning other parameters, the tracer test 0h had extreme values: the lowest $T_{initial}$ (i.e., 0.1h), representing a channeling; and the highest ratio Morrill dispersion index (i.e., T_{90}/T_{10}), 6.4, among all tracer experiments, indicating the high dispersion of the curve. The tracer test 24h presented a low T_{90}/T_{10} ratio of 3.0 due to the time-lag of $T_{initial}$, which is characterized by a plug flow (i.e., T_{90}/T_{10} ratio

Thèse accessible à l'adresse : https://theses.insa-lyon.fr/publication/2024ISAL0088/these.pdf © [C.K. Miyazaki], [2024], INSA Lyon, tous droits réservés

closer to 1 (Ling et al., 2015) with mixed flow (Levenspiel, 2012). Butterworth et al. (2016b) found T_{90}/T_{10} values similar to the current research in a no-aerated HF TW (4.5). Nevertheless, it shows that more flow heterogeneity is present when there is no aeration (preferential pathways, dead zones, different water velocities).

Overall, these findings highlight the influence of aeration on system homogenization, indicating that a decrease in aeration led to a reduction in the tracer mass recovery rate, $T_{initial}$, and an increase in tracer dispersion. Moreover, the results indicate that the system behaves differently when aeration is performed in the primary or secondary filter, with different responses of hydraulic mixing upon batch arrival.

3.3.2 Modelling outlet tracer curve

For all tracer tests except the non-aeration (0h), a mixture of two Gamma distributions presented the best fit, with a SSE below 0.002 in all cases. For the 0h test, a mixture of three Gamma distributions presented an SSE of 0.007, which better describes the curve behavior. The weighted parameters extracted from these fits are presented in Table 3.4.

Specifically in the tracer test 24h, 15% of the flow behaved as a tank with a HRT of 47.1h and NTIS of 3.9, while the remaining 85% of flow water behaved as a tank with a HRT of 35.8h and NTIS of 6.6. This observation implies the existence of two concurrent dynamics within the system, with a smaller fraction of the total volume approaching the CSTR behavior (Wallace and Knight, 2006), and a larger part behaving like a plug-flow reactor.

In tracer tests 24h, 9h1 and 6h, one of the two parallel paths dominated the flow, indicating a more homogeneous flow. In these tests, 85, 85 and 78% of the flow presented a HRT of 35.8h, 44.7h and 43.1h, respectively, and the other 15, 15 and 22% of the flow presented a HRT of 47.1h, 28.9h and 24.9h. On the contrary, the tracer tests 9h2 and 0h presented more heterogeneous pathways. For 9h2, the flow was split between 41% (distribution #1) and 59% (distribution #2), while for 0h, the behavior was split between 24% (distribution #1), 60% (distribution #2) and 16% (distribution #3). These results align with the findings outlined in section 3.3.1, emphasizing that aeration applied on the primary filter enhanced the overall mixing within the filter, while the absence of aeration in this filter led to more heterogeneity. Thus, an optimal hydraulic operation could be achieved with sequenced aeration of the primary filter and for a duration between 6h and 24h per day. The importance on aerating primary filter for total nitrogen removal was also proved by Chapter 4.

Upon comparing the weighted distribution NTIS, minimal variance was observed among the tracer test 24h, 9h1, 9h2, 6h and 0h (i.e., 6.2, 5.1, 5.5, 5.4, 5.8, respectively). These findings correspond with those observed in a study focusing on continuously aerated

Thèse accessible à l'adresse : https://theses.insa-lyon.fr/publication/2024ISAL0088/these.pdf © [C.K. Miyazaki], [2024], INSA Lyon, tous droits réservés

Table 3.4: Results for gamma fitting model for each aeration strategy. t = theoretical; e_v = volumetric efficiency; WD = weighted distribution; σ^2 = variance $\left(\int_0^\infty (time - HRT)^2 f(t)dt\right)$; σ_θ^2 = normalized variance $\left(\frac{\sigma^2}{HRT^2}\right)$. When appropriate, values are reported with the corresponding distribution (e.g., #1 referring to the first gamma distribution). *The weighted HRT was calculated by computing numerically the first moment of the gamma mixture. The weighted NTIS is the individual NTIS multiplied by their corresponding flow fractions.

Parameter	**24h**	**9h1**	**9h2**	**6h**	**0h**
SSE	0.001	0.001	0.001	0.002	0.007
$_t$HRT (h)	45.4	45.1	45.0	45.0	45.4
HRT (h)	47.1(#1) 35.8(#2)	28.9(#1) 44.7(#2)	22.6(#1) 45.1(#2)	24.9(#1) 43.1(#2)	14.8(#1) 33.7(#2) 88.8(#3)
NTIS	3.9 (#1) 6.6 (#2)	8.9 (#1) 4.4 (#2)	5.8 (#1) 5.3 (#2)	4.4 (#1) 5.7 (#2)	6.5 (#1) 5.1 (#2) 7.5 (#3)
Flow fraction	15%(#1) 85%(#2)	15%(#1) 85%(#2)	41%(#1) 59%(#2)	22%(#1) 78%(#2)	24%(#1) 60%(#2) 16%(#3)
WD.−HRT(h)*	37.4	42.2	35.9	39.1	37.8
e_v (%)	83%	93%	80%	87%	84%
WD.−NTIS*	6.2	5.1	5.5	5.4	5.8
σ^2	252.2	393.7	327	334.5	780
σ_θ^2	0.18	0.23	0.27	0.22	0.56

Thèse accessible à l'adresse : https://theses.insa-lyon.fr/publication/2024ISAL0088/these.pdf © [C.K. Miyazaki], [2024], INSA Lyon, tous droits réservés

HF TW, which reported a value of 5.2 for NTIS (Boog et al., 2020). However, they differ from those obtained for non-aerated HF TWs, with NTIS values of 11.3 (Seeger et al., 2013) and 11.0 (Kadlec and Wallace, 2009). Nevertheless, If N values are often used in N-k-C* model for design application (Von Sperling et al., 2023), the similar N values obtained in all conditions may be tricky to fit a global NTIS value on complex designed systems. Further studies is necessary to confirm if a N-k-C* model can be fitted with a common NTIS value for different aeration strategies or if the hybrid system should be divided by zones/compartments to combine different NTIS values.

The normalized variance measures the distribution variability as a function of the tracer detention time, being an useful parameter to compare the hydraulic performance between tracer tests. According to Wang and Jawitz (2006), higher hydraulic performance is achieved when the volumetric efficiency (e_v) increases and the normalized variance (σ_θ^2) decreases at the same time. In this current research, the results for the tracer test 24h had similar e_v than the tracer test 0h, 83% and 84%, respectively, but a considerably lower σ_θ^2 value (i.e., 0.18 vs 0.56, respectively). Despite the slight variation in e_v, the large drop in σ_θ^2 indicates that the 24h tracer test had better hydraulic performance, while the 0h tracer test presented greater dispersion due to hydraulic anomalies, such as potential short circuits, preferential pathways and dead zones. The heavy tail observed in the tracer test 0h was also seen by Butterworth et al. (2016b) in field experiences performed in a full-scale HF TW without aeration.

The tracer test 0h deserves further details due to its more complex behavior than the other tests. Its response curve had a unique shape, demanding a higher number of Gamma distributions to capture all its variations. Figure 3.5A presents the normalized frequency over time for each mixture of gamma distributions fitted to the data, up to three distributions. It can be seen that a single gamma distribution (1 gamma) cannot capture the heavy tail observed. Figure 3.5B shows the shape of each individual, unweighted, gamma that compose the final three-gamma adopted for this case. The transition of shapes from strong plug flow behavior (i.e., red curve) to CSTR behavior (i.e., orange curve) over time suggests the existence of multiple pathways and a variable flow within the filter, which largely deviates from other tracer test curves. According to Kadlec and Wallace (2009) the need for multiple gamma distributions to model complex response curves may indicate poor hydraulic behavior of TW. This important property suggests that the test with no aeration, 0h, may have had a more heterogeneity than the other tests, since three instead of two gamma distributions were necessary.

The complex behavior of the tracer inside the system suggests that measuring tracer concentration only at the outlet seems insufficient to comprehend the hydraulics of this hybrid system; such issues could have been impacted by variable internal flow, lateral and longitudinal movement and interference of vegetation density (Kadlec and

Thèse accessible à l'adresse : https://theses.insa-lyon.fr/publication/2024ISAL0088/these.pdf © [C.K. Miyazaki], [2024], INSA Lyon, tous droits réservés

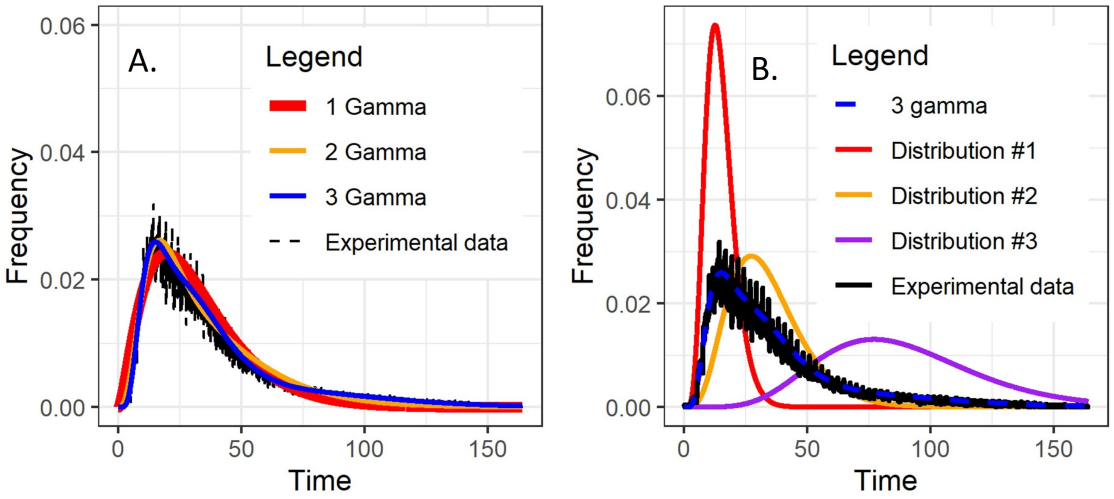

Figure 3.5: A (left) – Normalized frequency over time for overall result for each gamma distribution for tracer 0h. B (right) - Normalized frequency over time for each individual, unweighted, gamma that compose the final mixture distribution, which is the 3 gamma (tracer 0h).

Wallace, 2009). Besides, it is crucial to recognize that the underlying assumptions of the NTIS model do not align with the intuitive understanding of aeration processes. Thus, the characteristic shape of the response curves obtained, and the information provided on the hydraulic behavior of the system indicated that the tanks in parallel model coupled with fully mixed reactors to simulate dead zone might be a more suitable and realistic model for the system. Therefore, further studies to understand the hydraulic anomalies should focus on performing internal measurements that would allow going towards more complex and comprehensive model approach.

3.3.3 Internal tracer measurement

While sections 3.3.1 and 3.3.2 highlighted the impact of aeration from the point of view of a "black box" system, this present section explores possible hydraulic dysfunctions through internal measurements. Among all the experimental conditions assessed, only the internal behaviors of the 24h, 9h1, 9h2 and 6h tests were properly measured and are presented (section 3.2.4 pointed out the experimental limitations). As depicted in Table 3.5 and Figure 3.6, distinct responses were observed for each CM employed and for each aeration strategy.

The results for the 24h aeration strategy show that CM3, CM4, and CM5 had similar responses, both in terms of peak concentration time (17.8 h, 20.4 h and 21.7 h, respectively) and curve shape. Results for tracer test 9h1 pointed to similar mode times for the tracer reaching CM2, CM4 and CM5, indicating convergence in curve shapes (i.e., 20.1 h, 20.4 h and 23.1 h, respectively). Notably, CM2 presented channeling or bypassing in

Thèse accessible à l'adresse : https://theses.insa-lyon.fr/publication/2024ISAL0088/these.pdf © [C.K. Miyazaki], [2024], INSA Lyon, tous droits réservés

Table 3.5: Results for the salt tracer tests. $T_{initial}$ = time of the first detection of the tracer at the outlet; T_{median} = Time for exiting of 50% of measured tracer mass in the effluent; T_{mode} = time for reaching tracer concentration peak T_{90} = Time for exiting of 90% of measured tracer mass in the effluent

Tracer test	**Position (Figure 3.3)**	**$T_{initial}$ (h)**	**T_{median} (h)**	**T_{mode} (h)**	**T_{90} (h)**
SALT - 24h	CM2	0	19.6	14.3	43.4
	CM3	0.1	21.7	17.8	38.8
	CM4	0	22.1	20.4	48.2
	CM5	0.1	22.5	21.7	48.7
	Outlet	15.5	34.6	34.1	46.5
SALT - 9h1	CM2	0	24.8	20.1	45.9
	CM3	0	24.2	14.5	48.1
	CM4	0	26.4	20.4	48.5
	CM5	0	26.6	23.1	48.7
	Outlet	6.5	38.6	33.1	66.9
SALT - 9h2	CM2	0	11.5	8.2	30.8
	CM3	0	16	2.1	37.5
	CM4	0.3	13.3	7.8	36.6
	CM5	0	13.3	9.1	53
	Outlet	1.3	28.3	22.3	55.3
SALT - 6h	CM2	0.6	19.7	8.5	52.5
	CM3	0.6	26.2	22.4	57.8
	CM4	0.6	28.5	20	55.6
	CM5	2.1	28.9	23.1	53.4
	Outlet	0.6	35.8	30.6	60.2

Thèse accessible à l'adresse : https://theses.insa-lyon.fr/publication/2024ISAL0088/these.pdf © [C.K. Miyazaki], [2024], INSA Lyon, tous droits réservés

tracer tests 24h, 9h2 and 6h, exhibiting an accelerated water flow and potentially reducing the HRT to lower values than the theoretical HRT (Kadlec and Wallace, 2009). This pattern points the non-homogeneous distribution either of the batch on the surface of the filter and/or to the existence of a preferential pathway within this filter.

For 9h2, the T_{mode} for CM2 and CM3 indicated faster response times (9h2: CM2 = 8.2 h and CM3 = 2.1 h) than tracer 24h, 9h1 and 6h. These results suggest spatial heterogeneity when the primary filter is not aerated, aligning with the finding in section 3.3.1. In addition, Figure 3.6 shows high peaks and disturbances in internal measures.

Across all aeration strategies, no distinguishable variation was detected between CM4 and CM5 (Table 3.5, Figure 3.6), which were positioned vertically at two different depths (Figure 3.3). Hence, the hypothesis is that there exists uniform flow velocities within the vertical profile, while recognizing the possibility of mixing issues in the horizontal profile. In that case, the distribution of residence times might not be solely a consequence of mixing processes induced by aeration (Headley and Kadlec, 2007; Kadlec, 2000). Instead, it could result from variations in flow velocities in horizontal distribution.

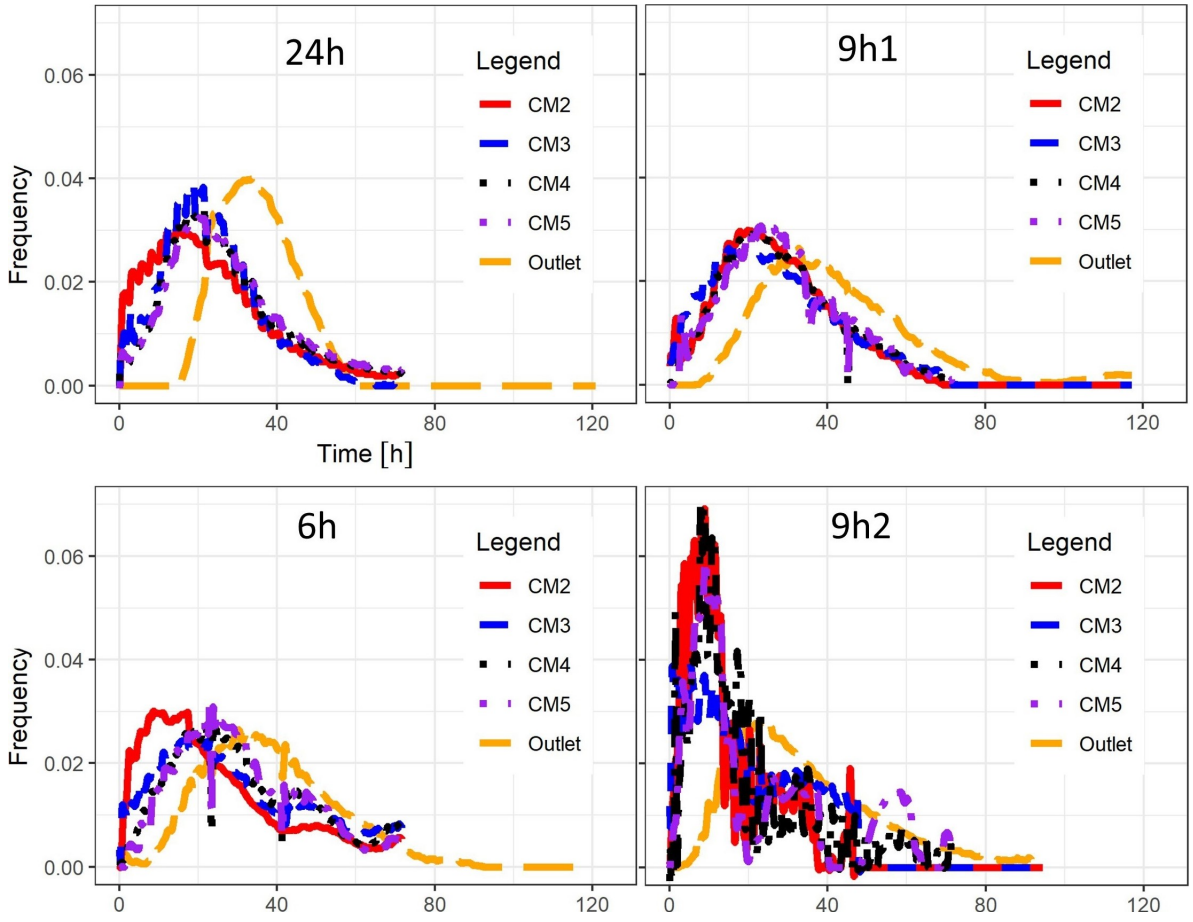

Figure 3.6: Normalized frequency over time for 24h, 9h1, 9h2 and 6h aeration per day. The conductivity meters were placed according to Figure 3.3. CM stands for conductivity meter.

Thèse accessible à l'adresse : https://theses.insa-lyon.fr/publication/2024ISAL0088/these.pdf © [C.K. Miyazaki], [2024], INSA Lyon, tous droits réservés

Particularly in the 6h aeration strategy, the CM2 (with concentration peak time at 8.5 h) was influenced by the vertical aeration, displaying a discernibly distinct response in comparison to the 24-hour strategy (with peak time at 14.3 h). The same observation was found in Table 3.3, where the T_{mode} for 24 h was slightly higher, meaning that the driplines on the bottom release air bubbles and go towards the surface. This movement conflicts with the horizontal flow, adding a vertical flow mixing. Thus, the tracer is kept inside the system for a longer time. Furthermore, substantial perturbations were evident in the background concentration, which remained uncorrected, given its continuous variability. This issue led to the presence of minor fluctuations at the tail in the tracer tests 9 h and 6 h. Overall, the internal measurements pointed to a noticeable spatial heterogeneity between filters primary and secondary, showcasing preferential pathways in CM2 and CM3, alongside with an effective vertical mixing.

3.3.4 Comparison between pilot versus full-scale

Figure 3.7 illustrates the normalized frequency over time for the pilot and full-scale. Both curves have similar shapes but different batch peaks over time. While the pilot has controlled batch hours, every 2h30 (4 m^3 per day), the full-scale has around 15 – 16 batches per day (around 17.7 m^3 per day), depending on the inflow. This difference between curves also affected the heavy tail on the full-scale, resulting in a tracer concentration of between 0.0035 and 0.0141 mg/L after 4 days (representing 5.5% of the total mass recovered). The heavy tail was also observed in another HF TW full-scale system aeration (Butterworth et al., 2016b).

Table 3.6 summarizes the main results from the gamma distribution analysis. In both tracer tests, the theoretical HRT were similar, 45.0 h (i.e., 1.9 days) and 42.7 h (i.e., 1.8 days) for pilot and full-scale, respectively. However, the actual detention time revealed that the full-scale system outperformed the pilot scale, demonstrating a volumetric efficiency of 97% compared with 87% for the pilot scale.

Table 3.6: Results for the pilot and full-scale

Parameter	**6h/d – Pilot scale**	**6h/d – Full-scale**
tHRT (h)	45.0	42.7
HRT (h)	39.1	41.4
Volumetric efficiency (%)	87	97
Mass recovery rate (%)	72	86
NTIS	5.4	4.1

Thèse accessible à l'adresse : https://theses.insa-lyon.fr/publication/2024ISAL0088/these.pdf © [C.K. Miyazaki], [2024], INSA Lyon, tous droits réservés

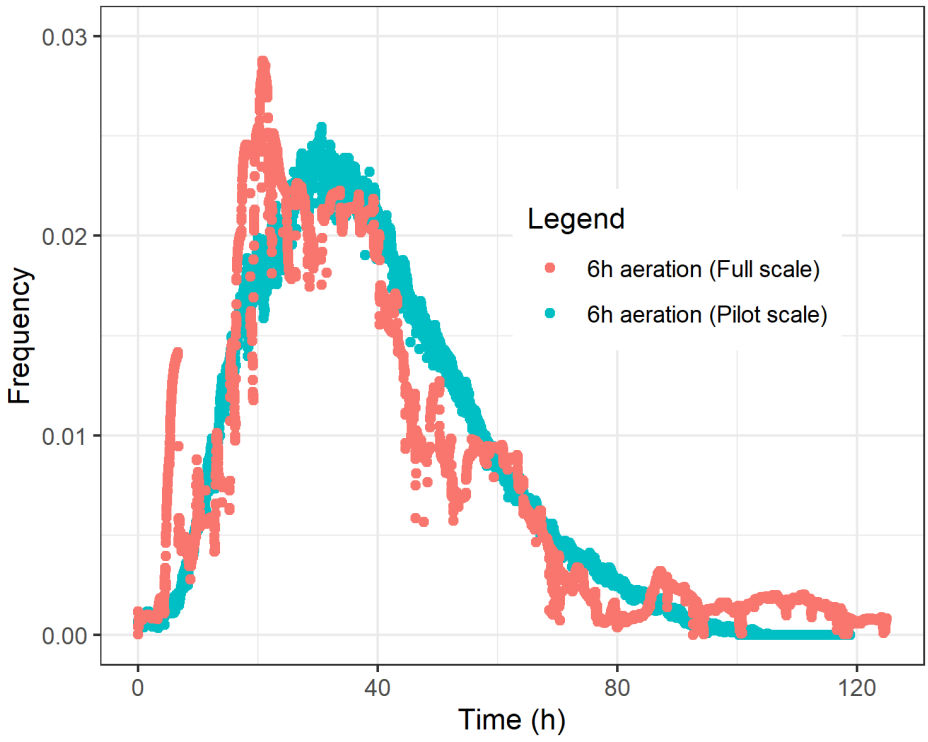

Figure 3.7: Normalized frequency over time for the pilot and full-scale with 6-hours of aeration per day

The NTIS was 5.4 and 4.1 for the pilot and full-scale system, respectively. The slight discrepancy could be attributed to the study periods, given that the pilot was conducted in spring and the full-scale in summer. Chazarenc et al. (2003) also noted an influence on the response curves when weather conditions varied. Overall, both values can be considered similar, suggesting that the results acquired in the pilot could be transposed on a large scale, even though there are a scale factor of five (the pilot system has 1 feeding point in 10 m^2 and the full-scale has 1 point every 50 m^2). These findings are a valuable link between pilot scale experimentation and real-world application, fulfilling a crucial need in applied research (Sustainability, 2019). The results also validate the repeatability and consistency of the results from a small scale (pilot scale) to a medium scale (full-scale). Given that the design guidelines for a French Vertical Flow TW recommend one feeding point every 50 m^2 (Dotro et al., 2017) to maintain a water distribution on the surface and that the full-scale system follows this feeding point density design, the tracer curve results for larger scales would likely be similar to those of the full-scale tracer test. Consequently, regardless the size of the system, either small or large facilities, the feeding point density and the surface water distribution will be the same. As consequence, the full-scale system used in this present study should be representative for larger scales.

Thèse accessible à l'adresse : https://theses.insa-lyon.fr/publication/2024ISAL0088/these.pdf © [C.K. Miyazaki], [2024], INSA Lyon, tous droits réservés

3.4 Conclusions and perspectives

The study investigated the effect of aeration on the hydrodynamics of a hybrid vertical and horizontal aerated TW by means of tracer tests and different aeration strategies in parallel. The results indicated a clear distinction between without aeration and with an aeration strategy of 24 hours. On one hand, the tracer test with 24 hours of aeration allows mixing the tracer within the filter, making flows more homogeneous and minimizing short-circuits; on the other hand, no aeration leads to greater flow heterogeneity, with different water velocity and dead zones. Concerning the aeration duration, comparison between tracer tests with 24 hours, 6 hours and 0 hours of aeration indicated a consistent relationship between the amount of oxygen supplied to the system and the mass recovery rate (i.e., 24 hours $>$ 6 hours $>$ 0 hours). Distinct hydraulic behavior was observed when aeration was performed on the primary (tracer test with 9 hours of aeration on the primary filter) or the secondary filter (tracer test with 9 hours of aeration on the secondary filter). Given the potential heterogeneity in the water distribution on the surface of the primary filter and the varied flow directions (vertical and horizontal), aeration of the primary filter becomes crucial. This aeration increases the mixing process and reduces preferential pathways.

The response curve at the outlet was modelled using two gamma distributions for most of the tracer tests, except for the case without aeration, where three gamma distributions were required. This finding indicated the existence of more complex hydraulic pathways within the system when there is no aeration. Optimal hydraulic operation would be achieved with sequenced aeration of the primary filter and for a duration of more than 6 h/d and less than 24 hours, which is consistent and compatible with the objective of reducing total nitrogen in this process (Chapter 4). Overall, the tracer tests show that aeration can change the hydrodynamics, but the outlet measurements are not able to detect the different zones (e.g., unsaturated or saturated) within the system. Consequently, future studies should incorporate internal measurements and explore more complex mechanistic or process engineering models to better describe the hydrodynamics in each compartment or in the system as a whole.

3.5 Learnings

Previous tracer studies tested limited conditions, without exploring the aeration strategies impact on hydraulics. This chapter we focused on exploring these limitations by implementing six parallel tracer tests on a pilot scale, using distinct aeration strategies (varying the aeration duration and differentiating the aeration between the primary and secondary filters) with sensors monitoring the middle and the outlet. We also conducted a tracer test on a full-scale system to verify the upscale results. We found that:

Thèse accessible à l'adresse : https://theses.insa-lyon.fr/publication/2024ISAL0088/these.pdf © [C.K. Miyazaki], [2024], INSA Lyon, tous droits réservés

- When establishing an aeration strategy, it is essential to consider the significant impact of aeration on the primary filter and the mixing process, which helps to minimize preferential pathways.
- The longer aeration duration prevents the formation of dead zones.
- Preferential pathways were identified with internal measurements.
- The hydraulic performance and, as consequence, the system performance, could be affected in case of reduction of aeration duration. Thus, for an optimal setting, it is recommended to aerated at least 6h per day.
- Full-scale results are in agreement with pilot scale system.

The significant findings helped us to identify the effects from the aeration strategies on the hydraulic behavior. The NTIS value results have been implemented on Chapter 5 to couple the hydraulic and kinetics on the N-k-C^* model.

Thèse accessible à l'adresse : https://theses.insa-lyon.fr/publication/2024ISAL0088/these.pdf © [C.K. Miyazaki], [2024], INSA Lyon, tous droits réservés

Thèse accessible à l'adresse : https://theses.insa-lyon.fr/publication/2024ISAL0088/these.pdf © [C.K. Miyazaki], [2024], INSA Lyon, tous droits réservés

Chapter 4

Aeration strategies and total nitrogen removal in a hybrid aerated treatment wetland

Abstract

This study investigates the impact of aeration strategy on the performance of total nitrogen (TN) removal in a compact hybrid aerated treatment wetland (TW), called Rhizosph'air®. The system combines a single-stage French vertical flow wetland with an aerated horizontal flow wetland, offering a unique and flexible approach for optimizing TN removal. In total, seven experimental conditions were tested, with different aeration modes, hydraulic loading rates, and ammonium addition. The wetland system demonstrated high performance in terms of COD removal (> 85%) and solids removal (> 90%), regardless of the experimental condition. However, TN removal was found to be directly impacted by operational changes. Increasing the hydraulic loading rate from 0.15 m/d to 0.25 m/d led to an improvement in TN removal, achieving over 60%. Furthermore, when ammonium was added to the inlet and when the aeration timing was synced with the timing of the influent batch load, the environmental conditions facilitated denitrification process, resulting in TN removal of approximately 70% and the lowest effluent NO_3-N concentrations (8.70 ± 4.40 mg/L). In summary, the timing of aeration strategy according to influent batch loading improved TN removal, suggesting its potential for optimization in future studies.

Keywords: Aerated wetland, Constructed wetland, French vertical flow, Horizontal flow, Wastewater

Thèse accessible à l'adresse : https://theses.insa-lyon.fr/publication/2024ISAL0088/these.pdf © [C.K. Miyazaki], [2024], INSA Lyon, tous droits réservés

This chapter was published as: Miyazaki, C.K., Morvannou, A., Higelin, E., Nivala, J., Molle, P., 2023. Aeration strategies and total nitrogen removal in a hybrid aerated treatment wetland. Blue-Green Systems 5, 321–335. https://doi.org/10.2166/bgs.2023.045

Thèse accessible à l'adresse : https://theses.insa-lyon.fr/publication/2024ISAL0088/these.pdf © [C.K. Miyazaki], [2024], INSA Lyon, tous droits réservés

4.1 Introduction

TWs have gained considerable attention for wastewater treatment due to their robustness, low operation and maintenance requirements, and ability to deliver high-quality effluent (Morvannou et al., 2015). TN in wastewater is usually removed through the use of the traditional nitrification-denitrification pathway. The process requires two steps: aerobic autotrophic nitrification to transform ammonia into nitrates and anoxic heterotrophic denitrification to transform the nitrates into nitrogen gas. Both phases demand specific environmental conditions, foremost the oxygen concentration and organic carbon source (Saeed and Sun, 2012). Passive TWs usually require two or three treatment stages to address TN removal by implementing separate aerobic and anoxic filters. Therefore, depending on the chosen design, the land requirement can vary between 4 to 10 m^2.population equivalent $(PE)^{-1}$, which is a disadvantage for these systems (Dotro et al., 2017) compared to conventional systems (0.12 – 0.3 $m^2.PE^{-1}$ for activated sludge).

In addition, passive TWs have some limitations regarding pollutant removal; namely, horizontal flow (HF) wetlands do not nitrify to a great extent, and vertical flow (VF) wetlands nitrify but are limited in their capacity to remove TN (Cross et al., 2021; Masih, 2017; Zhuang et al., 2019). While VF TWs exhibit almost complete ammonium removal (upwards of 90 %), passive TWs (either vertical or horizontal) achieve around only 20-50% TN removal (Cross et al., 2021). Consequently, considering the restrictions imposed on nutrient discharge and the problem of available land area in urban areas, intensified TW designs have been developed. The term "intensification" implies the use of energetic, chemical or operational modifications to increase pollutant removal (Fonder and Headley, 2010). By adopting an energy-oriented approach, it becomes possible to enhance the availability of oxygen within a TW, thereby promoting the removal of oxygen-requiring compounds such as carbon and ammonium.

Aeration in TW refers to the injection of air into the system, enabling aerobic conditions in a saturated zone. Aerated TW technology was created over 25 years ago (Wallace, 2001), and its implementation has witnessed a notable surge over the past decade. Today, approximately 500 aerated TW systems are operational on a global scale (Nivala et al., 2020). The main advantage of aerated TWs are their ability to completely nitrify (Cross et al., 2021; Masih, 2017; Zhuang et al., 2019), and their compactness compared to passive TWs (1 $m^2.PE^{-1}$ versus 4 – 5 $m^2.PE^{-1}$) (DWA, 2017); consequently, rendering them more viable for implementation where land availability is limited, such as in urban areas. Despite the disadvantage of increased energy costs, those systems operate at low pressure and consume less energy than conventional intensive wastewater treatment plants (Rochard, 2017b).

Moreover, intermittent or controlled aeration strategies (compared to continuous

Thèse accessible à l'adresse : https://theses.insa-lyon.fr/publication/2024ISAL0088/these.pdf © [C.K. Miyazaki], [2024], INSA Lyon, tous droits réservés

24/7 aeration) have demonstrated the potential to enhance denitrification processes in aerated wetlands (Dotro et al., 2017). Continuous aeration has been shown to achieve TN concentration removal ranging from 15% to 60% (Cross et al., 2021; Nivala et al., 2019a) and intermittent aeration has been found to optimize TN removal, yielding removal efficiencies of up to 90% (Masih, 2017).

Recent configurations and adaptations have been mixing the aeration and hybrid TW to go even further in the TN removal. One of this system, known as Rhizosph'air® (Troesch et al., 2020), allows the nitrification and denitrification processes in a single-stage TW. The aeration in this system provides increased oxygen transfer, resulting in the reduction of the system footprint from 2 $m^2.PE^{-1}$ (classical two-stage French VF wetland) to 0.8 – 1.2 $m^2.PE^{-1}$ depending on the conditions (Cross et al., 2021; Dou et al., 2016). This hybrid system have been installed around France (18 plants) and one of them was monitored during two years, treating domestic wastewater for 1,400 PE (Prost-Boucle and Molle, 2021). Regardless of the tested aeration mode, the treatment performances for COD, BOD_5, and TSS consistently remained high and stable. However, under the aeration mode of 12 hours per day divided into four cycles, nitrification was successfully achieved, while denitrification was limited due to insufficient carbon availability. To enhance TN removal, a reduction in the daily aeration duration proved beneficial. By adopting a four-cycle aeration mode with a total duration of 3 hours per day, the system was capable of remove 97% COD concentration and 82% TN concentration, remaining 19 mg TN/L at the outlet.

However, they tested limited aeration strategies with high variability in inflow and outflow. This current research intends to go further by testing the difference between each experimental condition in a controlled system, allowing a comparison to be made. Thus, to guarantee a stable and optimized nitrogen removal, it is crucial to adapt aeration strategies to meet specific treatment goals, ranging from complete nitrification to nearly complete removal of TN. Aeration strategies should be based on carbon and nitrification requirements, considering the absence of oxygen for denitrification. Therefore, this research aims to investigate the impact of aeration strategy in a hybrid aerated vertical/horizontal flows TW on the performance of TN removal.

4.2 Material and methods

4.2.1 Treatment wetland pilot

The industrial pilot-scale TW studied is part of the REFLET research platform (https://eng-reversaal.lyon-grenoble.hub.inrae.fr/equipment-platforms/reflet), located in Craponne, France, a commune situated in the Auvergne-Rhône-Alpes region. The pilot

Thèse accessible à l'adresse : https://theses.insa-lyon.fr/publication/2024ISAL0088/these.pdf © [C.K. Miyazaki], [2024], INSA Lyon, tous droits réservés

system had one month of start-up before starting the sampling campaign. Its commission started in January 2019. At total, the pilot covers an area of 20 m^2 (8 × 2.5 m). It replicates Rhizosph'air® system, which comprises a single-stage French VF TW, receiving raw wastewater directly on the surface of the filter, above an aerated HF TW. This arrangement enables the TW system to provide combined primary and secondary wastewater treatment.

The TW receives wastewater from around 4 m^3/d (26 PE), collected by a combined sewer from the upstream sewage basin produced by the community. The domestic wastewater has a ratio of COD/BOD_5 of approximately 2.0, showing that is a typical municipal untreated wastewater (Kadlec and Wallace, 2009).

The TW is planted with *Phragmites australis* and the upper layer is divided into two filters (10 m^2 each) by a PVC plate embedded up to the level of the filtration (0.2 m depth) and transition layers (0.15 m depth). While plants can impact nutrient transformation, sequestration and uptake (Val del Río et al., 2017) the main role of plants in this system is related to their mechanical role to avoid surface clogging. Indeed, nutrient uptake is minor compared to the load applied. This division allows for alternating feeding/resting phases of the filters (3.5 days each) to ensure mineralization of the organic deposit layer. The TW is fed by batches, and the filter that actively receives wastewater is referred to as the "primary filter" (PF), while the filter at rest is referred as the "secondary filter" (SF). The drainage system of the pilot system is designed such that during the feeding phase of the PF, the outflow is directed to the outlet of the SF, which is achieved through the opening and closing of associated electro-valves, as depicted in 4.1.

The saturation layer (1 m depth) is shared between the two parallel filters. Aeration of the system is accomplished by employing 120 driplines positioned at the bottom of the saturation layer (60 diffusers/m^2). The aeration process is facilitated by two side channel blowers (Becker SV 5.90/1). The estimated supply airflow rate for each blower is approximately 15 m^3/h (equivalent to 1.5 m^3/h/m^2). It is worth noting that no gas flow meter or temperature sensor was installed and therefore, the airflow rate estimation is based on these specifications.

4.2.2 Pilot operation and experimental conditions

In order to evaluate the influence of aeration timing on nitrogen removal dynamics in the hybrid aerated TW, seven experimental conditions were tested. Table 4.1 and Figure 4.2 present the experimental condition parameters. The nomenclature for each experimental condition follows the order: T or F (aeration based on time or feeding), sum total aeration time per day (the same aeration for both filters or differentiating aeration for each filter, in h/d), hydraulic loading rate (HLR) on the primary filter (in m/d), the addition or not of ammonium (NH_4-N).

Thèse accessible à l'adresse : https://theses.insa-lyon.fr/publication/2024ISAL0088/these.pdf © [C.K. Miyazaki], [2024], INSA Lyon, tous droits réservés

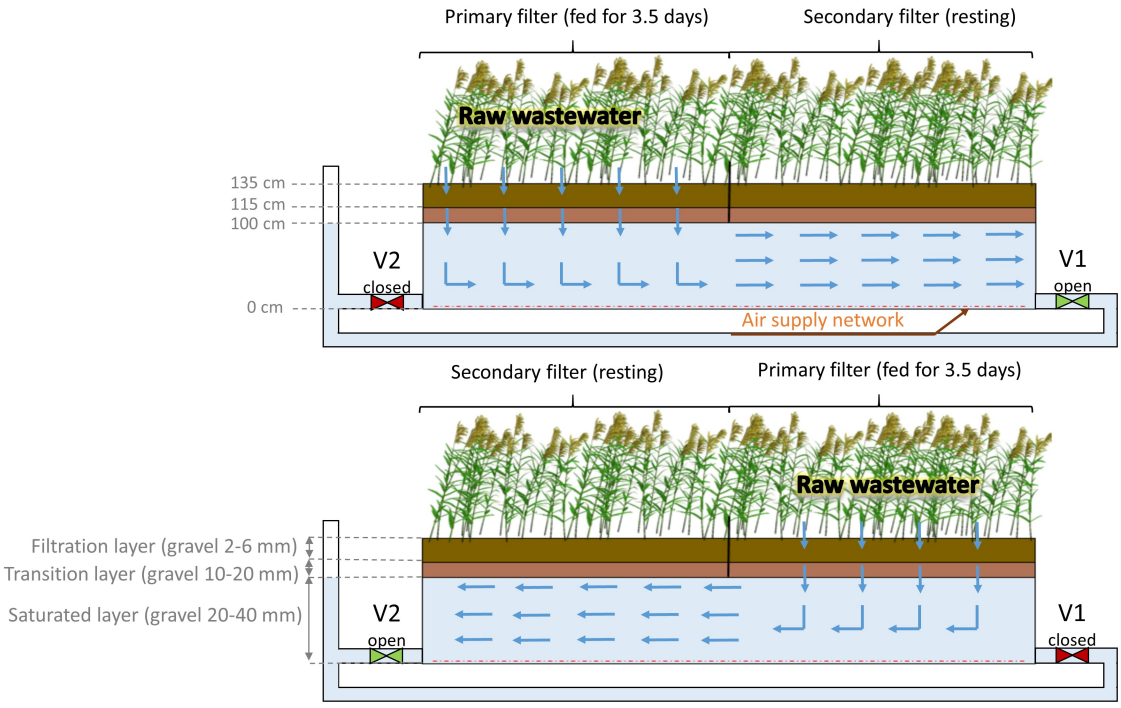

Figure 4.1: Hydraulic operating scheme of the hybrid aerated vertical/horizontal flow TW pilot

Aeration was based on time ("T" condition) for the first five experiments, e.g., hours of aeration per day spread across number of aeration cycles. Initially, a low HLR (0.15 m/d) with the longest aeration time (9 h) was tested as C1 condition to favour plant establishment as well as good aerobic performances: T-9h-0.15. The aim of this condition was to not overloading the system since the beginning and fasten nitrifying bacteria growth in winter. Then, the aeration time and number of aeration cycles were decreased (C2: T-3h-0.15). To better identify the treatment capacity of the system, the HLR was gradually increased (C3: T-3h-0.25 and C4: T-3h-0.35), and the pollutant load was increased by adding ammonia to the influent (C5: T-3h-0.35-NH_4). Since the influent comes from a combined sewer and, consequently, the inlet ammonium concentration was low, ammonium addition (the goal was to reach around 80 mg NH_4-N/L) allowed to test the capacity of the system for more stringent wastewater concentrations (C5, C6 and C7 conditions).

To increase denitrification, the timing of the aeration was coordinated with pulse feeding on the PF ("F" condition), optimizing the use of the available carbon in raw wastewater. Additionally, the aeration was decreased on the SF (C6: F-3.3h-1.7h-0.35-NH_4). For the last condition (C7: F-2.5h-0h-0.35-NH_4) aeration was decreased on the PF (2.5 h) and completely stopped on SF (0 h) to favor denitrification. In these cases, aeration was set to start 40 minutes before the batch and stop after 20 minutes for C6 and 15 minutes for C7 (time needed to degrade the oxygen inside the filter and remain in

Thèse accessible à l'adresse : https://theses.insa-lyon.fr/publication/2024ISAL0088/these.pdf © [C.K. Miyazaki], [2024], INSA Lyon, tous droits réservés

an anoxic environment).

Table 4.1: Experimental conditions parameters. T= time, F = feeding, PR = primary filter, SF = secondary filter, NB = number of cycles per day, Operation = aeration ON (min per cycle), Stop = aeration OFF (min per cycle), HLR = hydraulic loading rate (m/d)

Condition		**C1**	**C2**	**C3**	**C4**	**C5**	**C6**	**C7**
NH_4 addition		no	no	no	no	yes	yes	yes
Aeration (T or F)		T	T	T	T	T	F	F
Aeration PR	NB	6	4	4	4	4	10	10
	Operation	90	45	45	45	45	20	15
	Stop	150	315	315	315	315	130	135
Aeration SF	NB	6	4	4	4	4	10	0
	Operation	90	45	45	45	45	10	0
	Stop	150	315	315	315	315	140	0
HLR		0.15	0.15	0.25	0.35	0.35	0.35	0.35
Sampling period (start)		19/Jan	19/May	19/Jul	19/Oct	20/May	21/Jun	21/Aug
Sampling period (end)		19/May	19/Jul	19/Oct	20/Jan	20/Sep	21/Aug	21/Oct
Duration (days)		129	73	84	113	119	41	62
Number of samples		10	7	9	3	8	6	7

4.2.3 Pilot monitoring – chemical parameters

The pilot operation was monitored using a combination of continuously online sensors and laboratory analysis. Eight sensors were strategically installed along the filter, with measurements recorded at a 5-minute time step (Figure 4.3). Three of these sensors were dedicated to monitoring NH_4-N and NO_3-N concentrations (WTW, FDO 700IQ), positioned at the inlet, center and outlet of the pilot. The remaining sensors were oxygen sensors (WTW, VARION 700IQ), distributed within horizontal and vertical piezometers located inside the pilot.

The laboratory analysis occurred once per week, sampling the inlet and outlet through 24-hour composite samples. Each week, the filter was sampled alternated (different inlet and outlet). The following parameters were analyzed: total chemical oxygen demand (COD), filtered COD ($_f$COD), TSS, NH_4-N, NO_3-N, NO_2-N and TKN. The chemistry laboratory followed the European standard methods (NF EN 872, EN ISO 10304-1, NF EN ISO 14911, NF EN 25663, NF EN 6878, NF EN ISO 9963-1). TN was calculated as

Thèse accessible à l'adresse : https://theses.insa-lyon.fr/publication/2024ISAL0088/these.pdf © [C.K. Miyazaki], [2024], INSA Lyon, tous droits réservés

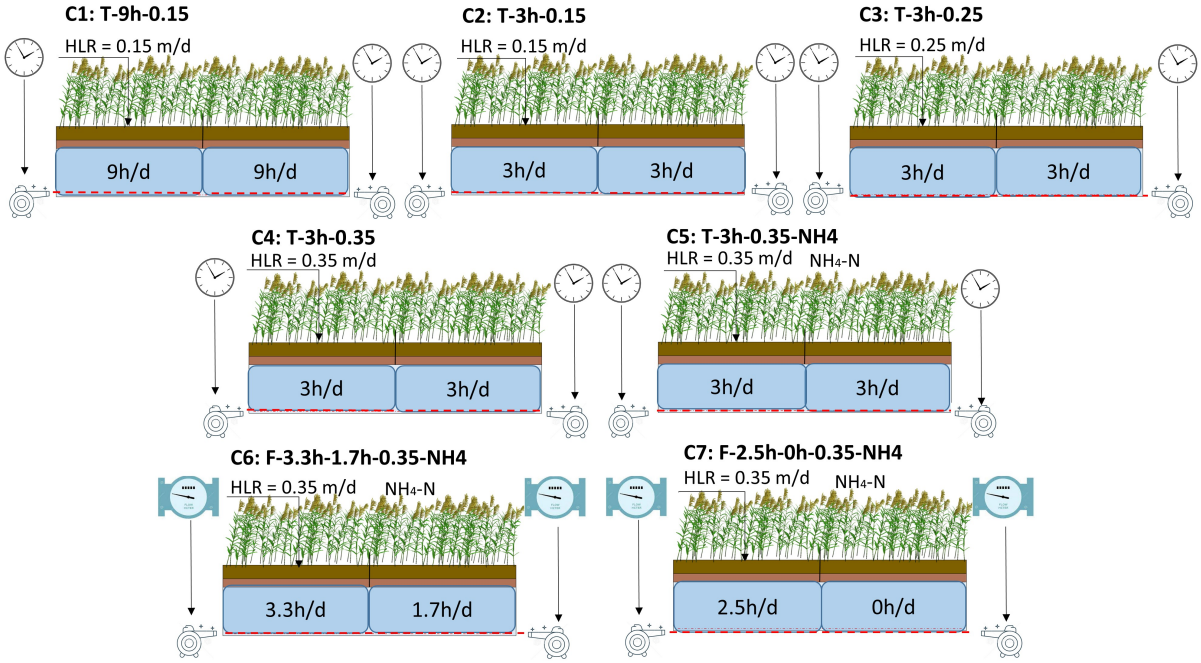

Figure 4.2: Parameters for each experimental condition.

the sum of NO_3-N, NO_2-N and TKN concentrations.

A statistical analysis was conducted to compare the treatment performance of each filter since they are fed alternately and heterogeneity could change the removal processes. This comparison was performed using a linear mixed model, which is suitable for analyzing grouped observations (Zuur et al., 2009). In our case, we considered each experimental condition as a random effect and the use of filter at the left or right side as a fixed effect. Eq. 4.1 to Eq. 4.3 describe such a relationship:

$$y_{ij} = (a + e_j) + b \cdot \text{filter}_{ij} + e_{ij} \qquad \text{(Eq. 4.1)}$$

$$e_j \sim N(0, \sigma_g^2) \qquad \text{(Eq. 4.2)}$$

$$e_{ij} \sim N(0, \sigma_h^2) \qquad \text{(Eq. 4.3)}$$

where: i is the observation, j is the experimental condition, a is the intercept term, e_{ij} is the random intercept term, b is the fixed effect, filter_{ij} is a dummy variable indicating the filter used (0 = left filter; 1 = right filter), e_{ij} the residual term, N is the normal distribution, σ_g and σ_h are the residual and random effect variance, respectively. If the results showed a low effect between the filter results, it means that they were homogeneous and can be processed together. The statistical analysis for all experimental conditions (refer

Thèse accessible à l'adresse : https://theses.insa-lyon.fr/publication/2024ISAL0088/these.pdf © [C.K. Miyazaki], [2024], INSA Lyon, tous droits réservés

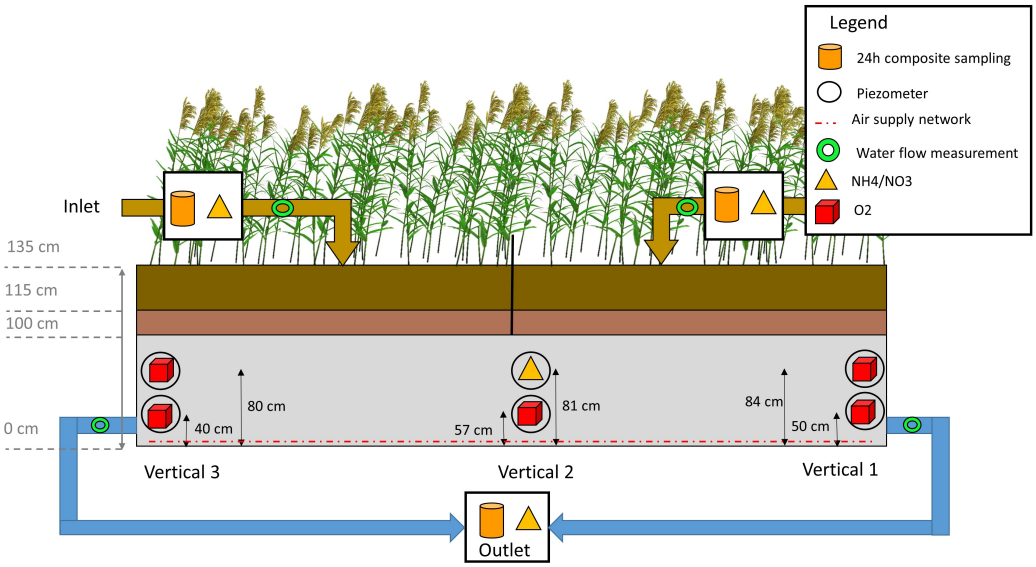

Figure 4.3: Position and type of sensor at the inlet, inside and outlet of the pilot, and location of the 24-hour composite sampling. The sensors were strategically placed to have a different vertical and horizontal profile and to have a view of the processes taking place in each filter and in half of the pathway.

Table 7.3 through Table7.7 in the Appendix for the results of the parametric coefficients) revealed a statistically insignificant difference between filters, indicating their homogeneity. Consequently, the results were treated collectively as representative of a single treatment system.

4.3 Results and discussion

4.3.1 Treatment performances and limitations: Timing aeration strategy

Table 4.2 presents the treatment performance for the experimental conditions employing the timing aeration strategies ("T"). Notably, the concentrations measured at the inlet exhibited variation across different conditions, evidenced by lower COD concentrations for C1 (T-9h-0.15) (384 mg COD/L) and C4 (T-3h-0.35) (280 mg COD/L), emphasizing the influence of seasonal factors. These periods corresponded to the winter season, characterized by wastewater dilution due to rainwater inflow and intrusion of a greater quantity of clear water in the combined sewer. Overall, the system demonstrated high performance in removing carbon and solids pollution regardless the experimental conditions, with an average outlet concentrations of less than 29 mg COD/L and 4 mg TSS/L. These results highlight the filtration capacity provided by the TW. Moreover, these

Thèse accessible à l'adresse : https://theses.insa-lyon.fr/publication/2024ISAL0088/these.pdf © [C.K. Miyazaki], [2024], INSA Lyon, tous droits réservés

findings align with previous studies on the treatment efficiency of similar full-scale systems (Petitjean et al., 2021), affirming the effectiveness and stability of the Rhizosph'air® in removing carbon and solids from raw wastewater.

Regarding ammonium removal, the nitrification process was nearly complete, regardless of the total aeration duration per day (C1: 9 h/d or C2, C3, C4: 3 h/d). The increase of HLR (C2: T-3h-0.15 and C3: T-3h-0.25) did not have significant impact on the nitrification process, since the treated loads were approximately equal to the applied loads (Figure 4.4a). The low output NH_4-N concentrations ($<$ 1 mg NH_4-N/L) and associated treated loads ($<$ 18 g NH_4-N/m^2/d) for conditions C1 (T-9h-0.15), C2 (T-3h-0.15), C3 (T-3h-0.25), and C4 (T-3h-0.35) demonstrated stable ammonium removal efficiency. These values fall within the lower ranges of reference values for the first stage of French VF TWs (Morvannou et al., 2015), with approximately 99% ammonium removal and production of nitrate.

However, when ammonium was added to the influent raw wastewater (C5: T-3h-0.35-NH_4), removal efficiency decreased to 89.2 ± 12.5%, indicating that nitrification had reached its maximum. To further enhance ammonium removal, the possible strategies are to increase the number of aeration cycles per day, the duration of aeration for each cycle or to automate the aeration using online sensors. Nevertheless, the result reinforces previous observations about the ability of a hybrid aerated TW to achieve ammonium removal over 90% (Prost-Boucle and Molle, 2021).

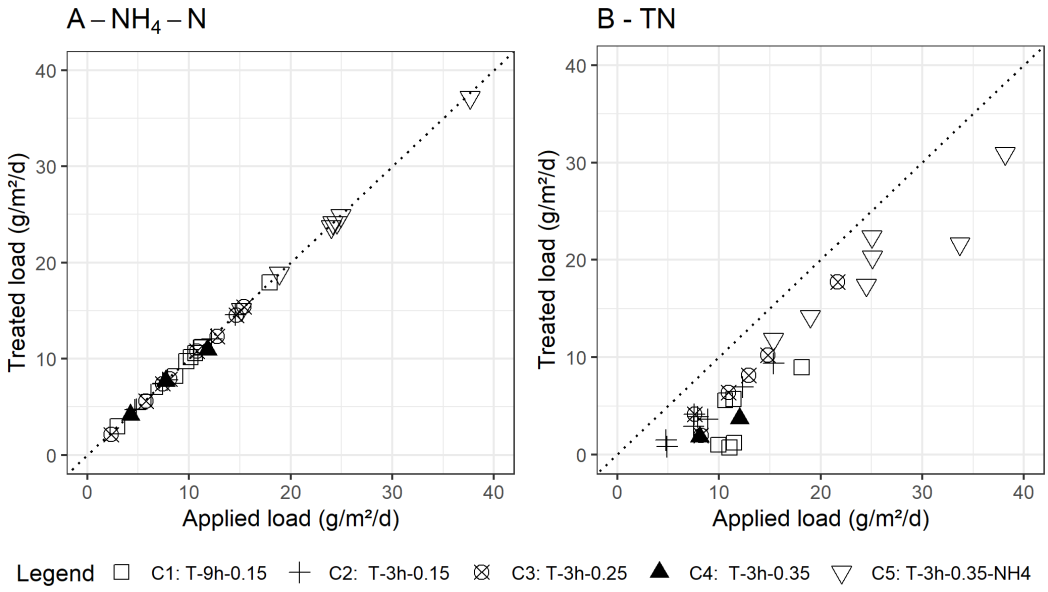

Figure 4.4: Applied and treated loads for NH_4-N (A) and TN (B), for experimental conditions C1 (T-9h-0.15), C2 (T-3h-0.15), C3 (T-3h-0.25), C4 (T-3h-0.35) and C5 (T-3h-0.35-NH_4)

In classical wastewater treatment process engineering, nitrification process is the

Thèse accessible à l'adresse : https://theses.insa-lyon.fr/publication/2024ISAL0088/these.pdf © [C.K. Miyazaki], [2024], INSA Lyon, tous droits réservés

Table 4.2: Inlet, outlet concentrations and concentration removal for each condition, considering temperature inside the filter, COD, TSS, TN, NH_4-N and NO_3-N, where Avg = average, Std dev = standard deviation and n= number of observations

C1: T-9h-0.15 (Temperature inside the filter: 8.4 ± 2.5°C)									
	In			Out			Concentration percent removal (%)		
Parameters	Median	Avg + Std dev	n	Median	Avg + Std dev	n	Median	Avg + Std dev	n
COD (mg/L)	325	384 ± 197	10	21	24 ± 6	10	93%	92 ± 4%	10
TSS (mg/L)	244	289 ± 146	10	<2	<2±0	10	99%	99 ± 1%	10
TN (mg/L)	36.1	33.9 ± 7.7	10	35.7	34.4 ± 5.7	10	5.50%	5.0 ± 12.7%	7
NH_4-N (mg/L)	34.7	32.3 ± 9.3	10	0.1	0.23 ± 0.48	10	99.70%	99.2 ± 1.7%	10
NO_3-N (mg/L)	0.83	1.33 ± 1.79	10	35.6	34.0 ± 5.9	10	-	-	-
C2: T-3h-0.15 (Temperature inside the filter: 17.2 ± 2.7°C)									
	In			Out			Concentration percent removal (%)		
Parameters	Median	Avg + Std dev	n	Median	Avg + Std dev	n	Median	Avg + Std dev	n
COD (mg/L)	642	723 ± 202.0	7	25	26 ± 2	7	96%	96 ± 1 %	7
TSS (mg/L)	570	585 ± 146	7	<2	<2 ± 1	7	99.60%	99.6± 0.2 %	7
TN (mg/L)	51.7	55.8 ± 19.4	7	24.1	26.4 ± 5.7	7	45.10%	47.2 ± 19.6 %	7
NH_4-N (mg/L)	45.5	43.0 ± 8.5	7	0.02	0.23 ± 0.31	7	99.90%	99.5 ± 0.7 %	7
NO_3-N (mg/L)	0.51	0.71 ± 0.43	7	22.6	25.3 ± 6.2	7	-	-	
C3: T-3h-0.25 (Temperature inside the filter: 19.9 ± 1.4°C)									
	In			Out			Concentration percent removal (%)		
Parameters	Median	Avg + Std dev	n	Median	Avg + Std dev	n	Median	Avg + Std dev	n
COD (mg/L)	554	545 ± 212	8	25	24 ± 4	8	96%	95 ± 3 %	8
TSS (mg/L)	380	434 ± 275	8	<2	<2±0	8	99.50%	99.4± 0.3 %	8
TN (mg/L)	35.3	41.1 ± 21.9	6	16.8	17.1 ± 1.8	5	66.40%	62.6 ± 17.7 %	4
NH_4-N (mg/L)	38.3	36.2 ± 16.2	8	0.47	0.65 ± 0.62	8	98.40%	97.6 ± 3.0 %	8
NO_3-N (mg/L)	0.49	0.75 ± 0.71	8	16.2	16.0 ± 2.4	7	-	-	-
C4: T-3h-0.35 (Temperature inside the filter: 12.0 ± 3.2°C)))									
	In			Out			Concentration percent removal (%)		
Parameters	Median	Avg + Std dev	n	Median	Avg + Std dev	n	Median	Avg + Std dev	n
COD (mg/L)	274	280 ± 112	3	<20	<20 ± 1	3	93%	92 ± 4 %	3
TSS (mg/L)	176	179 ± 91	3	<2	<2±0	3	99%	99 ± 1 %	3
TN (mg/L)	35.9	29.8 ± 12.2	3	15.4	15.0 ± 1.1	3	56.00%	42.8 ± 25.7 %	3
NH_4-N (mg/L)	23.3	23.9 ±11.1	3	0.24	0.65 ± 0.91	3	98.20%	97.8 ± 2.4 %	3
NO_3-N (mg/L)	0.74	1.17 ± 0.9	3	13.6	13.6 ± 0.2	3	-	-	-
C5: T-3h-0.35-NH_4 (Temperature inside the filter: 19.8 ± 1.7°C)									
	In			Out			Concentration percent removal (%)		
Parameters	Median	Avg + Std dev	n	Median	Avg + Std dev	n	Median	Avg + Std dev	n
COD (mg/L)	772	789 ± 242	6	28	29 ± 6	6	97%	96 ± 1 %	6
TSS (mg/L)	446	494 ± 145	6	3.7	3.9 ± 1.1	6	99%	99 ± 0.3 %	6
TN (mg/L)	106.4	108.2 ± 18.1	6	28.1	29.9 ± 11.1	6	75.20%	71.2 ± 12.8 %	6
NH_4-N (mg/L)	83.8	86.9 ± 19.0	6	6.09	8.17 ± 8.92	6	93.70%	89.2 ± 12.5 %	6
NO_3-N (mg/L)	0.45	0.48 ± 0.33	6	18	17.6 ± 4.9	6	-	-	-

Thèse accessible à l'adresse : https://theses.insa-lyon.fr/publication/2024ISAL0088/these.pdf © [C.K. Miyazaki], [2024], INSA Lyon, tous droits réservés

first step in TN removal. The challenge of TN removal is the second part, the denitrification process (Saeed and Sun, 2012). In the case of condition C1 (T-9h-0.075), the issue for initiating denitrification was excessive oxygenation within the filter, where the aerobic periods lasted 24h per day, as shown in Figure 4.5. The high dissolved oxygen (DO) concentration (in average 10 mg/L) led to the complete oxidation of ammonium (99.2 ± 1.7% removal), resulting in the reduction of ammonium nitrogen into nitrate and minimal removal of TN (concentration removal of 5.0 ± 12.7%, Table 4.2). Uggetti et al. (2016) tested a continuously aerated TW and found nearly complete nitrification, with 7-8 mg DO/L at the outlet.

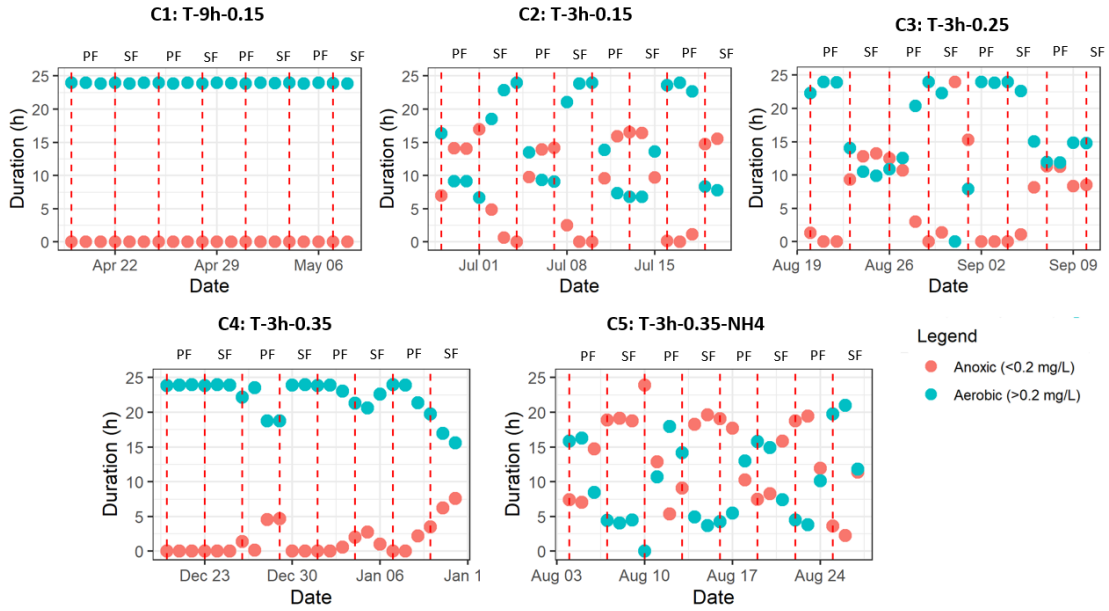

Figure 4.5: Duration in hours per day of aerobic condition (> 0.2 mg O2/L) and anoxic condition (< 0.2 mg O2/L) for the experimental conditions employing the time-based aeration strategy. A single oxygen sensor is exhibited for a period of one month. The red dash lines represent the filter alternation, PF stands for primary filter and SF for secondary filter

Comparing the C1 (T-9h-0.15) and C2 (T-3h-0.15) conditions (6 cycles versus 4 cycles of aeration/d), the C2 condition showed significantly higher denitrification, as indicated by the lower average outlet nitrate concentration (C1: 34 mg NO_3-N/L; C2: 25 mg NO_3-N/L), resulting in higher TN percent concentration removal for C2 of 47%. This can be attributed to the longer duration of anoxic condition, with an average of 13.1 h per day in the PF and 3.2h/d in the SF, which favored denitrifying bacteria activity. In Figure 4.5, for condition C2, whenever the filter is being fed, there is more carbon to degrade and the oxygen is rapidly consumed, while in the SF, the oxygen concentration increases, exhibiting longer aerobic conditions (3.2h/d for the PF and 20.5h/d for the SF).

When a similar aeration strategy (3 h/d) was applied but the HLR was increased

Thèse accessible à l'adresse : https://theses.insa-lyon.fr/publication/2024ISAL0088/these.pdf © [C.K. Miyazaki], [2024], INSA Lyon, tous droits réservés

from 0.15 m/d (C2) to 0.25 m/d (C3) and 0.35 m/d (C4), there was a decrease in the average effluent NO_3-N concentration (C2: 25.3 ± 6.2 mg /L; C3: 16.0 ± 2.4 mg/L; C4: 13.6 ± 0.2 mg/L). Consequently, TN removal increased from C2 (47.2 ± 19.6 %) to C3 (62.6 ± 17.7 %). The lower percent concentration TN removal in C4 (T-3h-0.35) (42.8 ± 25.7 %) was attributed to the lower inlet TN concentration and lower hydraulic retention time as the HLR was increased. During conditions C2 and C3, denitrification was more efficient as the HLR were higher, and higher inlet COD concentrations (about twice as high) provided higher availability of organic carbon. In addition, for these three experimental conditions, the loads applied in NH_4-N (2.3 – 18 g/m^2/d) and TN (2.4 – 21.7 g/m^2/d) remained within the same range of values, and the treated loads (2.1 – 17.9 g NH_4-N /m^2/d and 0.7 – 17.7 g TN /m^2/d) did not differ among the experimental conditions (Figure 4.4). These treated loads are higher than aerated VF (5.2 g NH_4-N /m^2/d) or aerated HF (7.3 g NH_4-N /m^2/d) (Dotro et al., 2017).

For condition C5, the condition with an ammonium addition (C5: T-3h-0.35-NH_4), the inlet average concentration was 108 ± 18 mg TN/L (between 9 to 19 g TN/m^2/d of applied load), approximately 2 to 4 times higher than the inlet TN concentration in other conditions. This operational condition achieved a high TN removal, reaching 71%. However, effluent NO_3-N concentrations were still measureable, indicating limitation in the denitrification process. The oxygen sensors reported an average of 18.1 h/d of anoxic conditions in the PF and 9.4 h/d in the SF. As Figure 4.5 shows, it is the first time that the duration of anoxic condition was constantly longer than aerobic condition. Therefore, with high nitrification and a long anoxic time during this experimental condition, it became clear that the limitation of denitrification is not due to a lack of nitrates or excessive oxygenation in the saturated zone, but probably to the lack of organic carbon in the saturated zone. This issue is commonly reported in the literature (Bezbaruah and Zhang, 2003; Wang et al., 2022; Yao et al., 2023).

Based on the assumptions of Morvannou et al. (2015) (80% concentration removal for COD and 50 % for TKN in the unsaturated zone of French VF TWs), the COD/NO_3-N ratio arriving in the saturated zone can be estimated. According to Morvannou et al., 2017, this ratio should be at least 2.0 at the entrance to the saturated zone (and a minimum residence time of 0.75 days) for an efficient denitrification. Estimations in this study would indicate that only condition C5 (T-3h-3.5-NH_4) lacked sufficient biodegradable carbon for denitrification. The deficit would be approximately between 40 and 120 mg COD/L (Table 7.9 through table 7.15 in the Appendix present these results).

It was not possible to match aeration requirements to the batch feeding by controlling aeration strategies on a temporal basis. When a batch arrived during a period of high DO concentration in the saturated zone, oxygen was used for carbon degradation resulting in a lack of carbon for denitrification during anoxic periods. Under the conditions tested

Thèse accessible à l'adresse : https://theses.insa-lyon.fr/publication/2024ISAL0088/these.pdf © [C.K. Miyazaki], [2024], INSA Lyon, tous droits réservés

from C1 to C5, the balance between nitrification and denitrification periods was not ideal for effectively transforming nitrogen forms while maintaining a sufficient carbon source for denitrification process. Thus, to remedy this deficiency and attempt to optimize denitrification, a new aeration strategy was tested that coordinated the aeration period and batch feeding.

4.3.2 Treatment performance and limitations: Aeration strategy according to batch feeding periods

Table 4.3 presents the treatment performance results for the experimental conditions employing the aeration strategy according to feeding time ("F"). The first condition C6 (F-3.3h-1.7h-0.175-NH_4) had similar influent concentrations to condition C4 (T-3h-0.175), characterized by diluted wastewater and subsequently, lower COD and NH_4-N influent concentrations. Despite this dilution, the system demonstrated a high efficiency in removing those pollutants, even in wet weather conditions (refer to Table 7.16 in the Appendix for the local rainfall data), demonstrating some flexibility in the performance of the system.

Table 4.3: Inlet, outlet concentrations and concentration removal s for each condition, considering temperature inside the filter, COD, TSS, TN, NH_4-N and NO_3-N, where Avg = average, Std dev = standard deviation and n= number of observations

C6: F-3.3h-1.7h-0.35-NH_4 (Temperature inside the filter: 19.5 ± 0.5°C)									
	In			Out			Concentration percent removal (%)		
Parameters	Median	Avg + Std dev	n	Median	Avg + Std dev	n	Median	Avg + Std dev	n
COD (mg/L)	286	252 ± 136	6	21	23 ± 4	6	91%	87 ± 10 %	6
TSS (mg/L)	201	189 ± 113	6	<2.0	<2.0 ± 0.0	6	99%	98 ± 2 %	6
TN (mg/L)	53.3	59.6 ± 42.8	6	31.5	35.3 ± 12.0	6	38.20%	24.7 ± 9.2 %	5
NH_4-N (mg/L)	52.7	47.1 ± 20.9	6	0.08	1.35 ± 3.01	6	99.60%	98.0 ± 4.4 %	5
NO_3-N (mg/L)	0.45	0.68 ± 0.55	6	30.5	30.3 ± 3.1	6	-	-	-
C7: F-2.5h-0h-0.35-NH_4 (Temperature inside the filter: 20.2 ± 0.5°C)									
	In			Out			Concentration percent removal (%)		
Parameters	Median	Avg + Std dev	n	Median	Avg + Std dev	n	Median	Avg + Std dev	n
COD (mg/L)	595	548 ± 137	7	40	34 ± 13	7	94%	94 ± 2 %	7
TSS (mg/L)	367	384 ± 85	7	7	7 ± 1	7	98%	98 ± 0%	7
TN (mg/L)	98	91.8 ± 41.6	7	29.6	27.0 ± 10.2	7	70.50%	70.7 ± 5.3 %	6
NH_4-N (mg/L)	97.3	91.3 ± 41.4	7	19.5	18.3 ± 7.1	7	80.50%	80.0 ± 5.3 %	6
NO_3-N (mg/L)	0.45	0.38 ± 0.16	7	9.76	8.70 ± 4.40	7	-	-	-

It is noteworthy that NH_4-N concentrations at the outlet were 20 times higher for condition C7 (F-2.5h-0h-0.175-NH_4) than for condition C6 (F-3.3h-1.7h-0.175-NH_4). However, condition C7 also exhibited the lowest NO_3-N outlet concentration among all experimental conditions (8.70 ± 4.40mg NO_3-N/L). This condition demonstrated its

Thèse accessible à l'adresse : https://theses.insa-lyon.fr/publication/2024ISAL0088/these.pdf © [C.K. Miyazaki], [2024], INSA Lyon, tous droits réservés

capability to effectively treat TN loads that were nearly twice as high as those of the other experimental conditions (as depicted in Figure 4.6). These applied and treated loads were much higher than the previous studies with aerated TW (Li et al., 2014; Uggetti et al., 2016; Zhang et al., 2010).

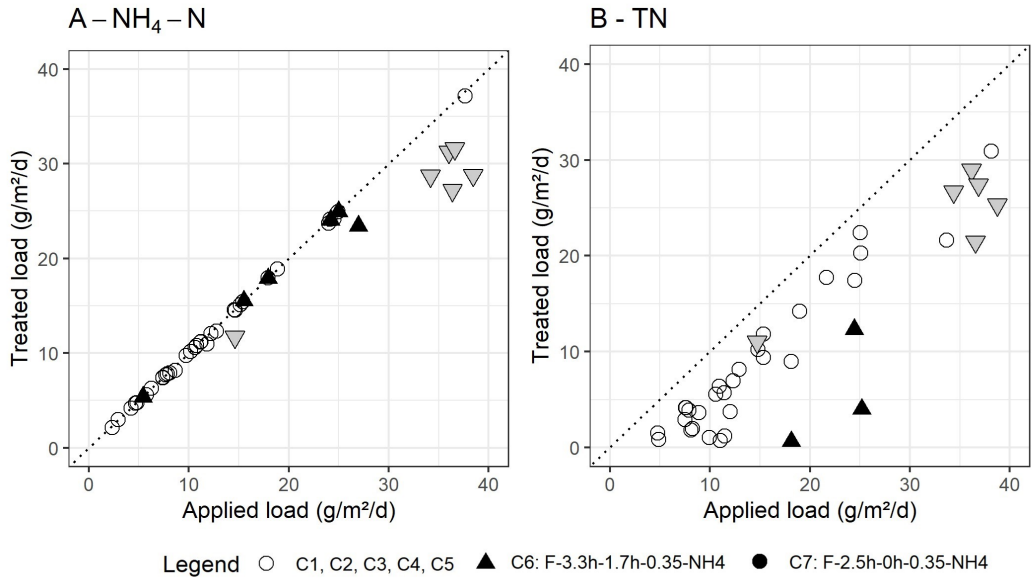

Figure 4.6: Applied and treated loads for NH_4-N and TN, for experimental conditions C1 (T-9h-0.15), C2 (T-3h-0.15), C3 (T-3h-0.25), C4 (T-3h-0.35), C5 (T-3h-0.35-NH_4), C6 (F-3.3h-1.7h-0.35-NH_4) and C7 (F-2.5h-0h-0.35-NH_4)

Figure 4.7 provides insight into the duration of aerobic and anoxic environment for experimental conditions with aeration strategy based on batch time. Condition C6 (F-3.3h-1.7h-0.175-NH_4) appeared to have a balance distribution between anoxic and aerobic environments, with an average duration of 14.7 h/d of anoxic in the PF and 5h/d in the SF and 7.8 h/d of aerobic in PF and 18h/d in SF. This balance seemed to favor only the nitrification process, since 30.3 ± 3.1 mg NO_3-N/L were measured at the outlet and the TN removal efficiency was only 24.7 ± 9.2 %. Nonetheless, the lack of biodegradable carbon (approximately 50 mg COD/L) was another reason for lack of denitrification.

In contrast, condition C7 (F-2.5h-0h-0.175-NH_4) exhibited an opposite trend compared to the other conditions: the majority of the day, the saturated zone remained anoxic (17.1 h/d in the PF and 22.9h/d in the SF), leading to an almost complete denitrification process at the saturated zone, with 8.70 ± 4.40 mg NO_3-N/L effluent concentration. However, as the aerobic environment decreased, 5.7h/d in PF and 0.9 h/d in SF, it also reduced the concentration removal of NH_4-N (80.0 ± 5.3 %). The DO concentration observed for the C7 condition (see Figure 7.11 in the Appendix) were similar to those observed by Uggetti et al. (2016), who also found an average removal of 66% for TN removal.

Thèse accessible à l'adresse : https://theses.insa-lyon.fr/publication/2024ISAL0088/these.pdf © [C.K. Miyazaki], [2024], INSA Lyon, tous droits réservés

Despite the extended anoxic periods, denitrification was again hindered by organic carbon limitation. The C/N ratios for C6 and C7 averaged 1.9 and 1.3, respectively. Thus, the carbon source from the batch was not sufficient to meet the denitrification requirement, causing nitrate accumulation (Wang et al., 2020). To overcome this, it would be necessary to increase the carbon source by using an external chemical product that is readily biodegradable, such as methanol or acetic acid (Fu et al., 2022).

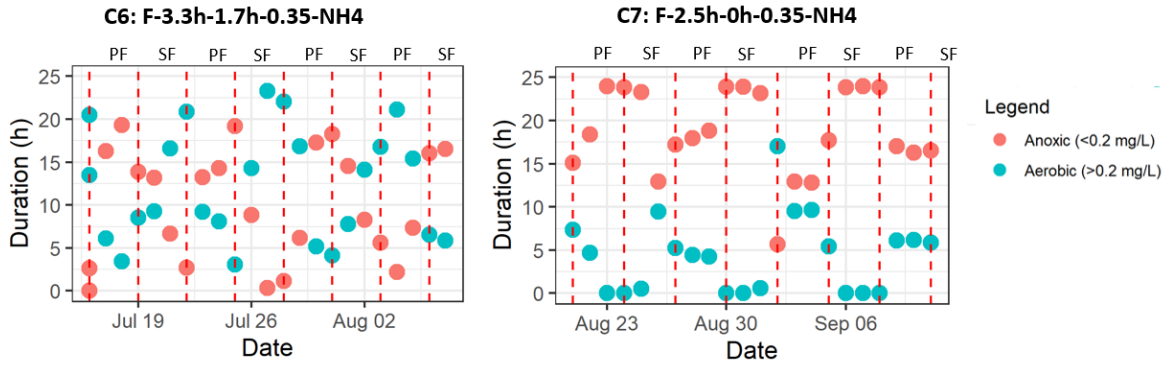

Figure 4.7: Duration in hours per day of aerobic condition ($>$ 0.2 mg O2/L) and anoxic condition ($<$ 0.2 mg O2/L) for the experimental conditions employing aeration strategy based on batch time. A single oxygen sensor is exhibited for a period of one month. PF = Primary filter and SF = secondary filter

Figure 4.8 illustrates the fluctuation in DO concentration over the course of the day for the C7 condition (F-2.5h-0h-0.175-NH_4). The aeration was set to start 40 minutes before the batch, it took around 10 minutes for the oxygen concentration reach its maximum value and then when the batch occurred, there were low oxygen concentration at the saturated layer (in average 0.3 mg/L and maximum 0.6 mg/L). Thus, the exact moment when the influent dose arrives, the environmental conditions are not completely anoxic. Nonetheless, Figure 4.7 pointed out that the environment was predominantly anoxic during the day, which created favorable conditions for denitrification. Consequently, the aeration strategy employed in C7 could be optimized if the aeration was timed early (to provide carbon when denitrification is occurring). To further improve understanding of nitrogen dynamics in aerated TWs, online sensors such as pH and redox could be useful monitoring and controlling the system through online monitoring instruments (Nivala et al., 2020). Such sensors would provide information about the characteristic patterns of biodegradation processes, including the detection of nitrification and denitrification phases. The advantage in this case is to know the timing and duration of nitrification periods or incomplete denitrification stages (Olsson, 2012). Ammonium and nitrate sensors are mainly used for nitrogen control; however, the high investment and maintenance costs of these sensors can make their use impractical. To overcome these problems, other physical-chemical parameters can be an option to measure indirectly, like DO, pH, oxidation-reduction

Thèse accessible à l'adresse : https://theses.insa-lyon.fr/publication/2024ISAL0088/these.pdf © [C.K. Miyazaki], [2024], INSA Lyon, tous droits réservés

potential (ORP) and oxygen uptake rate (OUR) (secondary variables) (Zanetti et al., 2012).

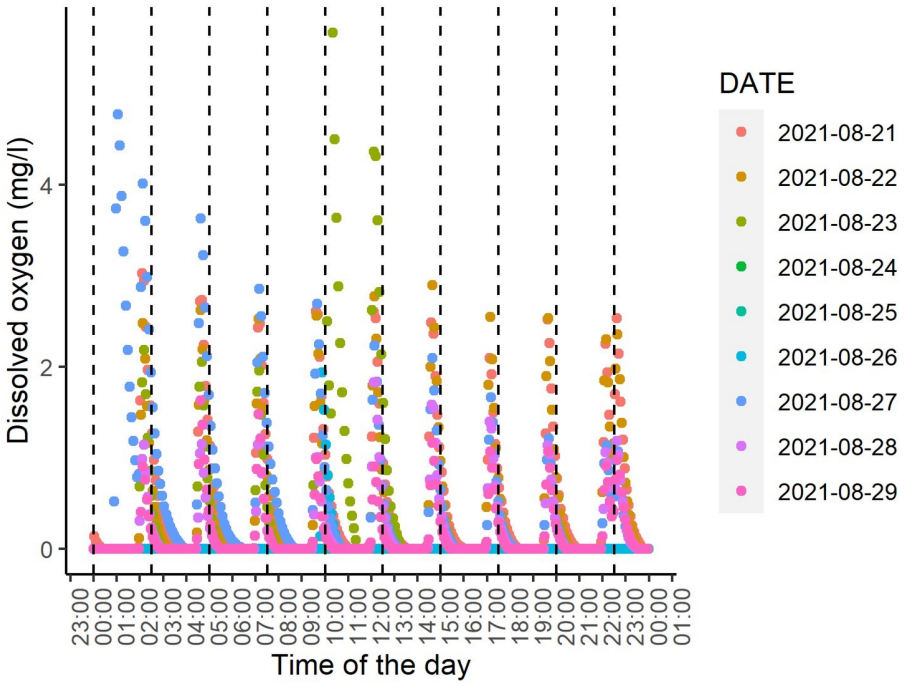

Figure 4.8: DO concentration during 24 hours for multiple days for the condition C7 (F-2.5h-0h-0.35-NH_4). A single oxygen sensor is exhibited, located at vertical 1 (84cm depth). Dash black lines represent the batches sent to the primary filter

4.4 Conclusion

The Rhizosph'air® hybrid aerated TW demonstrated high removal of carbon and suspended solids removal for all seven experimental conditions tested. The conditions varied with influent concentration, duration of aeration, timing of influent loading and aeration, different hydraulic loading rates, and addition of ammonium in the influent. TN removal was directly impacted by each operational change. In the experimental conditions with time-based aeration (C1 – C5), percent ammonium concentration removal exceeded 90 %. Aerating the system for 9 h total per day (6 cycles of 150 mins aeration on per cycle) resulted in the lowest TN removal (5%). Increasing the HLR (from 0.15 to 0.25 m/d) with 3h aeration per day, the TN removal improved from 47 % to 62 %. This is the result of a better balance between oxygen demand and supply. When ammonium was added to the influent (C5: T-3h-0.35-NH_4), nitrification was preserved while denitrification increased, reaching 71% TN concentration removal.

It is important to note the seasonal effect, particularly during winter when the influent to the pilot in this study was diluted by clear water intrusion (C4: T-3h-0.35 and

Thèse accessible à l'adresse : https://theses.insa-lyon.fr/publication/2024ISAL0088/these.pdf © [C.K. Miyazaki], [2024], INSA Lyon, tous droits réservés

C6: F-3.3h-1.7h-0.35-NH_4), resulting in lower influent COD and NH_4-N concentrations. Consequently, this had an impact on the efficiency of the system, by decreasing the TN removal, while preserving low outlet TN concentration (around 15 mgN/L). However, despite these effects, complete nitrification still occurred due to efficient oxygen transfer.

When aeration was set according to the batch feeding (C6: F-3.3h-1.7h-0.35-NH_4 and C7: F-2.5h-0h-0.35-NH_4), the subsurface conditions favored denitrification with longer periods of anoxic conditions and DO concentrations of approximately 0.2 and 0.9 mg DO/L. The condition C7 (F-2.5h-0h-0.35-NH_4) removed 71 % of TN, similar to the performance of condition C5 (T-3h-0.35-NH_4) (71 %). The change in aeration strategy from time-based to batch time provided an instantaneous source of carbon for denitrifying bacteria and consequently resulted in lower NO_3-N concentrations at the outlet. Nevertheless, this condition reached its maximum denitrification rates, but showed an increase in outlet ammonium concentrations (18.3 $\pm$ 7.1 mg NH_4-N/L effluent concentration). This underlines the importance of both oxygen supply and sequencing.

Therefore, to optimize the hybrid aerated TW system in this study and decrease effluent nitrate and TN concentrations without adding carbon, the following modifications are suggested:

- Optimize the use of carbon for denitrification by stopping aeration earlier before the influent batch feeding to ensure anoxic environmental conditions when the system is fed.
- Use online sensors (pH, redox or DO) to identify bending points or patterns related to nitrification and denitrification dynamics. This information could be used to control the operation of the aeration system based on the influent pollutant loads (e.g., treatment on demand).

4.5 Learnings

Previous intermittent aeration studies tested limited conditions, without exploring the impact on the variation with influent concentration, duration of aeration, timing of influent loading and aeration, different hydraulic loading rates, and addition of ammonium in the influent. This study explored different experimental conditions to understand the impact of aeration on the dynamics of nitrogen removal in a hybrid aerated TW. The learnings we had from the chapter are:

- The denitrification process is limited when the aeration is controlled according to time.
- The transition from time-based to inflow-based aeration strategy increased the denitrification process, resulting in the lowest NO_3-N concentrations at the outlet.

Thèse accessible à l'adresse : https://theses.insa-lyon.fr/publication/2024ISAL0088/these.pdf © [C.K. Miyazaki], [2024], INSA Lyon, tous droits réservés

The principal finding was that implementing an intermittent aeration strategy based on flow offers a notable advantage. This approach ensures the most effective aerobic and anoxic durations for nitrification and denitrification, occurring at the optimal time. The results supported defining the novel aeration strategy presented in the Chapter 5.

Thèse accessible à l'adresse : https://theses.insa-lyon.fr/publication/2024ISAL0088/these.pdf © [C.K. Miyazaki], [2024], INSA Lyon, tous droits réservés

Thèse accessible à l'adresse : https://theses.insa-lyon.fr/publication/2024ISAL0088/these.pdf © [C.K. Miyazaki], [2024], INSA Lyon, tous droits réservés

Chapter 5

Optimization of total nitrogen removal in a hybrid aerated vertical and horizontal treatment wetland

Abstract Passive treatment wetlands (TW) are robust systems that can effectively treat wastewater from small communities. However, their total nitrogen (TN) removal capacity is limited or requires different treatment stages. A single-stage TW offers a novel solution to this challenge. The system combines a first-stage French vertical flow TW with an aerated horizontal flow TW. Despite the successful demonstration of high performance in terms of ammonium (>80%), COD (>90%) and TSS (>90%) removal in the previous study, there is still a research gap regarding optimizing the aeration strategy and implementing rules to automate the system for TN removal. The aim of this study is to investigate TN removal performance using an innovative aeration strategy, test its limitations, examine the applicability of the N-k-C* model, and explore the potential for implementing aeration control strategies through online sensors, including the use of bending points and model predictions. The aeration strategy was intermittent and based on the inflow (in batch regime). The results showed that the aeration strategy proved effective in treating TN, with outlet concentration below 15 mg/L. At higher organic loadings, the system maintained high removal rates, though additional oxygenation was required to meet stricter TN limits. The N-k-C* model had a RMSE for TKN and TN 6.2 and 7.0 mg/L, respectively. These values does not allow its use for design purpose in case of strict compliance criteria. Bending-points were not consistently observed, and the concentrations at these points fluctuated making difficult to rely on them for aeration control. Finally, the potential use of a linear predictive model was explored, but the data demonstrated non-linear relationships among the variables. Therefore, future predictive modeling efforts should account for these factors.

Thèse accessible à l'adresse : https://theses.insa-lyon.fr/publication/2024ISAL0088/these.pdf © [C.K. Miyazaki], [2024], INSA Lyon, tous droits réservés

Keywords: Aerated wetland; aeration strategy; bending points; constructed wetland; wastewater

Thèse accessible à l'adresse : https://theses.insa-lyon.fr/publication/2024ISAL0088/these.pdf © [C.K. Miyazaki], [2024], INSA Lyon, tous droits réservés

5.1 Introduction

Treatment wetlands (TW) are engineered systems that mimic natural wetlands to control water pollution. They can treat high organic loads of carbon, but passive TWs have limited capacity for total nitrogen (TN) removal (Cross et al., 2021; Masih, 2017; Zhuang et al., 2019. The combination of vertical flow TW (VF TW) and horizontal flow TW (HF TW) in a hybrid system could achieve TN removal, so research trends have focused on different configurations with multiple stages (Vymazal, 2013). A single-stage configuration, the Rhizosph'air®, came up with an innovative process and high-tech system to achieve TN removal on a small footprint. Its great difference is the combination of French VF TW and an aerated HF TW, which can use intermittent aeration by air blowers across the bottom in the saturated zone. Such a design could enable the nitrification and denitrification process in a compact TW (0.8 - 1.2 $m^2.PE^{-1}$) (Troesch et al., 2020).

The aeration process improves oxygen transfer efficiency and reduces the system footprint (Cross et al., 2021; Dou et al., 2016), making it an relevant choice for implementation in urban areas. This hybrid system has been implemented throughout France, with one installation monitored over two years, treating 1,400 PE (293 m^3/d) of domestic wastewater (Prost-Boucle et al., 2021). The results showed a high performance in chemical oxygen demand (COD), biochemical oxygen demand (BOD_5), and total suspended solids (TSS) removal. In terms of nitrogen removal, the 12-hour aeration divided into four cycles could complete the nitrification process ($>$ 90% ammonium removal). However, denitrification was limited due to a lack of organic carbon, resulting in 60-65% TN removal. Reducing the daily aeration length to 3 hours improved TN removal, and the system achieved 80% removal of NH_4-N and 82% removal of TN (Prost-Boucle et al., 2021).

To enhance TN removal and assess the performance of the system under varying loads, other aeration strategies in a controlled system were studied on a pilot scale. Chapter 4 conducted an evaluation of the impact of seven different aeration strategies on TN removal. The first five experimental conditions, implemented an aeration strategy based on time, resulting in ammonium removal of over 90%. TN removal ranged from 5 $\pm$ 13% to 71 $\pm$ 13%. Denitrification process was limited due to a lack of carbon, with nitrate outlet concentrations ranging from 13.6 $\pm$ 0.2 to 34.0 $\pm$ 5.9 mg/L. The latter two experimental conditions demonstrated the interest of the optimization of carbon use for denitrification, with an aeration sequencing based on the inflow. This resulted in a notable decrease in nitrate outlet concentration to 8.70 $\pm$ 4.40 mg/L and a TN removal of 71%. The organic carbon from the batch arrival was consumed at a higher rate by the denitrified bacteria. In this aeration strategy, the aeration of the primary filter was coordinated with the batch feeding time , while the secondary filter was time-based. In this case, the hypothesis to further optimize the TN removal was to stop the aeration early

Thèse accessible à l'adresse : https://theses.insa-lyon.fr/publication/2024ISAL0088/these.pdf © [C.K. Miyazaki], [2024], INSA Lyon, tous droits réservés

enough before a feeding batch to guarantee an anoxic environment when the batch arrives to avoid aerobic degradation of COD and uses it during the denitrification process.

While Chapter 4 provided valuable insights to enhance the aeration strategies, further clarifications were needed regarding the limits of this aeration control based on the inflow. In the event of significant fluctuations in inlet concentration, particularly during periods of high organic loading, the robustness of this strategy remains uncertain. Regarding design purposes, the N-k-C* model has yet to be applied to this system. The remaining question is whether it is possible to apply a model based on inlet and outlet concentration, or whether compartmentalization is necessary to achieve greater precision (Chapter 3). Another potential strategy for further optimization could be the implementation of online sensors control of key parameters, such as dissolved oxygen concentration, nitrogen form concentration, or redox potential. This would offer a more efficient alternative to the current manual chemical measurement approach. Additionally, it would allow for improvements to the existing air blower configuration based on the inflow, enabling it to adapt to fluctuations of TN concentration in the inlet or within the filter, thereby enhancing TN removal (Zhang et al., 2020).

In this case, online sensors can be used to monitor and control the system through real-time monitoring instruments (Nivala et al., 2020). These online sensors have been implemented for a long time to control the aeration of activated sludge and sequencing batch reactors (Olsson, 2012). The control and optimization of the aeration strategy are linked to process control devices, ranging from the identification of bending-points to control the aeration phases (Jaramillo et al., 2018) to artificial intelligence (AI) control strategies (Monday et al., 2024). The bending-point strategy can be useful in providing information about characteristic patterns of the biodegradation processes, including the detection of nitrification and denitrification phases (Miao et al., 2022). The advantage in this case is to avoid long nitrification periods (i.e., which leads to a higher energy consumption) or incomplete denitrification stages.

In the case of aerated TW, this strategy requires the determination of a suitable activation and deactivation point for aeration from an empirical evaluation of the course of several measured variables. No fixed thresholds are used to activate the control or actuation processes. The patterns of online sensors behave differently for each design and operating mode in TW (Ruppelt et al., 2019), even depending on the location where they are installed. The sensor location could lead to an over or under aeration or miss load variation. Therefore, situation-dependent control commands are generated from the temporal course of the measured variables (Baumann et al., 2005).

Therefore, there is still a need for further research and development on nitrogen optimization by improving the aeration strategy and automating the TW (Parde et al.,

Thèse accessible à l'adresse : https://theses.insa-lyon.fr/publication/2024ISAL0088/these.pdf © [C.K. Miyazaki], [2024], INSA Lyon, tous droits réservés

2021). The objective of the present study is to evaluate the TN removal under a novel aeration strategy, to assess its limitations, to evaluate the application of the N-k-C* model, and to explore the potential use of aeration control strategies using online sensors, such as bending points and model prediction.

5.2 Material and methods

5.2.1 Treatment wetland pilot

The REFLET platform has nine TW pilots with different configurations, each with a surface area of 20 m^2 (INRAE, 2019). The study site is located in Craponne (France), and one of the pilots is a Rhizosph'air®. Further system details can be found in Chapter 3 and Chapter 4. The pilot was built in 2018 and the start-up period was in January 2019. The pilot was built in 2018, and the start-up period was January 2019. During the first few months of operation, the filter received a low hydraulic load to ensure the proper biomass and reed development. After two first studies (Chapter 3 and Chapter 4) on hydraulic characterization and aeration strategy evaluation, the present study started after five years of operation. The hybrid aerated TW has an upper layer divided into two filters (10 m^2 each, each 2.5 x 4m, as shown in Figure 5.1). The wastewater comes from a combined sewer system and the water quality can be highly diluted during the winter period. Therefore, to test the system capacity with a wide range of inlet concentrations regardless of the season, the site was equipped with two peristaltic pump doses to provide nitrogen (ammonium bicarbonate - $(NH_4)HCO_3$) and carbon (vegetable glycerin - 99.5% glycerol) sources at the station entrance manhole. The concentration added of each component is explored in section 5.2.2.

The upper layer receives raw wastewater and operates as a first-stage French VF TW. The wastewater flows vertically through an unsaturated layer filled with thin gravel (2 – 6 mm nominal size, 20 cm deep), then to a transition layer of medium size gravel (10 – 20 mm nominal size, 15 cm deep). Finally, the water reaches an aerated saturated zone of coarse gravel (20-40 mm nominal grain size, 100 cm deep). This last layer is a single compartment shared by the filters (without a physical separation). At the bottom, the aeration system includes 120 driplines, with a diffuser density of 60 diffusers/m^2, connected to two air blowers (one per filter). Each air blower was monitored with an airflow meter, a temperature sensor, and a pressure sensor. The pressure fluctuates around 160-180 mbar with an air flow rate of 5-6 $m^3/m^2/h$ for each blower.

The unsaturated layer is fed alternately every 3.5 days. The filter that receives the wastewater and the saturated zone below it are referred to as the "primary filter" (in the case of Figure 5.1). An electric valve at the inlet opens to feed the primary filter,

Thèse accessible à l'adresse : https://theses.insa-lyon.fr/publication/2024ISAL0088/these.pdf © [C.K. Miyazaki], [2024], INSA Lyon, tous droits réservés

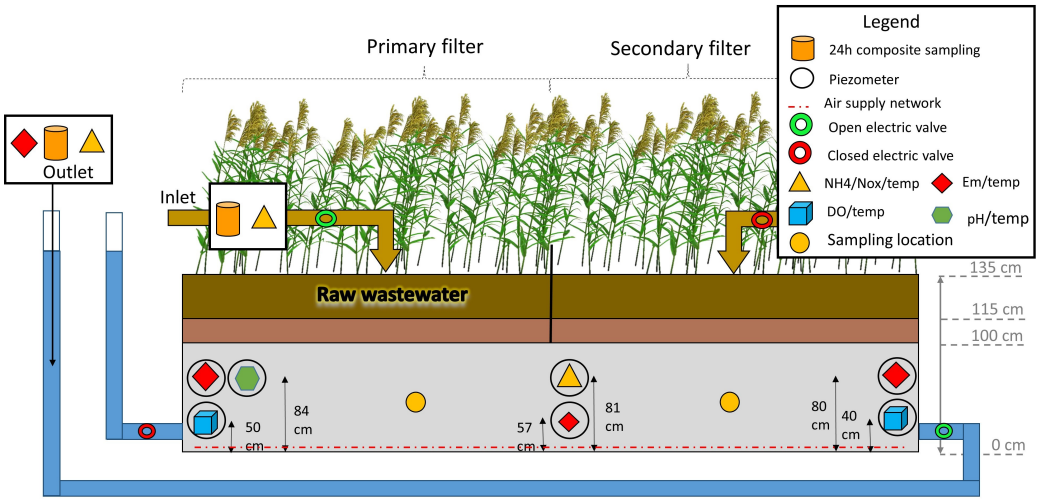

Figure 5.1: Position and type of sensors at the inlet, inside and outlet of the pilot, and location of the 24-hour composite sampling and for the bending-points validation. In this scheme, primary filter is on the left side and secondary filter is on the right side.

and the electric valve at the opposite outlet is coordinated and opens simultaneously to use the entire volume of the saturated layer. The electric valves are designed to operate automatically in accordance with the alternation of the feeding and rest filter. Then, the filter at rest and the saturated zone below it are referred to as the "secondary filter" (Figure 5.1 shows the secondary filter). This alternating operation ensures that the organic solids are mineralized on the surface, preventing them from seeping into the internal pores and clogging the system. A previous study determined that the hydraulic retention time is 1.9 days and that the aeration process on the primary filter plays a significant role in mixing the water in the saturated layer (3).

5.2.2 Optimizing total nitrogen removal

- Pilot operation

TWs are mainly used in decentralized systems and their influent characteristics are different from centralized systems. Decentralized systems range from 50 population equivalent (PE) to 10,000 PE, varying from individual onsite systems, to a series of larger clusters or semi-centralised (Risch et al., 2021). In small agglomerations, the organic load entering the TW corresponds to a normal to medium organic load, where the multiple contributions dilute the concentration (Mercoiret, 2009). In contrast, the high organic load represents domestic pollution discharged from a household, where the decentralization is extreme, and the daily variation for NH_4-N and COD could reach 220 mg/L and 2199 mg/L, respectively (Dubois et al., 2022). Therefore, the system was submitted to different ranges of organic loads to test its response and robustness. The normal organic load corresponded

Thèse accessible à l'adresse : https://theses.insa-lyon.fr/publication/2024ISAL0088/these.pdf © [C.K. Miyazaki], [2024], INSA Lyon, tous droits réservés

to an ammonium concentration < 100 mg NH_4-N/L or a COD concentration < 1200 mg COD/L, while the high organic load corresponded to an ammonium concentration > 100 mg NH_4-N/L or a COD concentration > 1200 mg COD/L.

The system operated in a batch regime with fixed hours, at total ten batches per day, every 2.5 hours to achieve a hydraulic loading rate of 0.4 m/d. The pilot was monitored weekly via laboratory analyses, which involved sampling inlet and outlet locations through the use of 24-hour composite samples. The analysis encompassed various parameters, including COD, filtered COD (fCOD), TSS, BOD_5 (once per month), NH_4-N, NO_3-N, NO_2-N, TKN (once per month) and TN (once per month) following European standard methods (NF EN 872, EN ISO 10304-1, NF EN ISO 14911, 135 NF EN 25663, NF EN 6878, NF EN ISO 9963-1).

- Aeration strategy

The oxygen consumption rate was calculated using a modified version of Platzer's equation (Platzer, 1999; Prost-Boucle and Molle, 2021). The inlet concentration was assumed to be 80 mg NH_4-N/L, and the COD was assumed to be 800 mg. To meet the oxygen demand, the equations used were based on those proposed by Boog et al. (2014) and Metcalf et al. (2004). The SOTE considered was 4.7%/m (Wallace et al., 2007), and the airflow rate was 7 m^3/h per air blower. Thus, the total daily aeration necessary to supply the demand was 11 hours. 3 recommended that the total duration of aeration on the primary filter should be longer than that on the secondary filter, and the primary filter should have a minimum of six hours for optimal hydraulic performance. Therefore, the total duration of eight hours on the primary filter was defined, while that on the secondary filter was set at three hours.

The aeration strategy was fractioned based on the previous experiment conducted by 4, which demonstrated the effectiveness of synchronizing aeration for the primary filter with feeding times. The aeration started 1.5 hours prior to each batch and lasted for 48 minutes, resulting in 10 aeration cycles per day. In contrast, the secondary filter was aerated on a time-based schedule, with each cycle occurring every five hours for a duration of 36 minutes (five cycles per day). Figure 5.2 illustrates the aeration cycles for the primary and secondary filters. This aeration strategy commenced in July 2023 and remained active until February 2024.

The primary objective of this aeration strategy was to use the primary filter to facilitate the nitrification and denitrification processes. The strategy is based on two key elements: first, aeration process transfers oxygen to the liquid phase, enabling the oxidation of ammonium to nitrate before the next batch arrives. As the nitrification process consumes oxygen, the environment tends to become anoxic. Second, this anoxic

Thèse accessible à l'adresse : https://theses.insa-lyon.fr/publication/2024ISAL0088/these.pdf © [C.K. Miyazaki], [2024], INSA Lyon, tous droits réservés

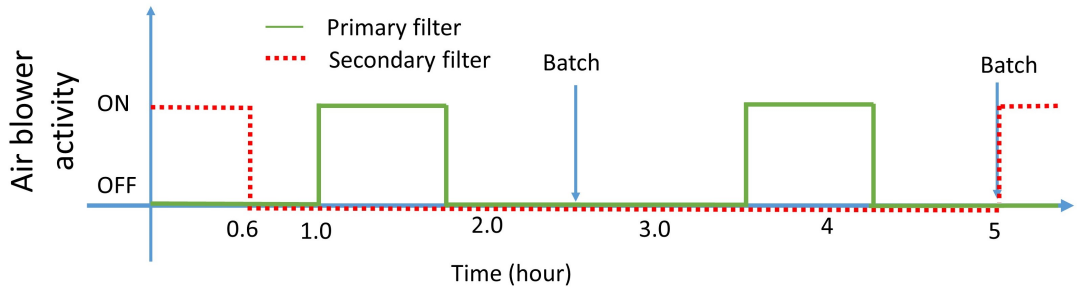

Figure 5.2: Aeration strategy for the current study.

environment, coupled with an input of organic carbon during the next batch, will encourage the reduction of nitrates and nitrites via the denitrification process. The secondary filter is used to polish the remaining pollutant concentration as a secondary treatment process.

- Statistical analysis

Principal Component Analysis (PCA) was used for exploring the relationships among various parameters associated with nitrification and denitrification processes. These include the efficiency of removal of the different forms of and variations in the concentrations of nitrogen compounds (Cui et al., 2021). This method reduces the dimensionality of a dataset (Jolliffe, 2002) and provides a visual representation of the key factors influencing the system performance.

The analysis focused on the following variables: TN concentration removal, NH_4-N outlet concentration, NO_3-N outlet concentration, daily durations of aerobic and anoxic conditions, water temperature and BOD_5/TKN. The aerobic duration was determined using a DO sensor, with conditions considered aerobic when DO levels exceeded 0.2 mg/L. Conversely, an anoxic environment was defined by DO levels below 0.2 mg/L. Since BOD_5 and TKN measurements were taken monthly, missing values were estimated using the median COD/BOD_5 ratio and the median (TKN - NH_4-N)/TSS ratio.

- Data analysis

The denitrification demand for organic carbon was calculated based on the assumption that 60% COD removal would be achieved in the unsaturated part. This value was selected because a first-stage French VF TW has been shown to achieve 77% COD removal at a depth of 53 cm (Morvannou et al., 2015). Additionally, a COD/NO_3-N ratio of 3 has been identified as optimal for denitrification (Morvannou et al., 2017). Therefore, the demand for COD is calculated by following Eq. 5.1.

$$\mathrm{COD_{demand}} = 3(\mathrm{TKN_{in}} - \mathrm{TKN_{out}}) - 0.8\mathrm{COD_{in}} \qquad \text{(Eq. 5.1)}$$

Thèse accessible à l'adresse : https://theses.insa-lyon.fr/publication/2024ISAL0088/these.pdf © [C.K. Miyazaki], [2024], INSA Lyon, tous droits réservés

- N-k-C* Model

The N-k-C* model is commonly employed to predict the effluent water quality and is used for design purposes (Kadlec and Wallace, 2009). This reaction model integrates the tanks-in-series (TIS) concept, accounts for background concentrations within the reactor, and considers hydraulic parameters. It also incorporates temperature-dependent first-order biodegradation (Kadlec and Wallace, 2009). To avoid the transport delay artifact (i.e., synoptic error), the training data was simplified to monthly averaged data (i.e., 8 data points from July 2023 until February 2024) (Kadlec and Wallace, 2009; Von Sperling et al., 2023). The target measure was the output variable of TKN and TN. An optimization algorithm was employed to find k_{v20} and θ, to achieve the lowest possible sum of squared errors between the predicted and the experimental values, with θ being constrained between 0.9 and 1.1 (Kadlec and Wallace, 2009). The equation to calculate removal coefficient correcting the water temperature is shown in Eq. 5.3.

$$k_v = k_{v20}\theta^{(T-20)} \qquad \text{(Eq. 5.2)}$$

where θ is the modified Arrhenius temperature factor (dimensionless), T is the water temperature measured with a sensor (°C), k_{v20} is the removal rate coefficient for a first-order reaction at 20°C (d^{-1}), and k_v is the removal rate coefficient for a first-order reaction at T °C (d^{-1}). The equation to predict the outlet concentration considering a first-order reaction is shown in Eq. 5.3.

$$C_{\text{out}} = C^* + \frac{(C_{\text{in}} - C^*)}{\left(1 + k_v \frac{\tau}{N}\right)^N} \qquad \text{(Eq. 5.3)}$$

where C_{in} is the inlet concentration to wetland (mg/L), C_{out} is the outlet concentration from wetland (mg/L), C^* is the background concentration (mg/L), N is the apparent number of tanks in series (NTIS) (dimensionless), and τ is the hydraulic retention time (HRT) (d) in the wetland. A previous study found NTIS and τ for different aeration strategies in the Rhizosph'air® system and these values were used for this model (Chapter 3). In such study, six tracer tests were conducted to evaluate the impact of different aeration strategies on NTIS and τ (Chapter 3). It should be noted, however, that none of the aforementioned tests precisely replicated the aeration strategy employed in the present experiment. As a result, the model was applied to the 9h1 (9h aeration only in the primary filter) and 6h (6h aeration in both filters) tracer tests, which are the closest to the current strategy, and the results were compared. No significant variance was observed between these tracer tests. Accordingly, only the results from the tracer test 9h1 were used.

The values determined for the removal rate coefficient k_{v20} were validated for the entire dataset. Two metrics were employed to assess the accuracy of the model: the root

Thèse accessible à l'adresse : https://theses.insa-lyon.fr/publication/2024ISAL0088/these.pdf © [C.K. Miyazaki], [2024], INSA Lyon, tous droits réservés

mean squared error (RMSE) and the coefficient of determination (R^2). The RMSE is a metric used to assess the inaccuracy of a model with the same unit as the target variable. It quantifies the dispersion of predicted values around the observed values, with lower RMSE values indicating higher precision. As the outcome target (either TKN or TN concentration) is a numeric value, RMSE is the primary metric used for the comparative analysis of algorithms, providing insights into the predictive performance of each model (Nguyen et al., 2021). The RMSE value, representing the root mean squared error, is computed using Eq. 5.4.

$$\text{RMSE} = \sqrt{\frac{1}{n}\sum_{i=1}^{n}(y_i - \hat{y}_i)^2} \qquad \text{(Eq. 5.4)}$$

where y_i is the observed value of the dependent variable for observation i, $\hat{y}_i$ is the predicted value of the dependent variable for observation i.

In contrast, R^2 evaluates the goodness of fit of the model to the data, with a range from 0 to 1. A value of 0 indicates that the model does not explain any of the variability of the response data around its mean. In contrast, a value of 1 indicates that the model can predict the exact same values as the one observed in the field. The R^2 value, also known as the coefficient of determination, is calculated using Eq. 5.5.

$$R^2 = 1 - \frac{\sum_{i=1}^{n}(y_i - \hat{y}_i)^2}{\sum_{i=1}^{n}(y_i - \bar{y}_i)^2} \qquad \text{(Eq. 5.5)}$$

where n is the number of observations, y_i is the observed value of the dependent variable for observation i, $\hat{y}_i$ is the predicted value of the dependent variable for observation i, and $\bar{y}_i$ is the mean of the observed values of the dependent variable.

5.2.3 Controlling total nitrogen removal with online sensors

- Online sensors

Simultaneous to the pilot operation, a total of ten online sensors were strategically positioned along the filter, with measurements taken at 5-minute intervals (Figure 5.1). Among these sensors, three monitored NH_4-N and NO_x-N concentrations (i.e., sensors WTW, VARION 700IQ), positioned at the inlet, middle, and outlet of the pilot system. The remaining sensors were oxygen (i.e., sensors WTW, FDO 700IQ), redox (i.e., sensors WTW SENSOLYT 700 IQ PTA), and pH (i.e., sensors WTW SENSOLYT 700 IQ SEA) sensors, distributed in piezometers situated inside the pilot in different depths and vertically spaced apart. The sensors were calibrated following the recommendations from the manufacturer. Every week, they were cleaned, maintained, or repaired when required. In the case of the

Thèse accessible à l'adresse : https://theses.insa-lyon.fr/publication/2024ISAL0088/these.pdf © [C.K. Miyazaki], [2024], INSA Lyon, tous droits réservés

nitrogen sensors, the weekly monitoring involved comparing its values against chemical laboratory results, while for the others, the monitoring was a simple verification of the values in a standard solution.

- Data pre-processing

The pre-processing data involved applying the calibration curve to the nitrogen and redox sensors. The data was visually inspected to identify punctual abnormalities that could come from perturbation in the cleaning process, such as outliers and missing values, which often occurred when a sensor was replaced. The redox potential standardized to the hydrogen reference (Eh) was calculated by adding the measured redox potential (Em) values (mV) and the potential of the Ag/AgCl reference against the standard hydrogen reference (Eref). The manufacturer provided this value, which varies according to the local temperature sensor.

- Bending-points control

The bending-point strategy employs indirect measurement to estimate the length of aerobic and anoxic conditions, thereby reducing energy consumption. When these variables are not controlled, it is possible to correlate their profiles with the nitrification / denitrification process and identify the endpoint of each reaction (Jaramillo et al., 2018). For example, the nitrate knee indicates the end of the denitrification process (examples of bending points strategy in Figure 7.12, Appendix). Ammonium and nitrate sensors are mainly used for nitrogen control. However, significant investment and maintenance costs associated with these sensors may render them impractical for some applications. To address these challenges, alternative physical-chemical parameters can be employed for indirect measurement, including dissolved oxygen (DO), pH, and redox potential (Eh) (Zanetti et al., 2012).

The online sensors were monitored throughout the pilot operation to gain insight into the curve pattern. Subsequently, two locations within the filter on either side (as illustrated in Figure 5.1) were chosen to collect grab samples to validate the correlation between the inflection points and the actual nitrification and denitrification processes. Samples were collected at ten-minute intervals. In total, five experimental conditions (EC) were conducted. A total of five experimental conditions (EC) were conducted. The first EC employed the aeration strategy depicted in Figure 5.3. The second to fifth EC employed a strategy of complete ammonium nitrification, stabilization of anoxic conditions, and batch launch. Thus, the aeration length depended on the field condition. The parameters monitored in each samples included Eh, DO, NH_4-N, NO_3-N, fCOD and HCO_3-.

Thèse accessible à l'adresse : https://theses.insa-lyon.fr/publication/2024ISAL0088/these.pdf © [C.K. Miyazaki], [2024], INSA Lyon, tous droits réservés

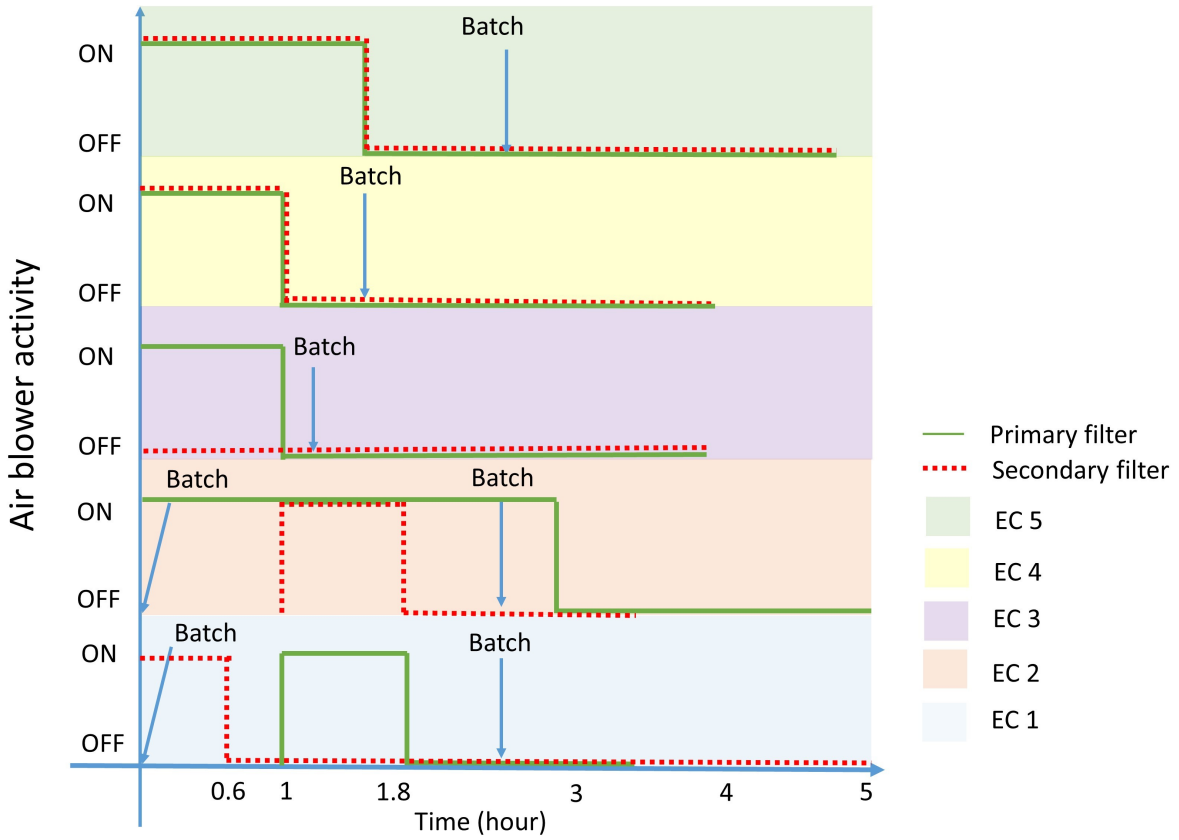

Figure 5.3: Aeration strategies applied for the bending-points validation experiments. EC = experimental conditions.

- Exploratory analysis for predictive modelling: Linear correlation between variables

It is crucial to analyze the potential interdependencies among variables to verify the applicability of linear predictive models. Examining all potential linear correlations between variables can assist in developing a selection criterion to further input in a predictive model for the system behavior (Bagherzadeh et al., 2021). In this case, a Pearson correlation matrix was used. All sensors were included as variables. Variables with normalized Pearson correlation coefficients of less than 0.01 or greater than 0.85 were systematically excluded. Based on the statistical guidelines of Cheng et al. (2023), this approach aims to retain only those variables demonstrating a moderate correlation with the target variable. Filtering out variables with weak or excessively strong correlations promotes robustness and generalizability in predictive performance Cheng et al. (2023).

Therefore, all temperature sensors were excluded from the analysis due to high correlation (Figure 7.13, Appendix), with the exception of the outlet temperature sensor. The decision was made to facilitate straightforward implementation within a full-scale context (Monday et al., 2024).

Thèse accessible à l'adresse : https://theses.insa-lyon.fr/publication/2024ISAL0088/these.pdf © [C.K. Miyazaki], [2024], INSA Lyon, tous droits réservés

5.3 Results and discussion

5.3.1 Optimizing total nitrogen removal

- System performance

In Figure 5.4, the biplot (Figure 7.14 presents the scree plot, Appendix) is used to represent the magnitude, direction, and correlation of each variable in relation to the first two principal components (PCs) as well as to depict individual observations. Variables with positive correlations are positioned close together in the same direction, while variables with negative correlations are situated on opposite sides. Uncorrelated variables appear to be nearly perpendicular (Kassambara, 2017). The dataset includes all data, and the individuals represent the TN removal. The data were classified into groups to capture the experimental outcomes and process mechanisms, as described previously in 2.2.2. The first two components of the PCA account for 72.6% of the total variance (PC1 = 46.5% and PC2 = 26.1%, Figure 5.4), which is a reasonable representation of the dataset in 2D (Jolliffe, 2002; Kassambara, 2017). The variables of duration of aerobic and anoxic conditions on the primary filter and water temperature made substantial contributions to PC1, while the inlet BOD_5/TKN ratio contributed to PC2 (refer to Figure 7.15 and Figure 7.16 in Appendix for a visual representation of the contribution of each variable to PC1 and PC2).

The biplot generated from the dataset indicates that the TN removal had a positive correlation with BOD_5/TKN inlet ratio. This suggests that a low BOD_5/TKN ratio may result in reduced organic carbon availability for the denitrification process, leading to an increase in nitrate concentration at the outlet and a reduction in TN removal. This supports the hypothesis that organic carbon as to be used as much as possible for denitrification during anoxic periods. Nitrate concentrations at the outlet were correlated with the duration of aerobic (positive correlation) or anoxic (negative correlation) environment in the primary filter. This demonstrates the importance of maintaining an equilibrium between nitrification and denitrification on the primary filter, particularly given that this filter has a longer aeration duration, an increased mixing effect (Chapter 3), and greater organic carbon availability (due to the supply from the batches). In contrast, ammonium concentrations at the outlet were found to be correlated with the state of the secondary filter, either the duration of the aerobic or the anoxic environment. The hypothesis is that the residual ammonium entering the secondary filter could potentially be nitrified, but not denitrified. In this case, the primary filter plays a significant role in the nitrification process and in the TN removal while the secondary filter mainly play a polishing role for nitrification. Therefore, ammonium and nitrate should be removed at maximum in the primary filter, leaving the residual ammonium to nitrify in the secondary filter.

Thèse accessible à l'adresse : https://theses.insa-lyon.fr/publication/2024ISAL0088/these.pdf © [C.K. Miyazaki], [2024], INSA Lyon, tous droits réservés

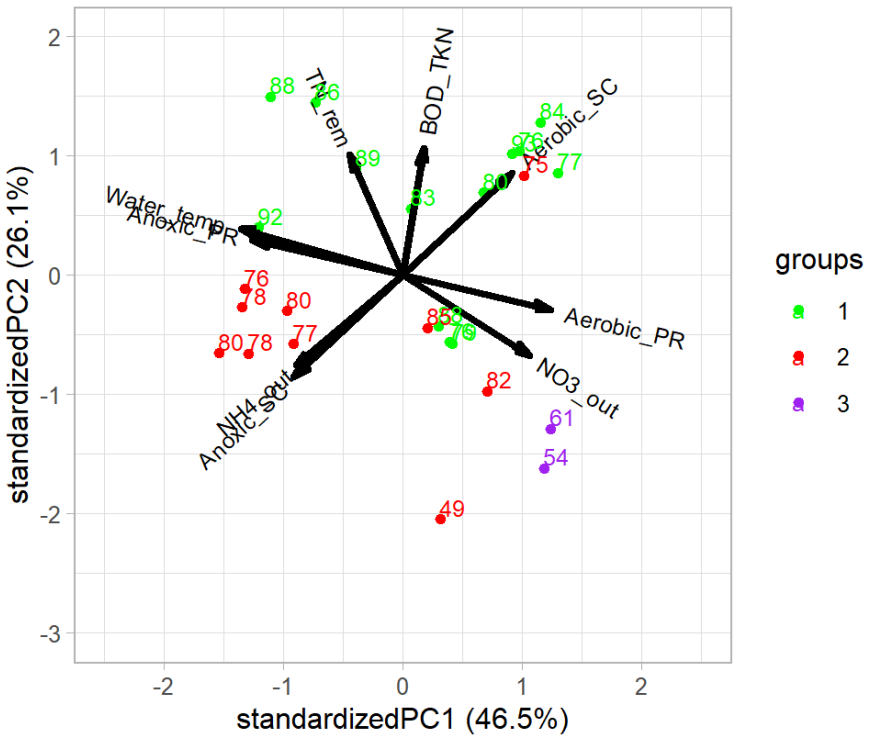

Figure 5.4: Principal component analysis showing the relationship between TN removal and other variables. The points represent the TN removal. TN_rem = TN removal, Water_temp = Water temperature, BOD_TKN = BOD_5inlet concentration / TKN inlet concentration, Anoxic_PR = Anoxic duration (< 0.2 mg O_2/L) in a day on the primary filter, Aerobic_PR = Aerobic (> 0.2 mg O_2/L) duration in a day on the primary filter, Anoxic_SC = Anoxic duration (< 0.2 mg O_2/L) in a day on the secondary filter, Aerobic_SC = Aerobic duration (> 0.2 mg O_2/L) in a day on the secondary filter, NH_4_out = NH_4-N concentration at the outlet, NO_3_out = NO_3-N concentration at the outlet, group 1 = normal organic loading, group 2 = high organic loading, group 3 = winter time.

The groups of Figure 5.4 cluster individuals according to similar performance of nitrogen removal. Samples with normal organic loading (Group 1) exhibited the highest TN removal (75 - 93%). Individuals with high organic loading rates (Group 2) achieved TN removal performances of between 49 and 80%. As the percentage of variance explained most of the dataset, it is possible to correlate individuals with variables (Jolliffe and Cadima, 2016). Therefore, most individuals in Group 2 exhibited a closer correlation with the duration of anoxic environments in the primary filter. In fact, the high oxygen consumption in this part of the filter led to longer periods of anoxic environments, which had an impact on TN removal. Group 3 demonstrates the impact of seasonal variations at the pilot location (lowest water temperature in the dataset of about 6°C), due to the fact that the individuals are on the opposite side of the water temperature variable. The individual points in Group 1 had the same inlet concentration (38.7 - 71.7 mg NH_4-N/L

Thèse accessible à l'adresse : https://theses.insa-lyon.fr/publication/2024ISAL0088/these.pdf © [C.K. Miyazaki], [2024], INSA Lyon, tous droits réservés

and 515 - 673 mg COD/L) but not the same water temperature (9.2 - 15.4°C). The lower performance in reducing the nitrate concentration was attributed to the absence of reeds due to the winter harvest and the lower temperature, which resulted in a reduction in the activity of denitrification bacteria.

Table 5.1 and Figure 7.17 (refer to Appendix for the results visualization) show the overall system performance for a dataset corresponding to low and high organic loadings. The figure demonstrates the variations in concentrations and removal efficiencies for COD, TSS, NH_4-N, and TN. The results for COD and TSS indicate that the treatment process is highly efficient, regardless of the inlet concentration. The concentration removal efficiencies are 96 ± 1% and 97 ± 1% for COD and 99 ± 1% and 99 ± 1% for TSS for normal and high organic loadings, respectively. Regarding nitrogen, the normal organic loading results indicate robust performance, with NH_4-N concentration removal of 90.3 ± 8.6%. The TN had a lower performance than other parameters, with 81.4 ± 5.8%, yet still reaching a reasonably lower outlet concentration of 13.7 ± 5.8 mg/L. The aeration strategy employed in the current study to better use organic carbon for the denitrification process had a superior performance for all the parameters, including NH_4-N and TN, compared to the seven strategies evaluated in Chapter 4, where the maximum TN concentration removal reached was 71 ± 5%.

Table 5.1: Inlet, outlet concentrations and concentration removal for normal and high organic loads, for COD, TSS, TN, NH_4-N and NO_3-N. Avg = average and Std dev = standard deviation.

Parameter		In		Out		Concentration removal (%)	
		Median	Avg ± Std dev	Median	Avg ± Std dev	Median	Avg ± Std dev
Normal organic loading	COD (mg/L)	819	805 ± 222	< 21	28 ± 10	96%	96 ± 1%
	TSS (mg/L)	204	253 ± 124	< 2	3 ± 2	99%	99 ± 1%
	NH_4-N (mg/L)	65.0	61.0 ± 22.4	3.7	6.0 ± 6.7	94.0%	90.3 ± 8.6%
	NO_3-N (mg/L)	< 0.5	< 0.6 ± 0.6	5.9	7.4 ± 6.1	-	-
	TN (mg/L)	78.9	74.8 ± 22.4	12.9	13.7 ± 6.4	80.0%	81.4 ± 5.8%
High organic loading	COD (mg/L)	1060	1080 ± 271	< 36	35 ± 9	96%	97 ± 1%
	TSS (mg/L)	420	372 ± 147	< 2	4 ± 3	99%	99 ± 1%
	NH_4-N (mg/L)	118.0	134.3 ± 37.4	13.5	20.7 ± 14.9	87.0%	85.6 ± 7.8%
	NO_3-N (mg/L)	< 0.5	< 0.5 ± 0.0	3.1	5.9 ± 5.9	-	-
	TN (mg/L)	142.5	158.2 ± 38.7	26.4	27.2 ± 12.9	82.0%	83.3 ± 5.3%

The results for this normal loadings comply with the European water policy (Council Directive of the European Communities, 1991) criteria for the maximum concentration in the effluent (15 mg TN/L) and the minimum concentration removal efficiency (70%). If further optimization is required, the limiting process is denitrification, with an outlet concentration of 7.39 ± 6.09 mg NO_3-N/L. As illustrated in Figure 5.4, the strong correlation between TN removal and BOD_5/TKN suggests a lack of organic carbon, which is relatively common in this type of system, thus the degradation of organic carbon should

Thèse accessible à l'adresse : https://theses.insa-lyon.fr/publication/2024ISAL0088/these.pdf © [C.K. Miyazaki], [2024], INSA Lyon, tous droits réservés

be optimized. The demand for organic carbon was calculated and the results indicates that some samples at the outlet showed a lack of organic carbon of up to 224 mg COD/L.

The high organic loading dataset (Table 5.1) accounts for the high organic loading, which exceeds 100 mg NH_4-N/L or 1200 mg COD/L. It should be noted that the total aeration duration of 11 hours was determined based on the normal organic load, with concentrations of 80 mg/L for NH_4 and 800 mg/L for COD. Thus, the aeration duration was fixed for the primary and secondary filters throughout the experiment. The results pointed out that the oxygen delivered was insufficient to meet the oxygen requirements of these high load ranges. These factors led to an increase in ammonium concentration at the outlet (on average 20.7 ± 14.9 mg/L). Even though the TN concentration removal (83.3 ± 5.3 %) was closer to normal organic loading, the TN outlet concentration increased to 27.2 ± 12.9 mg/L. Therefore, the high organic loading data indicates that the nitrification process limits higher performance, contrary to the findings of the normal organic loading data. Nevertheless, the system proved resilient despite a high inlet concentration of up to 236 mg TN/L, three times the average for typical wastewater in small communities (Mercoiret, 2009).

A previous study evaluated the effectiveness of an on-off air blower control strategy based on fixed time, with aerated and no-aerated phases, regardless of batch hours, and distributed during the day. The novel aeration strategy studied here is based on the inflow, where 1.5 hours prior to the batch arrival, the aeration process is initiated for a 48-minute period, followed by a 42-minute no-aeration phase until the batch hour. This strategy proved to be the most efficient of all the previous studies. The question then becomes how this can be applied on a full scale, given that the batch hours are not fixed and depend on the inflow. In addition, in some cases, the non-aeration phases could be short. Due to the scattered overnight batch hours, this aeration strategy can be readily implemented. However, the frequency of batch occurrences is higher during the day, which presents a challenge in maintaining an anoxic environment during the batch hour. This is due to the fact that the DO consumption depends on the batch occurrence. Furthermore, the nitrification and denitrification rates are also influenced by the microbial communities and their metabolic pathways (Miao et al., 2022). Further studies should focus on understanding the relationship between DO consumption rate and the other factors, such as ammonium inlet concentration, nitrification and denitrification kinetics, and the microbial activity. Additionally, this biochemical comprehension could be integrated with real-time control and automation of the system.

- N-k-C* model

Table 5.2 presents the results for the N-k-C* model, based on the average concentration of TKN and TN at the inlet and outlet for each month, and the primary

Thèse accessible à l'adresse : https://theses.insa-lyon.fr/publication/2024ISAL0088/these.pdf © [C.K. Miyazaki], [2024], INSA Lyon, tous droits réservés

model assumptions. The background concentrations were assumed to be 1 mg TKN/L (Kadlec and Wallace, 2009) and 2 mg TN/L (Gajewska and Cur, 2018). The values for the volumetric-based coefficient (k_{v20}) were 1.11 and 1.11 d^{-1} for TKN and TN, respectively.

Table 5.2: First-order reaction using the N-k-C* model approach, based on input and output average concentration for each month, as well as the main model assumptions. C^* stands for background concentration in mg/L.

Target parameter	**NTIS**	τ **(d)**	C^* **(mg/L)**	θ	k_{v20} **(d^{-1})**
TKN	5.1	1.8	1	0.96	1.11
TN	5.1	1.8	2	1.01	1.11

The similar values of removal rate coefficient for TKN and TN indicate that nitrification has a more significant impact than denitrification, which is expected given the very good TKN removal. The removal rate coefficients k_{v20} for TN was 20 times higher than those reported in a large dataset of passive HF TW (k_{v20} = 0.06 m/d) (Von Sperling et al., 2023) and 10 times higher than a passive HF TW in a cold climate (k_{v20} = 0.11 m/d) (Redmond et al., 2014). Both studies employed the P-k-C* approach. Furthermore, the removal rate coefficients for TN were five times greater than those observed in an aerated HF TW using an intermittent aeration strategy (k_{v20} = 0.27 m/d) (Redmond et al., 2014) and a continuously aerated HF TW (k_{v20} = 0.21 m/d) (Nivala et al., 2019a). The temperature correction (θ-value) for TKN and TN was 0.96 and 1.01, respectively, indicating that there is little, if any, temperature dependence on TKN and TN removal. Kadlec and Wallace (2009) also found the same results for non aerated HF TW, with a 10th to 90th percentile θ-value ranging from 0.951 to 1.011.

The results validation process entailed the application of θ and k_{v20} to the entire dataset. Figure 5.5 provides a comparison of the experimental and predicted values for each target parameter (TN and TKN), highlighting the accuracy of the model (R^2 and RMSE). The model for TKN demonstrated a strong correlation with the experimental values, with an R^2 value of 73%. By comparison, the R^2 value for the TN model was lower at 58%. This indicates that nearly half of the observed variability in the data set was accounted for. In terms of precision, the TKN model demonstrated superior performance compared to the TN model, with a RMSE of 6.19 and 7.01 mg/L, respectively. The RMSE values for the TKN and TN model were comparable to that of the TIS model applied in a free water surface (Canet-Martí et al., 2022). While the TKN model showed higher R^2 value and a good overall trend in predicting effluent concentrations, its precision (RMSE = 6.19 mg/L) is insufficient for accurately predicting values that would meet strict compliance standards. The TN model has also limitation, as it does not accurately reflect the dynamic response of the system and fails to adequately capture short-term fluctuations

Thèse accessible à l'adresse : https://theses.insa-lyon.fr/publication/2024ISAL0088/these.pdf © [C.K. Miyazaki], [2024], INSA Lyon, tous droits réservés

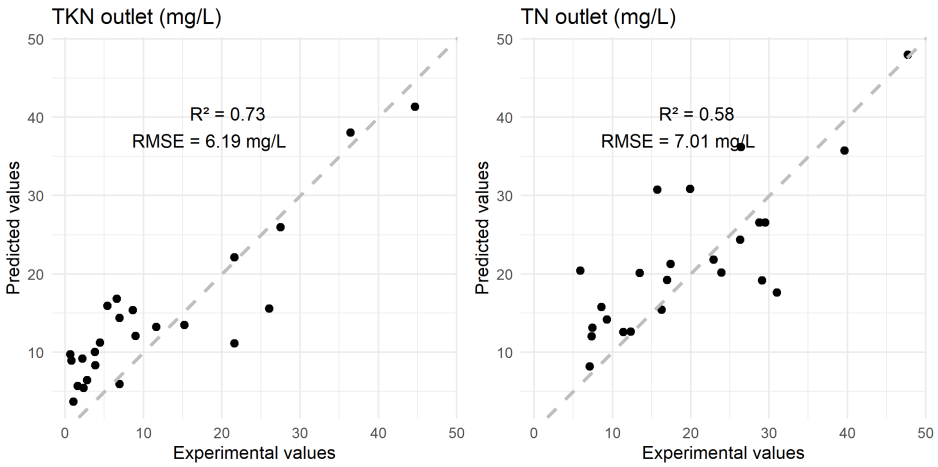

Figure 5.5: Comparison between experimental and predicted values for NTK and TN concentrations at the outlet. The model accuracy was pointed out as R^2 and RMSE.

in wastewater influent (Redmond et al., 2014).

Accordingly, as Chapter 3 demonstrated, the global NTIS values found in the different aeration strategies may present challenges in applying them in the N-k-C* model to represent complex systems, such as the Rhizosph'air®. The findings of this study confirm the previous hypothesis that a single NTIS value for the entire system is not a reasonable representation of reality. The most effective solution would be to divide the model into two disctinct compartments, one for the primary filter and the other for the secondary filter, given the distinct aeration strategies employed for each. Alternatively, a k_{v20} could be applied to each tank in series. These approaches may prove more effective in aligning with the actual outlet concentration, offering valuable insights for system design.

- Trend curves from online sensors

Figure 5.6 presents the trend curves for one day from each online sensor, with only periods where there were normal inlet ammonium concentrations. The concentrations of NH_4-N and NO_x-N in the middle of the filter remained stable during the day, with a mean concentration of 27.1 ± 19.9 mg NH_4-N/L and 0.5 ± 0.9 mg NO_x-N/L, respectively. At the outlet, the mean concentration of NH_4-N dropped to 3.0 ± 4.0 mg/L, while the concentration of NO_x-N increased to 11.3 ± 8.9 mg/L. This indicates that nitrification occurred not only in the primary filter, but also in the secondary filter. The primary filter had a dual role of oxidizing the ammonium and reducing the nitrate. In order to compare different trend curve periods, Figure 7.18 in the Appendix presents the results for the high inlet ammonium organic loading period. The mean concentration increased to 41.3 ± 23.9 mg NH_4-N/L and 1.6 ± 2.4 mg NO_x-N/L in the middle and 31.8 ± 16.4 mg NH_4-N/L and 3.9 ± 4.4 mg NO_x-N/L at the outlet. The oxidation of ammonium was first carried out on

Thèse accessible à l'adresse : https://theses.insa-lyon.fr/publication/2024ISAL0088/these.pdf © [C.K. Miyazaki], [2024], INSA Lyon, tous droits réservés

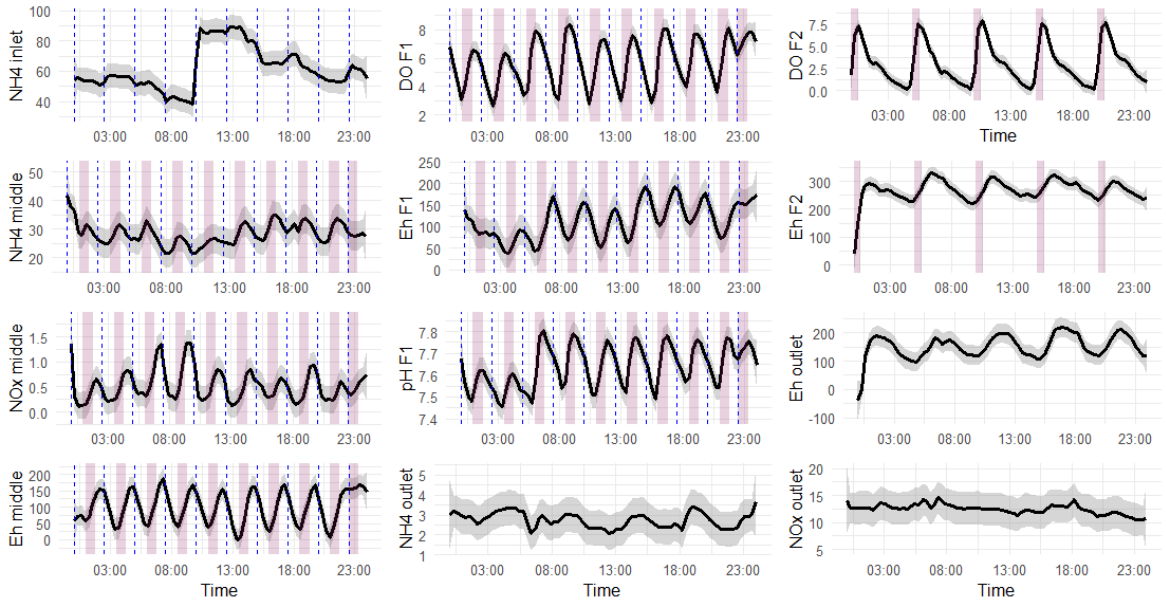

Figure 5.6: Trend curves for each online sensor considering only periods where the organic loading was $<$ 100 NH_4-N/L and $<$ 1200 mg COD/L. Black line represent the mean concentration, the grey region the 95% confidence interval, blue dashed line the batch hour, red region the aeration period. NH_4 middle, NO_x middle, Eh middle, O2 F1, Eh F1 and pH F1 were place in filter 1 and they are playing the primary filter. O2 F2 and Eh F2 were place in filter 2 and they are as secondary filter.

the primary filter, as also demonstrated in Table 5.1. In contrast to the normal organic loading scenario, the secondary filter did not play a significant role in the nitrification process. As outlined in section 5.3.1, nitrification was the primary limiting factor with high organic loading, while the performance on nitrate removal was highly effective.

The pH remained relatively stable throughout the experiment, fluctuating between 7.6 $\pm$ 0.3. This range is suitable for developing denitrified bacteria and does not hinder denitrification (Saeed and Sun, 2012). The Eh sensors inside the system demonstrated a range of -289 to 569 mV, aligning with the values observed in HF TW, which varied between -300 and 400 mV (Corbella et al., 2014), -400 and 800 mV (Dušek et al., 2008), -260 and 657 mV (Ruppelt et al., 2019) and VF TW with bottom saturated, varying between -450 and 700 mV (Silveira et al., 2015). During the aeration process, the Eh levels rose to 200-300 mV, within the range typically observed in aerobic zones (Kadlec and Wallace, 2009; Reddy et al., 2022). Once the aeration terminated, the Eh level declined to 50-100 mV, indicating a transition to an anoxic zone.

The DO sensor indicated a rapid increase in DO concentration at the start of aeration and a subsequent decrease when aeration was stopped. However, the rate of decline was contingent upon the consumption of bacteria. In the case of a normal ammonium organic loading, the DO concentration fluctuated between 8 mg/L at the

Thèse accessible à l'adresse : https://theses.insa-lyon.fr/publication/2024ISAL0088/these.pdf © [C.K. Miyazaki], [2024], INSA Lyon, tous droits réservés

end of aeration and 0 mg/L before a new oxygen supply. In the event of high organic loading, the DO concentration fluctuated between 2 and 0 mg/L (Figure 7.17, Appendix). The frequency of occurrence of the batch moment (considering an interval of 10 minutes before and after the batch) in anoxic environments (less than 0.2 mg DO/L) was 59-73% regardless of the organic loading. The frequency of occurrence increased to 85% in the cases where the DO concentration was less than 0.5 mg/L was considered, with an interval of 20 minutes before and after the batch. Therefore, the hypothesis of setting aeration on the primary filter before the batch hour to have an anoxic environment seems coherent. This indicates that denitrified bacteria readily consume organic carbon.

5.3.2 Exploratory control of total nitrogen removal with online sensors

- Bending points

The Eh and DO profiles for the primary and secondary filters are illustrated in Figure 7.19 for one day, in the Appendix. Both sensors on the primary filter indicated inflection points during and after the aeration period. The Eh sensor on the secondary filter displayed a more pronounced inflection point, which may represent the "nitrate knee", indicating the end of the denitrification according to Jaramillo et al. (2018). This occurred when no dissolved oxygen was available in an anoxic environment, allowing denitrification to take place and reducing nitrate and nitrite concentration.

The results of the validation method, as shown in Table 5.3, demonstrate the correlation between the Eh and DO inflection points and the chemistry data. Figure 5.7 illustrates the curves that identify the “DO elbow,” “ORP plateau,” and “Nitrate knee” (see Figure 7.12, Appendix, for bending-points strategies examples). The experiments identified inflection points correlated with ammonium and nitrate concentrations, with a total of two "DO elbow," one "ORP plateau," and three “Nitrate knee” (Table 5.3). The experimental condition (EC) 2 found a "DO elbow" when the ammonium concentration was 1.83 mg NH_4-N/L and the DO was 4.19 mg/L. In contrast, for the EC 4, the concentrations found were very different, at 16.7 mg NH_4-N/L and 1.08 mg DO/L. This indicates that the "DO elbow" was not a suitable indicator for the end of nitrification. The ORP plateau was identified during EC 5, when the Eh was 300 mV with 0 mg NO_3-N/L. This inflection point appears to identify the end of nitrification, but it only occurred once. Lastly, the bending point, which corresponds to the “Nitrate knee”, was identified in both the EC 1 (135 mV and 31.3 mg NO_3-N/L in the primary filter and 138 mV and 0 mg NO_3-N/L in the secondary filter) and EC 5. This suggests that denitrification reached its end point in two out of three occurences. However, the concentration during the experiment, which was identified as the “Nitrate knee”, ranged between 0 and 3.0 mg NO_3-N/L, indicating a relatively

Thèse accessible à l'adresse : https://theses.insa-lyon.fr/publication/2024ISAL0088/these.pdf © [C.K. Miyazaki], [2024], INSA Lyon, tous droits réservés

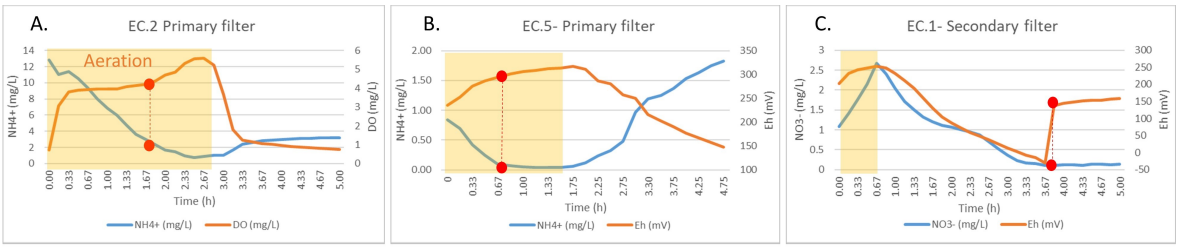

Figure 5.7: A. DO concentration versus ammonium concentration for the primary filter, the red dashed line represents the "DO elbow". B. Eh measurement versus ammonium concentration for the primary filter, the red dashed line represents the "ORP plateau". C. Eh measurement versus nitrate concentration for the secondary filter, the red dashed line represents the "Nitrate knee".

narrow range and potentially within the margin of error (see Figure 7.19, Appendix). As a result, there was minimal correlation between the Eh and DO bending points ("Nitrate knee", "DO elbow", and "ORP plateau") and ammonium or nitrate concentrations. Some studies in the literature (Fatone et al., 2008) indicated that these bending points are not easily discernible. The difficulties in identifying them can be attributed to two main factors: over-aeration conditions, where the optimal range is DO $<$ 2 mg/L, and under- or over-organic loading rates (Paul et al., 1998).

The validation method identified some bending points, but not all of them represent the actual end of the nitrification or denitrification process. Furthermore, the occurrences were not regular, and even the concentrations during the bending points were not the same. It should be noted that other environmental factors could potentially influence these points, including batches, internal hydraulic flow, and the end of the presence of organic matter. These efforts represent a pioneering study of the bending-point strategy on TWs in the literature. The majority of existing studies published in the literature in this field rely on online sensors for monitoring purposes (Arias et al., 2005; de Andrade Moraes et al., 2020; Garfí et al., 2014; Rizzo et al., 2020; Silveira et al., 2015) or they use a DO sensor to control aeration (Khan et al., 2022; Labella et al., 2015; Uggetti et al., 2016; Zhang et al., 2010). Further studies are required to optimize the use of this tool and could continue investigating the optimal activation and deactivation points for alternative aeration strategies and potentially testing other sensors (such as pH).

- Linear correlation and modelling implications

Figure 5.8 presents the Pearson correlation matrix with the corresponding significance levels in the upper-right, the density function and histograms in the diagonal, and the biplots in the lower-left for the online sensors. All sensors demonstrate a highly significant correlation with one another ($p < 0.001$). The highest positive correlation with NH_4-N

Thèse accessible à l'adresse : https://theses.insa-lyon.fr/publication/2024ISAL0088/these.pdf © [C.K. Miyazaki], [2024], INSA Lyon, tous droits réservés

Table 5.3: Nitrogen form concentrations at D0 and Eh inflexion points ("DO elbow", "ORP plateau", "Nitrate knee"). PR = primary filter, SC = secondary filter, - = no bending-points found.

Parameters		**EC 1**		**EC 2**		**EC 3**		**EC 4**		**EC 5**	
		PR	**SC**	**PR**	**SC**	**PR**	**SC**	**PR**	**SC**	**PR**	**SC**
Applied TKN Load ($g/m^3/d$)		92.4	-	25.9	-	22.5	-	22.5	-	90.0	-
"DO Elbow"	DO (mg/L)	-	-	4.19	-	-	-	-	1.08	-	-
	NH_4-N (mg/L)	-	-	1.83	-	-	-	-	16.7	-	-
"ORP Plateau"	Eh (mV)	-	-	-	-	-	-	-	-	300	-
	NH_4-N (mg/L)	-	-	-	-	-	-	-	-	0	-
"Nitrate knee"	Eh (mV)	135	138	-	-	-	-	-	-	250	-
	NO_3-N (mg/L)	31.3	0	-	-	-	-	-	-	0.88	-

concentrations at the outlet was observed with measurements of NH_4-N concentrations and pH in the middle of the primary filter. Conversely, the strongest negative correlation was seen with DO concentrations in the primary filter, Eh in the secondary filter and in the middle. With regard to the NO_x-N concentrations at the outlet, the highest positive correlation was observed with the Eh measured at the outlet and in the secondary filter. The lowest negative correlation was noted with the NH_4-N and NO_x-N concentrations measured in the middle. The histograms and density functions indicated that the data distributions for the majority of the sensors were highly skewed, with some exhibiting a bimodal pattern, such as the water temperature sensor. The aforementioned behavior was caused by the absence of data attributed to periods when the system was not operational or when the sensor was not functioning correctly and had to be replaced. Furthermore, the scatter plots highlighted the non-linear relationships between nutrient variables (NH_4-N and NO_x-N) and other variables.

Thèse accessible à l'adresse : https://theses.insa-lyon.fr/publication/2024ISAL0088/these.pdf © [C.K. Miyazaki], [2024], INSA Lyon, tous droits réservés

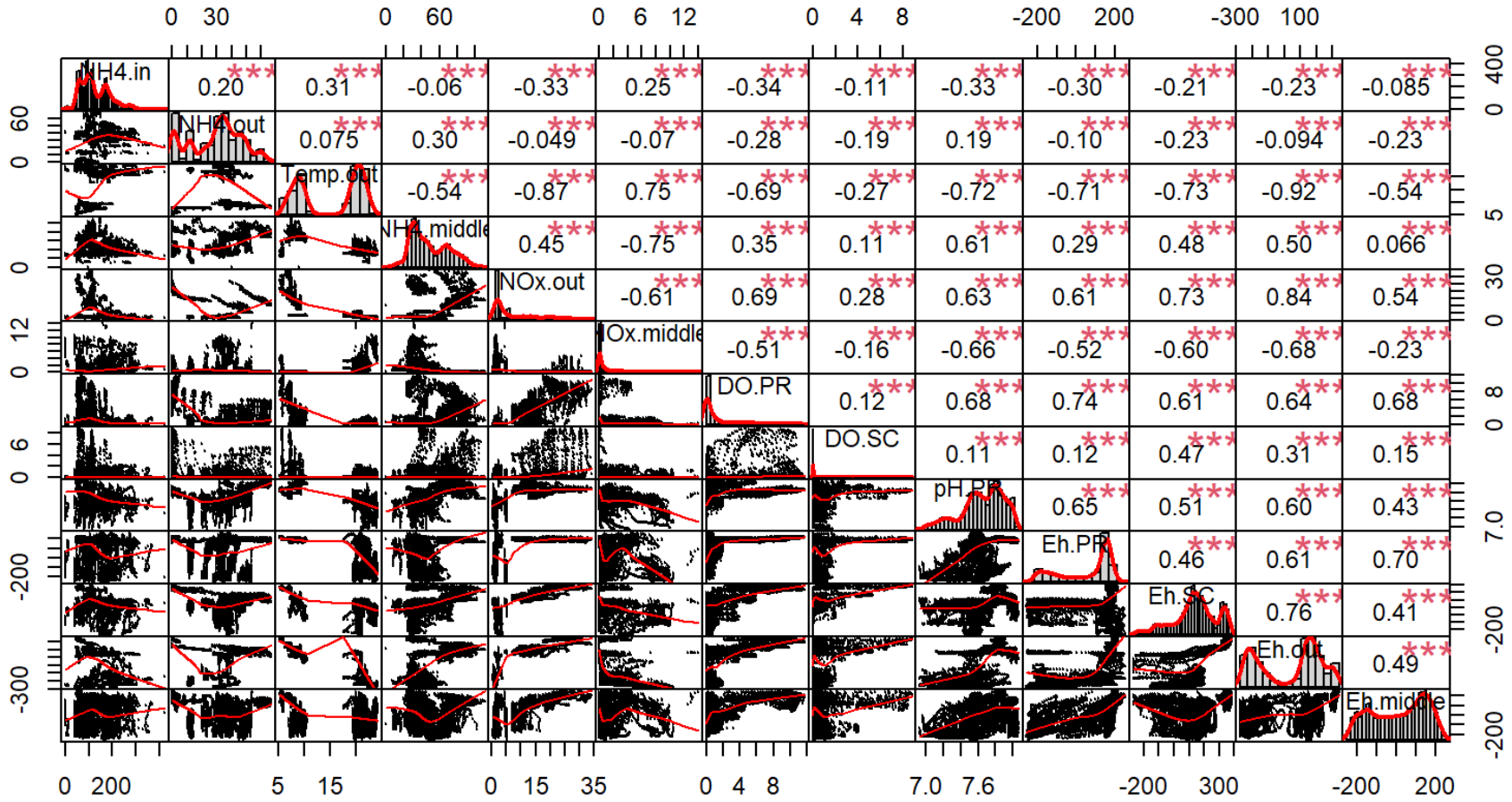

Figure 5.8: Pearson correlation matrix (upper-right), density function and histograms (diagonal), and scatter plot (lower-left) for the sensor. Statistical significance of rank correlations: dot means $p < 0.1$, *** means $p < 0.001$, ** means $p < 0.01$,* means $p < 0.05$. In the diagonal, the red curve represents the kernel density estimates, and below the diagonal, the red line represents the association between variables.

Thèse accessible à l'adresse : https://theses.insa-lyon.fr/publication/2024ISAL0088/these.pdf © [C.K. Miyazaki], [2024], INSA Lyon, tous droits réservés

A high correlation between variables can lead to issues in a multiple regression equation, a phenomenon known as multicollinearity (Allen, 1997). The degree of correlation between variables can impact the statistical significance of an independent variable, increasing uncertainty and making it challenging to interpret the effect of one variable on another (Siegel, 2012). Furthermore, it is recommended to normalize the error distributions to account for asymmetric curves and to apply parametric statistical techniques (Hammouri et al., 2020; Wilcox, 2003). Accordingly, these characteristics indicate that a linear regression model is unsuitable for predicting NH_4-N and NO_x-N concentrations at the outlet, necessitating a more robust model capable of taking these phenomena into account. As a result, researchers have turned their attention to alternative approaches. Recent technological advances have led to the development of online sensors for optimal control systems. The data-driven models used, based on machine learning, have proven to be effective in addressing the non-linear behavior of wastewater treatment plants and establishing accurate predictions that can be used in model-based control (Alvi et al., 2023). For instance, Alvi et al., 2022 employed hybrid network models to predict ammonium concentration using pH, DO, turbidity, TSS, and redox potential sensors as predictors, while Cheng et al., 2023 used a random forest model to predict COD concentrations from pH and temperature sensors.

5.4 Conclusions and perspectives

The system demonstrated robust performance under organic loadings comparable to those observed in small communities, with an inlet ammonium concentration of less than 100 mgNH_4-N/L. The system removed 90.3% of the ammonium and 81.4% of the TN, with a TN concentration at the outlet of less than 15 mg/L. The aeration strategy, based on the inflow, setting the aeration to start and finish between batches, and the non-aeration period occurring during batch time, proved effective in optimizing the removal of TN with normal organic loadings at the inlet. This strategy maximizes the degradation of organic carbon by denitrified bacteria. The aeration process in the primary filter effectively oxidized ammonium, while the non-aeration period preceding the batch provided an anoxic environment conducive to denitrification. The secondary filter was used to polish the nitrification process initiated in the primary filter. The system also demonstrated robust performance at high inlet ammonium concentrations, with a range of onsite treatment variations. In this case, removal rates were 85.6% and 83.3% for ammonium and TN, respectively. The main limitation was the nitrification process, which required further oxygenation in the case of a TN requirement less than 15 mg/L.

The N-k-C* model indicates that neither the TKN nor the TN model is suitable for design purposes in cases where low requirements are strictly enforced, as they are

Thèse accessible à l'adresse : https://theses.insa-lyon.fr/publication/2024ISAL0088/these.pdf © [C.K. Miyazaki], [2024], INSA Lyon, tous droits réservés

inaccurate. Future studies should incorporate different k_{v20} for each compartment by using specific kinetics coefficients or using one k_{v20} value for each tank in series. Online sensors were used to conduct an exploratory aeration control, with the objective of determining the feasibility of controlling the nitrogen treatment through the use of bending points or a linear predictive model. The experiments identified several bending points, including the "DO bend," the "ORP plateau," and the "nitrate knee," which represent the end of the nitrification or denitrification processes. However, the bending points did not appear consistently, and the concentrations at the bending points varied. Finally, the feasibility of using linear predictive models was investigated. However, the input variables exhibited issues with non-linear relationships. Therefore, it is recommended that future predictive modeling approaches consider these challenges.

5.5 Learnings

Chapter 5 consolidates the key findings from previous chapters to enhance the overall nitrogen removal efficiency of a hybrid aerated TW. The study centered on evaluating a novel aeration strategy, delineating its operational boundaries, developing an N-k-C* model, and investigating aeration control strategies with online sensors. The insights gained from this chapter are as follows:

- The aeration strategy based on inflow could optimize the TN removal.
- The primary filter has the major role of the nitrification and denitrification, and the secondary filter could potentially nitrify residual ammonium, but not denitrify.
- The aeration strategy is robust facing high organic loading, but additional aeration is required to meet stringent regulatory requirements.
- The N-k-C* model is not sufficiently precise for design purposes when outlet requirements are low.
- The inflection points (DO and Eh signals) were not consistently present, and when identified, the correlation between ammonium and nitrate concentration was not clear, with considerable variation in their concentrations.
- A linear prediction model would not be adequate to represent the complexity of the system.

Thèse accessible à l'adresse : https://theses.insa-lyon.fr/publication/2024ISAL0088/these.pdf © [C.K. Miyazaki], [2024], INSA Lyon, tous droits réservés

Thèse accessible à l'adresse : https://theses.insa-lyon.fr/publication/2024ISAL0088/these.pdf © [C.K. Miyazaki], [2024], INSA Lyon, tous droits réservés

Chapter 6

Conclusion and perspectives

6.1 General conclusion

The introduction of more stringent local regulations regarding nitrogen, coupled with the land constraints inherent to decentralized systems in urban areas, has prompted companies in the wetland treatment sector to invest in research and development to treat TN in smaller footprint TWs. As a result, the Rhizosph'air® was developed to be resilient, compact, robust, and aiming to be capable of serving communities between 500 and 10,000 PE. This thesis work is part of an effort to improve control of total nitrogen removal while addressing the operational challenges of protecting the receiving environment and developing wastewater reuse solutions. In Chapter 2, a literature review presented the key topics related to Rhizosph'air®, from NbS to aerated TW, and identifying research gaps and future perspectives in the literature. Then, two specific topics, oxygen transfer in aerated treatment wetlands and nitrogen dynamics in treatment wetlands, were described as part of the parameters of interest for this system. In Chapter 3, an evaluation of the impact of different aeration strategies on the hydrodynamics of the system was presented. This assessment used tracer tests to analyze both the outlet and internal system response. The hydraulic parameters and general hydraulic modeling (considered a "black-box" representation of hydraulics through process engineering), including HRT, volumetric efficiency, mass recovery rate, and NTIS, provided valuable insights into the hydraulic behavior of the system. Chapter 4 examined a range of experimental conditions (variation with influent concentration, duration of aeration, sequencing aeration according to batches, and different hydraulic and organic loading rates) and demonstrated that an aeration strategy based on inflow could improve nitrification while optimizing the use of organic carbon from the batch to enhance the denitrification process. As a perspective, this chapter proposes testing the same aeration strategy for enhancing TN removal, ensuring two underlying assumptions before the arrival of a batch: i) nitrification must be completed;

Thèse accessible à l'adresse : https://theses.insa-lyon.fr/publication/2024ISAL0088/these.pdf © [C.K. Miyazaki], [2024], INSA Lyon, tous droits réservés

ii) a sufficient no-aeration period must take place in order to return to anoxic conditions on the primary filter. If these conditions are met, carbon from the raw wastewater can be used to favor the denitrification process. The proposed aeration strategy, as well as its limitations and the resilience of the hybrid system, were tested and investigated in Chapter 5. This chapter also examined the applicability of the N-k-C* model for design purposes and explored the potential for implementing aeration control strategies through online sensors, including the use of bending points and model predictions.

These works led to the following conclusions:

- The hydraulic characterization demonstrated that aerating the primary filter enhances vertical mixing and reduces preferential pathways. Furthermore, longer aeration periods prevents from the formation of dead zones. The tracer test, conducted for 6h, 9h, and 24 hours of aeration per day in both filters (intermittent aeration with eight cycles per day), yielded comparable results. This indicates that a tracer test conducted for six hours per day is an appropriate and sufficient duration for achieving an effective hydraulic mix. The tracer tests resulted in NTIS values of between 5.1 and 6.2, depending on the aeration strategy employed. The tracer test without aeration exhibited a more heterogeneous hydraulic pathway, with different water velocity, dead zones and parallel flow paths.
- TN removal was influenced by factors such as influent concentration, aeration duration, and hydraulic loading rates. The aeration strategy based on fixed time (9h and 3h aeration per day, divided in 8 cycles per day) has the potential to achieve high ammonium removal rates, exceeding 90%. However, there is a limitation in denitrification. When the aeration duration per day is reduced from 9 hours to 3 hours (in both filters), the TN removal rate increases from 5% to 45%. By maintaining the 3-hours aeration duration per day (in both filters) and increasing the HLR (from 0.15 m/d to 0.35 m/d), the denitrification process was enhanced due to a reduction in aerobic degradation of carbon, thereby increasing carbon availability for denitrification, despite a decrease in the HRT. The transition from a time-based to a flow-based (timing the periods of aeration with the batch loading) aeration strategy enabled the system to optimize the use of organic carbon, resulting in a notable reduction in outlet nitrate levels from 17.6 $\pm$ 4.9 mgNO_3-N/L to 8.70 $\pm$ 4.40 mg$_3$-N/L.
- The system response under aeration strategy based on the inflow demonstrated robust performance under organic loads typical of small communities ($<$ 100 mg NH_4-N/L or $<$1200 mgCOD/L), with outlet TN concentrations below 15 mg/L. This aeration strategy, based on the inflow, proved effective in removing TN and maximizing carbon degradation. The primary filter was responsible for the main

Thèse accessible à l'adresse : https://theses.insa-lyon.fr/publication/2024ISAL0088/these.pdf © [C.K. Miyazaki], [2024], INSA Lyon, tous droits réservés

total nitrogen treatment, both ammonium and nitrate, while the secondary filter served as a polishing step for nitrification. The system demonstrated comparable TN removal under higher concentrations ($>$ 100 mg NH_4-N/L), but the higher NH_4-N and TN outlet concentration indicated that the control of aeration based on flow has some limitations if inlet concentrations vary considerably. This can make it challenging to guarantee low TN limits.

- The general N-k-C* model, when applied to TKN and TN, proved to be insufficiently accurate for design purposes when low outlet requirements are targeted (TN less than 15 mg/L). The root mean square error (RMSE) for TKN and TN was 6.19 and 7.01 mg/L, respectively. As an example, when the experimental value was 13.5 mgTN/L, the model predicted 20.1 mgTN/L.
- The experiments identified inflection points in DO and Eh correlated with ammonium and nitrate concentration. However, these inflection points were not consistently present, and when they were present, the correlation between ammonium and nitrate concentration was not evident, with variation in their NH_4-N and NO_3-N concentrations.
- It is not feasible to employ a linear prediction model in this instance as it is insufficient for capturing the level of complexity inherent to the system.

6.2 Perspectives

The primary objective of this thesis was to optimize the removal of total nitrogen in the Rhizosph'air treatment wetland system. While the study employed process engineering methodologies commonly used in the literature, the outcomes provided only general information about the system process. To gain deeper insights into system control, particularly the processes linked to hydrodynamics and total nitrogen treatment, a more internal analysis is necessary, such as the development of a mechanistic model. There are several potential research directions for continuing this study, including:

1. Gain a more detailed understanding of the internal hydrodynamics, including the identification of preferential pathways and dead zones. One approach is using electrical resistivity tomography (ERT) combined with two-phase modeling (gas-liquid).
2. Gain a more comprehensive understanding of biological activity, including bacterial populations and kinetic reactions.
3. Develop a model to improve accuracy and efficiency for design purposes under total nitrogen (TN) concentrations less than 15 mg/L.

Thèse accessible à l'adresse : https://theses.insa-lyon.fr/publication/2024ISAL0088/these.pdf © [C.K. Miyazaki], [2024], INSA Lyon, tous droits réservés

4. Develop an automated control system for TN removal.

The following topics provide comprehensive information on these studies, based on the knowledge accumulated over the past three years. This includes research that was initiated but not yet concluded, and therefore not included as a chapter.

6.2.1 Electrical resistivity tomography

During this PhD, the ERT method (refer to the Appendix for details of the methodology) was performed in parallel with the six tracer tests in Chapter 2. Despite the efforts made, in many of the 3D images a significant portion of the data was excluded due to the low sensitivity of a resistivity variance. These results were not straightforward to interpret due to the opposing effects of salt and aeration. The addition of salt will result in a decrease in resistivity, while the introduction of aeration will have the opposite effect, affecting the overall resistivity values. Two alternatives would be possible to avoid the outcome: i) use a different tracer that further increases the electrical resistivity, resulting in an increase in resistivity variation ; ii) change the number of electrodes and their position. To obtain comprehensive data coverage across the entire filter surface, it would be necessary to bury the electrodes at varying positions within the filter. Additionally, the inversion process (part of the 3D image generation methodology described in the Appendix) should be conducted more effectively in the future, and the number of quadripoles for each tracer test should be carefully filtered in order to facilitate comparison.

Once the 3D images for each tracer test have been generated, the next step will be to create a model of the hydrodynamics. This hydraulic model can be used to represent the system. Modifying parameters (HRT, aeration cycle, etc.) will enable characterization of flows and hydraulic properties. However, at this stage, it is not possible to use the ERT data without a two-phase (gas-liquid) flow model. By modeling aeration, the electrical resistivity of an equivalent heterogeneous medium can be simulated. By combining experimental data with mechanistic modeling approaches, researchers can propose improvements to the design and operation strategies for TWs.

The potential of applying a 2D hydraulic model (COMSOL Multiphysics$^{(R)}$) to the Rhizosph'air® system was explored in the framework of an internship. The preliminary study successfully modeled the flow without aeration, indicating a higher pressure on the primary filter side, particularly at the bottom of its saturated zone. The addition of air in the two-phase model (gas-liquid) was initiated with a simple version, without flow and biological activity consideration. The outcomes were then compared with data gathered from an aerated saturated column filled with fine gravel (2-4 mm). The air introduction in the model was validated for a fine gravel, which aligns with the fundamental hypothesis of constant equilibrium on capillarity. However, for coarser gravel, this hypothesis is not

Thèse accessible à l'adresse : https://theses.insa-lyon.fr/publication/2024ISAL0088/these.pdf © [C.K. Miyazaki], [2024], INSA Lyon, tous droits réservés

applicable. Given that the Rhizosph'air® system contains coarse gravel (gravel size of 20-40 mm) in the saturated layer, this model is not yet optimized for this system. For future studies, the 'Bubbly Flow' model (macroscopic modeling of mixed fluids and gas bubble interfaces (A. Sokolichin and Lapin, 2004) could be tested to more accurately represent the flow with aeration.

6.2.2 Biological activity

The aeration strategy outlined in Chapter 5 proved to be effective and the next step is to determine how this can be scaled for full implementation, especially given the variable time-interval between two batches, with a higher frequency of batch occurrences during the day. The aeration strategy requires a specific time interval between batches for complete nitrification as well as a return to an anoxic environment, followed by a batch supplying carbon to encourage the denitrification process. Further study is required to gain a deeper understanding of the key performance indicator, namely the bacterial communities and their activities. This will require an investigation into the factors that impact the activities of these communities, including temperatures, organic loads, dissolved oxygen consumption rates, aeration and no-aeration periods. The objective is to identify the optimal nitrification and denitrification rates. One of the limitations of the best aeration strategy applied in this work is linked to variations in inlet concentrations. When the aeration control is based on the inflow, high organic loading limits to reduce the TN outlet concentration due to the inability to adapt to inlet concentration fluctuations. Further studies could test the potential benefits of an aeration strategy based on flow as well as BOD and/or NH_4-N sensors at the inlet. In a full-scale system, it is not realistic to use expensive COD sensors. Therefore, studies could explore less expensive and more robust sensors related to BOD, such as microbial fuel cell.

During the implementation of the aeration strategy outlined in Chapter 5, the primary filter played a significant role in the nitrification and denitrification process, while the secondary filter was responsible for nitrifying the remaining ammonium concentration. In the event of nitrification, the NH_4-N will be transformed into NO_3-N, and denitrification will not occur due to the lack of organic carbon. One potential solution is to send batches with small volumes to secondary filters to address organic carbon deficiencies for denitrification processes. Future studies should investigate the viability of this strategy, determine the optimal frequency for applying these small batches, and assess the efficacy of an instantaneous aeration after the batch for proper mixing.

Thèse accessible à l'adresse : https://theses.insa-lyon.fr/publication/2024ISAL0088/these.pdf © [C.K. Miyazaki], [2024], INSA Lyon, tous droits réservés

6.2.3 Biokinetics model

During this PhD, efforts were made to improve the N-k-C* model with more precise data input. Two concurrent approaches were undertaken: (1) a kinetic experiment was conducted in situ for the primary and secondary filters (refer to Appendix for details of the methodology), and (2) a hydraulic process engineer model was explored. The objective of the kinetic experiment was to define the nitrification and denitrification kinetic rates for the primary and secondary filters.

Further analysis of the data will provide insights into the reaction order (one or two), the correlation between coefficient rates and temperature, the impact of ammonium applied load on coefficient rates, and the discrepancy between these rates on primary and secondary filters. Additionally, more data on Rhizosph'air® system with different operational conditions, such as aeration strategy and ratio C/N, can also improve the determination of kinetics rates.

The second phase of the project involved progressing towards hydraulic modelling. The gamma distribution model used in Chapter 2 revealed some limitations regarding the assumptions made, particularly in relation to the non-real NTIS value and the constant inflow (Dirac function). Therefore, future studies should investigate the integration of an existing model for an insaturated zone of French VF TW (dual-porosity model proposed by Morvannou et al. (2013)) with a saturated zone model. Additionally, this tool can be used to integrate the hydraulic and kinetic components, resulting in a robust model that can be used for design purposes.

6.2.4 Aeration control through models

The linear regression model is inadequate for predicting effluent NH_4-N and NO_x-N concentrations . A more robust model is required to account for these phenomena. The latest technological developments are focusing on online sensors for control systems. Data-driven models, based on machine learning, could address non-linear behavior of wastewater treatment plants and establish reliable predictions for use in model-based control. The random forest model was tested during this PhD to ascertain its suitability for use in this research context. The model had some limitations regarding the time-series input, and further studies should focus on how the data generated on the field could be used for training the model. Furthermore, the question arose as to whether all data could be incorporated simultaneously or if a time lag was necessary to accommodate the differences in sensor positions. If data were available on the hydraulic retention time for each position, the problem would be solved. However, no such information was available. Consequently, future studies should also consider this barrier to model implementation. This model could provide insights into which sensor was the most representative. By testing other

Thèse accessible à l'adresse : https://theses.insa-lyon.fr/publication/2024ISAL0088/these.pdf © [C.K. Miyazaki], [2024], INSA Lyon, tous droits réservés

aeration strategies, the DO sensor could be used to control the duration of aerobic and anoxic conditions for optimized TN removal. By integrating biochemical knowledge with real-time control and automation, TN removal could be further enhanced.

Thèse accessible à l'adresse : https://theses.insa-lyon.fr/publication/2024ISAL0088/these.pdf © [C.K. Miyazaki], [2024], INSA Lyon, tous droits réservés

Thèse accessible à l'adresse : https://theses.insa-lyon.fr/publication/2024ISAL0088/these.pdf © [C.K. Miyazaki], [2024], INSA Lyon, tous droits réservés

References

A. Sokolichin, G. E., & Lapin, A. (2004). Simulations of buoyancy driven bubbly flow: Established simplifications and open questions. *AIChE Journal*, *50*, 24–49. https://doi.org/https://doi.org/10.1002/aic.10003

Allen, C. R., Burr, M. D., Camper, A. K., Moss, J. J., & Stein, O. R. (2023). Seasonality, C:N ratio and plant species influence on denitrification and plant nitrogen uptake in treatment wetlands. *Ecological Engineering*, *191*, 106946. https://doi.org/10.1016/j.ecoleng.2023.106946

Allen, M. P. (Ed.). (1997). The problem of multicollinearity. In *Understanding Regression Analysis* (pp. 176–180). Springer US. https://doi.org/10.1007/978-0-585-25657-3_37

Alva, A. K., Paramasivam, S., Fares, A., Delgado, J. A., Mattos, D., & Sajwan, K. (2006). Nitrogen and Irrigation Management Practices to Improve Nitrogen Uptake Efficiency and Minimize Leaching Losses. *Journal of Crop Improvement*, *15*(2), 369–420. https://doi.org/10.1300/J411v15n02_11

Alvi, M., French, T., Cardell-Oliver, R., Keymer, P., & Ward, A. (2022). Cost Effective Soft Sensing for Wastewater Treatment Facilities. *IEEE Access*, *10*, 55694–55708. https://doi.org/10.1109/ACCESS.2022.3177201

Alvi, M., Batstone, D., Mbamba, C. K., Keymer, P., French, T., Ward, A., Dwyer, J., & Cardell-Oliver, R. (2023). Deep learning in wastewater treatment: A critical review. *Water Research*, *245*, 120518. https://doi.org/10.1016/j.watres.2023.120518

Araya, F., Vera, I., Sáez, K., & Vidal, G. (2016). Effects of aeration and natural zeolite on ammonium removal during the treatment of sewage by mesocosm-scale constructed wetlands [Publisher: Taylor & Francis _eprint: https://www.tandfonline.com/doi/pdf/10.1080/09593330.2015.1133715]. *Environmental Technology*, *37*(14), 1811–1820. https://doi.org/10.1080/09593330.2015.1133715

Archie, G. (1942). The electrical resistivity log as an aid in determining some reservoir-characteristics. *Trans. AIME 146*, 54–67.

Thèse accessible à l'adresse : https://theses.insa-lyon.fr/publication/2024ISAL0088/these.pdf © [C.K. Miyazaki], [2024], INSA Lyon, tous droits réservés

Arias, C., Brix, H., & Marti, E. (2005). Recycling of Treated Effluents Enhances Removal of Total Nitrogen in Vertical Flow Constructed Wetlands. *Journal of environmental science and health. Part A, Toxic/hazardous substances & environmental engineering*, *40*, 1431–43. https://doi.org/10.1081/ESE-200055882

Atanasova, N., Castellar, J. A., Pineda-Martos, R., Nika, C. E., Katsou, E., Istenič, D., Pucher, B., Andreucci, M. B., & Langergraber, G. (2021). Nature-Based Solutions and Circularity in Cities. *Circular Economy and Sustainability*, *1*(1), 319–332. https://doi.org/10.1007/s43615-021-00024-1

Audebert, M., Clément, R., Grossin-Debattista, J., Günther, T., Touze-Foltz, N., & Moreau, S. (2014a). Influence of the geomembrane on time-lapse ERT measurements for leachate injection monitoring. *Waste Management*, *34*(4), 780–790. https://doi.org/10.1016/j.wasman.2014.01.011

Audebert, M., Clément, R., Touze-Foltz, N., Günther, T., Moreau, S., & Duquennoi, C. (2014b). Time-lapse ERT interpretation methodology for leachate injection monitoring based on multiple inversions and a clustering strategy (MICS). *Journal of Applied Geophysics*, *111*, 320–333. https://doi.org/10.1016/j.jappgeo.2014.09.024

Austin, D., & Nivala, J. (2009). Energy requirements for nitrification and biological nitrogen removal in engineered wetlands. *Ecological Engineering*, *35*(2), 184–192. https://doi.org/10.1016/j.ecoleng.2008.03.002

Bagherzadeh, F., Mehrani, M.-J., Basirifard, M., & Roostaei, J. (2021). Comparative study on total nitrogen prediction in wastewater treatment plant and effect of various feature selection methods on machine learning algorithms performance. *Journal of Water Process Engineering*, *41*, 102033. https://doi.org/10.1016/j.jwpe.2021.102033

Baumann, P., Hansen, J., & Reichert, J. (2005). Steuerung der Stickstoffelimination auf Grundlage des Redox-Potenzials. Use of the Redox Potential for the Control of Nitrogen Elimination.

Bezbaruah, A. N., & Zhang, T. C. (2003). Performance of a constructed wetland with a sulfur/limestone denitrification section for wastewater nitrogen removal. *Environmental Science & Technology*, *37*(8), 1690–1697. https://doi.org/10.1021/es020912w

Blanchy, G., Saneiyan, S., Boyd, J., McLachlan, P., & Binley, A. (2020). ResIPy, an intuitive open source software for complex geoelectrical inversion/modeling. *Computers & Geosciences*, *137*, 104423. https://doi.org/10.1016/j.cageo.2020.104423

Boog, J., Kalbacher, T., Nivala, J., Forquet, N., Afferden, M. v., & Muller, R. A. (2020). Modeling the relationship of aeration, oxygen transfer and treatment performance

Thèse accessible à l'adresse : https://theses.insa-lyon.fr/publication/2024ISAL0088/these.pdf © [C.K. Miyazaki], [2024], INSA Lyon, tous droits réservés

in aerated horizontal flow treatment wetlands | Elsevier Enhanced Reader. https://doi.org/10.1016/j.watres.2019.03.062

Boog, J., Nivala, J., Aubron, T., Wallace, S., van Afferden, M., & Müller, R. A. (2014). Hydraulic characterization and optimization of total nitrogen removal in an aerated vertical subsurface flow treatment wetland. *Bioresource Technology*, *162*, 166–174. https://doi.org/10.1016/j.biortech.2014.03.100

Bozovic, R., Maksimovic, Č., Mijic, A., Smith, K., Suter, I., & Van Reeuwijk, M. (2017). *Blue Green Solutions. A Systems Approach to Sustainable, Resilient and Cost-Efficient Urban Development*. https://doi.org/10.13140/RG.2.2.30628.07046

Butterworth, E. (2014). *The use of artificial aeration in horizontal sub-surface flow constructed wetlands for tertiary nitrification* (PhD Theesis). Cranfield University. https://core.ac.uk/download/pdf/29409555.pdf

Butterworth, E., Richards, A., Jones, M., Dotro, G., & Jefferson, B. (2016a). Assessing the potential for tertiary nitrification in sub-surface flow constructed wetlands [Publisher: Taylor & Francis]. *Environmental Technology Reviews*. Retrieved May 22, 2024, from https://www.tandfonline.com/doi/abs/10.1080/21622515.2016.1188998

Butterworth, E., Richards, A., Jones, M., Mansi, G., Ranieri, E., Dotro, G., & Jefferson, B. (2016b). Performance of Four Full-Scale Artificially Aerated Horizontal Flow Constructed Wetlands for Domestic Wastewater Treatment [Number: 9 Publisher: Multidisciplinary Digital Publishing Institute]. *Water*, *8*(9), 365. https://doi.org/10.3390/w8090365

Canet-Martí, A., Grüner, S., Lavrnić, S., Toscano, A., Streck, T., & Langergraber, G. (2022). Comparison of simple models for total nitrogen removal from agricultural runoff in FWS wetlands. *Water Science and Technology*, *85*(11), 3301–3314. https://doi.org/10.2166/wst.2022.179

Chazarenc, F., Merlin, G., & Gonthier, Y. (2003). Hydrodynamics of horizontal subsurface flow constructed wetlands. *Ecological Engineering*, *21*(2), 165–173. https://doi.org/10.1016/j.ecoleng.2003.12.001

Cheng, Q., Chunhong, Z., & Qianglin, L. (2023). Development and application of random forest regression soft sensor model for treating domestic wastewater in a sequencing batch reactor [Publisher: Nature Publishing Group]. *Scientific Reports*, *13*(1), 9149. https://doi.org/10.1038/s41598-023-36333-8

Chislock, M. F., Doster, E., Zitomer, R. A., & Wilson, A. E. (2013). Eutrophication: Causes, Consequences, and Controls in Aquatic Ecosystems | Learn Science at Scitable. *Nature Education*. Retrieved March 27, 2024, from https://www.nature.com/scitable/

Thèse accessible à l'adresse : https://theses.insa-lyon.fr/publication/2024ISAL0088/these.pdf © [C.K. Miyazaki], [2024], INSA Lyon, tous droits réservés

knowledge/library/eutrophication-causes-consequences-and-controls-in-aquatic-102364466/

Cho, S., Kambey, C., & Nguyen, V. K. (2020). Performance of Anammox Processes for Wastewater Treatment: A Critical Review on Effects of Operational Conditions and Environmental Stresses [Number: 1 Publisher: Multidisciplinary Digital Publishing Institute]. *Water*, *12*(1), 20. https://doi.org/10.3390/w12010020

Corbella, C., Garfí, M., & Puigagut, J. (2014). Vertical redox profiles in treatment wetlands as function of hydraulic regime and macrophytes presence: Surveying the optimal scenario for microbial fuel cell implementation. *Science of The Total Environment*, *470-471*, 754–758. https://doi.org/10.1016/j.scitotenv.2013.09.068

Cota, R. S., von Sperling, M., & Penido, R. C. S. (2011). Tracer studies and hydraulic behaviour of planted and un-planted vertical-flow constructed wetlands. *Water Science and Technology*, *64*(5), 1056–1063. https://doi.org/10.2166/wst.2011.544

Council Directive of the European Communities. (1991). Council Directive of 21 May 1992 concerning urban wastewater treatment (91/271/EEC).

Cross, K., Tondera, K., Rizzo, A., Andrews, L., Pucher, B., Istenic, D., Karres, N., & McDonald, R. (2021). *Nature-Based Solutions for Wastewater Treatment: A Series of Factsheets and Case Studies* (IWA Publishing). https://doi.org/10.2166/9781789062267

Cui, F., Kim, M., Park, C., Kim, D., Mo, K., & Kim, M. (2021). Application of principal component analysis (PCA) to the assessment of parameter correlations in the partial-nitrification process using aerobic granular sludge. *Journal of Environmental Management*, *288*, 112408. https://doi.org/10.1016/j.jenvman.2021.112408

de Andrade Moraes, M. A., Zumalacarregui, J. A. G., Trein, C. M., & von Sperling, M. (2020). Dynamics of the behaviour of a vertical wetland (French system) operating in warm-climate conditions, evaluated by means of variables continuously measured in situ. *Water Science and Technology*, *82*(5), 954–966. https://doi.org/10.2166/wst.2020.399

Dececzaro, S. T., Wolff, D. B., Pelissari, C., Ramírez, R. J. M. G., Formentini, T. A., Goerck, J., Rodrigues, L. F., & Sezerino, P. H. (2019). Influence of hydraulic loading rate and recirculation on oxygen transfer in a vertical flow constructed wetland. *Science of The Total Environment*, *668*, 988–995. https://doi.org/10.1016/j.scitotenv.2019.03.057

Delgado-Gonzalez, L., Forquet, N., Choubert, J.-M., Boutin, C., Moreau, M., Moreau, S., & Clement, R. (2023). Flow path monitoring by discontinuous time-lapse ERT: An application to survey relationships between secondary effluent infiltration and roots

Thèse accessible à l'adresse : https://theses.insa-lyon.fr/publication/2024ISAL0088/these.pdf © [C.K. Miyazaki], [2024], INSA Lyon, tous droits réservés

distribution. *Journal of Environmental Management*, *326*, 116839. https://doi.org/10.1016/j.jenvman.2022.116839

Dong, J., & Kuang, S. (2024). Bibliometric Analysis of Nitrogen Removal in Constructed Wetlands: Current Trends and Future Research Directions [Number: 10 Publisher: Multidisciplinary Digital Publishing Institute]. *Water*, *16*(10), 1453. https://doi.org/10.3390/w16101453

Dotro, G., Langergraber, G., Molle, P., Nivala, J., Puigagut, J., Stein, O., & von Sperling, M. (2017). *Biological wastewater treatment series - Treatment wetlands (volume 7)* (Vol. 7). IWA Publishing. https://doi.org/10.2166/9781780408774

Dou, T., Troesch, S., Petitjean, A., Gabor, P. T., & Esser, D. (2016). Wastewater and Rainwater Management in Urban Areas: A Role for Constructed Wetlands. *Science direct - International Conference Green Urbanism*. Retrieved May 12, 2023, from https://cyberleninka.org/article/n/1498067/viewer

Dubois, V., Falipou, E., & Boutin, C. (2022). Quantification and qualification of the urban domestic pollution discharged per household and per resident. *Water Science and Technology*, *85*. https://doi.org/10.2166/wst.2022.064

du Plessis, A. (2022). Persistent degradation: Global water quality challenges and required actions. *One Earth*, *5*(2), 129–131. https://doi.org/10.1016/j.oneear.2022.01.005

Durot, M.-A., & Molle, P. (2017). Filtre planté de roseaux à aération forcée [Partenariat 2015-2018-Domaine eau et aménagements urbainsAction 40-2]. *«Evaluation des procédés nouveaux d'assainissement Conception et exploitation des stations de traitement des eaux usées des petites et moyennes collectivités (EPNAC)»*, 21. Retrieved November 9, 2021, from https://www.epnac.fr/content/download/3531/34184/version/2/file/20171023_note-gener-FPR-aeration-forcee-v-definitive.pdf

Dušek, J., Picek, T., & Čížková, H. (2008). Redox potential dynamics in a horizontal subsurface flow constructed wetland for wastewater treatment: Diel, seasonal and spatial fluctuations. *Ecological Engineering*, *34*(3), 223–232. https://doi.org/10.1016/j.ecoleng.2008.08.008

DWA. (2017). Standard DWA-A 262E: Principles for dimensioning, construction, and operation of wastewater treatment plants with planted and unplanted filters for treatment of domestic and municipal wastewater.

Eggermont, H., Balian, E., Azevedo, J. M. N., Beumer, V., Brodin, T., Claudet, J., Fady, B., Grube, M., Keune, H., Lamarque, P., Reuter, K., Smith, M., van Ham, C., Weisser, W. W., & Le Roux, X. (2015). Nature-based Solutions: New Influence for

Thèse accessible à l'adresse : https://theses.insa-lyon.fr/publication/2024ISAL0088/these.pdf © [C.K. Miyazaki], [2024], INSA Lyon, tous droits réservés

Environmental Management and Research in Europe. *GAIA - Ecological Perspectives for Science and Society*, *24*(4), 243–248. https://doi.org/10.14512/gaia.24.4.9

EPNAC. (2015). ELEMENTS DE METHODE POUR LA DEFINITION DES NIVEAUX DE REJETS DU PETIT COLLECTIF.

Ergaieg, K., Msaddek, M. H., Kallel, A., & Trabelsi, I. (2021). Monitoring of horizontal subsurface flow constructed wetlands for tertiary treatment of municipal wastewater. *Arabian Journal of Geosciences*, *14*(19), 2045. https://doi.org/10.1007/s12517-021-08419-y

European Environment Agency, Zal, N., Whalley, C., Christiansen, T., Kristensen, P., & Néry, F. (2018). *European waters: Assessment of status and pressures 2018*. Publications Office of the European Union. Retrieved March 26, 2024, from https://data.europa.eu/doi/10.2800/303664

Fan, J., Wang, W., Zhang, B., Guo, Y., Ngo, H. H., Guo, W., Zhang, J., & Wu, H. (2013). Nitrogen removal in intermittently aerated vertical flow constructed wetlands: Impact of influent COD/N ratios. *Bioresource Technology*, *143*, 461–466. https://doi.org/10.1016/j.biortech.2013.06.038

Fan, J., Zhang, J., Guo, W., Liang, S., & Wu, H. (2016). Enhanced long-term organics and nitrogen removal and associated microbial community in intermittently aerated subsurface flow constructed wetlands. *Bioresource Technology*, *214*, 871–875. https://doi.org/10.1016/j.biortech.2016.05.083

Farouk, A., Boumediene, B., Heran, M., & Harmand, J. (2020). *Flexibility of Waste Resource Recovery Facilities for water Reuse*.

Fatone, F., Battistoni, P., Bolzonella, D., Pavan, P., & Cecchia, F. (2008). Long-term experience with an automatic process control for nitrogen removal in membrane bioreactors. *Desalination*, *227*(1), 72–84. https://doi.org/10.1016/j.desal.2007.05.036

Faulwetter, J. L., Gagnon, V., Sundberg, C., Chazarenc, F., Burr, M. D., Brisson, J., Camper, A. K., & Stein, O. R. (2009). Microbial processes influencing performance of treatment wetlands: A review. *Ecological Engineering*, *35*(6), 987–1004. https://doi.org/10.1016/j.ecoleng.2008.12.030

Fonder, N., & Headley, T. (2010). Systematic nomenclature and reporting for treatment wetlands. In *Water and Nutrient Management in Natural and Constructed Wetlands* (pp. 191–220).

Fu, X., Hou, R., Yang, P., Qian, S., Feng, Z., Chen, Z., Wang, F., Yuan, R., Chen, H., & Zhou, B. (2022). Application of external carbon source in heterotrophic denitrification

Thèse accessible à l'adresse : https://theses.insa-lyon.fr/publication/2024ISAL0088/these.pdf © [C.K. Miyazaki], [2024], INSA Lyon, tous droits réservés

of domestic sewage: A review. *Science of The Total Environment*, *817*, 153061. https://doi.org/10.1016/j.scitotenv.2022.153061

Gajewska, M., & Cur, K. (2018). Kinetics of nitrogen removal processes in constructed wetlands. *E3S Web of Conferences*, *26*, 00001. https://doi.org/10.1051/e3sconf/20182600001

Garfí, M., Pedescoll, A., Carretero, J., Puigagut, J., & García, J. (2014). Reliability and economic feasibility of online monitoring of constructed wetlands performance. *Desalination and Water Treatment*, *52*(31-33), 5848–5855. https://doi.org/10.1080/19443994.2013.811443

Ghosh, D., & Gopal, B. (2010). Effect of hydraulic retention time on the treatment of secondary effluent in a subsurface flow constructed wetland. *Ecological Engineering*, *36*(8), 1044–1051. https://doi.org/10.1016/j.ecoleng.2010.04.017

Gikas, G., Papaevangelou, V., Moutsopoulos, K., & Tsihrintzis, V. (2017). Evaluation of clogging in HSF pilot-scale CWs using tracer experiments. *European Water*, *58*, 179–184.

Hallin, S., Philippot, L., Löffler, F. E., Sanford, R. A., & Jones, C. M. (2018). Genomics and Ecology of Novel N2O-Reducing Microorganisms. *Trends in Microbiology*, *26*(1), 43–55. https://doi.org/10.1016/j.tim.2017.07.003

Hameed, Y. T., Abdalqadir, N. A., & Nussrat, H. H. (2022). Evaluation of nitrification process in constructed wetlands: A review on novel biological nitrogen removal processes. Retrieved October 12, 2022, from https://jeasd.uomustansiriyah.edu.iq/index.php/jeasd/article/view/1147/1505

Hammouri, H., Sabo, R., Alsaadawi, R., & Kheirallah, K. (2020). Handling Skewed Data: A Comparison of Two Popular Methods. *Applied Sciences*, *10*. https://doi.org/10.3390/app10186247

Harris, S. L., Stephenson, T., & Pearce, P. (1996). Aeration investigation of biological aerated filters using off-gas analysis. *Water Science and Technology*, *34*(3), 307–314. https://doi.org/10.1016/0273-1223(96)00587-2

Headley, T. R., & Kadlec, R. H. (2007). Conducting hydraulic tracer studies of constructed wetlands: A practical guide. *Ecohydrology & Hydrobiology*, *7*(3-4), 269–282. https://doi.org/10.1016/S1642-3593(07)70110-6

Higelin, E. (2021). Amélioration des performances du procédé de filtre planté de roseaux vertical français avec aération forcée pour faire du traitement à la demande.

Thèse accessible à l'adresse : https://theses.insa-lyon.fr/publication/2024ISAL0088/these.pdf © [C.K. Miyazaki], [2024], INSA Lyon, tous droits réservés

Ilyas, H., & Masih, I. (2017). Intensification of constructed wetlands for land area reduction: A review. *Environmental Science and Pollution Research*, *24*(13), 12081–12091. https://doi.org/10.1007/s11356-017-8740-z

INRAE. (2019). Platform REFLET - INRAE. Retrieved January 2, 2024, from https://eng-reversaal.lyon-grenoble.hub.inrae.fr/equipment-platforms/reflet

IUCN. (2016). WCC-2016-Res-069-EN Defining Nature-based Solutions. https://portals.iucn.org/library/sites/library/files/resrecfiles/WCC_2016_RES_069_EN.pdf

Jaramillo, F., Orchard, M., Muñoz, C., Zamorano, M., & Antileo, C. (2018). Advanced strategies to improve nitrification process in sequencing batch reactors - A review. *Journal of Environmental Management*, *218*, 154–164. https://doi.org/10.1016/j.jenvman.2018.04.019

Jia, L., Wang, R., Feng, L., Zhou, X., Lv, J., & Wu, H. (2018). Intensified nitrogen removal in intermittently-aerated vertical flow constructed wetlands with agricultural biomass: Effect of influent C/N ratios. *Chemical Engineering Journal*, *345*, 22–30. https://doi.org/10.1016/j.cej.2018.03.087

Johnson, R. A., & Wichern, D. (2007). *Applied Multivariate Statistical Analysis*. Pearson Prentice Hall. Retrieved June 21, 2024, from https://www.pearson.com/en-us/subject-catalog/p/applied-multivariate-statistical-analysis-classic-version/P200000006217/9780137980963

Jolliffe, I. T., & Cadima, J. (2016). Principal component analysis: A review and recent developments. *Philosophical transactions. Series A, Mathematical, physical, and engineering sciences*, *374*(2065), 20150202. https://doi.org/10.1098/rsta.2015.0202

Jolliffe, I. (2002). *Principal ComponentAnalysis,Second Edition*. Springer.

Kadlec, R. (2000). The Inadequacy of First-Order Treatment Wetland Models. *Ecological Engineering*, *15*, 105–119. https://doi.org/10.1016/S0925-8574(99)00039-7

Kadlec, R. H. (2007). Tracer and spike tests of constructed wetlands. *Ecohydrology & Hydrobiology*, *7*(3), 283–295. https://doi.org/10.1016/S1642-3593(07)70111-8

Kadlec, R. H., & Wallace, S. D. (2009). *Treatment Wetlands, Second Edition* (CRC Press).

Kassambara, A. (2017). *Practical Guide to Principal Component Methods in R*. STHDA.

Khan, H., Groot, C., Schepers, O., Oirschot, D., Martens, M., Ronsse, F., & Rousseau, D. (2022). Effect of controlled aeration on COD and nitrogen removal in aerated constructed wetlands used for effluent polishing. *Journal of Environmental Chemical Engineering*, *10*, 108043. https://doi.org/10.1016/j.jece.2022.108043

Thèse accessible à l'adresse : https://theses.insa-lyon.fr/publication/2024ISAL0088/these.pdf © [C.K. Miyazaki], [2024], INSA Lyon, tous droits réservés

Kivaisi, A. K. (2001). The potential for constructed wetlands for wastewater treatment and reuse in developing countries: A review. *Ecological Engineering*, *16*(4), 545–560. https://doi.org/10.1016/S0925-8574(00)00113-0

Labella, A., Caniani, D., Hughes-Riley, T., Morris, R. H., Newton, M. I., Hawes, P., Puigagut, J., García, J., & Uggetti, E. (2015). Assessing the economic suitability of aeration and the influence of bed heating on constructed wetlands treatment efficiency and life-span. *Ecological Engineering*, *83*, 184–190. https://doi.org/10.1016/j.ecoleng.2015.06.028

Langergraber, G., & Simunek, J., Jirka. (2005). Modeling Variably Saturated Water Flow and Multicomponent Reactive Transport in Constructed Wetlands. *Vadose Zone Journal*, *4*. https://doi.org/10.2136/vzj2004.0166

Levenspiel, O. (2012). *Tracer Technology: Modeling the Flow of Fluids* (Vol. 96). Springer. https://doi.org/10.1007/978-1-4419-8074-8

Li, F., Lu, L., Zheng, X., & Zhang, X. (2014). Three-stage horizontal subsurface flow constructed wetlands for organics and nitrogen removal: Effect of aeration [Place: Amsterdam Publisher: Elsevier B.V]. *Ecological engineering*, *68*, 90–96. https://doi.org/10.1016/j.ecoleng.2014.03.025

Li, H., Liu, F., Luo, P., Chen, X., Chen, J., Huang, Z., Peng, J., Xiao, R., & Wu, J. (2019). Stimulation of optimized influent C:N ratios on nitrogen removal in surface flow constructed wetlands: Performance and microbial mechanisms. *Science of The Total Environment*, *694*, 133575. https://doi.org/10.1016/j.scitotenv.2019.07.381

Ling, Y., Xu, H., & Chen, X. (2015). Continuous multi-cell electrochemical reactor for pollutant oxidation. *Chemical Engineering Science*, *122*, 630–636. https://doi.org/10.1016/j.ces.2014.10.031

Liquete, C., Udias, A., Conte, G., Grizzetti, B., & Masi, F. (2016). Integrated valuation of a nature-based solution for water pollution control. Highlighting hidden benefits. *Ecosystem Services*, *22*, 392–401. https://doi.org/10.1016/j.ecoser.2016.09.011

Liu, F.-f., Fan, J., Du, J., Shi, X., Zhang, J., & Shen, Y. (2019). Intensified nitrogen transformation in intermittently aerated constructed wetlands: Removal pathways and microbial response mechanism. *Science of The Total Environment*, *650*, 2880–2887. https://doi.org/10.1016/j.scitotenv.2018.10.037

Liu, H., Hu, Z., Song, S., Zhang, J., Nie, L., Hu, H., Li, F., & Liu, Z. (2018). Quantitative Detection of Clogging in Horizontal Subsurface Flow Constructed Wetland Using the Resistivity Method [Number: 10 Publisher: Multidisciplinary Digital Publishing Institute]. *Water*, *10*(10), 1334. https://doi.org/10.3390/w10101334

Thèse accessible à l'adresse : https://theses.insa-lyon.fr/publication/2024ISAL0088/these.pdf © [C.K. Miyazaki], [2024], INSA Lyon, tous droits réservés

Liu, S., Zhang, Y., Feng, X., & Pyo, S.-H. (2024). Current problems and countermeasures of constructed wetland for wastewater treatment: A review. *Journal of Water Process Engineering*, *57*, 104569. https://doi.org/10.1016/j.jwpe.2023.104569

Lombard Latune, R., Laporte-Daube, O., Fina, N., Peyrat, S., Pelus, L., & Molle, P. (2017). Which plants are needed for a French vertical-flow constructed wetland under a tropical climate? *Water Science and Technology*, *75*(8), 1873–1881. https://doi.org/10.2166/wst.2017.064

Marzo, A., Ventura, D., Cirelli, G. L., Aiello, R., Vanella, D., Rapisarda, R., Barbagallo, S., & Consoli, S. (2018). Hydraulic reliability of a horizontal wetland for wastewater treatment in Sicily. *Science of The Total Environment*, *636*, 94–106. https://doi.org/10.1016/j.scitotenv.2018.04.228

Masi, F., Rizzo, A., & Regelsberger, M. (2018). The role of constructed wetlands in a new circular economy, resource oriented, and ecosystem services paradigm. *Journal of Environmental Management*, *216*, 275–284. https://doi.org/10.1016/j.jenvman.2017.11.086

Masih, I. (2017). The performance of the intensified constructed wetlands for organic matter and nitrogen removal: A review. *Journal of Environmental Management*, *198*, 372–383. https://doi.org/10.1016/j.jenvman.2017.04.098

Mercoiret, L. (2009). Application aux agglomérations d'assainissement inférieures à 2 000 Equivalent Habitants.

Metcalf, L., Eddy, H., & Tchobanoglous, G. (2004). *Wastewater engineering : Treatment, disposal, and reuse*. Retrieved June 16, 2022, from https://library.wur.nl/WebQuery/titel/1979505

Miao, Y., Zhang, L., Yu, D., Zhang, J., Zhang, W., Ma, G., Zhao, X., & Peng, Y. (2022). Application of intermittent aeration in nitrogen removal process: Development, advantages and mechanisms. *Chemical Engineering Journal*, *430*, 133184. https://doi.org/10.1016/j.cej.2021.133184

Mishra, S., Singh, V., Cheng, L., Hussain, A., & Ormeci, B. (2022). Nitrogen removal from wastewater: A comprehensive review of biological nitrogen removal processes, critical operation parameters and bioreactor design. *Journal of Environmental Chemical Engineering*, *10*(3), 107387. https://doi.org/10.1016/j.jece.2022.107387

Molle, P., Liénard, A., Grasmick, A., & Iwema, A. (2006). Effect of reeds and feeding operations on hydraulic behaviour of vertical flow constructed wetlands under hydraulic overloads. *Water Research*, *40*(3), 606–612. https://doi.org/10.1016/j.watres.2005.11.026

Thèse accessible à l'adresse : https://theses.insa-lyon.fr/publication/2024ISAL0088/these.pdf © [C.K. Miyazaki], [2024], INSA Lyon, tous droits réservés

Molle, P. (2003). *Filtres plantés de roseaux: Limites hydrauliques et rétention du phosphore* (Doctorat discipline Energétique génie des procédés). Université Montpellier II. Montpellier.

Molle, P. (2014). French vertical flow constructed wetlands: A need of a better understanding of the role of the deposit layer. *Water Science and Technology: A Journal of the International Association on Water Pollution Research*, *69*(1), 106–112. https://doi.org/10.2166/wst.2013.561

Molle, P., Lienard, A., Boutin, C., Merlin, g., & Iwema, A. (2005). How to treat raw sewage with constructed wetlands: An overview of the French systems. *Water science and technology : a journal of the International Association on Water Pollution Research*, *51*, 11–21. https://doi.org/10.2166/wst.2005.0277

Molle, P., Prost-Boucle, S., & Lienard, A. (2008). Potential for total nitrogen removal by combining vertical flow and horizontal flow constructed wetlands: A full-scale experiment study. *Ecological Engineering*, *34*(1), 23–29. https://doi.org/10.1016/j.ecoleng.2008.05.016

Monday, C., Zaghloul, M. S., Krishnamurthy, D., & Achari, G. (2024). A Review of AI-Driven Control Strategies in the Activated Sludge Process with Emphasis on Aeration Control [Number: 2 Publisher: Multidisciplinary Digital Publishing Institute]. *Water*, *16*(2), 305. https://doi.org/10.3390/w16020305

Morvannou, A., Forquet, N., Michel, S., Stéphane, T., & Molle, P. (2015). Treatment performances of French constructed wetlands: Results from a database collected over the last 30 years. *Water Science & Technology*, *71*, 1333. https://doi.org/10.2166/wst.2015.089

Morvannou, A., Choubert, J.-m., Vanclooster, M., & Molle, P. (2014). Modeling nitrogen removal in a vertical flow constructed wetland treating directly domestic wastewater. *Ecological Engineering*, *70*, 379–386. https://doi.org/10.1016/j.ecoleng.2014.06.034

Morvannou, A., Forquet, N., Vanclooster, M., & Molle, P. (2013). Which Hydraulic Model to Use for Vertical Flow Constructed Wetlands? *4th International Conference HYDRUS Software Applications to Subsur-face Flow and Contaminant Transport Problems*, p. 245 –p. 255.

Morvannou, A., Troesch, S., Esser, D., Forquet, N., Petitjean, A., & Molle, P. (2017). Using one filter stage of unsaturated/saturated vertical flow filters for nitrogen removal and footprint reduction of constructed wetlands. *Water Science and Technology*, *76*(1), 124–133. https://doi.org/10.2166/wst.2017.115

Thèse accessible à l'adresse : https://theses.insa-lyon.fr/publication/2024ISAL0088/these.pdf © [C.K. Miyazaki], [2024], INSA Lyon, tous droits réservés

Negi, D., Verma, S., Singh, S., Daverey, A., & Lin, J.-G. (2022). Nitrogen removal via anammox process in constructed wetland – A comprehensive review. *Chemical Engineering Journal*, *437*, 135434. https://doi.org/10.1016/j.cej.2022.135434

Neto, O. B. L., Haddon, A., Aichouche, F., Harmand, J., Mulas, M., & Corona, F. (2021). Predictive control of activated sludge plants to supply nitrogen for optimal crop growth. *IFAC-PapersOnLine*, *54*(3), 200–205. https://doi.org/10.1016/j.ifacol.2021.08.242

Nguyen, X. C., Ly, Q. V., Li, J., Bae, H., Bui, X.-T., Nguyen, T. T. H., Tran, Q. B., Vo, T.-D.-H., & Nghiem, L. D. (2021). Nitrogen removal in subsurface constructed wetland: Assessment of the influence and prediction by data mining and machine learning. *Environmental Technology & Innovation*, *23*, 101712. https://doi.org/10.1016/j.eti.2021.101712

Nivala, J., Boog, J., Headley, T., Aubron, T., Wallace, S., Brix, H., Mothes, S., van Afferden, M., & Müller, R. A. (2019a). Side-by-side comparison of 15 pilot-scale conventional and intensified subsurface flow wetlands for treatment of domestic wastewater. *Science of The Total Environment*, *658*, 1500–1513. https://doi.org/10.1016/j.scitotenv.2018.12.165

Nivala, J., Kahl, S., Boog, J., van Afferden, M., Reemtsma, T., & Müller, R. A. (2019b). Dynamics of emerging organic contaminant removal in conventional and intensified subsurface flow treatment wetlands. *Science of The Total Environment*, *649*, 1144–1156. https://doi.org/10.1016/j.scitotenv.2018.08.339

Nivala, J., Murphy, C., & Freeman, A. (2020). Recent Advances in the Application, Design, and Operations & Maintenance of Aerated Treatment Wetlands [Number: 4 Publisher: Multidisciplinary Digital Publishing Institute]. *Water*, *12*(4), 1188. https://doi.org/10.3390/w12041188

Nivala, J., Murphy, C., Stéphane, T., Wallace, S., & Esser, D. (2014). Intensified and modified wetland designs. *Sustainable Sanitation Practice Journal*, *18*, 15–20.

Nivala, J., Wallace, S., Headley, T., Kassa, K., Brix, H., van Afferden, M., & Müller, R. (2013). Oxygen transfer and consumption in subsurface flow treatment wetlands. *Ecological Engineering*, *61*, 544–554. https://doi.org/10.1016/j.ecoleng.2012.08.028

Olsson, G. (2012). ICA and me – A subjective review. *Water Research*, *46*(6), 1585–1624. https://doi.org/10.1016/j.watres.2011.12.054

Oral, H. V., Carvalho, P., Gajewska, M., Ursino, N., Masi, F., Hullebusch, E. D. v., Kazak, J. K., Exposito, A., Cipolletta, G., Andersen, T. R., Finger, D. C., Simperler, L., Regelsberger, M., Rous, V., Radinja, M., Buttiglieri, G., Krzeminski, P., Rizzo, A., Dehghanian, K., … Zimmermann, M. (2020). A review of nature-based solutions for

Thèse accessible à l'adresse : https://theses.insa-lyon.fr/publication/2024ISAL0088/these.pdf © [C.K. Miyazaki], [2024], INSA Lyon, tous droits réservés

urban water management in European circular cities: A critical assessment based on case studies and literature. *Blue-Green Systems*, *2*(1), 112–136. https://doi.org/10.2166/bgs.2020.932

Parde, D., Patwa, A., Shukla, A., Vijay, R., Killedar, D. J., & Kumar, R. (2021). A review of constructed wetland on type, treatment and technology of wastewater. *Environmental Technology & Innovation*, *21*, 101261. https://doi.org/10.1016/j.eti.2020.101261

Pascual, A., de la Varga, D., Soto, M., Oirschot, D., Kilian, R., Alvarez, J., Carvalho, P., Brix, H., & Arias, C. (2018). Aerated Constructed Wetlands for Treatment of Municipal and Food Industry Wastewater. https://doi.org/10.1002/9781119268376.ch3

Paul, E., Plisson-Saune, S., Mauret, M., & Cantet, J. (1998). Process state evaluation of alternating oxic-anoxic activated sludge using ORP, pH and DO. *Water Science and Technology*, *38*(3), 299–306. https://doi.org/10.1016/S0273-1223(98)00469-7

Petitjean, A., Daniau, P., Cano, R., Lara, E., Arbib, Z., Solis, G., & Troesch, S. (2022). Intensified French Treatment Wetlands – Influence of operating parameters on nitrogen removal. *Proceedings of the ICWS conference*.

Petitjean, A., Daniau, P., & Troesch, S. (2021). Constructed wetlands for domestic wastewater treatment: From classical "french" systems to optimized intensified treatment wetlands. In *International Congress Smallwat21v – Abstract book* (p. 548). International Congress Smallwat21v.

Petitjean, A., Solis, G., Blanco, I., Lara, E., Arbib, Z., Arias, C., & Troesch, S. (2023). Rhizosph'air - a single stage "french" treatment wetlands for nitrogen removal. 2-years monitoring of industrial-scale pilots. *Proceedings of the Wetpol conference*.

Platzer, C. (1999). Design recommendations for subsurface flow constructed wetlands for nitrification and denitrification. *Water Science and Technology*, *40*(3), 257–263. https://doi.org/10.2166/wst.1999.0170

Prost-Boucle, S., Chiboub, A., Seranne, L., & Molle, P. (2021). Les filtres plantés de roseaux avec aération forcée suivi de la station de Tarcenay, procédé Rhiwosph'air (syntea), HAL–03185685.

Prost-Boucle, S., & Molle, P. (2021). Intensified treatment wetlands: Forced aeration in Tarcenay, France. Case study. In *Nature-Based Solutions for Wastewater Treatment* (Katharine Cross, Katharina Tondera, Anacleto Rizzo, Lisa Andrews, Bernhard Pucher, Darja Istenič, Nathan Karres and Robert McDonald, 344p (180–185)). Science for Nature; People Partnership (SNAPP), IWA publishing.

Rampuria, A., Kulshreshtha, N. M., Gupta, A., & Brighu, U. (2021). Novel microbial nitrogen transformation processes in constructed wetlands treating municipal sewage:

Thèse accessible à l'adresse : https://theses.insa-lyon.fr/publication/2024ISAL0088/these.pdf © [C.K. Miyazaki], [2024], INSA Lyon, tous droits réservés

A mini-review. *World Journal of Microbiology and Biotechnology*, *37*(3), 40. https://doi.org/10.1007/s11274-021-03001-w

Reddy, K., Delaune, R., & Inglett, P. (2022). *Biogeochemistry of Wetlands: Science and Applications*. https://doi.org/10.1201/9780429155833

Redmond, E. D., Just, C. L., & Parkin, G. F. (2014). Nitrogen Removal from Wastewater by an Aerated Subsurface-Flow Constructed Wetland in Cold Climates [Publisher: Water Environment Federation]. *Water Environment Research*, *86*(4), 305–313. Retrieved July 3, 2024, from https://www.jstor.org/stable/24585116

Regmi, P., Stewart, H., Amerlinck, Y., Arnell, M., García, P. J., Johnson, B., Maere, T., Miletić, I., Miller, M., Rieger, L., Samstag, R., Santoro, D., Schraa, O., Snowling, S., Takács, I., Torfs, E., van Loosdrecht, M. C. M., Vanrolleghem, P. A., Villez, K., ... Rosso, D. (2018). The future of WRRF modelling – outlook and challenges. *Water Science and Technology*, *79*(1), 3–14. https://doi.org/10.2166/wst.2018.498

Ribaudo, M., Delgado, J., Hansen, L., Livingston, M., Mosheim, R., & Williamson, J. (2011). *Nitrogen in Agricultural Systems: Implications for Conservation Policy* (SSRN Scholarly Paper No. 2115532). Social Science Research Network. Rochester, NY. https://doi.org/10.2139/ssrn.2115532

Risch, E., Boutin, C., & Roux, P. (2021). Applying life cycle assessment to assess the environmental performance of decentralised versus centralised wastewater systems. *Water Research*, *196*, 116991. https://doi.org/10.1016/j.watres.2021.116991

Rizzo, A., Bresciani, R., Martinuzzi, N., & Masi, F. (2020). Online Monitoring of a Long-Term Full-Scale Constructed Wetland for the Treatment of Winery Wastewater in Italy [Number: 2 Publisher: Multidisciplinary Digital Publishing Institute]. *Applied Sciences*, *10*(2), 555. https://doi.org/10.3390/app10020555

Rochard, J. (2017a). Procédés de traitements des effluents de cave adaptés au secteur des vins biologiques : État des lieux et perspectives [Publisher: EDP Sciences]. *BIO Web of Conferences*, *9*, 02030. https://doi.org/10.1051/bioconf/20170902030

Rochard, J. (2017b). Processes of treatment of wineries effluents adapted to the organic wine sector: Current situation and prospects. *Proceedings of the fortieth World Congress of Vine and Wine (6 pp.). OIV, Sofia, Bulgaria.*

Rous, V., Vymazal, J., & Hnátková, T. (2019). Treatment wetlands aeration efficiency: A review. *Ecological Engineering*, *136*, 62–67. https://doi.org/10.1016/j.ecoleng.2019.06.006

Ruiz-Ocampo, H., Tondera, K., Paing, J., Molle, P., & Chazarenc, F. (2022). Long-term investigations on ammonium removal with zeolite in compact vertical flow treatment

Thèse accessible à l'adresse : https://theses.insa-lyon.fr/publication/2024ISAL0088/these.pdf © [C.K. Miyazaki], [2024], INSA Lyon, tous droits réservés

wetlands under field conditions. *Water Science and Technology*, *85*(3), 746–755. https://doi.org/10.2166/wst.2022.022

Ruppelt, J. P., Tondera, K., Vorenhout, M., Van der Weken, L., & Pinnekamp, J. (2019). Redox potential as a method to evaluate the performance of retention soil filters treating combined sewer overflows. *Science of The Total Environment*, *650*, 1628–1639. https://doi.org/10.1016/j.scitotenv.2018.09.043

Saeed, T., & Sun, G. (2012). A review on nitrogen and organics removal mechanisms in subsurface flow constructed wetlands: Dependency on environmental parameters, operating conditions and supporting media. *Journal of Environmental Management*, *112*, 429–448. https://doi.org/10.1016/j.jenvman.2012.08.011

Seeger, E. M., Maier, U., Grathwohl, P., Kuschk, P., & Kaestner, M. (2013). Performance evaluation of different horizontal subsurface flow wetland types by characterization of flow behavior, mass removal and depth-dependent contaminant load. *Water Research*, *47*(2), 769–780. https://doi.org/10.1016/j.watres.2012.10.051

Séranne, L., Molle, P., Clément, R., Gillot, S., Prost-Boucle, S., & Nivala, J. (2021). Influence of airflow, material type and dripline density on gas transfer and bubble pathways in aerated vertical flow treatment wetlands. *Submitted to Chemistry Journal*.

Shih, S.-S., Hong, S.-S., & Chang, T.-J. (2016). Flume Experiments for Optimizing the Hydraulic Performance of a Deep-Water Wetland Utilizing Emergent Vegetation and Obstructions [Number: 6 Publisher: Multidisciplinary Digital Publishing Institute]. *Water*, *8*(6), 265. https://doi.org/10.3390/w8060265

Siegel, A. F. (2012). Chapter 12 - Multiple Regression: Predicting One Variable from Several Others. In A. F. Siegel (Ed.), *Practical Business Statistics (Sixth Edition)* (pp. 347–416). Academic Press. https://doi.org/10.1016/B978-0-12-385208-3.00012-2

Silveira, D. D., Belli Filho, P., Philippi, L. S., Kim, B., & Molle, P. (2015). Influence of partial saturation on total nitrogen removal in a single-stage French constructed wetland treating raw domestic wastewater. *Ecological Engineering*, *77*, 257–264. https://doi.org/10.1016/j.ecoleng.2015.01.040

Stefanakis, A. (2024). Nature-Based Solutions for a Circular Water Economy: Examples of New Green Infrastructure. In A. Stefanakis, H. V. Oral, C. Calheiros, & P. Carvalho (Eds.), *Nature-based Solutions for Circular Management of Urban Water* (pp. 35–50). Springer International Publishing. https://doi.org/10.1007/978-3-031-50725-0_3

Stefanakis, A. I. (2019). The Role of Constructed Wetlands as Green Infrastructure for Sustainable Urban Water Management [Number: 24 Publisher: Multidisciplinary

Thèse accessible à l'adresse : https://theses.insa-lyon.fr/publication/2024ISAL0088/these.pdf © [C.K. Miyazaki], [2024], INSA Lyon, tous droits réservés

Digital Publishing Institute]. *Sustainability*, *11*(24), 6981. https://doi.org/10.3390/su11246981

Sustainability, N. (2019). From the lab to real-world use [Number: 11 Publisher: Nature Publishing Group]. *Nature Sustainability*, *2*(11), 989–989. https://doi.org/10.1038/s41893-019-0435-7

Tan, Y. Y., Tang, F. E., & Saptoro, A. (2021). Process-based models for nitrogen dynamics in subsurface flow constructed wetlands: A state-of-the-art review [Publisher: Canadian Science Publishing]. *Environmental Reviews*. https://doi.org/10.1139/er-2021-0001

Tang, S., Liao, Y., Xu, Y., Dang, Z., Zhu, X., & Ji, G. (2020). Microbial coupling mechanisms of nitrogen removal in constructed wetlands: A review. *Bioresource Technology*, *314*, 123759. https://doi.org/10.1016/j.biortech.2020.123759

Troesch, S., Dirk, E., Wallace, S., & Oirschot, D. V. (2020). Wastewater purification device and utilizations. US 10,526,222 B2. Rhizosph'air®. https://www.ecobird.fr/rhizosphair.pdf

Tsatsou, A., Frantzeskaki, N., & Malamis, S. (2023). Nature-based solutions for circular urban water systems: A scoping literature review and a proposal for urban design and planning. *Journal of Cleaner Production*, *394*, 136325. https://doi.org/10.1016/j.jclepro.2023.136325

Tunçsiper, B. (2009). Nitrogen removal in a combined vertical and horizontal subsurface-flow constructed wetland system. *Desalination*, *247*(1), 466–475. https://doi.org/10.1016/j.desal.2009.03.003

Uggetti, E., Hughes-Riley, T., Morris, R. H., Newton, M. I., Trabi, C. L., Hawes, P., Puigagut, J., & García, J. (2016). Intermittent aeration to improve wastewater treatment efficiency in pilot-scale constructed wetland. *Science of The Total Environment*, *559*, 212–217. https://doi.org/10.1016/j.scitotenv.2016.03.195

Val del Río, Á., Campos Gómez, J. L., Mosquera Corral, A., & Wang, Y. (Eds.). (2017). *Technologies for the Treatment and Recovery of Nutrients from Industrial Wastewater:* IGI Global. https://doi.org/10.4018/978-1-5225-1037-6

Valhondo, C., Martínez-Landa, L., Carrera, J., Hidalgo, J. J., Tubau, I., De Pourcq, K., Grau-Martínez, A., & Ayora, C. (2016). Tracer test modeling for characterizing heterogeneity and local-scale residence time distribution in an artificial recharge site [Publisher: Copernicus GmbH]. *Hydrology and Earth System Sciences*, *20*(10), 4209–4221. https://doi.org/10.5194/hess-20-4209-2016

Van Oirschot, D., Wallace, S., & Van Deun, R. (2015). Wastewater treatment in a compact intensified wetland system at the Badboot: A floating swimming pool in

Thèse accessible à l'adresse : https://theses.insa-lyon.fr/publication/2024ISAL0088/these.pdf © [C.K. Miyazaki], [2024], INSA Lyon, tous droits réservés

Belgium. *Environmental Science and Pollution Research*, *22*(17), 12870–12878. https://doi.org/10.1007/s11356-014-3726-6

Vera-Puerto, I., Campal, J., Martínez, S., Cortés-Rico, L., Coy, H., Tan, S., Arias, C. A., Baquero-Rodríguez, G., & Rosso, D. (2022). Effects of Environmental Conditions and Bed Configuration on Oxygen Transfer Efficiency in Aerated Constructed Wetlands. *Water*, *14*(20), 3284. https://doi.org/10.3390/w14203284

Von Sperling, M., Wallace, S., & Nivala, J. (2023). Representing performance of horizontal flow treatment wetlands: The Tanks In Series (TIS) and the Plug Flow with Dispersion (PFD) approaches and their application to design. *Science of The Total Environment*, *859*, 160259. https://doi.org/10.1016/j.scitotenv.2022.160259

Vymazal, J. (2005). Horizontal sub-surface flow and hybrid constructed wetlands systems for wastewater treatment. *Ecological Engineering*, *25*(5), 478–490. https://doi.org/10.1016/j.ecoleng.2005.07.010

Vymazal, J. (2007). Removal of Nutrients in Various Types of Constructed Wetlands. *The Science of the total environment*, *380*, 48–65. https://doi.org/10.1016/j.scitotenv.2006.09.014

Vymazal, J. (2008). Constructed Wetlands for Wastewater Treatment: A Review. *Proceedings of Taal 2007*, 965–980.

Vymazal, J. (2013). The use of hybrid constructed wetlands for wastewater treatment with special attention to nitrogen removal: A review of a recent development. *Water Research*, *47*(14), 4795–4811. https://doi.org/10.1016/j.watres.2013.05.029

Vymazal, J., & Kröpfelová, L. (2008). *Wastewater Treatment in Constructed Wetlands with Horizontal Sub-Surface Flow* [Google-Books-ID: IfqerCqRvg8C]. Springer Science & Business Media.

Wallace, S., & Austin, D. (2008). Emerging models for nitrogen removal in treatment wetlands. *Journal of Environmental Health*, *71*(4), 10–16.

Wallace, S., & Knight, R. L. (2006). *Feasibility, Design Criteria, and O&M Requirements for Small Scale Constructed Wetland Wastewater Treatment Systems*. IWA Publishing. https://doi.org/10.2166/9781780403991

Wallace, S., Oirschot, D., & Stefanakis, A. (2020). AERATED WETLANDS. In *Wetland Technology: Practical Information on the Design and Application of Treatment Wetlands* (pp. 105–107). IWA Publishing.

Wallace, S. (2001). System for Removing Pollutants from Water. U.S. Patent 6,200,469 B1.

Thèse accessible à l'adresse : https://theses.insa-lyon.fr/publication/2024ISAL0088/these.pdf © [C.K. Miyazaki], [2024], INSA Lyon, tous droits réservés

Wallace, S., Liner, M., Redmond, D., & Hildebrand, M. (2007). Oxygen transfer efficiency in aerated subsurface flow wetlands.

Wang, H.-c., Liu, Y., Yang, Y.-m., Fang, Y.-k., Luo, S., Cheng, H.-y., & Wang, A.-j. (2022). Element sulfur-based autotrophic denitrification constructed wetland as an efficient approach for nitrogen removal from low C/N wastewater. *Water Research*, *226*, 119258. https://doi.org/10.1016/j.watres.2022.119258

Wang, H., & Jawitz, J. W. (2006). Hydraulic analysis of cell-network treatment wetlands. *Journal of Hydrology*, *330*(3), 721–734. https://doi.org/10.1016/j.jhydrol.2006.05.005

Wang, J., Hou, J., Xia, L., Jia, Z., He, X., Li, D., & Zhou, Y. (2020). The combined effect of dissolved oxygen and COD/N on nitrogen removal and the corresponding mechanisms in intermittent aeration constructed wetlands. *Biochemical Engineering Journal*, *153*, 107400. https://doi.org/10.1016/j.bej.2019.107400

Wang, R., Xu, L., Xu, X., Xu, Z., Zhang, X., Cong, X., & Tong, K. (2023). Hydraulic characteristics of small-scale constructed wetland based on residence time distribution [Publisher: Taylor & Francis _eprint: https://doi.org/10.1080/09593330.2021.1994018]. *Environmental Technology*, *44*(8), 1061–1070. https://doi.org/10.1080/09593330.2021.1994018

Welz, P. J., Mbasha, W., Smith, I., Holtman, G., Terblanche, G., Le Roes-Hill, M., & Haldenwang, R. (2018). The influence of grain physicochemistry and biomass on hydraulic conductivity in sand-filled treatment wetlands. *Ecological Engineering*, *116*, 21–30. https://doi.org/10.1016/j.ecoleng.2018.02.017

Wilcox, R. R. (2003). 2 - probability and related concepts. In R. R. Wilcox (Ed.), *Applying Contemporary Statistical Techniques* (pp. 17–53). Academic Press. https://doi.org/10.1016/B978-012751541-0/50023-7

Xiong, C., Li, Q., Tam, N. F., Zhang, X., Tai, Y., Wu, R., Huang, L., Vymazal, J., Dai, Y., & Yang, Y. (2022). The combination sequence effect on nitrogen removal pathway in hybrid constructed wetlands treating raw sewage from multiple perspectives. *Science of The Total Environment*, *833*, 155200. https://doi.org/10.1016/j.scitotenv.2022.155200

Yao, D., Dai, N., Hu, X., Cheng, C., Xie, H., Hu, Z., Liang, S., & Zhang, J. (2023). New insights into the effects of wetland plants on nitrogen removal pathways in constructed wetlands with low C/N ratio wastewater: Contribution of partial denitrification-anammox. *Water Research*, *243*, 120277. https://doi.org/10.1016/j.watres.2023.120277

Zanetti, L., Frison, N., Nota, E., Tomizioli, M., Bolzonella, D., & Fatone, F. (2012). Progress in real-time control applied to biological nitrogen removal from wastewater. A short-review. *Desalination*, *286*, 1–7. https://doi.org/10.1016/j.desal.2011.11.056

Thèse accessible à l'adresse : https://theses.insa-lyon.fr/publication/2024ISAL0088/these.pdf © [C.K. Miyazaki], [2024], INSA Lyon, tous droits réservés

Zapater-Pereyra, M., Ilyas, H., Lavrnić, S., van Bruggen, J. J. A., & Lens, P. N. L. (2015). Evaluation of the performance and space requirement by three different hybrid constructed wetlands in a stack arrangement. *Ecological Engineering*, *82*, 290–300. https://doi.org/10.1016/j.ecoleng.2015.04.097

Zhang, H., Li, R., Shi, Y., & Pan, F. (2024). Effect of Aeration and External Carbon Source on Nitrogen Removal and Distribution Patterns of Related-Microorganisms in Horizontal Subsurface Flow Constructed Wetlands [Number: 5 Publisher: Multidisciplinary Digital Publishing Institute]. *Water*, *16*(5), 632. https://doi.org/10.3390/w16050632

Zhang, L.-y., Zhang, L., Liu, Y.-d., Shen, Y.-w., Liu, H., & Xiong, Y. (2010). Effect of limited artificial aeration on constructed wetland treatment of domestic wastewater. *Desalination*, *250*(3), 915–920. https://doi.org/10.1016/j.desal.2008.04.062

Zhang, W., Tooker, N. B., & Mueller, A. V. (2020). Enabling wastewater treatment process automation: Leveraging innovations in real-time sensing, data analysis, and online controls [Publisher: The Royal Society of Chemistry]. *Environmental Science: Water Research & Technology*, *6*(11), 2973–2992. https://doi.org/10.1039/D0EW00394H

Zhou, Y., Zhu, Y., Zhu, J., Li, C., & Chen, G. (2023). A Comprehensive Review on Wastewater Nitrogen Removal and Its Recovery Processes. *International Journal of Environmental Research and Public Health*, *20*(4), 3429. https://doi.org/10.3390/ijerph20043429

Zhu, H., Yan, B., Xu, Y., Guan, J., & Liu, S. (2014). Removal of nitrogen and COD in horizontal subsurface flow constructed wetlands under different influent C/N ratios. *Ecological Engineering*, *63*, 58–63. https://doi.org/10.1016/j.ecoleng.2013.12.018

Zhuang, L.-L., Yang, T., Zhang, J., & Li, X. (2019). The configuration, purification effect and mechanism of intensified constructed wetland for wastewater treatment from the aspect of nitrogen removal: A review. *Bioresource Technology*, *293*, 122086. https://doi.org/10.1016/j.biortech.2019.122086

Zuur, A. F., Ieno, E. N., Walker, N., Saveliev, A. A., & Smith, G. M. (2009). *Mixed effects models and extensions in ecology with R*. Springer. https://doi.org/10.1007/978-0-387-87458-6

Thèse accessible à l'adresse : https://theses.insa-lyon.fr/publication/2024ISAL0088/these.pdf © [C.K. Miyazaki], [2024], INSA Lyon, tous droits réservés

Thèse accessible à l'adresse : https://theses.insa-lyon.fr/publication/2024ISAL0088/these.pdf © [C.K. Miyazaki], [2024], INSA Lyon, tous droits réservés

Chapter 7

Appendix

7.1 Hydraulic characterization of a hybrid aerated vertical and horizontal treatment wetland

Table 7.1: Weather condition and water height for the different tracer experiments

Tracer test	**Rain (mm/day)**	**Soil temperature average (°C)**	**Water height (m)**
Tracer 24h	6.8	7.6	0.91-1
Tracer 9h1	0.4	6.8	0.92-0.95
Tracer 9h2	2.2	7.8	0.9-0.96
Tracer 6h	0.0	7.2	0.9-0.96
Tracer 0h	13.0	11.3	0.84-0.9

Table 7.2: Values used for calibration the amino-G acid

Tracer test	**a**	**b**
24h	-153.411	5.422533
9h	-160.5083	5.228849
9h1	-170.3215	5.558489
9h2	-179.8351	4.807591
6h	-139.0122	5.653042
0h	-242.1323	5.269554

Thèse accessible à l'adresse : https://theses.insa-lyon.fr/publication/2024ISAL0088/these.pdf © [C.K. Miyazaki], [2024], INSA Lyon, tous droits réservés

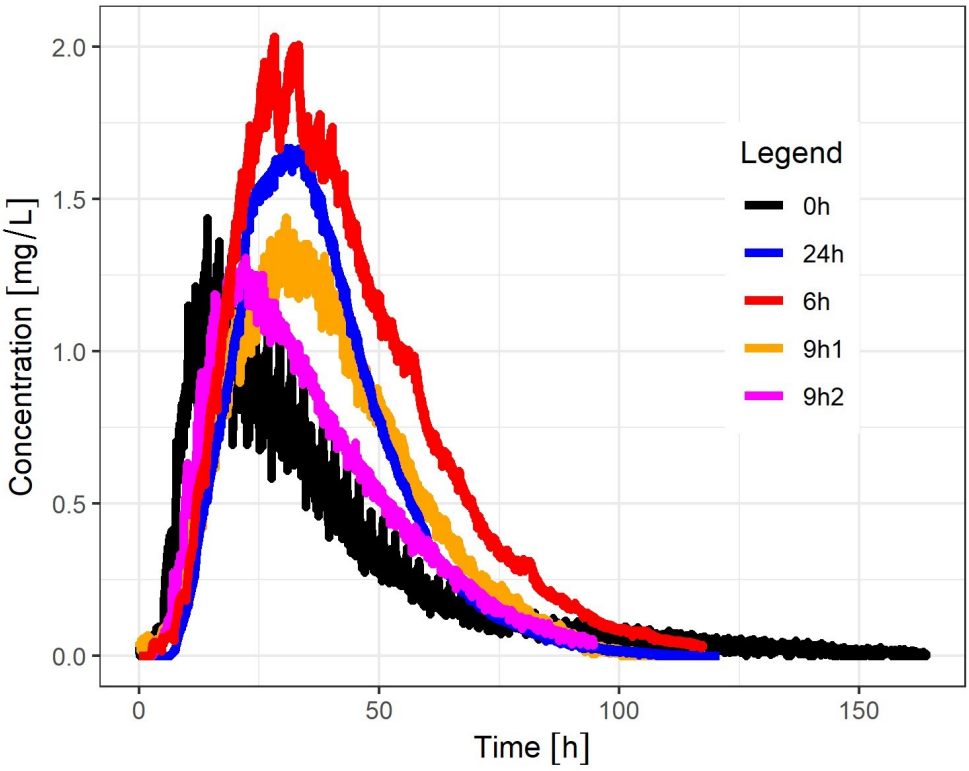

Figure 7.1: Concentration in amino-G acid (mg/L) at the pilot outlet over time for each aeration strategy.

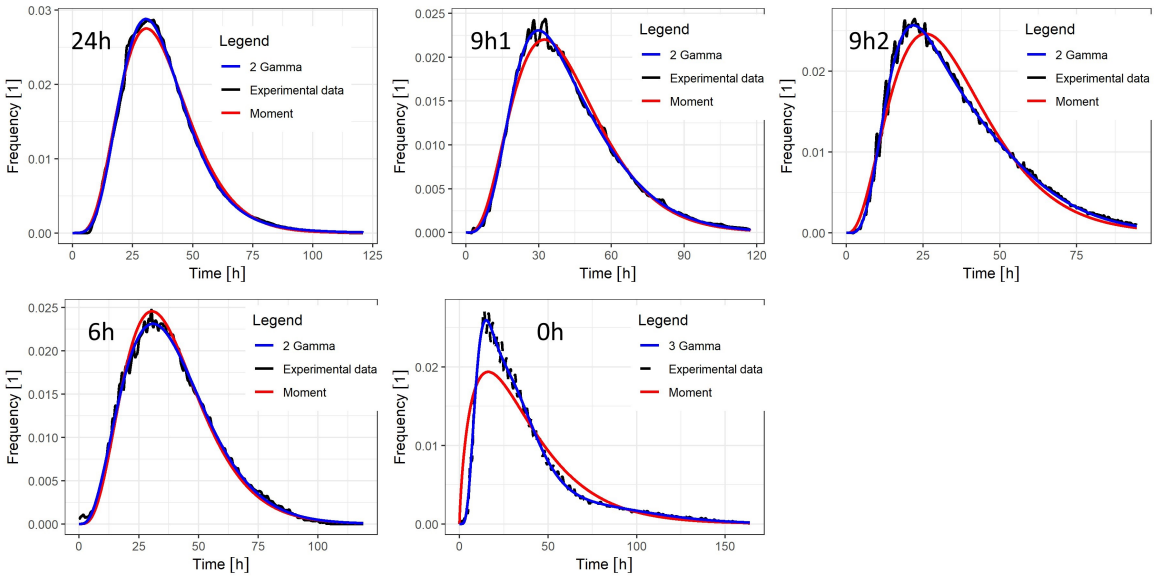

Figure 7.2: Comparison between different fitting methodologies for each tracer test.

Thèse accessible à l'adresse : https://theses.insa-lyon.fr/publication/2024ISAL0088/these.pdf © [C.K. Miyazaki], [2024], INSA Lyon, tous droits réservés

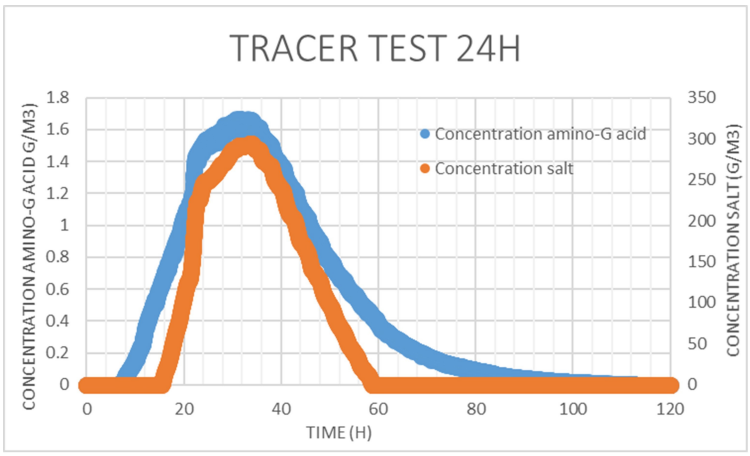

Figure 7.3: Comparison between amino-G acid and salt for the 24h tracer test.

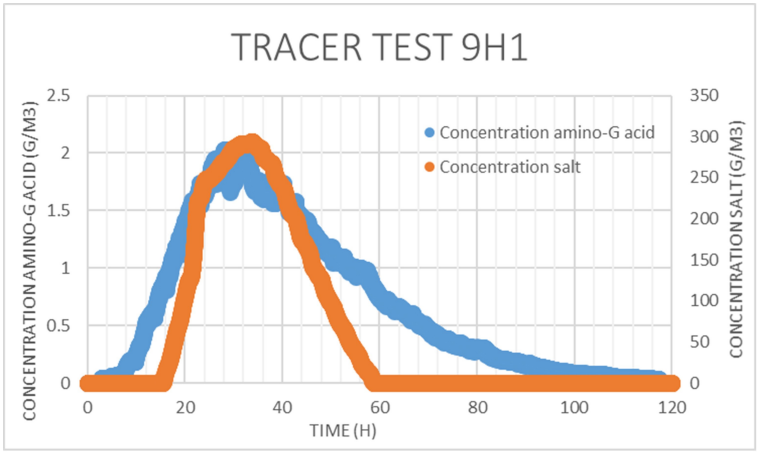

Figure 7.4: Comparison between amino-G acid and salt for the 9h1 tracer test.

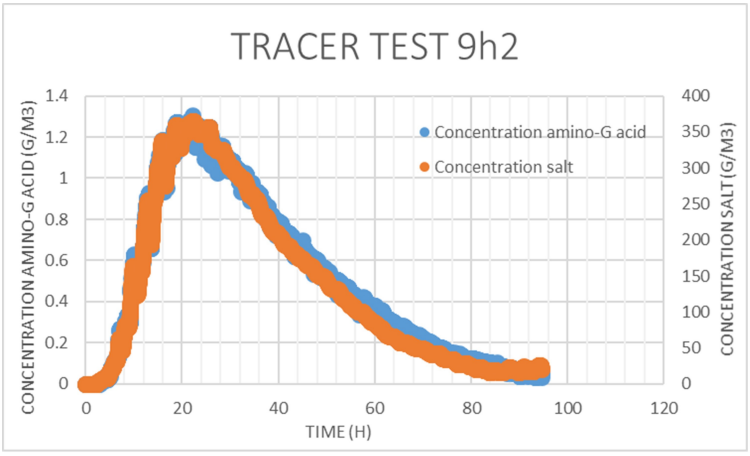

Figure 7.5: Comparison between amino-G acid and salt for the 9h2 tracer test.

Thèse accessible à l'adresse : https://theses.insa-lyon.fr/publication/2024ISAL0088/these.pdf © [C.K. Miyazaki], [2024], INSA Lyon, tous droits réservés

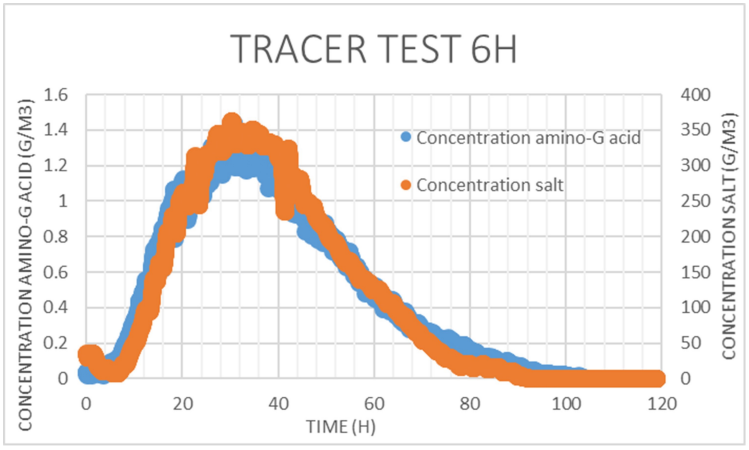

Figure 7.6: Comparison between amino-G acid and salt for the 6h tracer test.

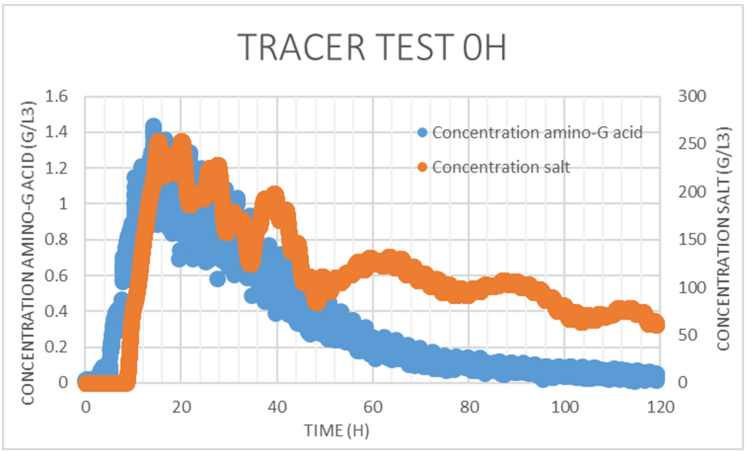

Figure 7.7: Comparison between amino-G acid and salt for the 0h tracer test.

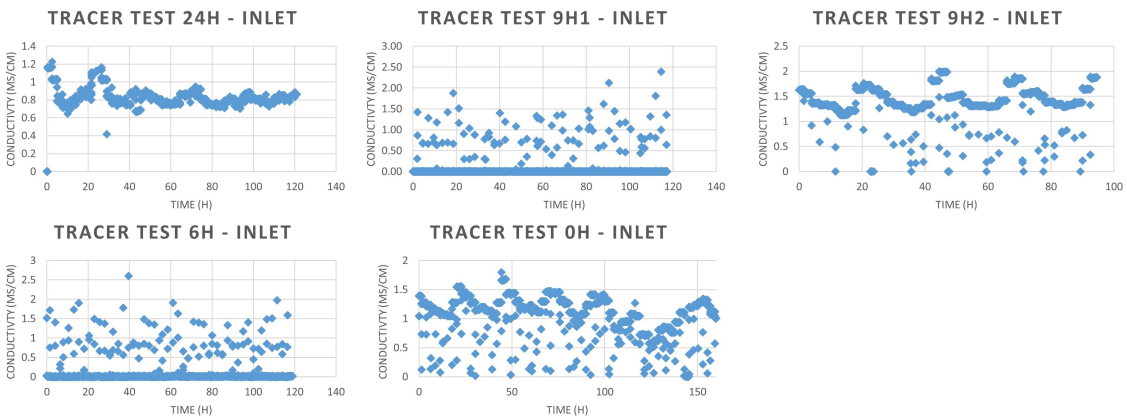

Figure 7.8: Inlet salt concentrations for each tracer test.

Thèse accessible à l'adresse : https://theses.insa-lyon.fr/publication/2024ISAL0088/these.pdf © [C.K. Miyazaki], [2024], INSA Lyon, tous droits réservés

7.2 Aeration strategies and total nitrogen removal in a hybrid aerated treatment wetland

Table 7.3: Parametric coefficients: COD

COD	Estimate	Standard error	t value	Pr (> |t|)
Intercept	0.928193	0.014861	62.457	< 2e-16
B	-0.003002	0.013278	-0.226	0.822

Aeration condition : p-value = 0.00417

Table 7.4: Parametric coefficients: fCOD

fCOD	Estimate	Standard error	t value	Pr (> |t|)
Intercept	0.66985	0.07075	9.467	7.71e-12
B	0.02945	0.04491	0.656	0.516

Aeration condition : p-value = 9.16e-06***

Table 7.5: Parametric coefficients: TSS

TSS	Estimate	Standard error	t value	Pr (> |t|)
Intercept	0.97562	0.01145	85.224	<2e-16
B	0.01332	0.01369	0.973	0.336

Aeration condition : p-value = 0.0896

Table 7.6: Parametric coefficients: NH_4-N

NH_4-N	Estimate	Standard error	t value	Pr (> |t|)
Intercept	0.95539	0.02694	35.468	<2e-1
B	-0.01615	0.01689	-0.956	0.345

Aeration condition : p-value = 6.63e-07 ***

Thèse accessible à l'adresse : https://theses.insa-lyon.fr/publication/2024ISAL0088/these.pdf © [C.K. Miyazaki], [2024], INSA Lyon, tous droits réservés

Table 7.7: Parametric coefficients: TN

TN	Estimate	Standard error	t value	Pr ($>$ |t|)
Intercept	0.4774	0.1216	3.925	0.0003381
B	-0.2174	0.1091	-1.991	0.053390

Aeration condition : p-value = 0.000689 ***

Thèse accessible à l'adresse : https://theses.insa-lyon.fr/publication/2024ISAL0088/these.pdf © [C.K. Miyazaki], [2024], INSA Lyon, tous droits réservés

Table 7.8: Inlet, outlet concentrations and concentration removal for each condition, considering temperature inside the COD,fCOD, TSS, TN, NH_4-N, NO_3-N,NO_2-N, PO_4-P,HCO_3-,where Avg = average, Std dev = standard deviation and n= number of observations

	Parameter	Inlet				Outlet				Concentration percent removal (%)			
		median	Avg	Std	n	median	Avg	Std	n	median	Avg	Std	n
	COD (mg/L)	325	385	197	10	21	24	6	10	93%	92%	4%	10
	fCOD (mg/L)	80.5	78	25	10	22	23	3	10	93%	68%	11%	10
	TSS (mg/L)	244	289	146	10	2	2	0	10	99%	99%	1%	10
	TN (mg/L)	36.1	33.9	7.7	10	35.7	34.4	5.7	10	5.50%	5.00%	12.70%	7
C1	NH_4-N (mg/L)	34.7	32.3	9.3	10	0.1	0.23	0.5	10	99.70%	99.20%	1.70%	10
	NO_3-N (mg/L)	0.83	1.33	1.79	10	35.6	34	5.9	10				
	NO_2-N (mg/L)	0.2	0.2	0.2	10	0.1	0.1	0.3	10				
	PO_4-P (mg/L)	2.9	2.7	0.7	10	3	3.2	0.9	10				
	HCO_3- (mg/L)	421.5	406.1	75.1	10	136.5	139.5	22.3	10				
	COD (mg/L)	642	723	202	7	25	26	2	7	96%	96%	1%	7
	fCOD (mg/L)	118	110	26	7	23	22	2	7	96%	79%	5%	7
	TSS (mg/L)	570	585	146	7	2	2	1	7	99.60%	99.60%	0.20%	7
	TN (mg/L)	51.7	55.8	19.4	7	24.1	26.4	5.7	7	45.10%	47.20%	19.60%	7
C2	NH_4-N (mg/L)	45.5	43	8.5	7	0.02	0.23	0.31	7	99.90%	99.50%	0.70%	7
	NO_3-N (mg/L)	0.51	0.71	0.43	7	22.6	25.3	6.2	7				
	NO_2-N (mg/L)	0.02	0.14	0.32	7	0.16	0.45	0.6	7				
	PO_4-P (mg/L)	3.4	3.5	0.6	7	4.6	4.7	0.2	7				
	HCO_3- (mg/L)	461	484.1	72.2	7	238	241.9	35.9	7				
	COD (mg/L)	554	545	212	8	25	24	4	8	96%	95%	3%	8
	fCOD (mg/L)	102	95	33	8	24	23	3	8	96%	71%	17%	8
	TSS (mg/L)	380	434	275	8	2	2	0	8	99.50%	99.40%	0.30%	8
	TN (mg/L)	35.3	41.1	21.9	6	16.8	17.1	1.8	5	66.40%	62.60%	17.70%	4
C3	NH_4-N (mg/L)	38.3	36.2	16.3	8	0.5	0.7	0.6	8	98.50%	97.60%	3.00%	8
	NO_3-N (mg/L)	0.5	0.8	0.7	8	16.2	16	2.4	7				
	NO_2-N (mg/L)	0	0	0.1	8	0.1	0.2	0.3	8				
	PO_4-P (mg/L)	2.9	2.7	1.5	8	4.3	4.1	1.3	8				
	HCO_3- (mg/L)	466.5	466.6	145	8	250	250.8	75.5	8				
	COD (mg/L)	274	280	112	3	20	20	1	3	93%	92%	3%	3
	fCOD (mg/L)	60	57	17	3	20	20	0	3	93%	62%	13%	3
	TSS (mg/L)	176	179	91	3	2	2	0	3	99%	99%	1%	3
	TN (mg/L)	35.9	29.8	12.2	3	15.4	15	1.1	3	56.00%	42.80%	25.70%	3
C4	NH_4-N (mg/L)	23.3	23.9	11.1	3	0.24	0.65	0.91	3	98.20%	97.80%	2.00%	3
	NO_3-N (mg/L)	0.72	0.66	0.57	3	12.2	12	2.8	3				
	NO_2-N (mg/L)	0.12	0.1	0.09	3	0.07	0.08	0.14	3				
	PO_4-P (mg/L)	2.1	1.9	1	3	2.4	2.5	0.7	3				
	HCO_3- (mg/L)	367.5	355.2	142.1	3	275	274.1	53.1	3				
	COD (mg/L)	417	417	123	2	23	23	4	2	95%	94%	1%	2
	fCOD (mg/L)	75	75	16	2	23	23	4	2	95%	69%	4%	2
	TSS (mg/L)	361	361	33	2	2	2	1	2	99.50%	99.50%	0.50%	2
	TN (mg/L)	35.7	35.7	7.8	2	30.4	30.4	3.2	2	13.20%	13.20%	4.90%	2
C5	NH_4-N (mg/L)	32.2	32.2	2.7	2	0.24	0.24	0.06	2	99.20%	99.20%	0.30%	2
	NO_3-N (mg/L)	0.78	0.78	0.06	2	29.9	29.9	3.2	2				
	NO_2-N (mg/L)	0.09	0.09	0.03	2	0.06	0.06	0.08	2				
	PO_4-P (mg/L)	2.8	2.8	1.4	2	3.2	3.2	1.3	2				
	HCO_3- (mg/L)	470.5	470.5	8.5	2	263.5	263.5	2.1	2				
	COD (mg/L)	650	611	95	5	24	24	3	5	95%	95%	1%	5
	fCOD (mg/L)	107	96	33	5	24	24	4	5	95%	75%	19%	5
	TSS (mg/L)	498	474	95	5	2	2	0	5	99.50%	99.60%	0.20%	5
	TN (mg/L)	42.4	44.6	13.4	5	25.4	22.5	2.1	5	56.60%	53.40%	5.90%	5
C6	NH_4-N (mg/L)	39.3	36.1	9.2	5	0.45	0.43	0.25	5	99.40%	98.80%	1.10%	5
	NO_3-N (mg/L)	0.6	0.8	0.2	5	23.3	22.8	2.2	5				
	NO_2-N (mg/L)	0.18	0.15	0.1	5	0.17	0.2	0.25	5				
	PO_4-P (mg/L)	2.6	2.8	0.3	5	3.4	3.3	1.2	5				
	HCO_3- (mg/L)	459	450.2	51.5	5	241	243.5	32.5	5				
	COD (mg/L)	696	634	198	6	30	28	5	6	95%	94%	2%	6
	fCOD (mg/L)	120	107	45	6	30	28	6	6	95%	74%	18%	6
	TSS (mg/L)	418	432	183	6	2	2	1	6	99.50%	99.50%	0.50%	6
	TN (mg/L)	30.4	39.4	19.8	6	16.7	18.1	5.3	6	48.70%	52.20%	19.60%	6
C7	NH_4-N (mg/L)	22.5	28.5	15.8	6	0.5	0.43	0.38	6	97.80%	97.40%	2.20%	6
	NO_3-N (mg/L)	0.4	0.5	0.2	6	16.7	17.7	7	6				
	NO_2-N (mg/L)	0.16	0.15	0.09	6	0.14	0.2	0.2	6				
	PO_4-P (mg/L)	2.7	2.6	1.2	6	3.6	3.3	1.5	6				
	HCO_3- (mg/L)	423.5	424.3	94.5	6	231	229.3	68.7	6				

Thèse accessible à l'adresse : https://theses.insa-lyon.fr/publication/2024ISAL0088/these.pdf © [C.K. Miyazaki], [2024], INSA Lyon, tous droits réservés

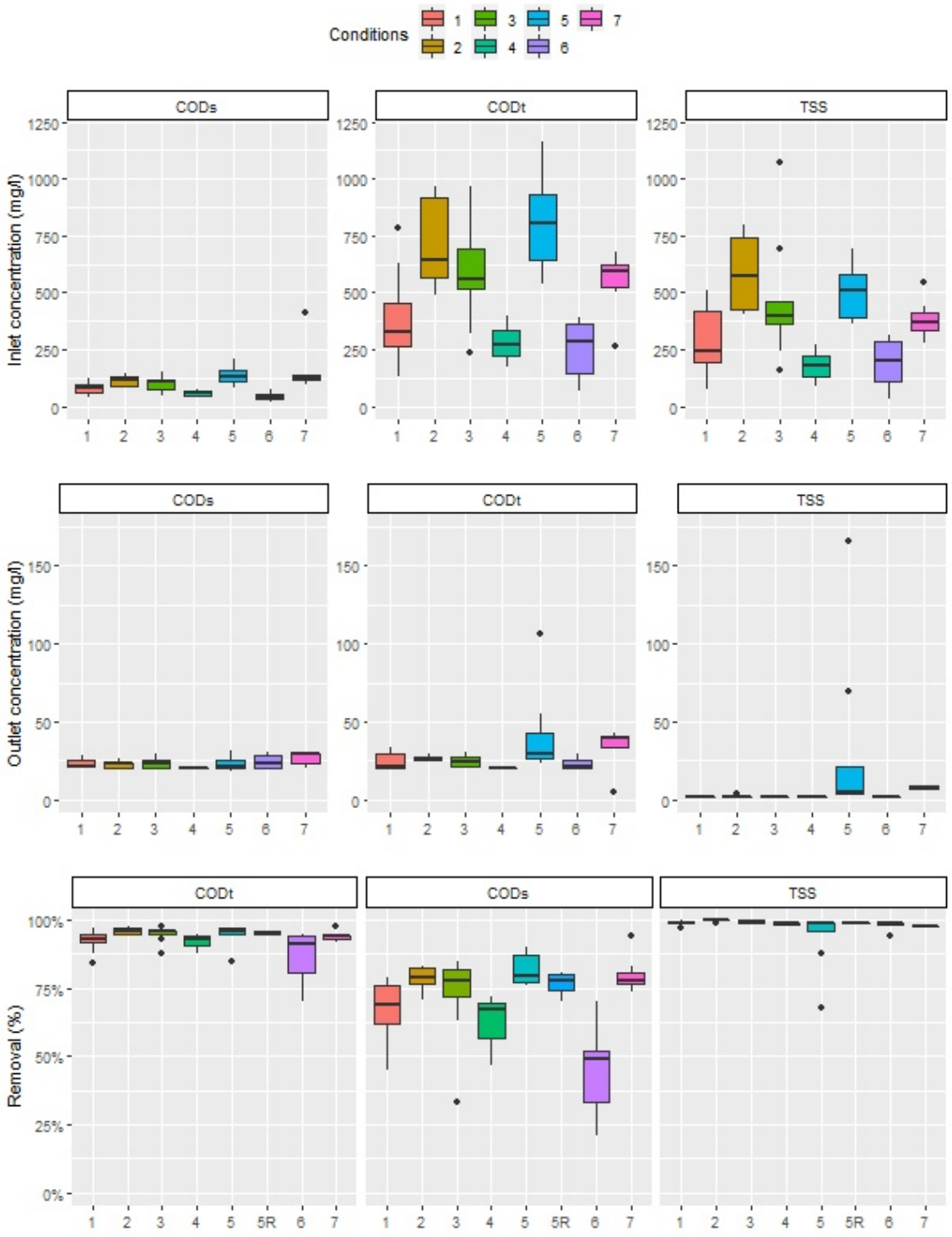

Figure 7.9: Inlet, outlet concentrations and concentration removal for the seven experimental condition tested, considering COD, fCOD and TSS.

Thèse accessible à l'adresse : https://theses.insa-lyon.fr/publication/2024ISAL0088/these.pdf © [C.K. Miyazaki], [2024], INSA Lyon, tous droits réservés

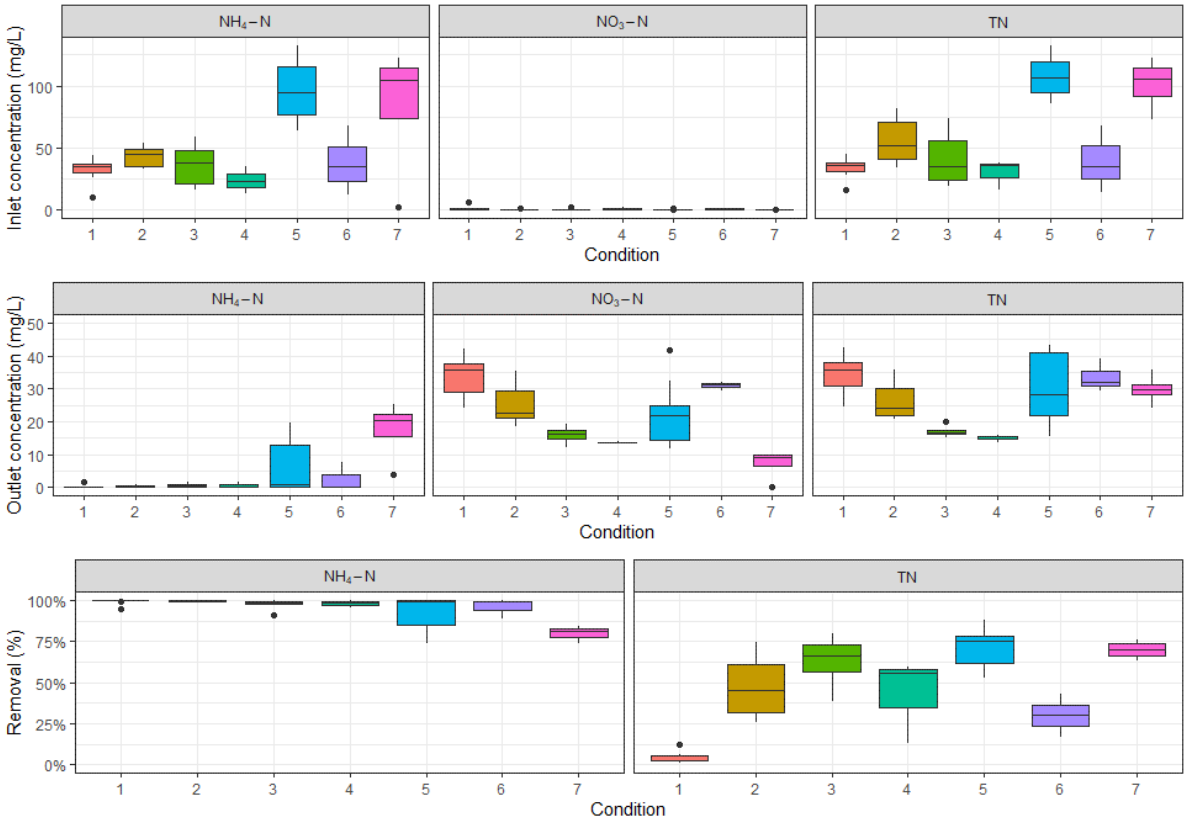

Figure 7.10: Inlet, outlet concentrations and concentration percent removal for the seven experimental conditions tested, considering NH_4-N, NO_3-N and TN.

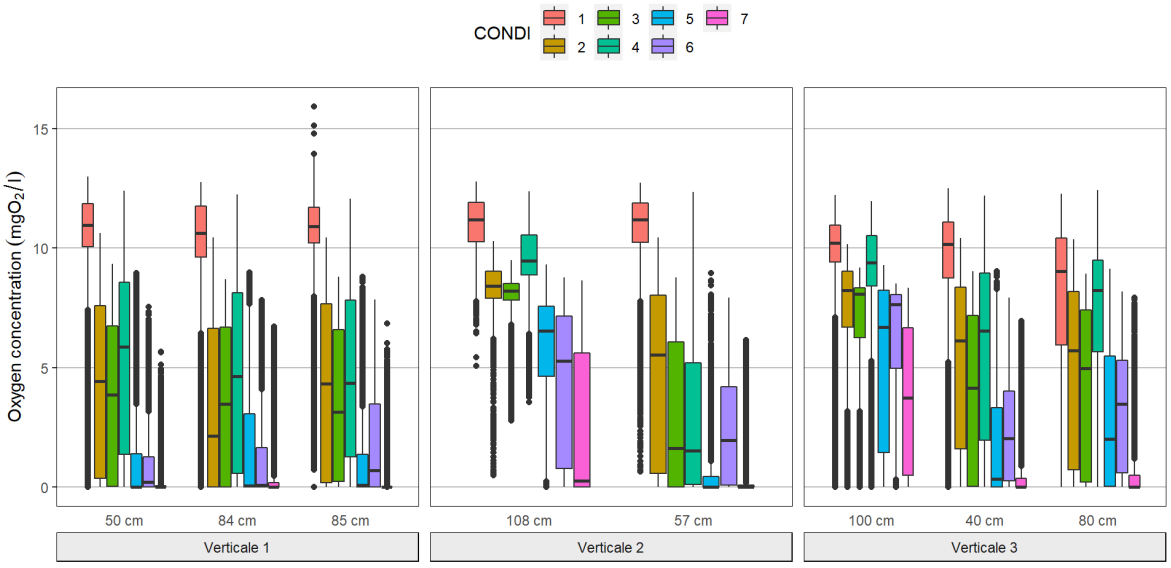

Figure 7.11: Dissolved oxygen concentrations measured at different pilot depths for the seven experimental conditions tested. Depths are indicated from the bottom of the pilot

Thèse accessible à l'adresse : https://theses.insa-lyon.fr/publication/2024ISAL0088/these.pdf © [C.K. Miyazaki], [2024], INSA Lyon, tous droits réservés

Table 7.9: Analysis of the lack of organic carbon for C1: T-9h-0.15

N to denitrify	CODt	CODe	CODn	CODn - CODa
mg/L	mg/L	mg/L	mg/L	mg/L
37	238	48	75	27
35	429	86	71	-15
37	631	126	74	-52
44	782	156	89	-68
26	313	63	52	-11

CODe = COD entering the saturated zone

CODn = COD needed; CODa = COD available

Table 7.10: Analysis of the lack of organic carbon for C2: T-3h-0.15

N to denitrify	CODt	CODe	CODn	CODn - CODa
mg/L	mg/L	mg/L	mg/L	mg/L
45	603	121	91	-30
46	642	128	91	-37
33	491	98	66	-32
34	530	106	67	-39

CODe = COD entering the saturated zone

CODn = COD needed; CODa = COD available

Table 7.11: Analysis of the lack of organic carbon for C3: T-3h-0.25

N to denitrify	CODt	CODe	CODn	CODn - CODa
mg/L	mg/L	mg/L	mg/L	mg/L
15	235	47	29	-18
44	514	103	88	-15
47	566	113	93	-20
58	695	139	116	-23

CODe = COD entering the saturated zone

CODn = COD needed; CODa = COD available

Thèse accessible à l'adresse : https://theses.insa-lyon.fr/publication/2024ISAL0088/these.pdf © [C.K. Miyazaki], [2024], INSA Lyon, tous droits réservés

Table 7.12: Analysis of the lack of organic carbon for C4: T-3h-0.35

N to denitrify	CODt	CODe	CODn	CODn - CODa
mg/L	mg/L	mg/L	mg/L	mg/L
13	171	34	26	-8
23	274	55	47	-8
34	394	79	67	-12

CODe = COD entering the saturated zone
CODn = COD needed; CODa = COD available

Table 7.13: Analysis of the lack of organic carbon for C5: T-3h-0.35-NH_4

N to denitrify	CODt	CODe	CODn	CODn - CODa
mg/L	mg/L	mg/L	mg/L	mg/L
47	670	134	94	-40
74	927	185	147	-38
116	956	191	231	40
90	732	146	180	33
115	540	108	230	122
131	1161	232	263	30

CODe = COD entering the saturated zone
CODn = COD needed; CODa = COD available

Table 7.14: Analysis of the lack of organic carbon for C6: F-3.3h-1.7h-0.35-NH_4

N to denitrify	CODt	CODe	CODn	CODn - CODa
mg/L	mg/L	mg/L	mg/L	mg/L
60	473	95	120	25
62	504	101	125	24
12	260	52	24	-28
45	434	87	90	3
35	412	82	70	-13

CODe = COD entering the saturated zone
CODn = COD needed; CODa = COD available

Thèse accessible à l'adresse : https://theses.insa-lyon.fr/publication/2024ISAL0088/these.pdf © [C.K. Miyazaki], [2024], INSA Lyon, tous droits réservés

Table 7.15: Analysis of the lack of organic carbon for C7: F-2.5h-0h-0.35-NH_4

N to denitrify	CODt	CODe	CODn	CODn - CODa
mg/L	mg/L	mg/L	mg/L	mg/L
68	411	82	136	54
73	505	101	147	46
72	546	109	144	35
68	629	126	135	9
103	595	119	205	86
106	678	136	213	77
91	621	124	182	58

CODe = COD entering the saturated zone

CODn = COD needed; CODa = COD available

Thèse accessible à l'adresse : https://theses.insa-lyon.fr/publication/2024ISAL0088/these.pdf © [C.K. Miyazaki], [2024], INSA Lyon, tous droits réservés

Table 7.16: Weather condition - Part 1

Condition 1		Condition 2		Condition 3	
DATE	RAIN (mm/d)	DATE	RAIN (mm/d)	DATE	RAIN (mm/d)
27/02/2019	0.2	04/07/2019	0	24/07/2019	0
28/02/2019	0	05/07/2019	0	25/07/2019	0
01/03/2019	0	06/07/2019	10	26/07/2019	1.6
02/03/2019	3.4	07/07/2019	0	27/07/2019	7.8
03/03/2019	0	08/07/2019	0.2	28/07/2019	16
04/03/2019	0.2	09/07/2019	0	29/07/2019	0.2
05/03/2019	0.2	10/07/2019	0	30/07/2019	0.2
06/03/2019	0	11/07/2019	0	31/07/2019	0
07/03/2019	7.8	24/06/2019	0	01/08/2019	0
27/02/2019	0.2	25/06/2019	0	02/08/2019	0
28/02/2019	0	26/06/2019	0	03/08/2019	0
01/03/2019	0	27/06/2019	0	04/08/2019	0
02/03/2019	3.4	28/06/2019	0	05/08/2019	0.6
03/03/2019	0	29/06/2019	0	06/08/2019	10.8
04/03/2019	0.2	30/06/2019	0	07/08/2019	3.4
05/03/2019	0.2	01/07/2019	1	08/08/2019	0
06/03/2019	0	02/07/2019	0	09/08/2019	7.13
07/03/2019	7.8	03/07/2019	0	10/08/2019	28.8
12/02/2019	1.8	27/05/2019	0	11/08/2019	16.2
13/02/2019	0	28/05/2019	1.4	12/08/2019	3
14/02/2019	0.2	29/05/2019	0	13/08/2019	0
15/02/2019	0.2	30/05/2019	0	14/08/2019	0
16/02/2019	0.2	31/05/2019	0	15/08/2019	0
17/02/2019	0	01/06/2019	0	16/08/2019	0
18/02/2019	0.2	02/06/2019	0	17/08/2019	0
05/04/2019	0.4	03/06/2019	0	18/08/2019	0
06/04/2019	0.2	04/06/2019	0	19/08/2019	12.8
07/04/2019	0	05/06/2019	2.2	20/08/2019	15.2
08/04/2019	0	06/06/2019	1	21/08/2019	0
09/04/2019	0	07/06/2019	0.4	22/07/2019	0
10/04/2019	1	08/06/2019	0	23/07/2019	0
11/04/2019	0	09/06/2019	13	22/08/2019	0
12/04/2019	0	10/06/2019	11.6	23/08/2019	0
13/04/2019	0	11/06/2019	1.6	24/08/2019	0
14/04/2019	0	12/07/2019	0.2	25/08/2019	0
15/04/2019	0	13/07/2019	0	26/08/2019	1
16/04/2019	3	14/07/2019	0	27/08/2019	0
17/04/2019	0	15/07/2019	0	28/08/2019	0
18/04/2019	0	16/07/2019	0		
19/04/2019	0	17/07/2019	0		
20/04/2019	0	12/06/2019	8.6		
21/04/2019	0	13/06/2019	0		
22/04/2019	0	14/06/2019	8.4		
19/02/2019	0.2	15/06/2019	16		
20/02/2019	0	16/06/2019	0		
21/02/2019	0.2	17/06/2019	0		
22/02/2019	0	18/06/2019	0		
23/02/2019	0.2	19/06/2019	0		
24/02/2019	0	20/06/2019	10		
25/02/2019	0.2	21/06/2019	2.8		
26/02/2019	0	22/06/2019	16		
10/05/2019	0.4	23/06/2019	0		

Thèse accessible à l'adresse : https://theses.insa-lyon.fr/publication/2024ISAL0088/these.pdf © [C.K. Miyazaki], [2024], INSA Lyon, tous droits réservés

Table 7.17: Weather condition - Part 2

Condition 4		Condition 5	
DATE	RAIN (mm/d)	DATE	RAIN (mm/d)
19/12/2019	0	25/06/2020	0
20/12/2019	6.2	26/06/2020	13.6
21/12/2019	8	27/06/2020	0.2
22/12/2019	2.4	28/06/2020	0.4
23/12/2019	1	29/06/2020	0
24/12/2019	3	30/06/2020	0.2
25/12/2019	0.2	01/07/2020	11.8
26/12/2019	0.2	30/07/2020	0
27/12/2019	4.6	31/07/2020	0
28/12/2019	0	01/08/2020	0.6
29/12/2019	0	02/08/2020	0
30/12/2019	0	03/08/2020	1.2
31/12/2019	0.2	04/08/2020	0
01/01/2020	0.2	05/08/2020	0
02/01/2020	0	06/08/2020	0
03/01/2020	0.8	07/08/2020	0
04/01/2020	0.6	08/08/2020	0
05/01/2020	0.8	09/08/2020	0
06/01/2020	0.4	10/08/2020	2
07/01/2020	0.2	11/08/2020	0
08/01/2020	1.2	12/08/2020	0
09/01/2020	0	13/08/2020	6
10/01/2020	0.8	14/08/2020	0
11/01/2020	0	15/08/2020	0
12/01/2020	0	16/08/2020	3.8
13/01/2020	0.2	17/08/2020	0
13/01/2020	0.2	18/08/2020	0
14/01/2020	0.2	19/08/2020	0
15/01/2020	0	20/08/2020	0
16/01/2020	0.2	21/08/2020	0
17/01/2020	5	22/08/2020	5.8
18/01/2020	0.2	23/08/2020	5.8
19/01/2020	0	24/08/2020	0
		25/08/2020	0
		26/08/2020	0
		27/08/2020	0
		28/08/2020	27.8
		29/08/2020	0
		30/08/2020	0
		31/08/2020	0
		01/09/2020	0
		02/09/2020	0
		29/05/2020	0
		30/05/2020	0
		31/05/2020	0
		01/06/2020	0
		02/06/2020	0.2
		03/06/2020	4.4
		02/07/2020	0
		03/07/2020	0
		04/07/2020	0
		05/07/2020	0

Thèse accessible à l'adresse : https://theses.insa-lyon.fr/publication/2024ISAL0088/these.pdf © [C.K. Miyazaki], [2024], INSA Lyon, tous droits réservés

Table 7.18: Weather condition - Part 3

Condition 6		Condition 7	
DATE	RAIN (mm/d)	DATE	RAIN (mm/d)
29/06/2021	5.2	09/08/2021	0
30/06/2021	0.2	10/08/2021	0
01/07/2021	0	11/08/2021	0
02/07/2021	0	09/08/2021	0
03/07/2021	3.6	10/08/2021	0
04/07/2021	15.8	11/08/2021	0
05/07/2021	0	22/08/2021	0
06/07/2021	42.8	23/08/2021	0
07/07/2021	0	24/08/2021	0
08/07/2021	0.8	25/08/2021	0
09/07/2021	0	26/08/2021	0
10/07/2021	7.8	27/08/2021	0
11/07/2021	0.2	28/08/2021	0
12/07/2021	44.2	29/08/2021	0
13/07/2021	9.4	30/08/2021	0
14/07/2021	15.6	31/08/2021	0
15/07/2021	8.2	01/09/2021	0
16/07/2021	4	02/09/2021	0
17/07/2021	0	03/09/2021	6.6
18/07/2021	0	04/09/2021	0.2
19/07/2021	0	05/09/2021	0
20/07/2021	0	09/08/2021	0
21/07/2021	0	10/08/2021	0
22/07/2021	0.2	11/08/2021	0
23/07/2021	0	12/08/2021	2.6
24/07/2021	0.8	13/08/2021	0.2
25/07/2021	0	14/08/2021	0
26/07/2021	0	15/08/2021	0
27/07/2021	0.2	16/08/2021	0
28/07/2021	6.8	17/08/2021	0.2
19/07/2021	0	18/08/2021	0
20/07/2021	0	19/08/2021	0
21/07/2021	0	20/08/2021	0
22/07/2021	0.2	21/08/2021	0
23/07/2021	0	06/09/2021	0
24/07/2021	0.8	07/09/2021	0
25/07/2021	0	08/09/2021	0
26/07/2021	0	09/09/2021	0.4
27/07/2021	0.2	10/09/2021	2.8
28/07/2021	6.8	11/09/2021	2.8
29/07/2021	0	12/09/2021	0
30/07/2021	4.8	13/09/2021	0
31/07/2021	3.8		
01/08/2021	0.6		
02/08/2021	0		
03/08/2021	12		
04/08/2021	8.8		
29/06/2021	5.2		
30/06/2021	0.2		
01/07/2021	0		
02/07/2021	0		
03/07/2021	3.6		

Thèse accessible à l'adresse : https://theses.insa-lyon.fr/publication/2024ISAL0088/these.pdf © [C.K. Miyazaki], [2024], INSA Lyon, tous droits réservés

7.3 Optimization of total nitrogen removal in a hybrid aerated vertical and horizontal treatment wetland

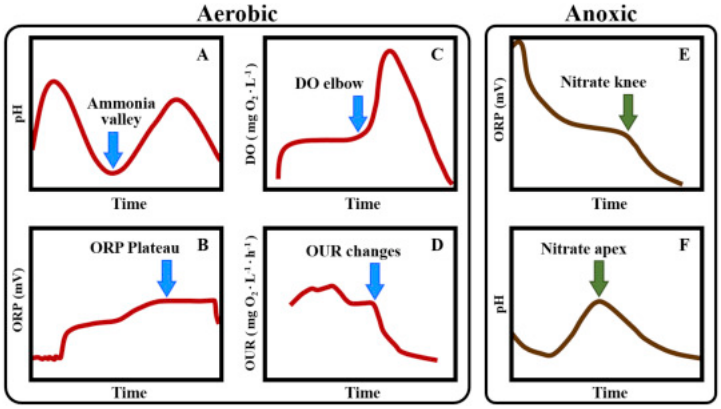

Figure 7.12: Bending points strategy for aerobic and anoxic phase. Source: Jaramillo et al. (2018)

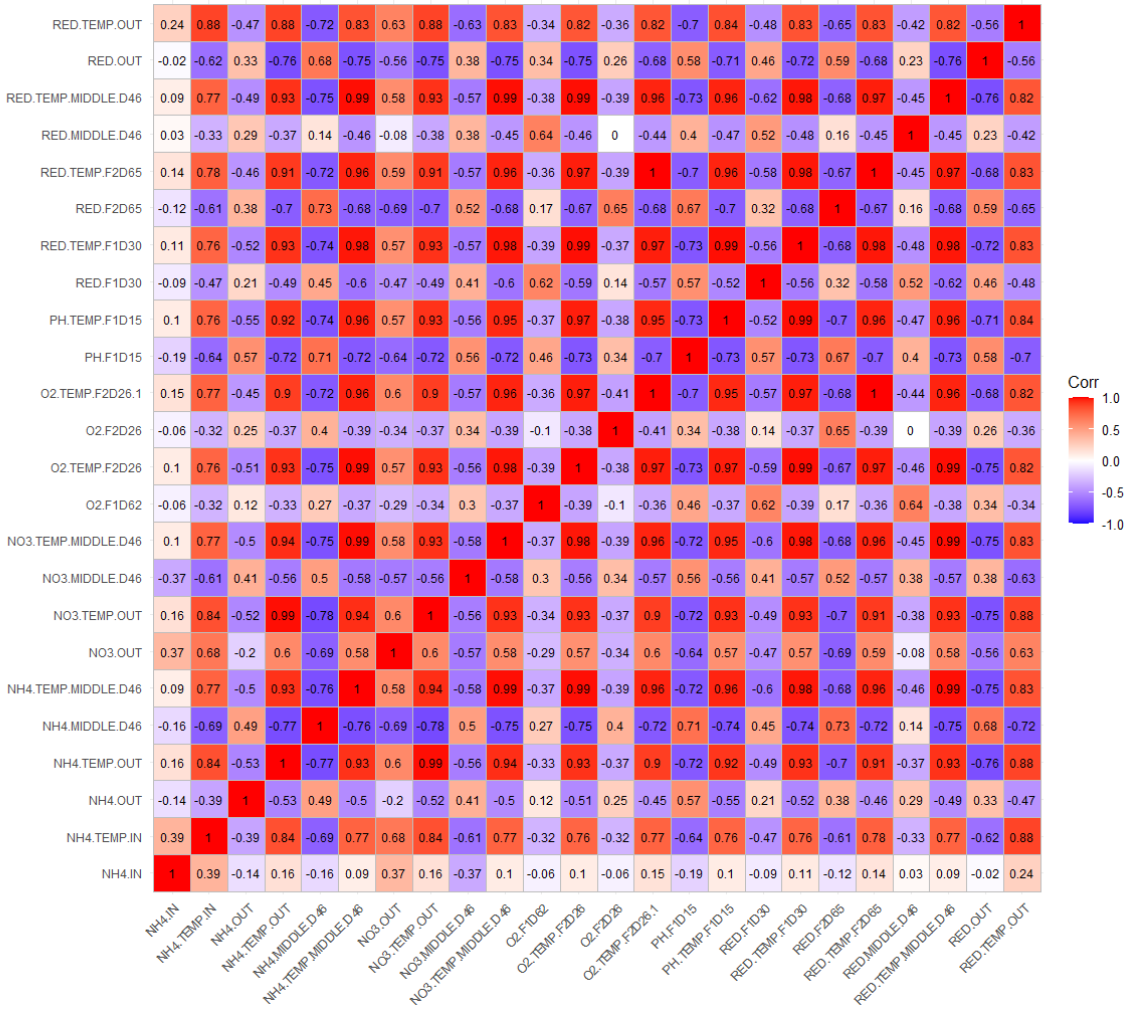

Figure 7.13: Matrix of correlation result (all variables)

Thèse accessible à l'adresse : https://theses.insa-lyon.fr/publication/2024ISAL0088/these.pdf © [C.K. Miyazaki], [2024], INSA Lyon, tous droits réservés

The Scree plot below indicates that the elbow is located at the third dimension. Consequently, for values where the dimension is greater than 3, the eigenvalues are small. Therefore, two principal components can be used to summarize the sample variance (Johnson and Wichern, 2007).

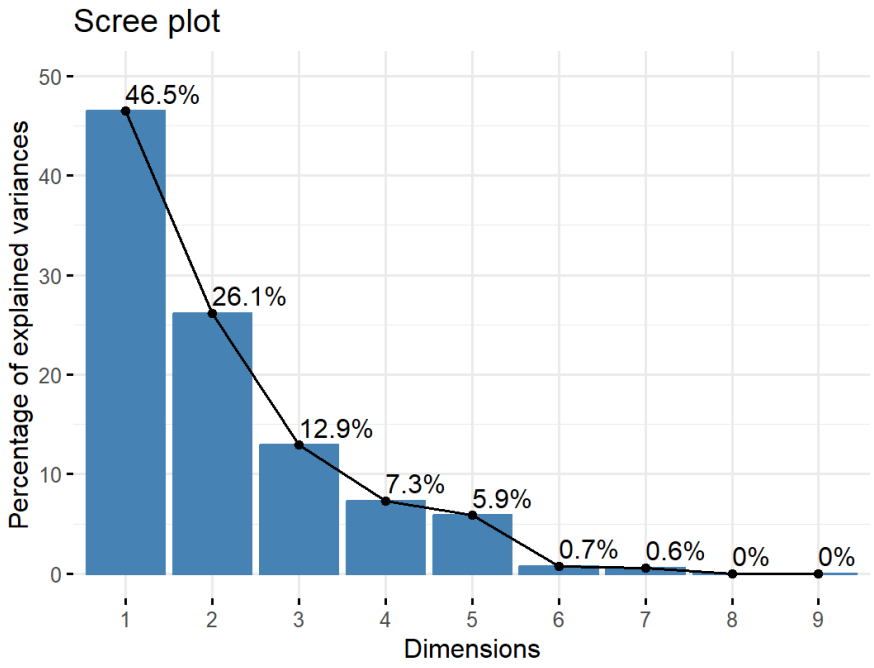

Figure 7.14: Scree plot for PCA analysis using the dataset

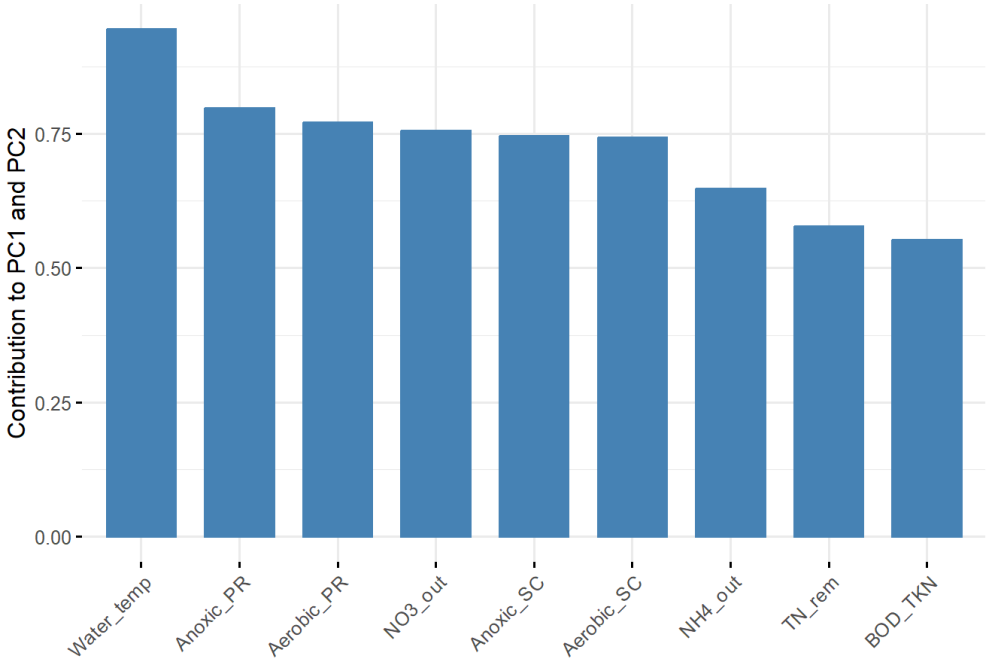

Figure 7.15: Contribution of each variable to PC1.

Thèse accessible à l'adresse : https://theses.insa-lyon.fr/publication/2024ISAL0088/these.pdf © [C.K. Miyazaki], [2024], INSA Lyon, tous droits réservés

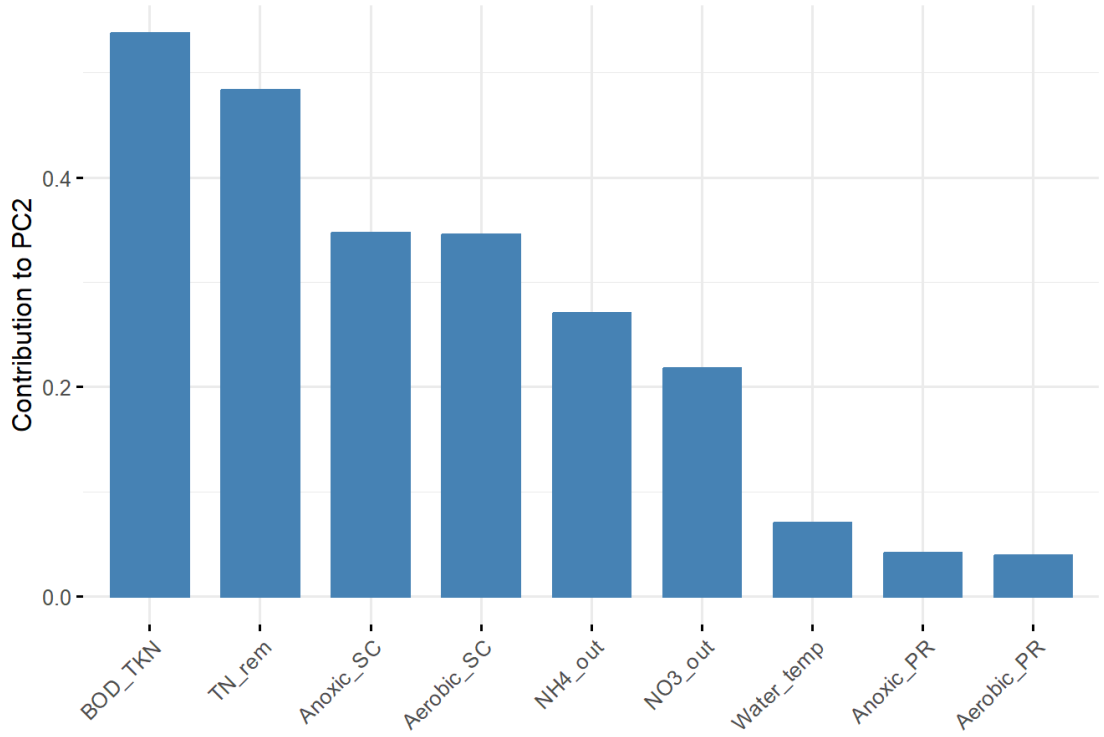

Figure 7.16: Contribution of each variable to PC2.

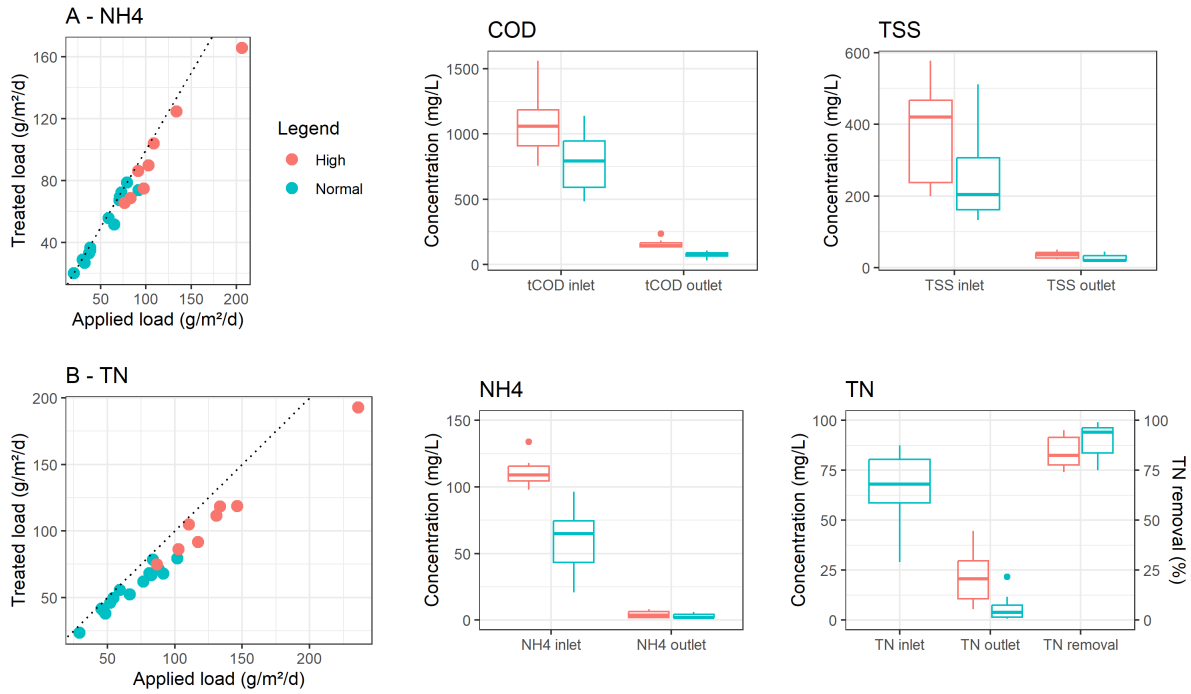

Figure 7.17: Left side – Applied load versus treated load for NH_4-N and TN. Right side - Inlet and outlet concentrations for COD, NH_4-N and TN. The TN concentration removal on the right y-axis represent the values in percentage.

Thèse accessible à l'adresse : https://theses.insa-lyon.fr/publication/2024ISAL0088/these.pdf © [C.K. Miyazaki], [2024], INSA Lyon, tous droits réservés

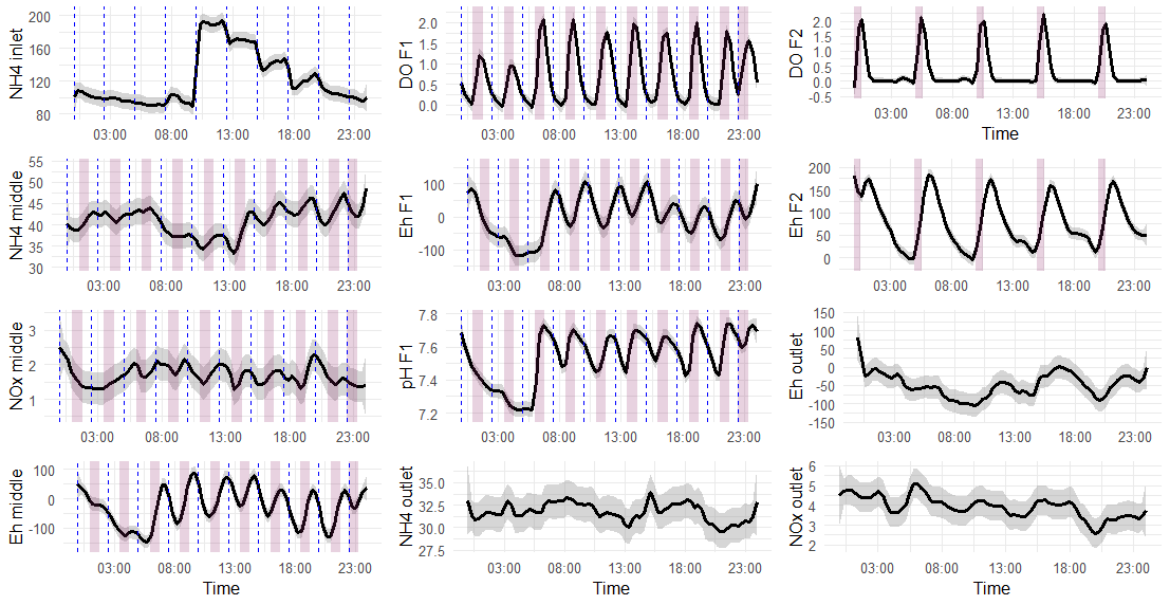

Figure 7.18: Curves characteristics for each online sensor considering only periods where the organic loadings were > 100 mg NH_4-N/L and > 1200 mg COD/L. Black line represent the mean concentration, the grey region the 95% confidence interval, blue dashed line the batch hour, red region the aeration period.

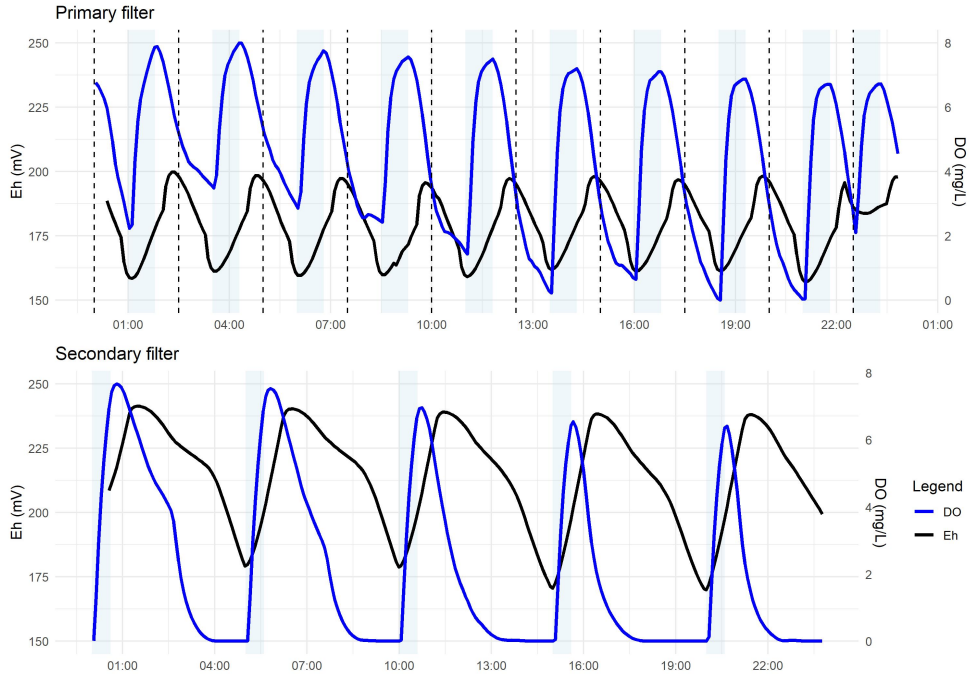

Figure 7.19: Eh and DO curve patterns for primary and secondary filters. Black dashed lines represent the batch hour and the blue region the aeration period.

Thèse accessible à l'adresse : https://theses.insa-lyon.fr/publication/2024ISAL0088/these.pdf © [C.K. Miyazaki], [2024], INSA Lyon, tous droits réservés

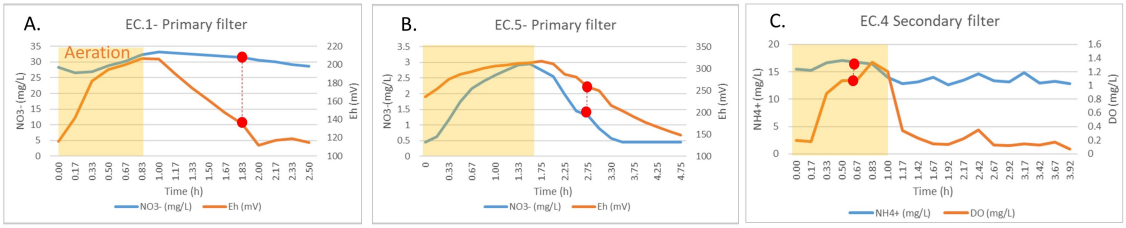

Figure 7.20: A. Eh measurement versus nitrate concentration for the primary filter, the red dashed line represents the "Nitrate knee". B. Eh measurement versus nitrate concentration for the primary filter, the red dashed line represents the "Nitrate knee". C. DO concentration versus ammonium concentration for the secondary filter, the red dashed line represents the "DO elbow".

Thèse accessible à l'adresse : https://theses.insa-lyon.fr/publication/2024ISAL0088/these.pdf © [C.K. Miyazaki], [2024], INSA Lyon, tous droits réservés

7.4 Methodology for hydraulic characterization based on ERT

This section represents an abstract intended for submission to a conference. However, improvements are needed before it can be validated and submitted. Limitations are highlighted in the perspectives section.

Summary: *An innovative methodology is proposed as a complementary technique for the classical tracer study, which aims to characterize the hydraulic dynamic in a closed system. The Electrical Resistivity Tomography (ERT) is capable of tracking a temporal sequence and producing multiple images. However, it becomes unwieldy to draw inferences when the frequency of time steps is high. Thus, a singular image could better simplify the interpretation. The proposition involves extracting the maximum amplitude and the corresponding time step for each tetrahedron to create this image.*

7.4.1 Introduction

There are many types of wastewater treatment system and one of them is the treatment wetland (TW). It's a closed tank filled with gravel and plants at the top of the filter. The performance of TW in terms of pollutant removal is significantly influenced by various hydraulic characteristics, such as hydraulic retention time (HRT), dead zones, and short-circuiting (Headley and Kadlec, 2007). Conventionally, hydraulic characterization has been accomplished through tracer studies aimed at determining tracer retention time and identifying potential anomalies. However, this technique is not adapted to understand the spatial heterogeneity, encompass observations limited to the outlet, and cannot capture the dynamic inside the filter (Delgado-Gonzalez et al., 2023). In this context, electrical resistivity tomography (ERT) can be a complementary technique for assessing dysfunctions within treatment wetlands. Over the past 20 years, geophysical methods have been democratized for their numerous applications in biotechnologies studies. Among these fields, electrical resistivity tomography has emerged as a prominent technique for studying water infiltration in porous media in both 2D or 3D (Audebert et al., 2014a). In TW, the application of ERT has primarily focused on evaluating clogging (Ergaieg et al., 2021; Marzo et al., 2018). However, its potential can be expanded to identify the flow patterns, including short-circuited flow, dead zones, and assess the effectiveness of mixing and aeration. Consequently, this research aims to evaluate the potential utilization of ERT for hydraulic characterization by a complementary methodology to the classical tracer study.

Thèse accessible à l'adresse : https://theses.insa-lyon.fr/publication/2024ISAL0088/these.pdf © [C.K. Miyazaki], [2024], INSA Lyon, tous droits réservés

7.4.2 Methodology

- Tracer test

The tracer test estimate the actual residence time of the water, as well as provide valuables information, e.g. median time, volumetric efficiency, dispersion number and equivalent number of apparent tanks in series (Headley and Kadlec, 2007). This tool involves an addition of a known quantity of tracer at the inlet through a single impulse injection. Subsequently, the concentration of the tracer, as well as the flow rate, is continuously monitored at the system's outlet over the course of several days.

- 3D Electrical Resisitivity Tomography

Electrical resistivity refers to a physical parameter that characterize the medium's capacity to oppose the passage of an electric current. It is influenced by many factors, such as the porosity of the medium, the water content, the conductivity of the solution and the temperature (Archie, 1942). In the case of a horizontal treatment wetland, the system can be conceptualized as a closed tank with a single inlet and outlet, operating within a controlled environment and achieving complete saturation. Consequently, the propagation of water flow cannot be directly observed using ERT. Thus, a tracer, such as salt, should be added to create an electrical resistivity contrast.

The tracer study in a horizontal TW can typically last between 2 and 10 days, resulting in a time-series of images. Thus, interpreting the tracer flow pose significant challenges due to the substantial volume of data generated. To address this, the present study proposes the generation of a singular image representing the maximum amplitude time of different spatial locations and its corresponding time. The tank mesh is divided into multiples tetrahedra, each displaying a curve that depicts resistivity changes across the time. The minimum point of the ratio curve (Eq. SM.1) signifies the maximum amplitude, and all these informations are consolidated into a single image (Figure 7.21).

$$\text{ratio} = 100 \cdot \left(\frac{\rho_f}{\rho_i} - 1 \right) \qquad \text{(Eq. SM.1)}$$

- Study case

In order to validate the methodology, a hybrid treatment wetland was selected as the study case. The chosen system features a forced aeration mechanism with driplines distributed across the entire bottom, allowing air injection at the saturated zone. This technology represent a current trend in the TW sector. The pilot has an area of 20 m2 and it is located in France. For the experimental setup, electrodes were installed at the surface of the whole filter (144 electrodes, 6 lines of 24 electrodes) and a resistivity-meter

Thèse accessible à l'adresse : https://theses.insa-lyon.fr/publication/2024ISAL0088/these.pdf © [C.K. Miyazaki], [2024], INSA Lyon, tous droits réservés

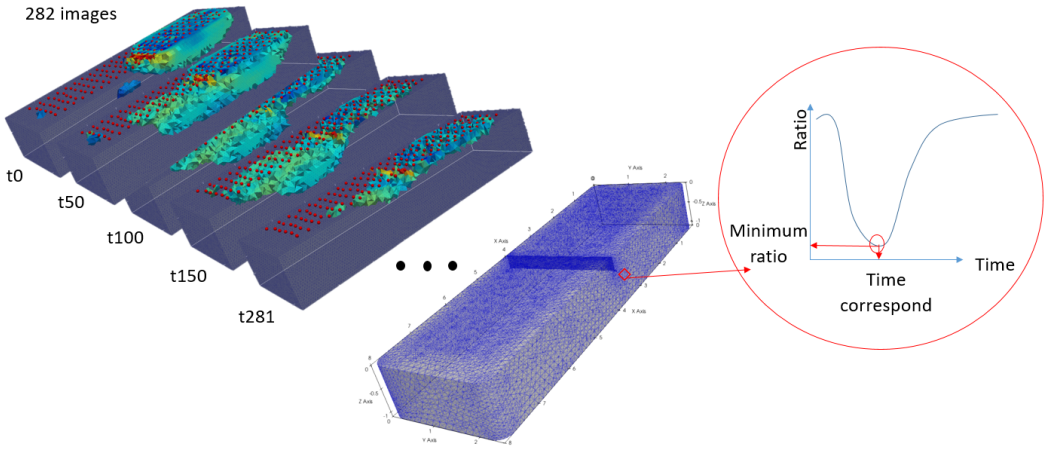

Figure 7.21: Methodology for ERT data treatment

was employed for measurement (Syscal Pro, Iris Instrument, France) at intervals of 15 minutes, enabling continuous monitoring of the system's dynamic behavior over time. Each acquisition had a duration of 13 min, with 1144 quadripoles (Wenner and dipole-dipole arrays), which thus generating 282 images. The collected data sets were subsequently inverted using the Resipy software to reconstruct a three-dimensional (3D) representation of electrical resistivity imaging (Blanchy et al., 2020). The system is completely isolated by a geomebrane, thereby a closed 3D model was created, excluding boundary. For the time-lapse inversion, inversion errors were calculated using normal and reciprocal measurement inversion before the saline tracer test. The time-lapse inversion was performed using an inversion set as reference model. The reference model is the measurement before the injection of the saline tracer for all images (Audebert et al., 2014b). The acquired data considered a standard temperature of 25°C, and the resistivity values were corrected based on the local temperature sensors using the following formula (Eq. SM.2):

$$\rho_T = \frac{\rho_{T_{\text{reference}}}}{1 + \alpha_T \cdot (T - T_{\text{reference}})} \qquad \text{(Eq. SM.2)}$$

The Paraview software was used to visualize the ratio in the tank over each time-step. In terms of tracer study, the tracer batch involved the addition of 3 kg of salt (NaCl) and 12 mg of amino-G acid at the beginning of the experiment. The aeration condition was maintained continuously for 24 hours per day throughout the entire filter. At the outlet of the system, a fluorimeter and a conductivity meter were installed to measure and monitor the tracer concentration.

Thèse accessible à l'adresse : https://theses.insa-lyon.fr/publication/2024ISAL0088/these.pdf © [C.K. Miyazaki], [2024], INSA Lyon, tous droits réservés

7.4.3 Results

- ERT validation

In order to establish a comparison between the ERT data and local sensors, four conductivity meters were strategically installed at the midpoint of the filter. The purpose of this installation was to assess the consistency and agreement between the measurements obtained from the ERT technique and the readings acquired from the local sensors. Figure 7.22 illustrates the graphical representation of this comparison, demonstrating that the two curves (ERT and sensors) has the same shape. Nonetheless, only Figure 7.22C has a good fit, the others could have a better correlation if the porosity is homogenous throughout the entire filter. The experimental site is operating for 5 years and different biomass accumulation according to zones is mostly probable. Thus, based on this observation, it can be concluded that the ERT data is validated and capable of providing reliable and accurate responses.

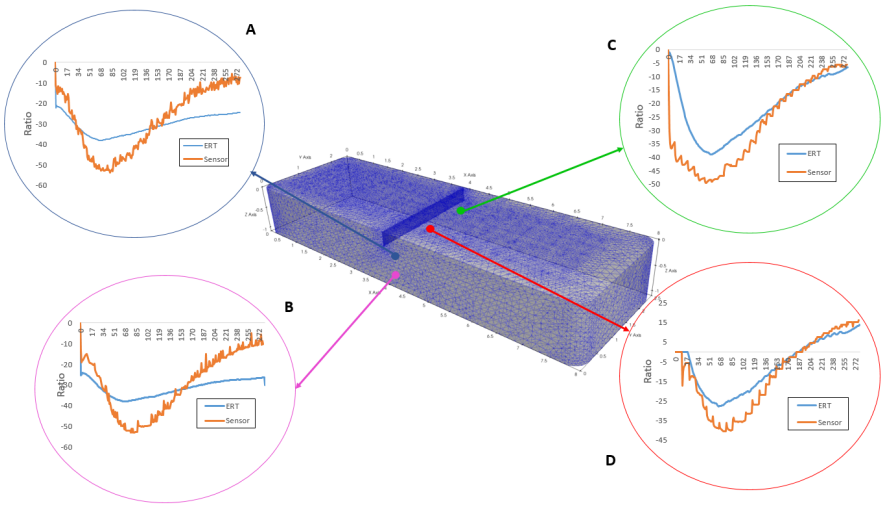

Figure 7.22: Validation for the ERT data

- ERT response

Figure 7.23A provide a view of the maximum amplitude in a y-axis slice. The lower part indicates a high ratio, while the upper part signifies a low ratio. This distribution suggests that the water predominantly flows closer to the surface, possibly due to the aeration effect. Overall, the salt concentration is distributed homogenously. Figure 7.23B and C introduce an additional element by depicting the corresponding time for each ratio using a black and white scale. Figure 7.23B illustrates where the salt had the maximum concentration, occurring between 56 and 130 time-step (13h to 33h after the tracer batch). It suggest a short-circuited zone, indicating a water preferential pathway.

In Figure 7.23 (from 33h to 50h after the tracer batch), the salt start to disperse

Thèse accessible à l'adresse : https://theses.insa-lyon.fr/publication/2024ISAL0088/these.pdf © [C.K. Miyazaki], [2024], INSA Lyon, tous droits réservés

throughout the filter, towards to border areas and it reaches the outlet. The calculated tracer retention time, based on the classical methodology described by Headley and Kadlec (2007), amounts to 41 hours. Both methods converge towards the same result, meaning that the water spends approximately 1.7 days inside the filter.

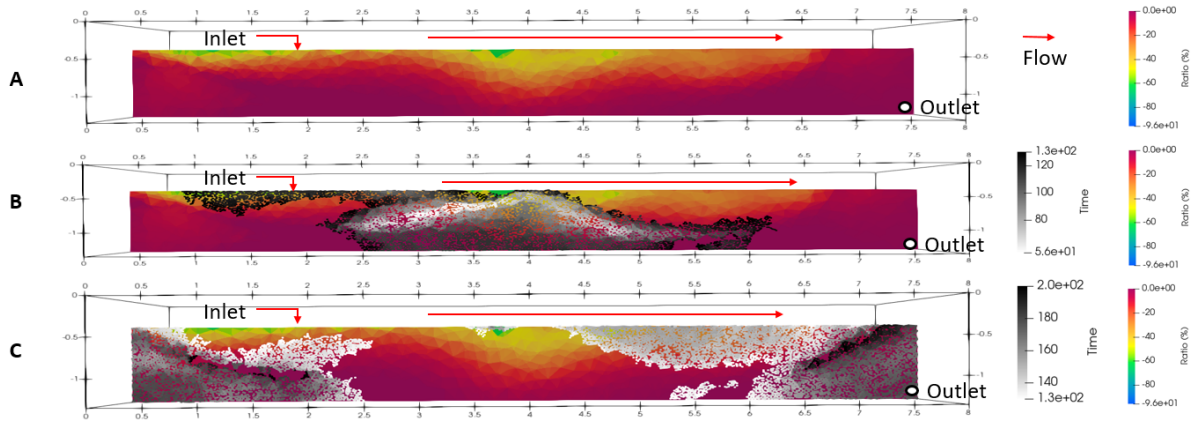

Figure 7.23: ERT results from the study case in a y-axis slice. A = minimum ratio (%), B = minimum ratio (%) at the back and minimum time from 56 to 130 time-step, C = minimum ratio (%) at the back and minimum time from 130 to 200 time-step

7.4.4 Conclusions

This experimental setup and data collection strategy allowed the validation and assessment of the proposed methodology for hydraulic characterization in treatment wetlands. The study case highlighted that the full-time aeration can homogenize the lower part, but the filter is not used at the same time. Certain areas exhibited preferential pathways where the water flow faster, while other areas, there are slower flow rates or even temporary stagnation. Therefore, the current study gives a visual representation of the hydraulics dynamics. This visualization offers valuable insights into the heterogeneity of flow patterns and the presence of potential dead zones. However, it is worth noting that further investigations could delve deeper into numerical analyses, such as quantifying the exact extent of dead zones, if feasible through modeling approaches. Future studies may explore numerical modeling techniques to gain more precise quantitative results, enabling a comprehensive understanding of the hydraulic behavior. By combining experimental data with sophisticated modeling approaches, researchers can propose improvements on the design and operation strategies for treatment wetlands.

Thèse accessible à l'adresse : https://theses.insa-lyon.fr/publication/2024ISAL0088/these.pdf © [C.K. Miyazaki], [2024], INSA Lyon, tous droits réservés

7.5 Methodology for nitrogen kinetics

The objective of this experiment is to ascertain the nitrification and denitrification rates, as well as the requisite time to establish an anoxic environment prior to the batch arrival. A total of five experimental conditions (EC) were assessed. Samples were collected at two points on the saturated layer of the primary and secondary filters at ten-minute intervals (Figure 7.24). The following parameters were monitored: redox, O_2, NH_4-N, NO_3-N, fCOD, and HCO_3^-. Please note that the data has not been included in this PhD thesis as it is still undergoing processing and treatment.

The first EC used the identical aeration strategy outlined in Chapter 5. The second, third, fourth and fifth ECs had both the primary and secondary filters subjected to the same conditions. Initially, the filter was aerated until the concentration of NH_4 in the filter reached 0 mg/L. Once aeration has ceased, the dissolved oxygen (DO) concentration was monitored with the DO sensor to determine the necessary time for establishing an anoxic environment (0 mg DO/L). Then, a 400-liter batch was launch at the surface of the filter. Furthermore, the filter was aerated for a period of 10 minutes to ensure complete mixing of the batch and the availability of the carbon source necessary for denitrification throughout the filter. Subsequently, the nitrate concentration was monitored with the nitrate sensor until it reached zero.

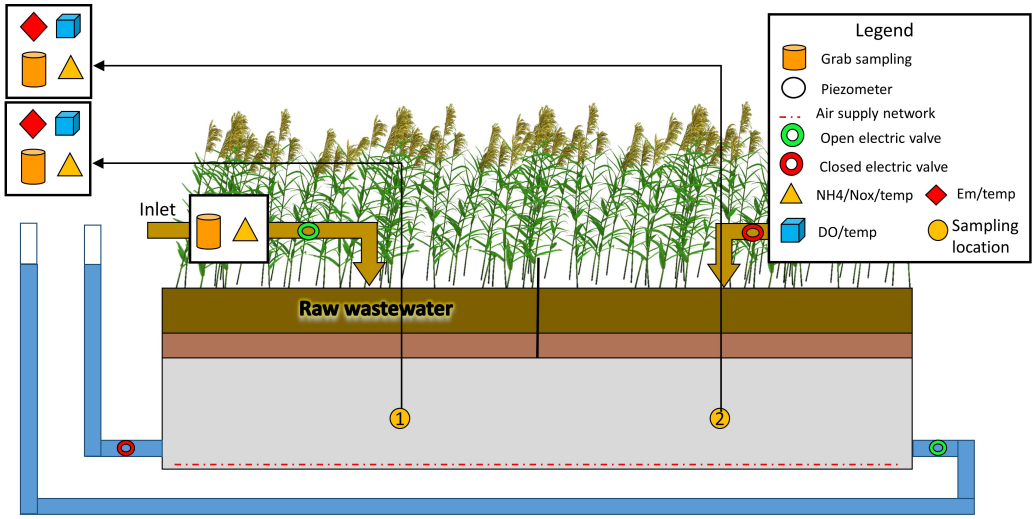

Figure 7.24: Sampling location and the sensors used for the kinetic experiment.

Thèse accessible à l'adresse : https://theses.insa-lyon.fr/publication/2024ISAL0088/these.pdf © [C.K. Miyazaki], [2024], INSA Lyon, tous droits réservés

FOLIO ADMINISTRATIF
THESE DE L'INSA LYON, MEMBRE DE L'UNIVERSITE DE LYON

NOM : **MIYAZAKI** DATE de SOUTENANCE : **13/11/2024**

Prénoms : **Caroline Kimie**

TITRE : **Optimization of hybrid aerated vertical/horizontal flow treatment wetland**

NATURE : **Doctorat** Numéro d'ordre : **2024ISAL0088**

École Doctorale : **Ćhimie**

Spécialité : **Génie des procédés**

RÉSUMÉ :
La combinaison de réglementations locales plus strictes et le besoin d'installations de plus grande capacité ont incité les entreprises du secteur du traitement des filtres plantés des roseaux (FPR) à donner la priorité aux initiatives de recherche et de développement visant à améliorer l'élimination de l'azote total (AT) et à minimiser l'empreinte des systèmes. En réponse à ces défis, le système Rhizosph'air a été créé pour être résilient, compact et robuste, avec une capacité de desservir des communautés de 2 000 à 10 000 EH. Cette thèse contribue à l'optimisation de l'élimination de l'AT tout en répondant aux défis opérationnels liés à la protection de l'environnement et à la réutilisation des eaux usées. Cette thèse est organisée en quatre chapitres principaux. Le chapitre 2 fournit une vue d'ensemble des sujets clés liés au système Rhizosph'air, y compris les solutions basées sur la nature et les FPR aéré. Il identifie les principaux domaines de recherche à améliorer, y compris le transfert d'oxygène et la dynamique de l'azote, afin d'améliorer l'élimination de l'azote naturel. Le chapitre 3 est consacré à l'analyse de l'impact des stratégies d'aération sur l'hydrodynamique du système. A cette fin, des tests de traçage ont été utilisés pour évaluer les réponses internes et de sortie. Les paramètres hydrauliques et la modélisation ont fourni des informations précieuses sur le comportement du système. Le chapitre 4 examine une série de conditions expérimentales, démontrant que les stratégies d'aération basées sur l'écoulement favorisent l'équilibre entre les environnements aérobies et anoxiques, optimisant ainsi l'élimination des AT. En outre, la stratégie suggère d'utiliser le filtre primaire pour générer des nitrates pendant l'aération et de permettre aux bactéries dénitrifiantes de les consommer pendant les périodes de non-aération et l'heure de traitement discontinu. L'utilisation du carbone organique des eaux usées brutes est également un aspect clé de cette stratégie. Enfin, le chapitre 5 examine la stratégie d'aération proposée, ses limites et la résilience du système hybride. Il évalue également l'applicabilité du modèle N-k-C* et étudie le potentiel de contrôle de l'aération en temps réel à l'aide de capteurs en ligne, y compris les points de flexion et les prédictions du modèle. Cette recherche fait progresser la compréhension des processus d'aération et de l'élimination des AT, offrant des stratégies innovantes pour améliorer la performance du traitement des FPR dans les petites communautés.

MOTS-CLÉS : **Aerated wetland; aeration strategy; constructed wetland; hydraulic; wastewater**

Laboratoire(s) de recherche : **INRAE - REVERSAAL**

Directeur de thèse : **Pascal MOLLE**

Président du Jury :

Composition du Jury :

MOLLE Pascal, Directeur de recherche (HDR), INRAE
NIVALA Jaime, Directrice de recherche (HDR), INRAE
GALVAO Ana, Professor(PhD), University of Lisbon
ROUSSEAU Diederik, Professor (PhD), Ghent University
GAUTIER Mathieu, Maître de conference (HDR), INSA-Lyon
MASI Fabio, Directeur technique/R&D (PhD), IRIDRA
MORVANNOU Ania, Chargée de recherche (PhD), Ecobird

Thèse accessible à l'adresse : https://theses.insa-lyon.fr/publication/2024ISAL0088/these.pdf © [C.K. Miyazaki], [2024], INSA Lyon, tous droits réservés